AD_____

Award Number: DAMD17-99-1-9547

TITLE: Genetic and Epigenetic Mechanisms Underlying Acute and Delayed Neurodegenerative Consequences of Stress and Anticholinesterase Exposure

PRINCIPAL INVESTIGATOR: Hermona Soreq, Ph.D.

CONTRACTING ORGANIZATION: Hebrew University of Jerusalem
91904 Jerusalem, Israel

REPORT DATE: August 2000

TYPE OF REPORT: Annual

PREPARED FOR: U.S. Army Medical Research and Materiel Command
Fort Detrick, Maryland 21702-5012

REPORT DOCUMENTATION PAGE

Form Approved
OMB No. 074-0188

1. AGENCY USE ONLY (Leave blank)	2. REPORT DATE	3. REPORT TYPE AND DATES COVERED
	August 2000	Annual (15 Jul 99 – 14 Jul 00)

4. TITLE AND SUBTITLE
Genetic and Epigenetic Mechanisms Underlying Acute and Delayed Neurodegenerative Consequences of Stress and Anticholinesterase Exposure

5. FUNDING NUMBERS
DAMD17-99-1-9547

6. AUTHOR(S)
Hermona Soreq, Ph.D.

7. PERFORMING ORGANIZATION NAME(S) AND ADDRESS(ES)
Hebrew University of Jerusalem
91904 Jerusalem, Israel

E-MAIL:
soreq@shum.huji.ac.il

8. PERFORMING ORGANIZATION REPORT NUMBER

9. SPONSORING / MONITORING AGENCY NAME(S) AND ADDRESS(ES)
U.S. Army Medical Research and Materiel Command
Fort Detrick, Maryland 21702-5012

10. SPONSORING / MONITORING AGENCY REPORT NUMBER

11. SUPPLEMENTARY NOTES
Report contains color graphics.

12a. DISTRIBUTION / AVAILABILITY STATEMENT
Approved for public release; Distribution unlimited

12b. DISTRIBUTION CODE

13. ABSTRACT ***(Maximum 200 Words)***

To characterize neuropathological consequences of excess acetylcholinesterase (AChE), we employed transgenic mice developed under previous US Army support. These mice demonstrated association between such excess and adverse responses (in brain and intestine) to pyridostigmine and diisopropylfluorophosphonate. The stress-associated "readthrough" AChE-R variant was seen also in progenitor blood cells, suggesting its use as a surrogate marker for anti-AChE responses. Moreover, AChE-R accumulates in the brain following head injury, its pre-injury excess exacerbates damage, and its antisense suppression improves survival and recovery. Using a 2-hybrid yeast screen we discovered a previously unknown interaction of AChE-R with RACK1, a protein kinase cargo protein involved in signaling processes. Animals carrying a tetracycline-inducible anti-AChE antisense sequence are being characterized for further studies of these interactions. At the extended promoter of the *ACHE* gene, we found a 4 bp deletion that over-induces transcription and hypersensitivity to pyridostigmine through impairment of HNF3ß interaction, and discovered a novel mutation that disrupts the glucocorticoid binding site. Finally, we found AChE-R-specific inhibitor interactions in mouse brain that reflect the specific increase in the AChE-R variant after psychological stress. The AChE-R variant thus emerges as the key scavenger and acetylcholine-hydrolyzing agent in several mammalian tissues under various stress insults.

14. SUBJECT TERMS
Neurotoxin

15. NUMBER OF PAGES
167

16. PRICE CODE

17. SECURITY CLASSIFICATION OF REPORT	18. SECURITY CLASSIFICATION OF THIS PAGE	19. SECURITY CLASSIFICATION OF ABSTRACT	20. LIMITATION OF ABSTRACT
Unclassified	Unclassified	Unclassified	Unlimited

Table of Contents

Introduction

To characterize neuropathological consequences of excess acetylcholinesterase (AChE), we employed transgenic mouse models that had been developed under previous USARMED support. These mice demonstrated an association between an excess of AChE and acutely adverse responses (in brain and intestine) to pyridostigmine and diisopropylfluorophosphonate, respectively a carbamate and an organophosphate inhibitor of AChE. The stress-associated "readthrough" AChE-R variant is seen also in progenitor blood cells, which suggests that it may prove to be a surrogate marker for reactions to anti-AChE agents and for studies on protection against them. Moreover, AChE-R accumulates in the brain of mice following head injury; its pre-injury excess exacerbates tissue damage; and its suppression by antisense agents improves survival and recovery of the animals. In an effort to discover the chain of cellular events that link the excess of AChE with the long-term pathological consequences, we used a 2-hybrid yeast screen to discover an interaction of AChE-R with RACK1, a protein kinase cargo protein that is involved in signaling processes. Animal models that carry a tetracycline-inducible antisense sequence designed to destroy AChE mRNA upon administration of low doses of a tetracycline, are now being characterized. Within the extended promoter of the *ACHE* gene, we found a 4 bp deletion that induces excess transcription and hypersensitivity to pyridostigmine through impairment of a transcription factor (HNF3ß) binding site, and discovered a novel mutation that disrupts the glucocorticoid binding site. Finally, we found that AChE-R, which specifically increases following psychological stress, has inhibitor sensitivities that are quantitatively different from those of the synaptic form of the enzyme. The AChE-R variant thus emerges as the key scavenger and acetylcholine-hydrolyzing agent in several mammalian tissues under various stress insults.

In greater detail, results are reported according to the tasks enumerated in the grant application, except for task 4, which is awaiting approval for human studies:

1. To characterize the sensory, cognitive and neuromotor consequences of a transgenic excess in AChE variants.
2. To employ transgenic mouse models with up to 300-fold differences in peripheral AChE levels for demonstration of direct correlation between AChE dosage and protection from stress and chemical warfare agents and to test their responses to pyridostigmine administration.
3. To develop RT-PCR tests in peripheral blood cells of model animals, and additional surrogate markers, for follow-up of responses and protection.
4. To adapt such tests to use in humans following accidental exposure to agricultural anti-ChEs.
5. To employ the transgenic mouse models to test effects of sudden changes in AChE levels at all the above sites and functions.
6. To delineate the protein partners through which AChE exerts non-catalytic signals which lead to delayed symptoms.
7. To develop tetracycline-inducible animal models in which AChE activity can be induced or antisense-suppressed at will.
8. To continue the search for promoter sequence polymorphisms which lead to natural variations in human AChE levels and correlate them with responses to anti-ChEs.
9. To expedite transgenic models for production from milk of recombinant human AChE, as a potential scavenger.

Task 1: Characterize consequences of excess AChE variants in transgenic animals.

Excess AChE-R attenuates but AChE-S intensifies neurodeterioration correlates

Acute stress increases the risk for neurodegeneration, but the molecular signals regulating the shift from transient stress responses to progressive disease are not yet known. The "readthrough" variant of acetylcholinesterase (AChE-R) (Fig. 1) accumulates in the mammalian brain under acute stress (Fig. 2). Therefore, markers of neurodeterioration were examined in transgenic mice overexpressing either AChE-R or the "synaptic" AChE variant, AChE-S (Fig. 3). Several observations demonstrate that excess AChE-R attenuates, whereas AChE-S intensifies, neurodeterioration. In the somatosensory cortex, AChE-S transgenics, but not AChE-R or control FVB/N mice, displayed a high density of curled neuronal processes indicative of hyperexcitation (Table 1). In the hippocampus, AChE-S and control mice, but not AChE-R transgenics presented progressive accumulation of clustered, heat shock protein 70–immunopositive neuronal fragments (Fig. 4), and displayed a high incidence of reactive astrocytes (Fig. 5). Our findings suggest that AChE-R serves as a modulator that may play a role in preventing the shift from transient, acute stress to progressive neurological disease, with its characteristic astrocyte reactivity (Fig. 6). This work has appeared as Sternfeld et al. (2000) *Proc. Natl. Acad. Sci. USA* 97, 8647-8652.

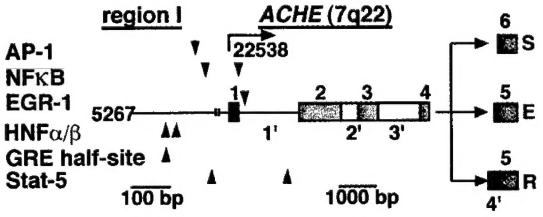

Fig. 1. Organization of the *ACHE* gene. The human gene is located at q22 on chromosome 7. Its coding region is comprised of 6 exons, the first of which encodes a leader sequence and the next 4 of which encode the core protein that is part of each AChE variant. Alternative splicing of the pre-mRNA gives rise to three variants, the synaptic (S), erythrocytic (E) and readthrough (R) forms, depending upon whether exons 5 and 6 and pseudointron 4 are included.

In both stress and injury, the physiological response to insult is the up-regulation of AChE-R expression. In one possible scenario, AChE is generally beneficial. Its elevation following chronic low-level exposure to anti-cholinesterases or stress may be sufficient to mitigate or reverse the deleterious effects. In the case of a high-level exposure to an anti-AChE or to severe stress, this response may be inadequate, and the deterioration overwhelms the body's protective mechanism. The expression of AChE-R may therefore be considered "good" but not always good enough. Alternatively, AChE-R may serve the short-term goal of preventing the over-stimulation of cholinergic mechanisms, but at the cost of long-term deleterious effects. In the short term, the up-regulation of AChE levels would prevent seizures by restoring normal cholinergic neurotransmission. In contrast, in the long term, as AChE is a homolog of cell adhesion molecules, it may disrupt the architecture of synapses and/or the blood-brain barrier. In this case, the long-term effect of AChE-R is "bad". Further studies will be required to satisfactorily resolve this issue. As part of this effort, we prepared a polyclonal rabbit antiserum selective for the C-terminal peptide that is unique to AChE-R

Preparation of antibodies directed at the AChE Readthrough Peptide (ARP)

The DNA sequence encoding ARP was PCR amplified from AChE-R cDNA using the following primers: GCT GGA TCC ATC GAG GGG CGA GGT ATG CAG GGG CCA GCG GGC (upstream) and TAT AAG CTT CTA GGG GGA GAA GAG AGG GGT (downstream). The resultant fragment was introduced into the open reading frame of a pGEX-KG plasmid (Pharmacia) and expressed in *E. coli* to yield a glutathione-S-transferase (GST)-ARP fusion protein. Contamination of bacterial proteins was removed from the *E. coli* lysates by 20 min incubation at 37 °C with 0.2 mM Mg-ATP. GST and ARP-GST fusion protein were purified from the supernatant of *E. coli* lysates by affinity chromatography on glutathione-Sepharose (Pharmacia) in the presence of protease inhibitors, aprotinin (10 μg/ml; Boehringer/Mannheim; Germany), benzamidine (5 mM; Sigma, Israel), Pefabloc SC (0.2 mM; Merck, Darmstadt, Germany) and EDTA (1 mM). Elution with 10 mM reduced glutathione in 50 mM Tris-HCl, pH 8.0, was followed by dialysis against 0.1 M ammonium acetate buffer, pH 7.0 and lyophilization of aliquot samples. Protein purity was tested by SDS-PAGE. New Zealand female rabbits were immunized subcutaneously with 0.3 mg fusion protein in complete Freund's adjuvant. Monthly reimmunizations were with 0.2 mg fusion protein in incomplete Freund's adjuvant. Ten days after immunization, specific antibodies were detected in the sera by ELISA, using immobilized fusion protein, in the presence of excess soluble GST (20 μg/ml). Immobilized ARP-GST, GST, and *E. coli* lysate were prepared using Affigel 10 beads (Bio-Rad) according to manufacturer's recommendations. Crude IgG fraction was prepared from the reactive sera by 50% saturated $(NH_4)_2SO_4$ precipitation and dialysis (100 mM Tris-HCl, pH 8.0). To eliminate antibodies against anti-GST or bacterial proteins, IgG fractions were repeatedly incubated with bead-bound GST or heat-shocked *E. coli* lysate proteins (overnight, 4 °C). Antibodies were eluted with 4.5 M $MgCl_2$. Unbound fractions were then incubated with ARP-GST beads (2 h, room temp. or overnight, 4°C). The bound fraction, eluted with 3.5 M $MgCl_2$, was dialyzed against 10 mM Tris-HCl, pH 8.0, and then against PBS, containing 0.025% NaN_3. This antibody has been transferred to Dr. M. Mesulam of Northwestern University School of Medicine for investigations into Alzheimer's disease.

Table 1. Suppressed stress-associated morphological features in AChE-R transgenics

Morphological Abnormality	Measurement	AChE-S	AChE-R	control
curled processes, (NFT 200)	cumulative length 0.48 mm^2 (μm)	3080 ± 210 p<0.0001	1410 ± 150	1070 ± 170
cortex thickness (μm)		230 ± 7	240 ± 8	230 ± 5
GABAergic interneurons (parvalbumin)	cells cortical layers 1-3	210 ± 4	190 ± 14	190 ± 19
	cells cortical layers 4-6	250 ± 12	270 ± 14	250 ± 10
	cell area (μm^2)	68 ± 3	66 ± 3	60 ± 3
GABAergic interneurons (calbindin D28K)	cells cortical layers 1-3	290 ± 10	300 ± 6	260 ± 15
	cells cortical layers 4-6	67 ± 5	73 ± 2	76 ± 5

	cell area (μm^2)	57 ± 2	55 ± 1.5	54 ± 2
neuronal fragment clusters, (NFT 200)	clusters per section	3.3 ± 0.8	0.4 ± 0.2 p<0.02	1.7 ± 0.4
	cluster area (μm^2)	3470 ± 370	2090 ± 500 *	2060 ± 230
	fragments/ cluster	110 ± 16 p<0.002	70 ± 15 *	46 ± 4
	fragment density in cluster	0.032± 0.002 p<0.03	0.035± 0.008 *	0.023± 0.002
neuronal fragment clusters, (HSP 70)	clusters per section	6.2 ± 2.1 p<0.005	0.4 ± 0.3	1.7 ± 0.7
	cluster area (μm^2)	2690 ± 380 p<0.03	1370 ± 280 *	1690 ± 240
	fragments/ cluster	50 ± 6 p<0.02	30 ± 7 *	31 ± 4
	fragment density in cluster	0.020 ± 0.001	0.022± 0.004 *	0.019± 0.001
astrocytes (GFAP)	total number of cells	270 ± 9	250 ± 10	270 ± 10
	percent of hypertrophic cells	24 ± 2	16 ± 3 p<0.03	24 ± 2

Presented are average values ± standard error of the mean (s.e.m.) for the measurements of morphological features noted in text. The antibody used for staining is noted in parentheses. Age groups of 4 and 8-10 month old mice were combined for calculations, except for the clustering phenomenon, which increased with age and for which the data presented (pooled from 3 mice) is for the 8-10 month group. A normal distribution could not be assumed and non-parametric tests were used: Kruskal-Wallis's for the main effects of transgenic line or age and Mann-Whitney's for multiple comparisons of transgenic lines. Significant p values (in comparison to control mice) are noted where appropriate.

*In AChE-R transgenics, the small number of clusters found precluded any statistical comparison of cluster area and number of fragments/cluster.

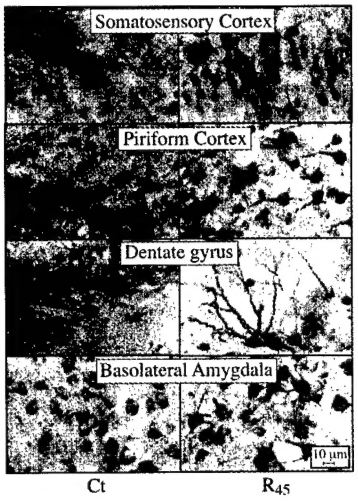

Fig. 2. AChE-R immunoreactivity in transgenic brain. Shown is AChE-R immunoreactivity in high magnification photomicrographs of coronal sections 1.2 mm posterior to Bregma from the brains of control (Ct) mice and the AChE-R_{45} transgenics (R_{45}). Note that ARP immunostaining is apparent only in neurons, that both somata and processes are stained and that the intensity of neuronal staining is highly variable between the different brain regions

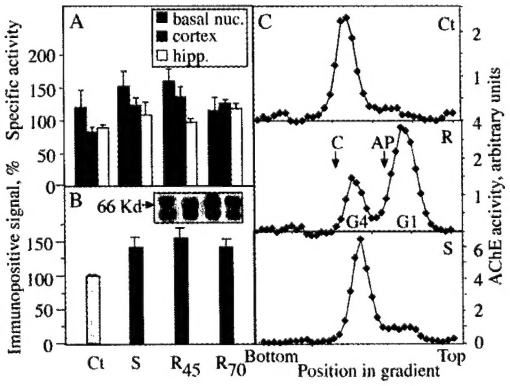

Fig. 3. Overexpression of AChE in transgenic brain.

A. AChE activity in brain regions of transgenic mice. Shown are rates of acetylthiocholine hydrolysis/min/mg protein in homogenates of basal nuclei (basal nuc.), cortex and hippocampus (hipp.) of AChE-S (S), AChE-R of line 45 (R_{45}) or 70 (R_{70})

transgenics and control (Ct) mice, all from the FVB/N strain. Bars present averages ± s.e.m. for homogenates from 4-5 mice of each pedigree. Note that elevation in catalytic AChE activity, though non-significant, is common to all transgenic lines.

B. AChE immunoreactivity in cortex of transgenic mice. Shown are average intensities ± s.e.m. of immuopositive bands following SDS-PAGE, immunoblot and densitometric analysis of cortical homogenates from transgenic and control mice. The antibody employed was targeted against the common N-terminal domain of AChE; the positive signal obtained with this antibody in control mouse samples (see inset) demonstrates massive cross reactivity with the mouse enzyme. Intensities were determined for the 3 main immunopositive bands (see inset) from 5-8 lanes loaded with protein from individual mice of each strain and are presented as percentage of control values within the same gel. Note that elevation in immunoreactivity, though non-significant, is common to all transgenic lines. Inset: an example of an immunoblot film, showing the main bands in each lane for each of the transgenics and controls at the same order as in the bar graph.

C. Altered multimeric assembly Shown are sucrose gradient profiles for AChE in the cortex of control (Ct), AChE-S (S) and AChE-R (line R45) mice. Arrows denote the sedimentation of bovine catalase (C; 11.4 S) and alkaline phosphatase (AP; 6.1 S). Note elevation in AChE tetramers (G4; ~10 S) or monomers (G1; ~4.4 S) and the altered ratio between these isoforms in the different transgenics.

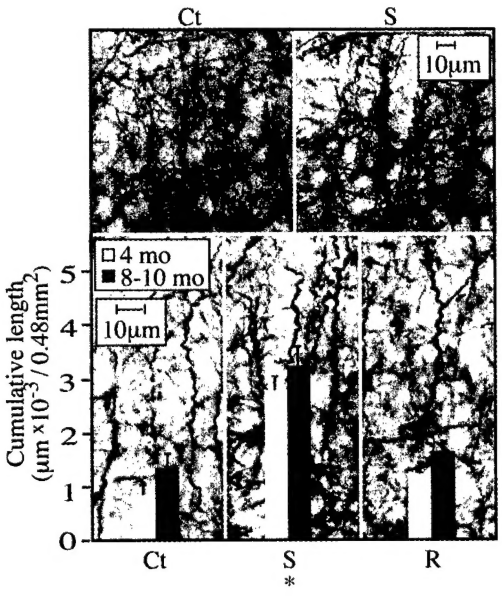

Fig. 4. Evidence for neuronal process malformation in AChE-S transgenic mice.
Above: example micrographs from control (Ct) and AChE-S transgenics (S) immunolabeled for neurofilament (NFT) 200. Below: cumulative length (averages ± s.e.m.) of all axonal or dendritic segments displaying a corkscrew-like pattern are displayed on high magnification micrographs from the parietal cortex of 4 or 8- 10 month old AChE-S (S) and AChE-R (R) transgenics and control mice. Numbers were derived from three coronal sections containing the somatosensory cortex, 1-2 mm posterior to Bregma from each of 6 male mice per group. Analysis using the Seescan Image Analysis system (Seescan plc, Cambridge, UK) was on 32 subfields, of 150 μm (width) x 100 μm (height) (total area of 0.48 mm^2). * $p<0.001$.

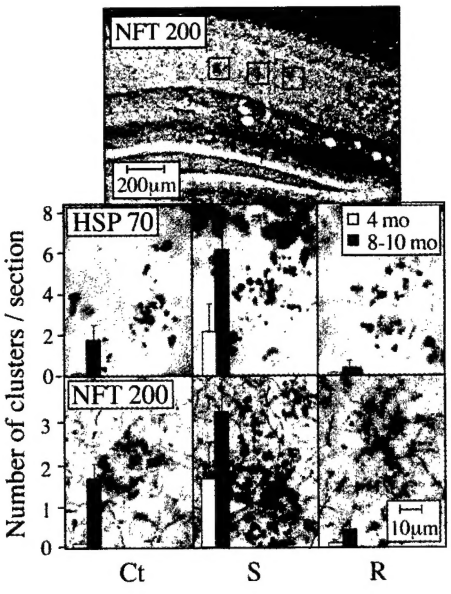

Fig. 5. Clustered neuronal fragments.
Shown are coronal brain sections from 8-10 month old control and transgenic mice following immunostaining of neurofilament 200 (NFT 200) or heat-shock protein 70 (HSP 70) with cresyl violet counter staining. Top: Low magnification image, in which gray-black clusters of neuronal fragments immunopositive for NFT 200 (surrounded by red frames) are apparent in the stratum radiatum layer of hippocampal CA1-3 regions (1.6-2.8 mm posterior to Bregma). Center and bottom rows: High magnification images of the framed regions, stained for HSP 70 and NFT 200, respectively. Clusters including over 10 neuronal fragments were counted in 3 sections from each mouse, 2 to 4 mm posterior to Bregma. Bars present counted clusters per section as average ± s.e.m. for 6 mice from each strain and age group (4 and 8-10 month old). Ct- control FVB/N mouse; S- AChE-S transgenic mouse; R- AChE-R transgenic mouse.

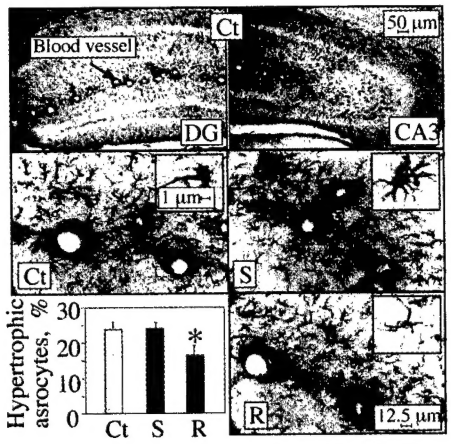

Fg. 6. Astrocyte reactivity.
Normal and reactive astrocytes were counted in the stratum lacunosum moleculare in hippocampal sections 2 to 4 mm posterior to Bregma, (3 from each of 6 mice in each strain). Shown is GFAP astrocyte labeling in coronal brain sections from 4 month old transgenic and control mice. Note that in normal astrocytes, only dendrites are stained and soma are pale or invisible, while reactive cells display highly immunoreactive soma and enhanced dendritic staining. Top: example low magnification micrographs of dentate gyrus (DG; left) and CA3 (right) hippocampal regions of control (Ct) mice. Center and bottom: high magnification images of stratum lacunosum moleculare from the hippocampal CA3 subregion from control, AChE-S (S) and AChE-R (R) mice. Insets: individual astrocytes stained for GFAP. Inset size bar equals 1 μm. Bar graph: percent reactive astrocytes out of the total counted astrocytes (average ± s.e.m. of n = 6 mice for each group). * $p<0.05$.

Task 2: To employ transgenic mouse models with up to 300-fold differences in peripheral AChE levels for demonstration of direct correlation between AChE dosage and protection from stress and chemical warfare agents and to test their responses to pyridostigmine administration.

Hypersensitivity to anti-AChE agents in seen in humans and in transgenic mice. Hypersensitivity to acetylcholinesterase inhibitors (anti-AChEs) causes severe nervous system symptoms under low dose exposure. In our study, three individuals were identified as being heterozygous for a 4 bp deletion in the extended *ACHE* promoter region. Proband 1, a 30-year-old woman, of Ashkenazi Jewish origin and no significant history of adverse drug responses, received a single oral dose of 30 mg pyridostigmine, a dose considered safe, which is given prophylactically under anticipation of chemical warfare. Within 1 hr, peripheral blood AChE fell to an almost undetectable level, increasingly severe muscle fasciculations developed, accompanied by intense headache, rhinnorea, lacrimation and frequent urination. These acute symptoms continued for 3 days, and resolved into a 5-day period of extreme fatigue, muscle weakness and general malaise. Proband 2, a 72-year old man, was hospitalized due to a multi-infarct dementia (MID), a condition caused by blood flow deprivation during a multi-focal stroke, which damages several brain regions. Proband 3 was a 39 year old woman of Turkish origin with a history of 3 spontaneous abortions performed under general anesthesia who suffered from excessive unexplained vomiting during a fourth pregnancy. The conclusion from these findings is that there are serious consequences of a constitutive overexpression of AChE. As other carrier members of the families of the probands were asymptomatic, one must conclude that the additional genetic and/or non-genetic factors affect the phenotype of the mutation.

This phenomenon was explored in experimental animals. AChE-overexpressing transgenic mice, unlike normal FVB/N mice, displayed anti-AChE hypersensitivity and failed to transcriptionally induce AChE production following exposure to anti-AChEs. Moreover, AChE transgenics were found to overexpress the stress-associated transcription factor HNF3ß in brain neurons. This work has appeared as Shapira et al. (2000) *Hum. Mol. Gen.* 9, 1273-1281.

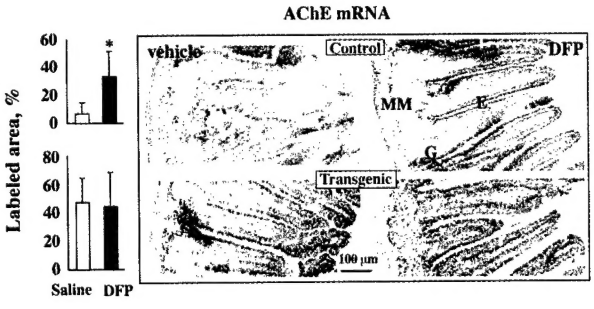

Fig. 1. Anti-AChE exposure induces trasncriptional AChE activation in the intestine of normal but not AChE-overexpressing transgenic mice. Presented are representative transverse ileum sections prepared from mice 2 hrs post-injection (i.p., 1 mg/Kg body weight) of DFP or saline. Columns present AChE-R mRNA signal quantified in similar micrographs as percentages of labeled area out of the villus area (means of 2-5 villi from 2-6 animals, 1-3 separate experiments for each animal ± s.d.). Asterisks denote statistically-significant differences (Scheffe's test, $p<0.01$). Note the drastic increase in AChE-R mRNA levels within the intestinal epithelium (E), the muscularis mucosa (MM) and the intestinal gland (G) regions of DFP-treated normal mice.

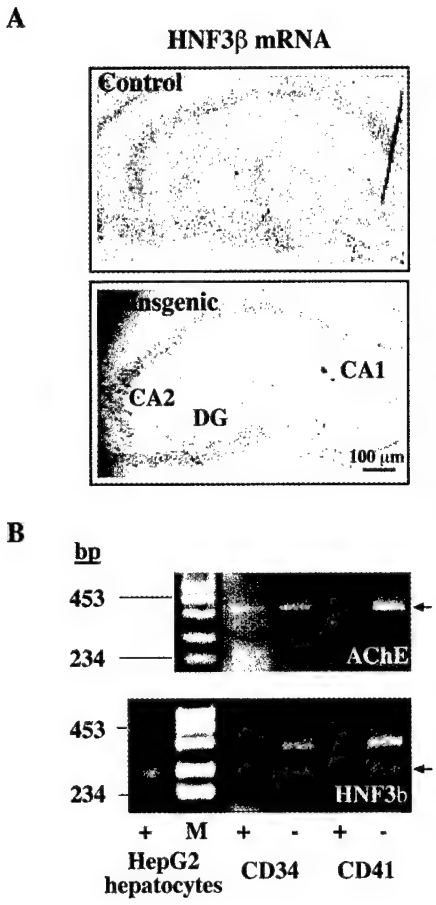

Fig. 2. HNF3β is elevated in the brain of hAChE-overexpressing mice and is co-expressed with AChE in diverse human hematopoietic lineages.

Hippocampal expression of HNF3β increases in transgenic mice. Representative micrographs of *in situ* hybridization experiments performed on FVB/N mouse saggital brain sections obtained from control and transgenic mice (n = 2 for each group). Shown are the CA1, CA2 and the dentate gyrus (DG) hippocampal structures, known to express AChE. Note the increase in HNF3β mRNA, (red signal) in both regions of transgenic mice.

B. Hematopoietic expression. Presented are RT-PCR products amplified using primers specific for the domain common to all human AChE splice variants (top) or for rat HNF3β (bottom), from RNA of human hematopoietic cells, sorted by flow cytometry from umbilical cord blood. Shown are products from CD34-positive progenitor cells ($CD34^+$), CD34-negative fully-committed white blood cells and megakaryocytes ($CD34^-$), mature megakaryocytes ($CD41^+$) and white blood cells ($CD41^-$). All express AChE and the expected ca. 300-bp HNF3β product (arrow; also produced in the liver carcinoma HepG2 cell line) accompanied by a ~400-bp unidentified product. M, size marker. No products appeared in control reactions containing no RT (data not shown).

Task 3: To develop RT-PCR tests in peripheral blood cells of model animals, and additional surrogate markers, for follow-up of responses and protection.

ARP, a peptide derived from acetylcholinesterase modulates blood cell composition under stress

Because we have now found that *in situ* hybridization coupled with confocal imaging gives a higher sensitivity than PCR, and, of course a spatial resolution that is impossible with PCR, we have chosen to use this method for analysis of mRNA on the cellular level.

Psychological stress induces rapid and long-lasting changes in blood cell composition, implying deterministic events in gene expression. Here, we report that 0.6 μM cortisol elevates "readthrough" acetylcholinesterase (AChE-R) mRNA levels in human $CD34^+$ hematopoietic progenitor cells. Nanomolar concentrations of ARP, a synthetic peptide corresponding to the unique C-terminal domain of AChE-R, effectively replaced both cortisol and stem cell factor in promoting expansion of progenitor cells into myeloid and megakaryocyte lineages *ex vivo*. Following forced swim stress a peptide reacting with anti-ARP antiserum accumulated in mouse blood. In stressed mice, exogenous ARP augmented hematopoietic expansion *ex vivo*. In contrast, antisense suppression of AChE-R mRNA blocked hematopoietic expansion, prevented accumulation of immunoeactive peptide in bone marrow, and suppressed hematopoietic responses. Our findings demonstrate a potent hematopoietic growth-factor activity for ARP, and point to a role for AChE in the hematopoietic response to stress that is attributable to the C-terminal peptide of AChE-R.

Table 1. The effect of various conditions on cultured cell count[a]

treatment	total viable cells	$CD34^+$ (early progenitors)	$CD33^+$ (early myeloids)	$CD33^+$ and $CD15^+$ (total myeloids)	$CD41^+$ (megakaryocytes)
control	61.0	1.0	7.2	12.3	30.9
ARP, 2 nM	570.0	87.2	329.0	530.0	42.3[b]
cortisol, 1.2 μM	80.0	13.0	45.0	73.0	10.1[b]
ASP, 2 nM	100.0	7.2	10.0	13.0	4.6[b]
SCF, 50 ng/ml	118.0	6.3	69.0	72.0	2.6[b]
AS1, 20 pM	81.2	1.4	2.4	5.0	30.9
PBAN, 2 nM	105.0	1.7	1.6	3.1	52.9

[a]Cultures were seeded at 50,000 cells/well. Shown are cells per culture x 10^{-3} on day 14; 1 of 3 reproducible experiments .

[b]These are also $CD34^+$ positive early cells with expansion potential.

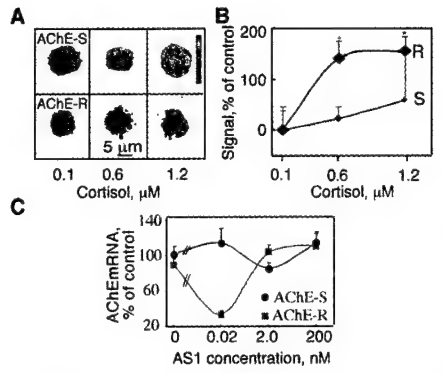

Fig. 1. Cortisol enhances and AS1 suppresses AChE-R mRNA in human CD34$^+$ cells A. Confocal images of human CD34$^+$ cells incubated for 24 hr with the noted cortisol concentrations following *in situ* hybridisation with cRNA probes for the noted transcripts. Right: pseudocolour-coded scale of staining intensity. B. Average ± standard deviation fluorescent signal measured in confocal projections (10-20 cells per group) of CD34$^+$ treated with cortisol and subjected to in situ hybridization with AChE-S and -R specific probes. Asterisks note statistically significant differences from control ($p<0.001$, Student's t test). C. Figure shows an inverted, selective, dose-dependent suppression of AChE-R mRNA in CD34$^+$ cells by AS1, an antisense oligonucleotide targeted to exon 2 in AChE mRNA.

Fig. 2. ARP accumulates in mouse serum following stress

A. Amino acid sequence of synthetic human ARP, starting at the splice site from the AChE core domain. β Strand was predicted using the GCG software package (University of Wisconsin). Hydrophobic residues are shown in red.

B. Immunoblot labeling with affinity-purified anti-GST-ARP antibodies. Lanes: recombinant (r) AChE-R from transfected COS cells mixed with synthetic ARP; rAChE-S (Sigma) mixed with synthetic AChE-S C-terminal peptide (ASP); serum from saline-injected (control) or stressed mouse 24 hr post-treatment.

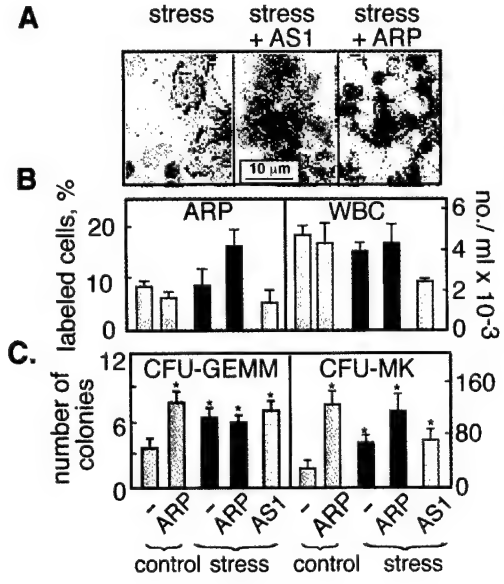

Fig. 3. ARP has short- and long-term effects on blood cells composition *in vivo* A. Bone marrow smears, 24 hr post-stress (with or without AS1 or ARP treatment) immunolabeled with anti GST-ARP antibodies. B. Left: No. of ARP-immunopositive cells in 5 fields of bone marrow smears (avg ± s.e.m. for 3 mice in each group). Right: White blood cell counts (at least 3 mice per group). C. 1 week clonogenic cultures of bone marrow cells derived from mice receiving the noted treatments.

Task 5: To employ the transgenic mouse models to test effects of sudden changes in AChE levels at all the above sites and functions.

Antisense prevention of neuronal damages following head injury in mice.

Closed head injury (CHI) is an important cause of death among young adults and a prominent risk factor for non-familial Alzheimer's disease. Emergency intervention following CHI should therefore strive to improve survival, promote recovery, and prevent delayed neuropathologies. We employed high-resolution non-radioactive *in situ* hybridization to demonstrate that a single intracerebroventricular (i.c.v.) injection of 500 ng 2'-O-methyl RNA-capped antisense oligonucleotide (AS-ODN) (Fig. 1) against acetylcholinesterase (AChE) mRNA blocks overexpression of the stress-related *readthrough* AChE (AChE-R) mRNA splicing variant in head-injured mice (Figs. 2,3). Silver-based Golgi staining revealed pronounced dendrite outgrowth in somatosensory cortex of traumatized mice 14 days post-injury that was associated with sites of AChE-R mRNA overexpression and suppressed by anti-AChE AS-ODNs (Fig. 4). Furthermore, antisense treatment reduced the number of dead CA3 hippocampal neurons in injured mice (Fig. 5), and facilitated neurological recovery as determined by performance in tests of neuro-motor coordination (Fig. 6). In trauma-sensitive transgenic mice overproducing AChE, antisense treatment reduced mortality from 50% to 20%, similar to that displayed by head-injured control mice (Fig. 7). These findings demonstrate the potential of antisense therapeutics in treating acute injury, and suggest antisense prevention of AChE-R overproduction to mitigate the detrimental consequences of various traumatic brain insults. This study has appeared as Shohami et al. (2000) *J. Mol. Med.* 78, 228-236.

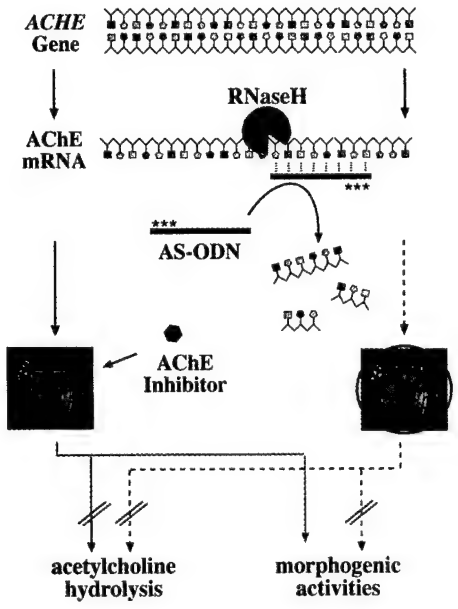

Fig. 1. The antisense strategy.
AChE displays two independent biological activities. Some activities depend on the hydrolysis of actylcholine; others, on non-enzymatic features of the protein that are presumed to mediate cell adhesion processes. Conventional pharmacology targets the enzyme's catalytic activity by either blocking access of substrate to the active site, or by inactivating the catalytic triad through the formation of non-regenerating enzyme intermediates. Commonly used therapeutic AChE inhibitors do not differentiate between AChE isozymes and do not inhibit the non-cataltyic activities of the protein In contrast, AS-ODNs targeting AChE mRNA, block *de novo* synthesis of AChE protein, thereby blocking both its catalytic and non-catalytic activities. The low cellular abundance of AChE mRNA, the high specificity of antisense agents, and the differential stabilities of the various alternative AChE-encoding mRNAs, allow the use of very low doses of ODNs to target specific ACHE isoforms.

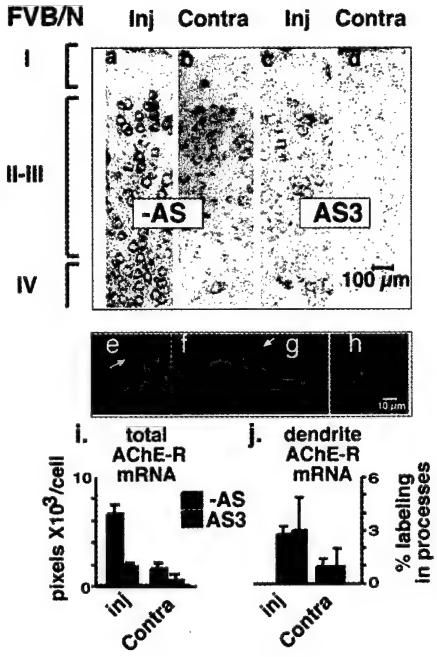

Fig. 2. Antisense oligonucleotides suppress trauma-induced accumulation of readthrough AChE-R mRNA in mouse brain. Male adult FVB/N mice were subjected to controlled closed head injury (left side of the head), injected after 1 hr into the left ventricle with either saline or 500 ng of the partially 2'O-methyl-protected 20-mer AS-ODN AS3 and sacrificed 14 days later. In situ hybridization was performed on 5 µm paraffin-embedded brain sections using a 50-mer biotinylated 2'-0-methyl cRNA probe targeted to intron I4 in mouse AChE-R mRNA. Staining was with Fast Red.

a-d. Brightfield digital photomicroscopy images of cortical layers I-IV from injured (a,c) and contralateral (b,d) hemispheres. Sites of AChE-R mRNA accumulation are indicated by red staining. Note the intense staining of cortical neurons on the injured vs. contralateral side of the brain and the pronounced bilateral reduction in staining following a single unilateral injection of AS3.

e-h. Shown are representative confocal images of neurons from somatosensory cortex. Note the massive accumulation of AChE-R mRNA in both somata and apical dendrites (white arrows). AS3 dramatically suppressed the accumulation of AChE-R mRNA in neurons from both the injured (e vs. g) and contralateral (f vs. h) hemispheres and in both subcellular compartments.

i-j. Densitometric analysis was performed on confocal images of cortical neurons as depicted in Fig. 2e-h. (i). Columns represent the total number and standard deviation of pixels/cell for 10-20 neurons in each group (left) or the percent of total pixels detected within dendrites (right) for the injured and contralateral hemispheres of mice injected with saline or AS3. Note the disproportionately high levels of AChE-R mRNA-specific fluorescence in neurons from the injured as compared to contralateral hemisphere, and the 4-6-fold reduced levels of staining in animals treated with AS3. The relative fraction of AChE-R mRNA appearing in dendrites was unmodified by antisense intervention (j).

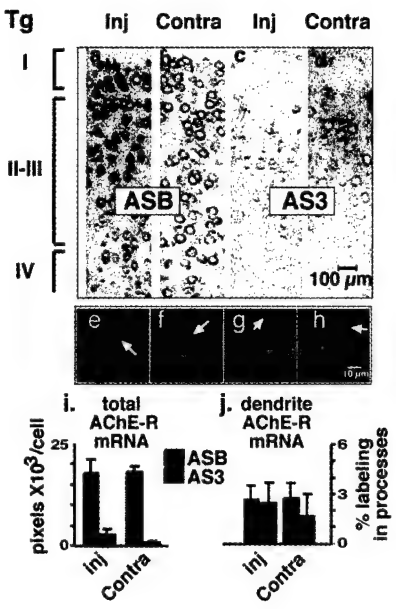

Fig. 3. Head trauma elicits pronounced bilateral accumulation of endogenous AChE-R mRNA in AChE transgenic mice. Experimental details were as in Fig. 1 except that saline was replaced with an irrelevant oligonucleotide , ASB (see Methods), as control. Note that transgenic mice, as opposed to control FVB/N mice display prominent overexpression of AChE-R mRNA in both the injured and non-injured brain hemispheres following head injury.

a-d. Brightfield microscopy. In brains from traumatized AChE transgenic mice with preexisting AChE excesses, similarly intense red hybridization signals were observed in cell bodies and dendrites of neurons from both the injured and contralateral hemispheres. AS3 effectively suppressed AChE-R mRNA expression in both hemispheres.

e-h. Confocal microscopy as in Fig. 1.

i-j. Densitometric analysis as in Fig. 1, note the more intense staining and higher dendrite localization of AChE-R mRNA in the contralateral hemisphere of transgenics as compared to FVB/N mice.

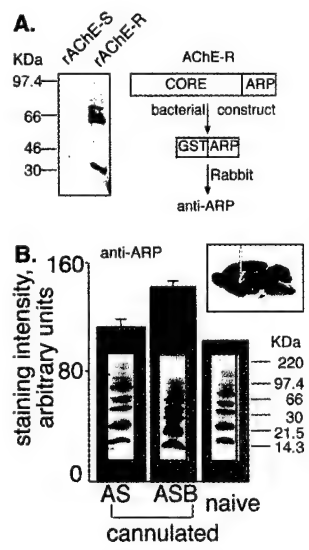

Fig. 4. AS3 suppresses trauma-induced overproduction of immunoreactive AChE-R protein. A. Selective immunodetection of the AChE-R protein. To selectively label the AChE-R variant, rabbits were immunized with a recombinant fusion protein of glutathione transferase (GST) with the 26 amino acid C-terminal peptide unique to AChE-R (ARP). The resultant antiserum, affinity purified to remove anti-GST antibodies, selectively labeled recombinant (r) AChE-R produced in transfected Cos cells (66-67 Kd) and an apparent AChE-R degradation product (~ 30 Kd), but not purified rAChE-S (Sigma, St. Louis) in immunoblot analysis.B. AS3 suppresses AChE-R labeling. Cortical homogenates from AChE transgenic mice injected icv with either AS3 or ASB on two consecutive days were subjected to SDS-PAGE on a 4-20% reducing gel and probed with anti-ARP antiserum. Shown are the corresponding chemiluminescence-labeled lanes as insets within a bar graph representing the summation of densitometric analyses of the six most prominent bands in each lane. Inset in the right-hand corner illustrates the position of the cannula. Columns represent avg ± SEM for homogenates from 6 AS3- and 4 ASB-treated mice, respectively. A single representative control, untreated, non-operated animal is shown (naive).

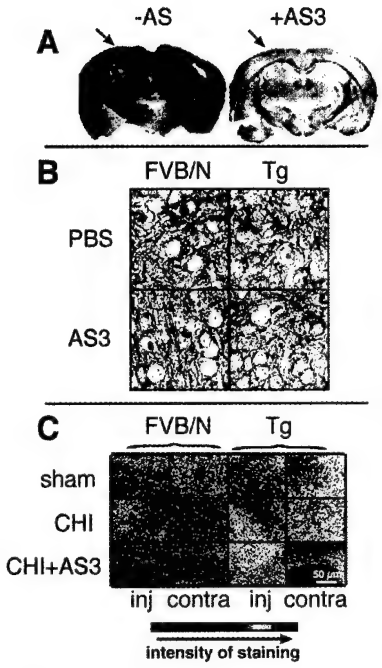

Fig. 5. Antisense treatment suppresses AChE-R mRNA and neurite growth and promotes neuron survival following head trauma.

A. Low magnification image of whole brain sections from head-injured FVB/N mice subjected to in situ hybridization as in Fig. 1A. Note that AChE-R mRNA is intensively expressed in the injured hemisphere (left), especially in the cortex, close to the site of injury (arrows). AS3 significantly suppressed AChE-R mRNA accumulation in both hemispheres.

B. Golgi staining was performed on brain sections from FVB/N or Transgenic (Tg) mice subjected to CHI and injected i.c.v. with either PBS or AS3. Shown are representative high magnification (x1000) images from layer IV of somatosensory cortex on the injured hemisphere 14 days following head injury. Note that AS3 treatment notably reduced the density of stained neurites in both FVB/N and transgenic mice.

C. Golgi staining performed on brain sections depicted in B was semi-quantified in sections from uninjured (sham) FVB/N or AChE transgenic (Tg) mice and from mice untreated (CHI) or treated with AS3 (CHI + AS3) following closed head injury. Presented are pseudocolor representations of cortical sections in which stained neurites appear red. Note the intense Golgi staining, representing high neurite density in cortex from the injured hemisphere of FVB/N mice and the higher intensity in transgenic mice. Red signal was significantly reduced in both FVB/N and Tg mice treated with AS3.

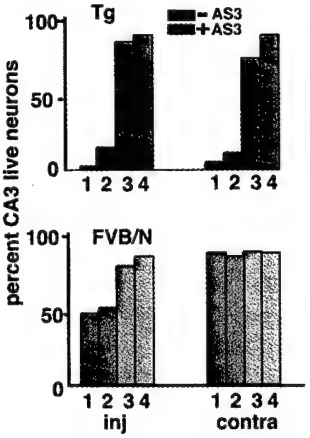

Figure 6. Live and dead neurons in the CA3 hippocampal region were counted in 2 consecutive sections from 4 control and 4 transgenic mice 14 days following closed head injury with or without antisense treatment. Overt neuronal cell death was identified by the presence of pyknotic black cell bodies. 150-200 cells were counted for each mouse. Columns represent the percent of live neurons counted for individual mice. Note the dramatic bilateral neuron loss suffered by transgenic as compared with FVB/N mice and the minimal neuron loss observed among antisense treated animals.

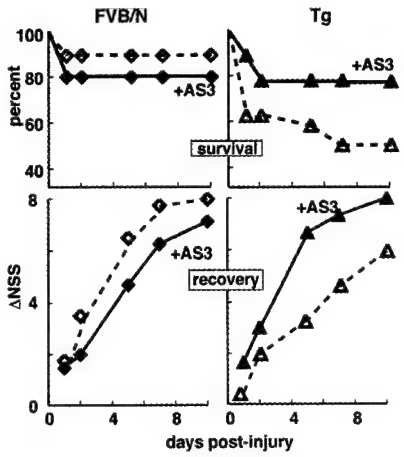

Fig. 7. Antisense treatment rescues survival and neurological recovery of injured mice.
Survival and neurological recovery of FVB/N and AChE transgenic mice were monitored following CHI. One hour following trauma, a neurological evaluation of the mice was taken using a graded balancing task of 2 and 3 cm wide beam crossing. Recovery was monitored at various time points post-trauma for each mouse. Presented are percentages of surviving mice (top) and average percent successes for surviving mice in the beam task (bottom) on the noted days following trauma. Note the high mortality and slow recovery of transgenic mice compared to controls and the improved outcome following a single AS3 treatment. Starting n = 20-24 mice per group.

Task 6: To delineate the protein partners through which AChE exerts non-catalytic signals which lead to delayed symptoms.

The C-terminal domain of AChE-R interacts with RACK1, a protein kinase C intracellular receptor of the WD family of proteins

To identify potential protein partners of the C-terminal domain of AChE-R, we utilized the Gal4 two-hybrid system, using as "bait" a peptide with the sequence of the C-terminal 53 amino acid residues of AChE-R. A human fetal brain two-hybrid cDNA library containing 10^7 independent clones was screened for interacting proteins.

Using the two-hybrid system for detection of AChE-R binding partners, we have discovered at least one pathway through which AChE-R can exert its intracellular signaling. In the yeast two-hybrid screen, we found that a C-terminal fragment of AChE-R interacts tightly with RACK1, a G protein homology WD domain protein that binds protein kinase C. Using brain extracts, we have further shown that RACK1 creates 66 KDa complexes refractory to SDS-PAGE with yet unidentified protein(s) in the stressed brain.

Fig. 1. Amino acid sequence ACHE-ARP1 used as bait for the two hybrid system. The first 26 amino acids belong to the AChE common domain and the underlined part belongs to the actual ARP-peptide.

PLEVRRGLRAQACAFWNRFLPKLLSAT<u>GMQGPAGSGWEEGSGSPPGVTPLFSP</u>

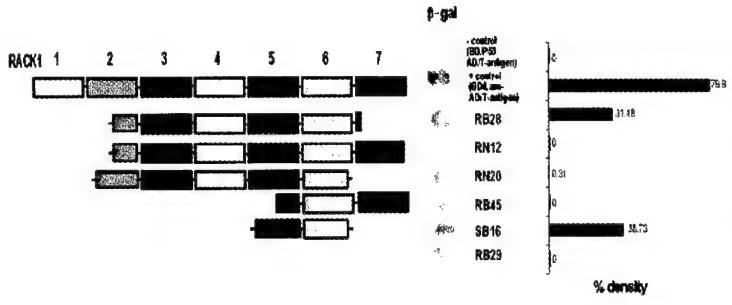

Fig. 2. Identification of AChE-R binding protein. All of the successful clones induced the WD domains 5,6 and 7, suggesting that this region in the RACK1 protein is both necessary and sufficient for AChE-R – RACK1 interaction. Amino acid sequence alignment of RACK1 with the sequence obtained from the two-hybrid positive clone shows close to 100% homology. Furthermore, only part of the protein was expressed, which narrowed our search to this part.

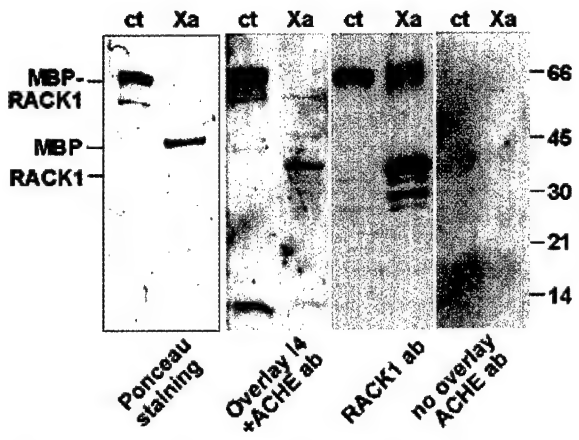

Fig. 3. Overlay assay for AChE-R-RACK1 binding.

Purified RACK1 samples were separated on a 4-20% denaturing polyacrylamide gel and blotted on an nitrocellulose membrane, which was stained with Ponceau S. Three identical strips were used for parallel experiments: one was overlaid with a homogenate of PC12 cells overproducing recombinant ACHE-I4 and developed with antibody to AChE N-terminus; second strip serving as a negative control underwent the same treatment but without I4 homogenate; and the third strip was developed with anti-RACK1 antibody to identify bands containing RACK1. Maltose binding protein served as an internal control for binding specificity. Note that AChE interacts with RACK1 either in fusion with MBP or alone, but not with MBP.

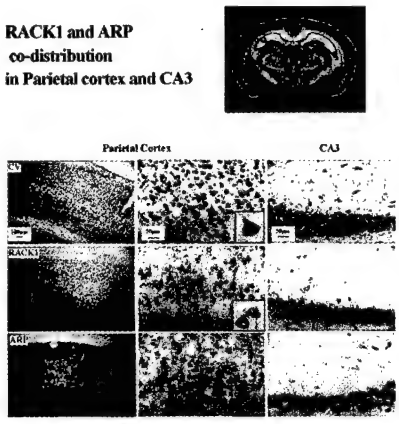

Fig. 4. Accumulation of RACK1 immunoreactive species in the post-stress mouse brain.

As AChE-R was implicated in long-term neuronal stress responses, we decided to test for neuronal expression of RACK1 and examine its level in the post-stress mouse brain. Immunohistochemical analyses with anti-RACK1 antibodies demonstrated neuronal expression of this protein. Immunoreactive RACK1 was clearly observed in the cytoplasm and proximal processes of pyramidal neurons, both in the mouse cortex and hippocampus. In particular, RACK1 expression was prominent in layers 3 and 5 of the frontal, parietal and piriform cortex and in regions CA1-3 of the hippocampus. A subset of these neurons also expresses AChE-R under acute psychological stress. Moreover, AChE-R expression like that of RACK1, is more pronounced in hippocampal CA1-3 neurons than in the dentate gyrus. Thus, RACK1 and AChE-R are co-expressed in large stress-responsive neuron populations.

Fig. 5. Distribution of AChE-R and RACK1 in mouse brain.

A. AChE-R and RACK1 display parallel neuronal distribution in the piriform cortex. To further explore the neuron populations expressing AChE-R and RACK1, adjacent sections from the same brains were immunolabeled with anti-RACK1 and anti-AChE-R antibodies. Piriform cortex neurons displayed co-distribution with these two antibodies, indicating a co-localization of RACK 1 and AChE-R.

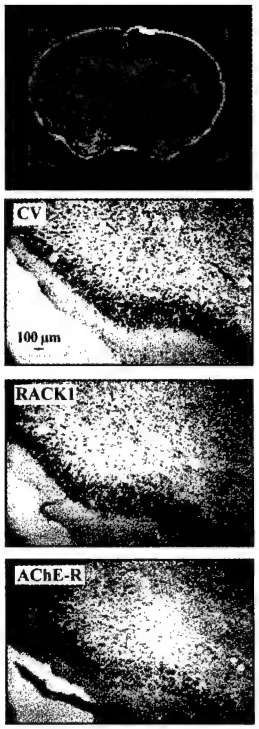

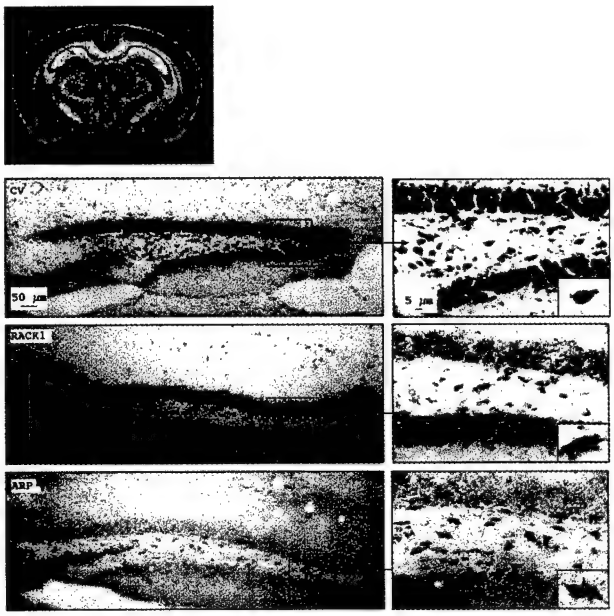

B. RACK1 and AChE-R display distinct distributions in the dentate gyrus. Unique distribution patterns were found for AChE-R and RACK1 in the hippocampal dentate gyrus, where RACK1 expression efficacy paralleled its expression in CA3, but where AChE-R's expression was considerably weaker than that of AChE-R. Intriguingly, single neurons of the hippocampal region that is enriched with stem cells that are capapble of proliferation at the adult phase display both AChE-R and RACK1.

Task 7: To develop tetracycline-inducible animal models in which AChE activity can be induced or antisense-suppressed at will.

The Tet-On Gene Expression Systems allow high-level, regulated gene expression in response to varying concentrations of tetracycline (Tc) or Tc derivatives such as doxycycline (Dox). In the Tet-Off System, gene expression is turned on in the *absence* of Tc or Dox. In contrast, gene expression is activated in the Tet-On System in the *presence* of Dox. The tet system uses the tetracycline resistance operon from *E. coli* to control gene expression in eukaryotic cells. The system is based on two regulatory elements derived from the tetracycline-resistance operon of the *E. coli* Tn10 transposon—the tetracycline repressor protein (TetR) and the tetracycline operator sequence (*tetO*) to which TetR binds. The gene to be expressed (in our case RZ or AS) is cloned into the pTRE2 "response" plasmid, which contains the $P_{hCMV*-1}$ promoter upstream of a multiple cloning sites (MCS). $P_{hCMV*-1}$ is a compound promoter consisting of the tetracycline-responsive element (TRE), which contains seven copies of *tetO*, and the minimal immediate early promoter of cytomegalovirus (P_{minCMV}). The second key component of the system is a "regulator" plasmid which expresses a hybrid protein known as the Tc-controlled transactivator (tTA). tTA is encoded by pTet-Off and is a fusion of the wild-type TetR to the VP16 activation domain (AD) of herpes simplex virus. tTA binds the tetO sequences which brings the VP16 activation domain into close proximity with the $P_{hCMV*-1}$ - and thereby activates transcription - in the absence of Tc. Thus, as Tc is added to the culture medium, transcription is turned off in a dose-dependent manner. The Tet-On System is based on the "reverse" TetR (rTetR), which differs from the wild-type TetR by four amino acid changes. When fused to the VP16 AD, rTetR creates a "reverse" tTA (rtTA) that activates transcription in the presence of Dox.

<u>Construction of Ribozyme (RZ) and Antisense (AS) expression cell lines and transgenic mice under the control of the Tet-on system</u>

DNA fragments encoding for 150 nt antisense (AS-AChE) RNA and 37 nt ribozyme (RZ-AChE) targeted to AChE mRNA were cloned into a plasmid vector under tetracycline controlled promoter (Fig. 1). Both AS and RZ are capable of destroying AChE mRNA in a sequence-specific manner. Non-selective effects over AChE-homologous proteins were prevented by positioning the binding sites for the AS and RZ at the AChE mRNA region encoding for the C-terminal sequence, which shows no homology to other genes in the GeneBank. However, this sequence is present in all AChE variants produced by 3'-alternative splicing. Moreover, it has previously been demonstrated in our lab that this site displays particular vulnerability to ribozyme degradation. *In vitro* synthesized RZ-AChE successfully cleaved an *in vitro* transcribed fragment of mouse AChE cDNA. Selection of individual stably transfected PC12-TetON clones resulted in the establishment of several (tet) AS-AChE and (tet) RZ-AChE cell lines. These displayed over 50% reduction in basal AChE level upon addition of the inducer doxycycline. More than one cell line of each type was selected to exclude the influence of the integration site. The relevant DNA constructs were futher injected into fertilized mouse eggs to yield transgenic pedigrees, which are currently being characterized. We intend to employ the identified partners in the *in vivo* conditional suppression models for studying the states and molecular mechanisms through which AChE variants confer their C-terminal specific morphogenic functions.

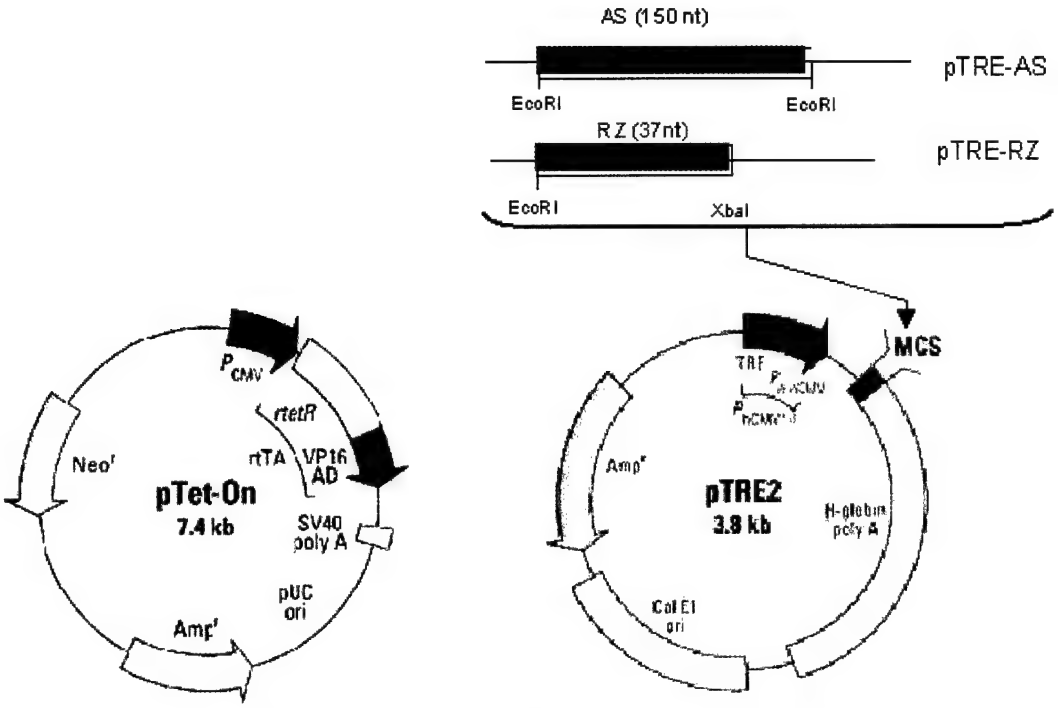

Fig. 1. Teracycline controlled expression of AChE ribozyme and antisense constructs. The gene to be expressed (in our case RZ or AS) is cloned into the pTRE "response" plasmid, which contains the $P_{hCMV*-1}$ promoter upstream of a multiple cloning sites (MCS). The second key component of the system is a "regulator" plasmid, which expresses a hybrid protein. When the hybrid protein is fused to the VP16 AD, it activates transcription in the presence of Dox.

Task 8: To continue the search for promoter sequence polymorphisms which lead to natural variations in human AChE levels and correlate them with responses to anti-ChEs.

A transcription-activating polymorphism in the *ACHE* promoter associated with acute sensitivity to anti-AChEs

Hypersensitivity to acetylcholinesterase inhibitors (anti-AChEs) causes severe nervous system symptoms under low dose exposure. In search of a direct genetic origin(s) for this sensitivity, we studied six regions in the extended 22 Kb promoter of the *ACHE* gene in individuals who presented adverse responses to anti-AChEs and in randomly-chosen controls (Figs. 1, 2). Two contiguous mutations, a T→A substitution, disrupting a putative glucocorticoid response element, and a 4-bp deletion abolishing 1 of 2 adjacent HNF3 binding sites, were identified 17 Kb upstream to the transcription start site. Allele frequencies for these mutations were 0.006 and 0.012, respectively, in 333 individuals of various ethnic origins, with a strong linkage between the deletion and the biochemically-neutral H322N mutation in *ACHE*'s coding region. Heterozygous carriers of the deletion included a proband who presented acute hypersensitivity to the anti-AChE pyridostigmine and another with unexplained excessive vomiting during a fourth pregnancy following 3 spontaneous abortions. Electromobility shift assays, transfection studies and measurements of AChE levels in immortalized lymphocytes as well as in peripheral blood from both carriers and non-carriers, revealed functional relevance for this mutation both *in vitro* and *in vivo* and showed it to increase AChE expression, probably by alleviating a competition between the 2 HNF3 binding sites (Fig. 3). Moreover, AChE-overexpressing transgenic mice failed to transcriptionally induce AChE production following exposure to anti-AChEs (Fig. 4). Our findings point to promoter polymophism(s) in the *ACHE* gene as dominant susceptibility factors for adverse responses to exposure to or treatment with anti-AChEs. This work has appeared as Shapira et al. (2000) *Hum. Mol. Gen.* 9, 1273-1281.

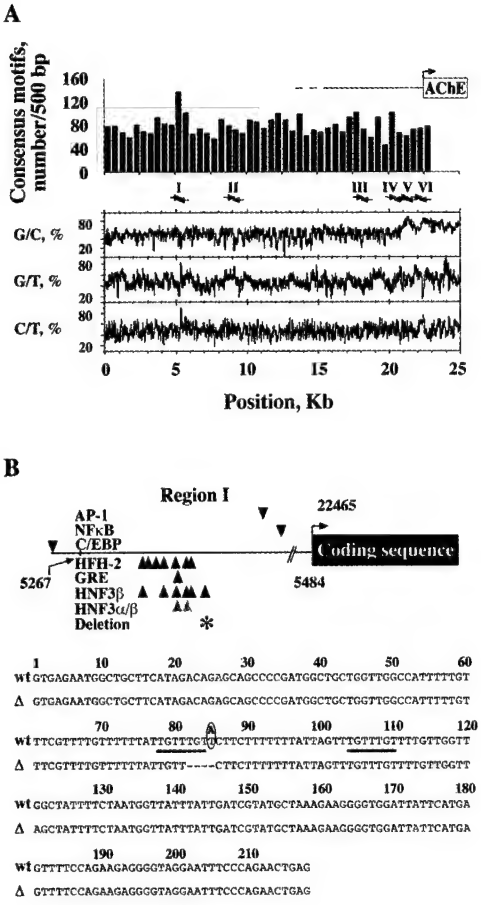

Fig. 1. *ACHE* promoter polymorphism in the hypersensitive proband I.

A. Selecting domains prone to effective polymorphism in the h*ACHE* upstream region. Top: Density of consensus motifs. Shown are cumulative numbers of consensus motifs in 500 bp regions along the af002993 cosmid reverse DNA sequence. Arrow above represents the *ACHE* transcription start site (nt. 22465 in the cosmid sequence. Bottom: Nucleotide pair patterns. Shown are percentages of the noted nucleotide pairs counted in 60 bp windows and 3 nucleotide shifts along the af002993 DNA. Peaks and troughs represent homogeneous sequences; arrow-delineated Roman numerals represent approximate positions of primer pairs designed to amplify the regions of interest. Note the high number of consensus motifs located in region I.

B. Characteristics of the polymorphic region I. Top: Consensus binding sites for transcription factors in region I. Presented (wedges) are approximate positions within region I of binding sites for the transcription factors designated on the left. Sites with complete consensus sequences as well as the GRE half-palindromic site, TGTTCT, were located using FindPatterns of the GCG software package and the MatInspector program. Grey wedges represent consensus sequences known to bind either HNF3α or HNF3β; asterisk designates the mutated binding site. First and last nucleotides of region I as well as the transcription start site are marked. Bottom: Region I sequence. Presented is the normal region I sequence (wt; the T/A substitution is circled) aligned with the mutant sequence allele carrying the 4-bp deletion (Δ); nucleotide 1 is 5267 in the af002993 cosmid reverse sequence. The two HNF3 consensus binding sites are underlined.

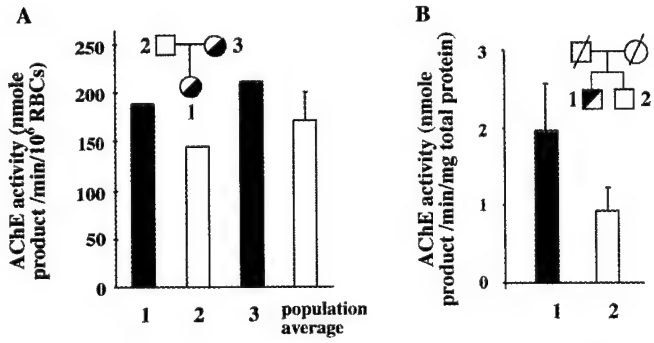

Fig. 2. Increased AChE activity levels in blood from carriers of the 4-bp deletion.

Red blood cell (RBC) AChE levels in proband I, family and control individuals. Shown is proband I's pedigree, with the proband and her mother heterozygous for the 4-bp deletion (half-filled circles, see below).

Columns present means of triplicate measurements of specific AChE activity in RBC fractions from members of the proband's family. For the control population, presented are average ± s.d. (n = 20).

B. AChE levels in EBV-transformed lymphoblasts from a deletion-carrying individual and his non-carrier brother. Presented are AChE activity levels in homogenates of EBV-transformed lymphoblast cell lines established from peripheral blood of proband II, a carrier of the 4-bp deletion and his non-carrier brother, as depicted in the pedigree. Shown are averages and standard deviations of AChE levels in 7 separate homogenates normalized to total protein measured with the Bio-Rad $^{D}_{C}$ protein assay kit (Bio-Rad, Hercules, CA).

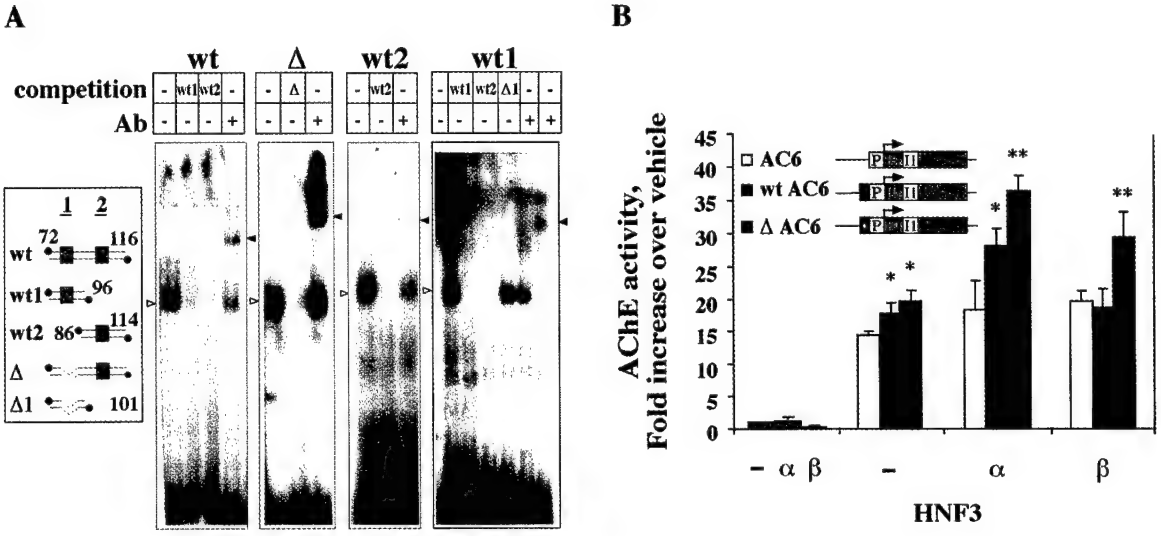

Fig. 3. Functional characterization of region I deletion.

Gel mobility shift assays reveal differential HNF3β affinities for the two normal and one mutant region I sites. EMSA gel images show shifted probe bands (open wedges), as well as supershifted bands (filled wedges; Ab, antibody in a 1:1000 or 1:500 dilutions for wt1 in the two right lanes, respectively). Probes used for each assay are designated above the respective table.

Inset: Presented are the 5' end-labeled (filled circles) double-stranded oligodeoxynucleotides tested for the binding capacities of the normal and mutant domains in region I. Numbers are as in Fig. 1B bottom. Putative HNF3-binding sites on these probes, are boxed and numbered.

B. Differences in transcription activation abilities of the normal and mutant region I sequences. Inset: Presented are AChE expression constructs used for transfection experiments. Designated are region I normal and variant fragments (dark grey boxes; deletion dotted), the minimal promoter (P), intron 1 (I1), and numbered exons (E). Columns show fold increase values of AChE activities in COS cells transfected with AC6 (white bars), wtAC6 (black bars) or the ΔAC6 vector (grey bars), either alone or together with constructs encoding the designated rat transcription factors, both under control of the rat phosphoglycerate kinase-1 promoter. Cross-hatched columns represent transfections with constructs encoding the transcription factors alone. Shown are average specific AChE activities in cell lysates from 5 transfection experiments as

compared with those of cells treated with Lipofectamine alone, in the same set (-). Asterisks mark activities significantly different ($p < 0.01$; Scheffe's test) from those in lysates of cells transfected with AC6 alone. Double asterisks mark an additional significant difference between the wild type and mutant groups.

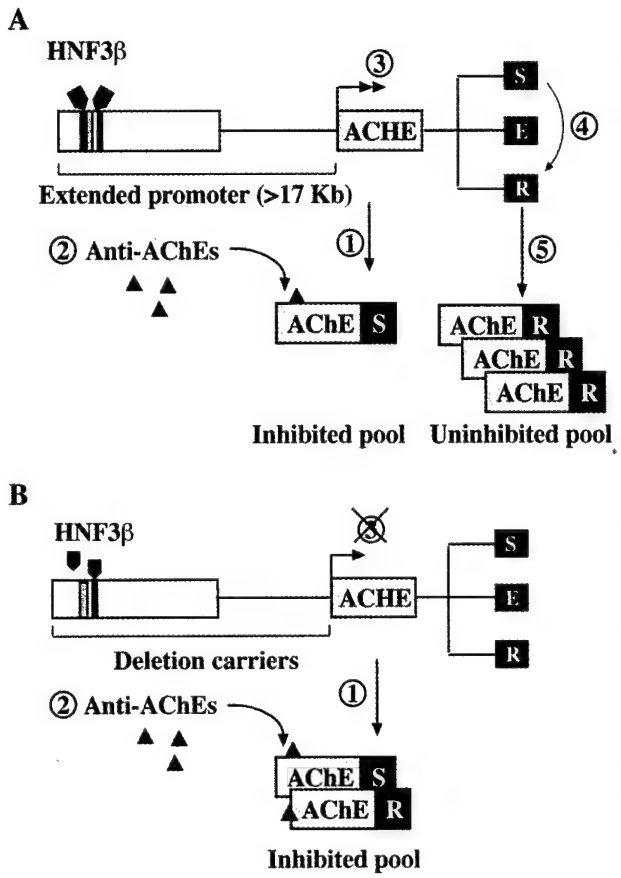

Fig. 4. Constitutive AChE overproduction impairs the feedback response to anti-AChEs.

A. Transcriptional AChE overproduction and alternative splicing confer protection by increasing scavenging capacity. The scheme shows the *ACHE* gene and its extended promoter, with the 2 adjacent HNF3β binding sites (black boxes) and an additional binding site for the glucocorticoid receptor (diagonally-striped box). Numbered steps display the tentative pathway of anti-AChEs responses, as follows: (1) under normal conditions, the major transcript in both the central and peripheral nervous systems is the synaptic variant (AChE-S); hematopoietic cells express preferentially the GPI-anchored AChE-E isoform. (2) Anti-AChEs bind to the active site in the core domain common to all AChE isoforms. This elevates acetylcholine levels, causes cholinergic excitation and thus mimics stress conditions. (3) Cholinergic excitation causes enhanced transcription, possibly via the c-fos transcription factor which is thought to activate AChE transcription under stress. (4) Newly transcribed AChE mRNA is produced. Alternative splicing preference is for production of AChE-R mRNA instead of AChE-S mRNA. (5) Consequently, a new pool of uninhibited, hyper-sensitive AChE-R molecules accumulates in the tissue, increasing its inhibitor scavenging capacity.

B. Deletion carriers may fail to respond by transcriptional overproduction due to constitutive AChE accumulation. With one HNF3β site missing, the remaining site is more effectively activated by the transcription factor, causing constitutive AChE overproduction (1). This leads to AChE accumulation, of which at least some is AChE-R. Anti-AChEs (2) would therefore inhibit preferentially the more sensitive AChE-R variant, leaving some enzyme (possibly AChE-S, or AChE-E in the case of hematopoietic cells) uninhibited. However, the feedback response (3) is impaired. This is apparently crucial for replenishing the enzyme pool to an extent sufficient to suppress acute post-exposure symptoms.

Task 9: To expedite transgenic models for production from milk of recombinant human AChE, as a potential scavenger.

The stress-associated AChE-R displays distinct inhibitor sensitivities

Establishment of anti-cholinesterase therapies for Alzheimer's disease revealed several levels of responsiveness, but the molecular origin of such diversity is unclear. Here, we report differences between the anti-cholinesterase sensitivities of the 3 C-terminally distinct human acetylcholinesterase (AChE) isoforms produced by alternative splicing from the original transcript of the single *ACHE* gene: the major "synaptic" AChE-S, the "erythrocytic" AChE-E and the stress-associated "readthrough" AChE-R. The 3 AChE variants display distinct electrophoretic mobilities and are immunochemically distinguishable by region-specific antibodies. Unlike AChE-S and AChE-E, the C-terminal sequence of AChE-R does not support dimerization or coupling to a glylcophosphatidoinositide moiety. When produced in transgenic mice, AChE-R remained low salt-soluble and monomeric (Figs. 1, 2 and Table 1). *In vitro* inhibition curves indicated significantly higher sensitivities of AChE-R than those of recombinant AChE-S or purified AChE-E for the organophosphates diisopropylfluorophosphonate and paraoxon, as well as for the pseudoirreversible carbamate, rivastigmine (Exelon™) (Fig. 3 and Table 2). In contrast, all AChE isoforms were similarly sensitive to tacrine (Cognex™) and donepezil (Aricept™); and AChE-R was 4-fold less sensitive than AChE-S to the peripheral site inhibitor, propidium. Transgenic C-terminally truncated "core" AChE-C protein presented similar inhibitor sensitivities to those of AChE-R. *In vivo*, somatosensory cortex extracts from AChE-R transgenics and acutely stressed mice had larger proportions of monomeric enzyme and displayed higher sensitivity to rivastigmine, but not donepezil, as compared to strain- and age-matched control mice and AChE-S transgenics (Fig. 4). Our findings demonstrate previously unsuspected differences among drug responses of alterntaive AChE isoforms and predict stress-related and drug-induced changes in the responsiveness to certain anti-cholinesterases.

Table 1. Production of human AChE variants in milk of transgenic mice

Three DNA constructs encoding alternative isoforms of recombinant human AChE (Sternfeld et al., 1998) were used for introduction into transgenic mouse pedigrees. Milk of females from each of these lines was collected from nursing mice 7 days post partum. Milk and muscle hydrolysis rates of ATCh were determined spectrophotometrically using a modification of Ellman's assay (Andres et al., 1997), in the presence or absence of 10-5 M of the selective BuChE inhibitor iso-OMPA. Activity is expressed as nmol ATCh hydrolyzed/min/ml milk or /mg protein.

promoter	protein	total milk activity	milk activity[a]	muscle activity[a]
hp	AChE-S	3.9 ± 0.2	0.5 ± 0.2	35.9 ± 1.3[b]
cmv	AChE-C	13 ± 2	7.1 ± 0.6	352 ± 59[c]
cmv	AChE-R (line 45)	11 ± 1	7.4 ± 0.3	190 ± 23[d]
cmv	AChE-R (line 70)	121 ± 4	115 ± 4.0	2700. ± 250.[d]
FVB/N control		4.1 ± 0.4	0.5 ± 0.3	7.6 ± 0.6[d]

[a]Activity determined in the presence of 10^{-5} M iso-OMPA.

[b]Data taken from Andres et al. (1997)

[c]Values from 2 male mice (personal communication from T.Evron, Jerusalem).

[d]Data taken from Sternfeld et al. (Sternfeld et al., 1998).

Table 2. K_i values (_M) of human AChE variants for peripheral and active site inhibitors
The source of AChE-R was transgenic mouse milk and of AChE-S and AChE-E, the commercial recombinant and erythrocyte enzymes. The experiments were performed in triplicate.

inhibitor	AChE-R	AChE-S	AChE-E	AChE-R/ AChE-S
rivastigmine	2.8 ±0.2	24.5 ± 3.3	16.6 ± 0.3	0.11
paraoxon	0.032 ± 0.002	0.18 ± 0.01	0.088 ± 0.005	0.17
donepezil	0.0098 ± 0.0011	0.018 ± 0.002	0.19 ± 0.001	0.54
DFP	0.048 ± 0.004	0.12 ± 0.03	0.18 ± 0.04	0.40
tacrine	0.034 ± 0.002	0.040 ± 0.003	0.046 ± 0.007	0.85
pyridostigmine	0.071 ± 0.005	0.071 ± 0.004	0.10 ± 0.03	1.00
propidium	1.3 ± 0.2	0.32 ± 0.04	2.9 ± 0.6	4.1

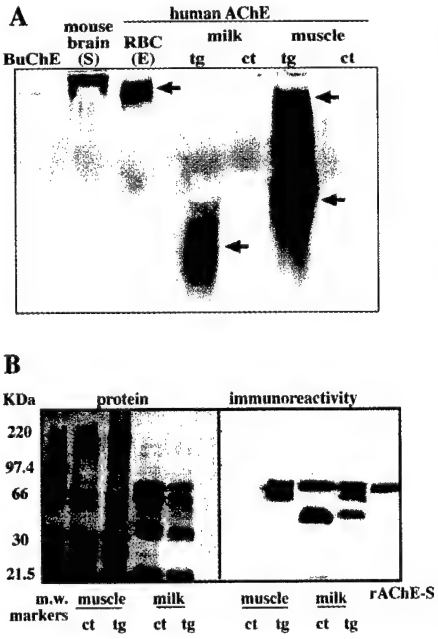

Fig. 1. AChE-R transgenic mice produce distinct AChE variants in muscle and milk
A. Activity gel. Samples of cholinesterases (with activity of ΔA_{405} of approx. 0.4/min in the Ellman's assay) were electrophoresed on non-denaturing polyacrylamide gels. Cholinesterase activity was detected using the Karnovsky method. Shown are (from left to right): human serum BuChE; AChE-S from transgenic mouse brain; AChE-E from erythrocytes; milk and muscle extracts from AChE-R transgenic and control mice. Upper bands (upper arrows) denote slowly migrating AChE-E. Lower bands (lower arrows) denote AChE-R. The different mobilities are probably due to different post-translational processing.
B. Immunodetection of recombinant human AChE in milk and muscle of transgenic mice. Right: Immunoblot; samples of milk and muscle extracts (40 µg of total protein) from AChE-R transgenic and control FVB/N mice, and purified recombinant AChE-S (6 I.U.) were subjected to 8% SDS-PAGE and blotted onto nitrocellulose filters. After blocking, the blot was reacted with monoclonal antibodies raised against denatured AChE-C (core) and then with horseradish peroxidase-conjugated goat anti-mouse IgG and subjected to chemiluminescent detection. Two immunoreactive bands (72 and 54 KDa) appear both in transgenic and non-transgenic milk. The upper band, markedly stained by the Ponceau, co-migrates with mouse serum albumin which is abundant in mouse milk. However, a 62 KDa band, the predicted size of the AChE-R protein, appears in the milk and muscle of AChE-R transgenic, but not control mice. In the transgenic muscle, an additional immunopositive band of 70 KDa was detected, not found in non-transgenic muscle. This band most likely reflects muscle-specific production of AChE. Left: Ponceau staining of the proteins on the nitrocellulose filter.

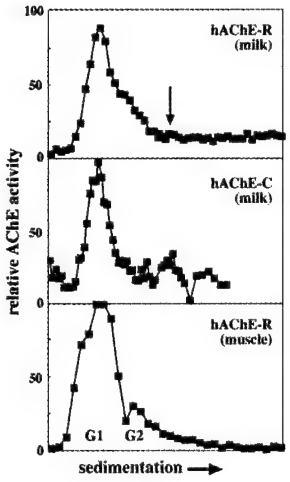

Fig. 2. Sedimentation profiles of variant AChEs from milk and muscle of female transgenic mice

Presented are one of 4 replicate sedimentation profiles in 5-20% sucrose gradients of AChE activities from milk and whole muscle extract from mice expressing the AChE-R trangene and of milk from mice expressing AChE-C. All sedimentation profiles were aligned with bovine catalase as a sedimentation marker (11.4 S), whose position is indicated in the upper panel. Note the prominent peak of the AChE-R monomer (G1), in milk of transgenics expressing either AChE-R or AChE-C; the similar sedimentation properties of AChE-R and AChE-C are compatible with the two monomers differing only by a short, hydrophilic sequence. An additional shoulder of AChE-E dimers (G2), is detectable in muscle from AChE-R transgenics.

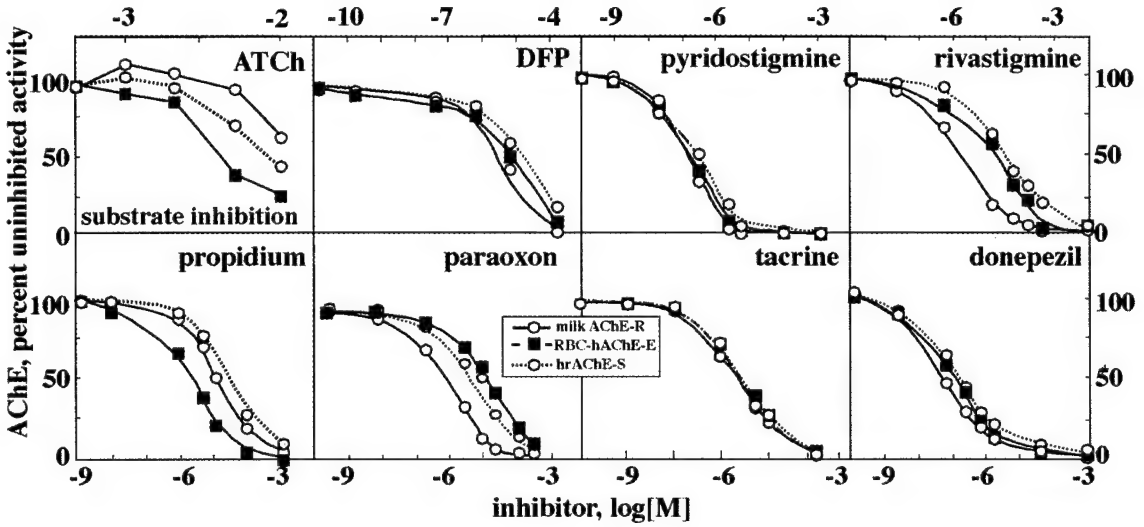

Fig. 3. AChE from transgenic AChE-R mouse milk displays high sensitivity to inhibitors

AChE from the milk of AChE-R transgenic mice, human erythrocytes (RBC-hAChE-E) and human recombinant AChE-S (hrAChE-S) were pre-incubated for 10 min with the indicated concentrations of inhibitors in Ellman's reagent and AChE activity was measured. Data are presented for each AChE isoform as percent of uninhibited activity. Note that milk AChE-R, as expressed in AChE-R transgenic mice (filled squares), is more sensitive to the organophosphates DFP and paraoxon and to the carbamate inhibitor rivastigmine than are the other AChE variants; AChE-R displays the same sensitivity as AChE-S and AChE-E to the carbamate pyridostigmine and tacrine, and is less sensitive than AChE-S to propidium.

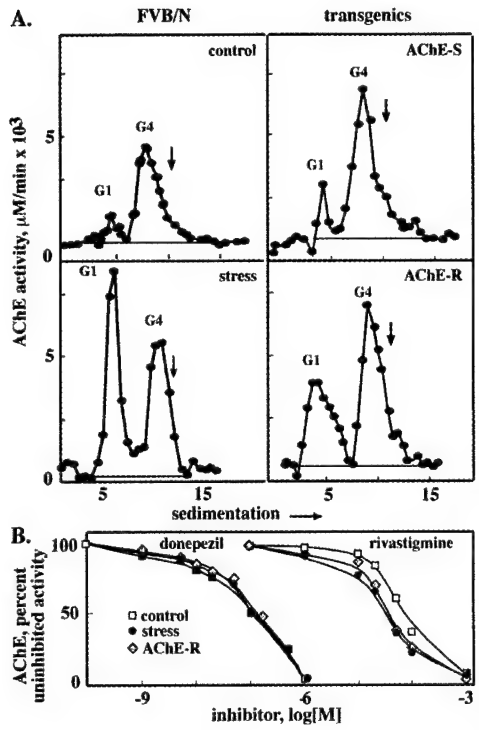

Fig. 4. Transgenic- and stress-induced alterations in brain AChE sedimentation profiles and inhibitor sensitivities

A. Shown are one of four sedimentation patterns of catalytically active AChE from the somatosensory cortices of untreated and 90 min post-stress FVB/N mice and from untreated AChE-S and -R transgenic mice. The total AChE activity of the control preparation was 0.97 ± 0.19; for the stressed group, 1.12 ± 0.16; for the AChE-S transgenics, 1.48 ± 0.34; and for the AChE-R transgenics, 1.36 ± 0.18 mmol/min/mg wet tissue weight. The G1:G4 ratios for these preparations, caclulated from the areas under the peaks and above the lines constructed below them, are: control, 0.14; stress, 1.05; AChE-S, 0.12; and AChE-R, 0.65. B. Shown are inhibition curves of pooled somatosensory cortex homogenates from 4 mice, in each case, of the above model systems (control and stressed FVB/N mice and AChE-R transgenics). Inhibition was with increasing doses of donepezil and rivastigmine. Note the increased sensitivity to the latter in experimental, as compared to control, samples.

Key research accomplishments

- Excess AChE-R attenuates but AChE-S intensifies neurodeterioration correlates
- Transgenic mice that overexpress ACHE are hypersensitive to anti-AChE agents.
- ARP, a peptide derived from acetylcholinesterase modulates blood cell composition under stress
- Antisense prevention of neuronal damages following head injury in mice.
- The C-terminal domain of AChE-R interacts with RACK1, a protein kinase C intracellular receptor of the WD family of proteins
- Progress toward a tetracycline-inducible animal model for the induction or antisense suppression of AChE activity.
- A transcription-activating polymorphism in the *ACHE* promoter associated with acute sensitivity to anti-AChEs
- The stress-associated AChE-R displays distinct inhibitor sensitivities
- Preparation of antibodies directed at the AChE Readthrough Peptide (ARP)
- Involvement in acquired and inherited diseases of polymorphisms in the extended promoter region of the human *ACHE* gene.

Reportable outcomes

Publications

- Shapira, M., Grant, A., Korner, M., and Soreq, H. (2000) Genomic and transcriptional characterization of the human ACHE locus indicates complex involvement with acquired and inherited diseases. Isr. Med. Assoc. J., 2, 470-473.
- Shapira, M., Grant, A., Korner, M., and Soreq, H. (2000) Human acetylcholinesterase gene expression is controlled by an exceptionally long stress-responding promoter. Ital. J. Psych. Behav. Sci. (in press).
- Shapira, M., Livny, N., Bosgraaf, L., Grisaru, D., Grant, A., Korner, M., Tur-Kaspa, I. Ebstein, R. and Soreq, H. (2000). A transcription-activating polymorphism in the ACHE promoter associated with acute sensitivity to anti-cholinesterase. Hum. Mol. Genet., 9, 1273-1281.
- Shohami, E., Kaufer, D., Chen, Y., Cohen, O., Ginzberg, D., Melamed-Book, N., Seidman, S., Yirmiya, R. and Soreq, H. (2000). Antisense prevention of neuronal damages following head injury in mice. J. Mol. Med., 78, 228-236.
- Soreq, H. and Seidman, S. (2000). Antisense approach to anticholinesterase therapeutics. Isr. Med. Assoc. J., 2, 81-85.
- Soreq, H. and Seidman, S. (2000). Antisense approach to isoform – specific blockade of acetylcholinesterase. In: Antisense Drug Technology: Principles, Strategies and Applications. S. T. Crooke, Ed. Marcel Dekker, Inc., Carlsbad, CA.
- Sternfeld, M. and Soreq, H., (2000) Acetylcholinesterase variants in mammalian stress: catalytic short-term and structural long-term roles. In press in: Mol. Genet. Mental Disorders, M. Briley, Ed.
- Sternfeld, M., Shoham, S., Klein, O., Flores-Flores, C., Evron, T. Idelson, G.H., Kitsberg, D., Patrick, J.W. and Soreq, H. (2000). Excess "readthrough" acetylcholinesterase attenuates but the "synaptic" variant intensifies neurodeterioration correlates. Proc. Natl. Acad. Sci. USA, 97, 8647-8652.
- Grisaru, D., Deutsch, V., Shapira, M., Sternfeld, M., Melamed-Book, N., Kaufer, D., Galyam, N., Lessing, J.B., Eldor, A. and Soreq, H., ARP, a peptide derived from acetylcholinesterase modulates blood cell composition under stress (submitted for publication).
- Salmon, A.Y., Ginzberg, D., Sternfeld, M., Mor, I., Glick, D. and Soreq, H., The stress-associated " readthrough" acetylcholinesterase variant displays distinct inhibitor sensitivities (submitted for publication).

Awards

Israel Ministry of Health, to Hermona Soreq, for excellence in research.

Degrees obtained

Daniela Kaufer, Ph.D., Hebrew University of Jerusalem, "The Molecular mechanisms underlying stress responses in the mammalian brain"

Nilli Galyam, M.Sc., Hebrew University of Jerusalem, "Neuronal and hematopoietic consequences of antisense acetylcholinesterase suppression".

Nadav Livny, M.Sc., Hebrew University of Jerusalem, "Genetic and epigenetic contributions toward anticholinesterase insults".

Nelly Gluzman, M.Sc. Hebrew University of Jerusalem, "Site-directed mutagenesis approach to drug interactions of human cholinesterases".

Tools for evaluation of neuropathologies

Transgenic animal models, currently under evaluation as a model for Alzheimer's disease, laboratory of S. Brimijoin, Mayo Clinic Foundation, Rochester, MN.

Anti-AChE-R antibody, currently under evaluation for analysis of Alzheimer's disease pathology in laboratory of M. Mesulam, Northwestern University School of Medicine, Chicago, IL.

Informatics

The 22 Kb upstream sequence of the human *ACHE* gene (GeneBank accession no. af002993).

Funding applied for, based on work supported by this grant

US-Israel Binational Science Foundation, grant 1999/115.

Research opportunities resulting from work on this grant

Daniela Kaufer, fellowship from Human Frontiers, at Stanford University Department of Biological Sciences

Michael Shapira, post-doctoral application to Stanford University, Department of Genetics.

Conclusions

Accumulated findings implicate genetic polymorphism and recently described regulatory processes that control expression of the *ACHE* gene in unexpected responses to AChE inhibitors. In particular, induction of a prolonged and exaggerated *ACHE* expression, associated with both immediate and long-term changes in acetylcholine metabolism following acute psychological stress, closed-head injury (itself, a known AD risk factor) and exposure to AChE inhibitors. All of these insults elicit rapid, transient excitation of cholinergic neurons in the CNS. Such excitation activates a feedback response that dramatically up-regulates AChE production. This response causes, within one hour and for at least several days, a beneficial calming of brain hyperactivity by suppression of the increased acetylcholine levels. However, studies with AChE-transgenic mice suggest that excesses of the AChE protein in neurons can also cause late-onset limitation of dendrite branching and depletion of dendritic spines (i.e. impaired networks) in cortical pyramidal neurons. This leads to progressively impaired performance in tests of memory and muscle strength. At least some of the delayed phenomena induced by AChE excess are caused by the AChE protein *per se*, independently of its hydrolytic activity.

The biomedical and environmental implications of human AChE research indicate that genomic polymorphisms in the coding sequence and/or promoter of the *ACHE* gene (and possibly additional loci) may modulate individual responses to AChE inhibitors in a complex and yet not fully predictable manner, affecting both the nervous and the hematopoietic systems. Recent cosmid sequencing and genotyping efforts have revealed novel polymorphisms in the *ACHE* upstream promoter sequence. Such polymorphisms can alter *ACHE* expression and/or properties, affecting both short- and long-term manifestations of cholinergic functions in a manner that may increase the risk for neurodegenerative disease due to physical, chemical or psychological insults.

References

Alber R, Sporns O, Weikert T, Willbold E, Layer PG. Cholinesterases and peanut agglutinin binding related to cell proliferation and axonal growth in embryonic chick limbs. Anat Embryol Berl 1994; 190:429-38.

Allderdice PW, Gardner HA, Galutira D, Lockridge O, LaDu BN, McAlpine PJ. The cloned butyrylcholinesterase (BCHE) gene maps to a single chromosome site, 3q26. Genomics 1991; 11:452-454.

Andres C, Beeri R, Friedman A, et al. Acetylcholinesterase-transgenic mice display embryonic modulations in spinal cord choline acetyltransferase and neurexin Ibeta gene expression followed by late-onset neuromotor deterioration. Proc Natl Acad Sci U S A 1997; 94:8173-8.

Appleyard ME. Secreted acetylcholinesterase: non-classical aspects of a classical enzyme. Trends Neurosci 1992; 15:485-90.

Beeri R, Andres C, Lev Lehman E, et al. Transgenic expression of human acetylcholinesterase induces progressive cognitive deterioration in mice. Curr Biol 1995; 5:1063-71.

Beeri R, Gnatt A, Lapidot Lifson Y, et al. Testicular amplification and impaired transmission of human butyrylcholinesterase cDNA in transgenic mice. Hum Reprod 1994; 9:284-92.

Beeri R, Le Novere N, Mervis R, et al. Enhanced hemicholinium binding and attenuated dendrite branching in cognitively impaired acetylcholinesterase-transgenic mice. J Neurochem 1997; 69:2441-51.

Birikh KR, Berlin YA, Soreq H, Eckstein F. Probing accessible sites for ribozymes on human acetylcholinesterase RNA. RNA 1997; 3:429-37.

Chatonnet A, Lockridge O. Comparison of butyrylcholinesterase and acetylcholinesterase. Biochem J 1989; 260:625-34.

Coyle JT, Price DL, DeLong MR. Alzheimer's disease: a disorder of cortical cholinergic innervation. Science 1983; 219:1184-1190.

Donger C, Krejci E, Serradell AP, et al. Mutation in the human acetylcholinesterase-associated collagen gene, COLQ, is responsible for congenital myasthenic syndrome with end-plate acetylcholinesterase deficiency (Type Ic). Am J Hum Genet 1998; 63:967-75.

Dupree JL, Maynor EN, Bigbee JW. Inverse correlation of acetylcholinesterase (AChE) activity with the presence of neurofilament inclusions in dorsal root ganglion neurons cultured in the presence of a reversible inhibitor of AChE. Neurosci Lett 1995; 197:37-40.

Ehrlich G, Ginzberg D, Loewenstein Y, et al. Population diversity and distinct haplotype frequencies associated with ACHE and BCHE genes of Israeli Jews from trans-Caucasian Georgia and from Europe. Genomics 1994; 22:288-95.

Ehrlich G, Patinkin D, Ginzberg D, Zakut H, Eckstein F, Soreq H. Use of partially phosphorothioated "antisense" oligodeoxynucleotides for sequence-dependent modulation of hematopoiesis in culture. Antisense Res Dev 1994; 4:173-83.

Ehrlich G, Viegas Pequignot E, Ginzberg D, Sindel L, Soreq H, Zakut H. Mapping the human acetylcholinesterase gene to chromosome 7q22 by fluorescent in situ hybridization coupled

with selective PCR amplification from a somatic hybrid cell panel and chromosome-sorted DNA libraries. Genomics 1992; 13:1192-7.

Friedman A, Kaufer D, Shemer J, Hendler I, Soreq H, Tur Kaspa I. Pyridostigmine brain penetration under stress enhances neuronal excitability and induces early immediate transcriptional response. Nat Med 1996; 2:1382-5.

Futerman AH, Low MG, Ackermann KE, Sherman WR, Silman I. Identification of covalently bound inositol in the hydrophobic membrane- anchoring domain of Torpedo acetylcholinesterase. Biochem Biophys Res Commun 1985; 129:312-7.

Gennarelli TA, Graham DI. Neuropathology of the Head Injuries. Semin Clin Neuropsychiatry 1998; 3:160-175.

Getman DK, Eubanks JH, Camp S, Evans GA, Taylor P. The human gene encoding acetylcholinesterase is located on the long arm of chromosome 7. Am J Hum Genet 1992; 51:170-7.

Giacobini E. Cholinergic foundations of Alzheimer's disease therapy. J Physiol Paris 1998; 92:283-7.

Gnatt A, Prody CA, Zamir R, Lieman-Hurwitz J, Zakut H, Soreq H. Expression of alternatively terminated unusual human butyrylcholinesterase messenger RNA transcripts, mapping to chromosome 3q26-ter, in nervous system tumors. Cancer Res 1990; 50:1983-7.

Grifman M, Galyam N, Seidman S, Soreq H. Functional redundancy of acetylcholinesterase and neuroligin in mammalian neuritogenesis. Proc Natl Acad Sci U S A 1998; 95:13935-40.

Grifman M, Soreq H. Differentiation intensifies the susceptibility of pheochromocytoma cells to antisense oligodeoxynucleotide-dependent suppression of acetylcholinesterase activity. Antisense Nucleic Acid Drug Dev 1997; 7:351-9.

Grisaru D, Lev-Lehman E, Shapira M, et al. Human osteogenesis involves differentiation-dependent increases in the morphogenically active 3' alternative splicing variant of acetylcholinesterase. Mol Cell Biol 1999; 19:788-95.

Grisaru D, Sternfeld M, Eldor A, Glick D, Soreq H. Structural roles of acetylcholinesterase variants in biology and pathology. Eur J Biochem 1999:(in press).

Hata Y, Butz S, Sudhof TC. CASK: a novel dlg/PSD95 homolog with an N-terminal calmodulin-dependent protein kinase domain identified by interaction with neurexins. J Neurosci 1996; 16:2488-94.

Ichtchenko K, Nguyen T, Sudhof TC. Structures, alternative splicing, and neurexin binding of multiple neuroligins. J Biol Chem 1996; 271:2676-82.

Inestrosa NC, Alvarez A, Perez CA, et al. Acetylcholinesterase accelerates assembly of amyloid-beta-peptides into Alzheimer's fibrils: possible role of the peripheral site of the enzyme. Neuron 1996; 16:881-91.

Irie M, Hata Y, Takeuchi M, et al. Binding of neuroligins to PSD-95. Science 1997; 277:1511-5.

Karpel R, Ben Aziz Aloya R, Sternfeld M, et al. Expression of three alternative acetylcholinesterase messenger RNAs in human tumor cell lines of different tissue origins. Exp Cell Res 1994; 210:268-77.

Karpel R, Sternfeld M, Ginzberg D, Guhl E, Graessmann A, Soreq H. Overexpression of alternative human acetylcholinesterase forms modulates process extensions in cultured glioma cells. J Neurochem 1996; 66:114-23.

Kaufer D, Friedman A, Seidman S, Soreq H. Acute stress facilitates long-lasting changes in cholinergic gene expression. Nature 1998; 393:373-7.

Kaufer D, Friedman A, Soreq H. The vicious circle: long-lasting transcriptional modulation of cholinergic neurotransmission following stress and anticholinesterase exposure. The Neuroscientist 1999; 5:173-183.

Koenigsberger C, Chiappa S, Brimijoin S. Neurite differentiation is modulated in neuroblastoma cells engineered for altered acetylcholinesterase expression. J Neurochem 1997; 69 (4):1389-1397.

Krasowski MD, McGehee DS, Moss J. Natural inhibitors of cholinesterases: implications for adverse drug reactions. Can J Anaesth 1997; 44:525-34.

La Du BN. Identification of human serum cholinesterase variants using the polymerase chain reaction amplification technique. Trends Pharmacol Sci 1989; 10:309-13.

Lapidot-Lifson Y, Prody CA, Ginzberg D, Meytes D, Zakut H, Soreq H. Coamplification of human acetylcholinesterase and butyrylcholinesterase genes in blood cells: correlation with various leukemias and abnormal megakaryocytopoiesis. Proc Natl Acad Sci U S A 1989; 86:4715-4719.

Levey AI, Wainer BH, Rye DB, Mufson EJ, Mesulam MM. Choline acetyltransferase-immunoreactive neurons intrinsic to rodent cortex and distinction from acetylcholinesterase-positive neurons. Neuroscience 1984; 13:341-53.

Lev-Lehman E, Deutsch V, Eldor A, Soreq H. Immature human megakaryocytes produce nuclear-associated acetylcholinesterase. Blood 1997; 89:3644-53.

Llinas RR, Greenfield SA. On-line visualization of dendritic release of acetylcholinesterase from mammalian substantia nigra neurons. Proc Natl Acad Sci U S A 1987; 84:3047-50.

Loewenstein Lichtenstein Y, Schwarz M, Glick D, Norgaard Pedersen B, Zakut H, Soreq H. Genetic predisposition to adverse consequences of anti-cholinesterases in 'atypical' BCHE carriers. Nat Med 1995; 1:1082-5.

Massoulie J, Pezzementi L, Bon S, Krejci E, Vallette FM. Molecular and cellular biology of cholinesterases. Prog Neurobiol 1993; 41:31-91.

McGuire MC, Nogueira CP, Bartels CF, et al. Identification of the structural mutation responsible for the dibucaine- resistant (atypical) variant form of human serum cholinesterase. Proc Natl Acad Sci U S A 1989; 86:953-7.

Mesulam MM, Geula C. Acetylcholinesterase-rich neurons of the human cerebral cortex: cytoarchitectonic and ontogenetic patterns of distribution. J Comp Neurol 1991; 306:193-220.

Mollgard K, Dziegielewska KM, Saunders NR, Zakut H, Soreq H. Synthesis and localization of plasma proteins in the developing human brain. Integrity of the fetal blood-brain barrier to endogenous proteins of hepatic origin. Dev Biol 1988; 128:207-221.

Neville LF, Gnatt A, Loewenstein Y, Seidman S, Ehrlich G, Soreq H. Intramolecular relationships in cholinesterases revealed by oocyte expression of site-directed and natural variants of human BCHE. EMBO J 1992; 11:1641-9.

Neville LF, Gnatt A, Loewenstein Y, Soreq H. Aspartate-70 to glycine substitution confers resistance to naturally occurring and synthetic anionic-site ligands on in-ovo produced human butyrylcholinesterase. J Neurosci Res 1990; 27:452-60.

Pakaski M, Kasa P. Glial cells in coculture can increase the acetylcholinesterase activity in human brain endothelial cells. Neurochem Int 1992; 21:129-33.

Paoletti F, Mocali A, Vannucchi AM. Acetylcholinesterase in murine erythroleukemia (Friend) cells: evidence for megakaryocyte-like expression and potential growth-regulatory role of enzyme activity. Blood 1992; 79:2873-9.

Patinkin D, Lev Lehman E, Zakut H, Eckstein F, Soreq H. Antisense inhibition of butyrylcholinesterase gene expression predicts adverse hematopoietic consequences to cholinesterase inhibitors. Cell Mol Neurobiol 1994; 14:459-73.

Primo-Parmo SL, Bartels CF, Wiersema B, van der Spek AF, Innis JW, La Du BN. Characterization of 12 silent alleles of the human butyrylcholinesterase (BCHE) gene. Am J Hum Genet 1996; 58:52-64.

Prody CA, Dreyfus P, Zamir R, Zakut H, Soreq H. De novo amplification within a "silent" human cholinesterase gene in a family subjected to prolonged exposure to organophosphorous insecticides. Proc Natl Acad Sci USA 1989; 86:690-694.

Prody CA, Zevin-Sonkin D, Gnatt A, Goldberg O, Soreq H. Isolation and characterization of full-length cDNA clones coding for cholinesterase from fetal human tissues. Proc Natl Acad Sci U S A 1987; 84:3555-9.

Razon N, Soreq H, Roth E, Bartal A, Silman I. Characterization of activities and forms of cholinesterases in human primary brain tumors. Exp Neurol 1984; 84:681-95.

Schwarz M, Glick D, Loewenstein Y, Soreq H. Engineering of human cholinesterases explains and predicts diverse consequences of administration of various drugs and poisons. Pharmacol Ther 1995; 67:283-322.

Seidman S, Cohen O, Ginsberg D, et al. Multilevel approaches to AChE-induced impairments in learning and memory. In: Doctor BP, Taylor P, Quinn DM, Rotundo RL, Gentry MK, eds. Structure and Function of Cholinesterases and Related Proteins. New York: Plenum Press, 1998:183-184.

Seidman S, Eckstein F, Grifman M, Soreq H. Antisense technologies have a future fighting neurodegenerative diseases. Antisense Nucleic Acid Drug Dev 1999; (in press).

Seidman S, Sternfeld M, Ben Aziz Aloya R, Timberg R, Kaufer Nachum D, Soreq H. Synaptic and epidermal accumulations of human acetylcholinesterase are encoded by alternative 3'-terminal exons. Mol Cell Biol 1995; 15:2993-3002.

Shapira M, Korner M, Bosgraaf L, Tur-Kaspa I, Soreq H. The human ACHE locus includes a polymorphic enhancer domain 17 Kb upstream from the transcription start site. In: Doctor BP, Taylor P, Quinn DM, Rotundo RL, Gentry MK, eds. Structure and Function of Cholinesterases and Related Proteins. New York: Plenum Press, 1998:111.

Shoham S, Sternfeld M, Milay T, Patrick JW, Soreq H. Transgenic human AChE variants display different capacities of inducing "corkscrew-like" neuronal processes in mouse somatosensory cortex. Neurosci. Lett. 1998; Suppl. 51:S38.

Soreq H, Ben-Aziz R, Prody CA, et al. Molecular cloning and construction of the coding region for human acetylcholinesterase reveals a G + C-rich attenuating structure. Proc Natl Acad Sci U S A 1990; 87:9688-92.

Soreq H, Malinger G, Zakut H. Expression of cholinesterase genes in human oocytes revealed by in-situ hybridization. Hum Reprod 1987; 2:689-93.

Soreq H, Patinkin D, Lev-Lehman E, et al. Antisense oligonucleotide inhibition of acetylcholinesterase gene expression induces progenitor cell expansion and suppresses hematopoietic apoptosis ex vivo. Proc Natl Acad Sci USA 1994; 91:7907-11.

Soreq H, Zakut H. Human Cholinesterases and Anticholinesterases. San Diego: Academic Press, 1993.

Sternfeld M, Ming G, Song H, et al. Acetylcholinesterase enhances neurite growth and synapse development through alternative contributions of its hydrolytic capacity, core protein, and variable C termini. J Neurosci 1998; 18:1240-9.

Sternfeld M, Patrick JD, Soreq H. Position effect variegations and brain-specific silencing in transgenic mice overexpressing human acetylcholinesterase variants. J Physiol (Paris) 1998; 92:249-55.

Sternfeld M, Rachmilewitz J, Loewenstein-Lichtenstein Y, et al. Normal and atypical butyrylcholinesterases in placental development, function, and malfunction. Cell Mol Neurobiol 1997; 17:315-32.

Sussman JL, Harel M, Frolow F, et al. Atomic structure of acetylcholinesterase from Torpedo californica: a prototypic acetylcholine-binding protein. Science 1991; 253:872-9.

Taylor P. Agents acting at the neuromuscular junction and autonomic ganglia. In: Hardman JG, Limbird LE, Molinoff PB, Ruddon RW, eds. Goodman and Gilman's The Pharmacological Basis of Therapeutics. New York: McGraw-Hill, 1996:177-197.

von der Kammer H, Mayhaus M, Albrecht C, Enderich J, Wegner M, Nitsch RM. Muscarinic acetylcholine receptors activate expression of the EGR gene family of transcription factors. J Biol Chem 1998; 273:14538-44.

Whittaker M. Cholinesterase. Basel: Karger, 1986.

Wright CI, Guela C, Mesulam MM. Protease inhibitors and indoleamines selectively inhibit cholinesterases in the histopathologic structures of Alzheimer disease. Proc Natl Acad Sci U S A 1993; 90:683-6.

Zakut H, Ehrlich G, Ayalon A, et al. Acetylcholinesterase and butyrylcholinesterase genes coamplify in primary ovarian carcinomas. J Clin Invest 1990; 86:900-8.

Zakut H, Even L, Birkenfeld S, Malinger G, Zisling R, Soreq H. Modified properties of serum cholinesterases in primary carcinomas. Cancer 1988; 61:727-37.

Zakut H, Lapidot-Lifson Y, Beeri R, Ballin A, Soreq H. In vivo gene amplification in non-cancerous cells: cholinesterase genes and oncogenes amplify in thrombocytopenia associated with lupus erythematosus. Mutat Res 1992; 276:275-284.

Zakut H, Lieman Hurwitz J, Zamir R, Sindell L, Ginzberg D, Soreq H. Chorionic villus cDNA library displays expression of butyrylcholinesterase: putative genetic disposition for ecological danger. Prenat Diagn 1991; 11:597-607.

Genomic and Transcriptional characterization of the human *ACHE* locus indicates complex involvement with acquired and inherited diseases

Michael Shapira MSc[1], Alastair Grant BSc[1], Mira Korner PhD[1] and Hermona Soreq PhD[1,*]

[1] Department of Biological Chemistry, The Life Sciences Institute, The Hebrew University of Jerusalem, Israel 91904.

* To whom correspondence should be addressed (Fax 972-2-6520258, Tel 972-2-6585109, e-mail: soreq@shum.huji.ac.il)

Running title: The *ACHE* locus and human disease

Abstract

Background: Abnormal levels of the acetylcholinesterase enzyme (AChE) or aberrations involving the long arm of chromosome 7, harboring the *ACHE* gene at 7q22, occur in various diseases (e.g. Alzheimer's or Parkinson's diseases, leukemias). However, the cause(s) for these abnormalities are still unknown.

Objective: In search for the genomic elements and transcriptional processes controlling *ACHE* gene expression and the plausible stability of its locus, we initiated a study aimed at isolating, sequencing and characterizing the human (h)ACHE locus and its mRNA products.

Methods: Three clones containing the *ACHE* gene were isolated from a human chromosome 7 cosmid library. Two of these clones were thereafter sequenced and searched for repetitive elements, open reading frames and corresponding expressed sequence tags (ESTs). RT-PCR was employed to further explore these findings.

Results: The locus harboring the G,C-rich *ACHE* gene was found to be exceptionally rich in Alu repeats. It includes an additional, inversely-oriented gene (h*ARS*), tentatively associated with arsenite resistance. EST clones corresponding to both genes were found in cDNA libraries from 11 different human tissue sources, with ARS expressed in 10 additional tissues. Co-regulation of brain *ACHE* and *ARS* was suggested from their mutually increased expression following acute psychological stress.

Conclusions: The abundance of Alu retrotransnposones may predispose the *ACHE* locus to chromosomal rearrangements. Additionally, coordinated transcriptional regulation is implied from the joint ARS-AChE expression in stress insult responses. Disease-related changes in AChE may therefore reflect locus-specific regulation mechanisms affecting multiple tissues.

Keywords: acetylcholinesterase; arsenite-reseistance; inherited diseases; transcriptional actication; gene-locus.

Introduction

The acetylcholine hydrolysing enzyme acetylcholinesterase (acetylcholine acetylhydrolase, AChE, EC 3.1.1.7) terminates cholinergic neurotransmission and thus controls central and peripheral nervous systems functions. AChE abnormalities were reported in various pathologies, including nervous system diseases (e.g. Alzheimer's or Parkinson diseases and myasthenia gravis) or cases of intoxication with chemical warfare agents [1]. AChE abnormalities also occur in diseases involving non-cholinergic tissues and cell types (e.g. in nocturnal hemoglobinuria [2]). These diseases may reflect non-catalytic activities of the enzyme, which shares sequence homologies and functional properties with a series of non-enzyme cell-cell interaction proteins (reviewed in [3]). In addition to changes in AChE expression, chromosomal aberrations involving band 7q22, harboring the human (h)*ACHE* locus, are associated with various types of leukemias [4].

AChE inhibitors (anti-AChEs; e.g. commonly used agricultural insecticides [5]), increase the risk for non-Hodkin's lymphomas [6]. Chemicals with anti-AChE capabilities also include chemical warfare agents, prophylactic drugs aimed to protect from exposure to such agents [7] and a wide range of anti-AChE drugs used for treating Alzheimer's disease and myasthenia gravis patients ([8] and [9], respectively). However, both exposure to anti-AChEs and acute psychological stress induce AChE overproduction [10,11]. Moreover, transgenic mouse models with AChE overproduction presented early cognitive deterioration [12], progressive neuromuscular deformities [13] and typical characteristics of stress insults in their brain (Sternfeld et al., submitted). This suggests long-lasting delayed consequences for AChE accumulation. To evaluate the scope of such consequences, we combined molecular genetic approaches with searches of genomic databases to explore the h*ACHE* locus.

Materials and Methods

Reverse transcription PCR (RT-PCR). Primers used for PCR amplification were 5'-CAGGTCCCGATATTCCACAAT-3' and 5' GGGCTGACCATAGGGCATCA-3' for mARS, 5'-TGAAACAACATACAATTCCATCATGAAGTGTGAC-3' and 5'-AGGAGCGATAATCTTGATCTTCATGGTGCT-3' for actin and primers complementary to exon 2 of mAChE which is common to all AChE isoforms [10]. Samples of PCR products were withdrawn every third cycle starting at cycle 18 for AChE and actin and every second cycle starting at cycle 26 for ARS.

Sequence analyses. Searches for open reading frames (ORFs) in the hACHE locus, G,C content as well as repetitive sequences in the *ACHE* upstream sequence and expression sequence tags (ESTs) derived from this locus were performed using the programs Grail (http://avalon.epm.ornl.gov/Grail-bin/EmptyGrailForm), Window (the University of Wisconsin GCG software package), Repeat Masker 2 (http://ftp.genome.washington.edu) and Blast (http://www.ncbi.nlm.nih.gov/BLAST/), respectively.

Results

To extend the genomic analysis at the *ACHE* locus, the cloned human *ACHE* gene has been used as a probe for screening a cosmid library [14]. Three cosmid clones were isolated, two of which included a PCR-amplifyable sequence located immediately upstream to the *ACHE* transcription start site (Fig. 1). One of the two cosmid clones containing the *ACHE* upstream region was fully sequenced and the third clone, not containing this region, was used to extend the sequenced portion downstream to *ACHE*. This yielded a 38 Kb sequence. A search for ORFs demonstrated two inversely-oriented active genes in this locus, *ACHE* and *ARS*, the latter showing high similarity to a rodent gene which is overexpressed in cells exposed to arsenite [15].

Searching the *ACHE* locus for repetitive elements unraveled an extremely high prevalence of Alu repeats, non-viral retrotransposons which are part of the family of short interspersed elements (SINEs; Fig. 2). Thirty nine of these repeats were identified along 23 Kb of *ACHE* upstream sequence. In addition, this region was found to be markedly lower in its G,C content than the *ACHE* gene itself.

To find out which tissues express hAChE and hARS, the expression sequence tags (EST) database was searched. ESTs originating from AChE and hARS mRNA transcripts were found in many different tissues, including both adult (brain, intestine, skeletal muscle, colon and kidney) and fetal tissues (liver and spleen, lung and heart) (Fig. 3). hARS mRNA was considerably more abundant; different alternatively spliced hARS mRNA sequences were found in all of the above tissues as well as in B cells, breast tissue, placenta, pituitary gland, fetal lung, cervix, thymus, T cells and fibroblasts.

The partial overlap in tissue distribution of mRNA transcripts of hARS and hAChE, together with their close genomic proximity in both primates and rodents (data not shown), raised the possibility of coordinated transcriptional regulation of this entire chromosomal domain. To test whether this is the case, we compared the levels of AChE and ARS in the brain of control mice to those in mice subjected to the forced-swim protocol causing psychological stress [10]. Stressed mice displayed, as expected, increased AChE mRNA levels in their brain [11]. In addition, these mice displayed massive co-induction in the brain of the *ARS* gene 2 hrs post-stress, while maintaining unchanged actin mRNA levels (Fig. 4). This supports the notion of a stress-associated regulation of gene expression in the *ACHE* locus.

Discussion

Our findings demonstrate ubiquitous expression of the adjacent h*ACHE* and hARS genes in many different fetal, adult and tumor tissues. This, and the co-induction of mouse (m)AChE and mARS expression under acute psychological stress provide a tentative genomic explanation for the reports of modulated AChE expression in different diseases.

Reported transfection studies mostly referred to the proximal sequence, including up to 300 base pairs (bp) of the *ACHE* promoter, as essential for its normal expression [16]. In transgenic mice, the proximal 600 bp of the h*ACHE* promoter failed to induce detectable expression in extra-CNS tissues [12]. Either the transgene insertion site in the host mouse genome or species-specific differences in *ACHE* regulation could be responsible for that. We have recently found that transcription factor binding sites located 17 Kbp upstream of the *ACHE* transcription start site regulate osteogenic *ACHE* gene expression [17]. We conclude that similarly to the albumin gene [18] (and several others), exceptionally distal enhancer elements are required for *ACHE*'s proper expression.

The rodent ARS gene (*ARS2*; [15]) is overexpressed under arsenite exposure and was therefore tentatively identified as an arsenite-responsive protein. Its human homologue is located downstream to *ACHE*, inversely oriented close to it and co-regulated with it. The sequence of the *ARS* translation product does not resemble any known protein, including the cloned bacterial arsenite resistance protein. As the two genes must have individual promoters, each on a different DNA strand, their co-expression may reflect joint opening of the *ACHE* and *ARS* DNA domains for transcriptional induction. This, in turn, predicts hARS accumulation under all of those conditions that induce AChE overproduction, including acute psychological stress, and exposure to AChE inhibitors [11]. One of these inhibitors is arsenite [19], which would induce feedback accumulation of its AChE scavenger, just as it occurs in response to pyridostigmine [10,11]. This suggests that *ARS* accumulates under arsenite exposure only because of co-localization and co-regulation with *ACHE* but is not causally involved in arsenite resistance. The *ACHE* locus thus emerges as a jointly controlled domain, perhaps similar to the β-globin locus [20].

AChE accumulation under various stress insults may contribute, through its non-catalytic properties, towards the variable symptoms of Gulf War veterans [21], of patients exposed to agricultural insecticides [5] and of anti-AChE treated Alzheimer's disease patients [22]. Its ubiquitous expression may further predict involvement in many more tissues than the nervous system. Moreover, the remarkable abundance of SINE elements, in particular Alu repeats, in the *ACHE* locus implies exceptional susceptibility for tranposition events, which are assisted by the existence of chromosomal breakages [23]. Additionally, Alu repeats may also facilitate unequal crossing-over [24], altogether contributing to instability of this region. Chromosomal rearrangements could result in the loss of upstream transcription factor binding sites, and thus affect *ACHE* gene expression and its capacity to accumulate under stress or exposure to anti-AChEs. This explains the reported chromosomal aberrations involving 7q22 in leukemic patients [25]. The increased risk for non-Hodgkin's lymphoma of farmers exposed to anti-cholinesterases [6] may hence be relevant both to inhibitor-induced accumulation of the AChE protein and to

abnormal replication of this locus in lymphocytes. Genomic and transcriptional analysis thus points at the *ACHE* locus as an intersection involved in many pathways, several of which may lead to disease.

Acknowledgements

The authors are grateful to Dr. Lap-Chi Tsui, Toronto, for the 7q22 cosmids. This study was supported by the Medical Research and Development Command of the US Army (DAMD17-99-1-9547), the Israel Science Foundation (590/97), the German-Israel Foundation (I-0512-206.01/96), the Israel Ministry of Science (8433-1-97) and Ester Neuroscience, Ltd. (to H.S.). A.G. is an incumbent of a fellowship by the Friends of the Hebrew University, London.

Legends

Figure 1. Identification of 7q22 cosmids containing the *ACHE* gene. Shown on top is a schematic description of the PCR identification of cosmids containing the *ACHE* gene from a 7q22 cosmid library and the structure of the *ACHE* gene, with exons represented by filled boxes numbered above and introns represented by open boxes numbered below. Black box represents 600 bp of the proximal promoter with a right-bent arrow designating the transcription start site. Below, the position of the analyzed cosmid on chromosome 7 is drawn and a gel image shows a 294 bp-long PCR product (marked with a red arrow) amplified using primers depicted at the top scheme with thick arrows. This fragment could be amplified from cosmid A (Genebank accession no. Af002993) but not from cosmid C (accession no af237614), both located at 7q22. Plus sign designates a PCR reaction with the plasmid containing *ACHE*'s proximal promoter, serving as template.

Figure 2. Analysis of the ACHE extended Promoter. Presented is an analysis of the *ACHE* extended promoter (22.5Kb) in terms of G,C content (drawn line), repeatless regions (red boxes) and variable repeat elements (simple sequence DNA, low complexity sequence, SINEs, retroviral long terminal repeats (LTRs) and the SRP SINE subtype). Note the abundant SINE sequences, most of which are Alu repeats. Cumulative G,C content (percent) for each of these subgroups is shown (right).

Figure 3. Expession from the 7q22 locus as reflected in the EST database. Shown is the graphical output of the Blast program (http://www.ncbi.nlm.nih.gov/BLAST/) run against the expression sequence tags (EST) database using the af002993 cosmid as a query sequence and restricting the search to human sequences. The identified ESTs are aligned against the corresponding regions of the query sequence, which is shown in red and scaled in bp. ESTs are colored according to their alignment score as depicted in the color key bar (black-hatched portions represent incontinuities in the alignments and therefore indicate introns). Designated are the *ARS* and *ACHE* gene regions and the tissue origins of the different ESTs, with uppercase letters showing highly-represented tissues. Asterisks designate tissues expressing both ARS and AChE.

Figure 4. Psychological stress increases both AChE and ARS mRNA levels in the mouse medulla. Shown is one out of 3 reproducible experiments presenting a semi-quantitative kinetic follow-up of RT-PCR evaluation. Arrow-labeled are AChE, ARS and actin cDNA products in extracts prepared from the brain stem (medulla) region of either a control mouse (C) or two different mice subjected to psychological stress (S) [11]. Densitometry of the fluorescent signals presented 8-fold stress-related increases for the AChE transcripts. Four-fold increases were detected for ARS products in brains of stressed as compared to control mice. Actin products showed no difference associated with stress, demonstrating specificity of the AChE and ARS increases. m, size marker.

References

1. Moretto A. Experimental and clinical toxicology of anticholinesterase agents. *Toxicol Lett* 1998;102-103:509-13.

2. Ueda E, Kinoshita T, Terasawa T, Shichishima T, Yawata Y, Inoue K, Kitani T. Acetylcholinesterase and lymphocyte function-associated antigen 3 found on decay-accelerating factor-negative erythrocytes from some patients with paroxysmal nocturnal hemoglobinuria are lost during erythrocyte aging. *Blood* 1990;75(3):762-9.

3. Grisaru D, Sternfeld M, Eldor A, Glick D, Soreq H. Structural roles of acetylcholinesterase variants in biology and pathology. *Eur J Biochem* 1999;264:672-686.

4. Johnson E, Cotter FE. Monosomy 7 and 7q--associated with myeloid malignancy. *Blood Rev* 1997;11(1):46-55.

5. Soreq H, Glick D. Novel roles for cholinesterases in stress and inhibitor responses. In: Giacobini E, ed. Cholinesterases and cholinesterase inhibitors: basic, preclinical and clinical aspects: Martin Dunitz Ltd., 1999.

6. Brown LM, Blair A, Gibson R, Everett GD, Cantor KP, L.M. S, Burmeister LF, Van Lier SF, Dick F. Pesticide exposure and other agricultural risk factors for leukemia among man in Iowa and Minnesota. *Cancer Res* 1990;50:6585-6591.

7. Keeler JR, Hurst CG, Dunn MA. Pyridostigmine used as a nerve agent pretreatment under wartime conditions [see comments]. *Jama* 1991;266(5):693-5.

8. Winkler J, Thal LJ, Gage FH, Fisher LJ. Cholinergic strategies for Alzheimer's disease. *J Mol Med* 1998;76(8):555-67.

9. Wittbrodt ET. Drugs and myasthenia gravis. An update. *Arch Intern Med* 1997;157(4):399-408.

10. Friedman A, Kaufer D, Shemer J, Hendler I, Soreq H, Tur-Kaspa I. Pyridostigmine brain penetration under stress enhances neuronal excitability and induces early immediate transcriptional response. *Nat Med* 1996;2:1382-1385.

11. Kaufer D, Friedman A, Seidman S, Soreq H. Acute stress facilitates long-lasting changes in cholinergic gene expression. *Nature* 1998;393(6683):373-7.

12. Beeri R, Andres C, Lev Lehman E, Timberg R, Huberman T, Shani M, Soreq H. Transgenic expression of human acetylcholinesterase induces progressive cognitive deterioration in mice. *Curr Biol* 1995;5(9):1063-71.

13. Andres C, Beeri R, Friedman A, Lev-Lehman E, Henis S, Timberg R, Shani M, Soreq H. Acetylcholinesterase-transgenic mice display embryonic modulations in spinal cord choline acetyltransferase and neurexin Ibeta gene expression followed by late-onset neuromotor deterioration. *Proc Natl Acad Sci U S A* 1997;94(15):8173-8.

14. Melmer G, Sood R, Rommens J, Rego D, Tsui LC, Buchwald M. Isolation of clones on chromosome 7 that contain recognition sites for rare-cutting enzymes by oligonucleotide hybridization. *Genomics* 1990;7(2):173-81.

15. Rossman TG, Wang Z. Expression cloning for arsenite-resistance resulted in isolation of tumor-suppressor fau cDNA: possible involvement of the ubiquitin system in arsenic carcinogenesis. *Carcinogenesis* 1999;20(2):311-6.

16. Getman DK, Mutero A, Inoue K, Taylor P. Transcription factor repression and activation of the human acetylcholinesterase gene. *J Biol Chem* 1995;270(40):23511-9.

17. Grisaru D, Lev-Lehman E, Shapira M, Chaikin E, Lessing JB, Eldor A, Eckstein F, Soreq H. Human osteogenesis involves differentiation-dependent increases in the morphogenically active 3' alternative splicing variant of acetylcholinesterase. *Mol Cell Biol* 1999;19(1):788-95.

18. Herbst RS, Friedman N, Darnell JE, Jr., Babiss LE. Positive and negative regulatory elements in the mouse albumin enhancer. *Proc Natl Acad Sci U S A* 1989;86(5):1553-7.

19. Wilson IB, Silman I. Effects of quaternary ligands on the inhibition of acetylcholinesterase by arsenite. *Biochemistry* 1977;16(12):2701-8.

20. Hardison R, Slightom JL, Gumucio DL, Goodman M, Stojanovic N, Miller W. Locus control regions of mammalian beta-globin gene clusters: combining phylogenetic analyses and experimental results to gain functional insights. *Gene* 1997;205(1-2):73-94.

21. Haley RW, Kurt TL, Hom J. Is there a Gulf War Syndrome? Searching for syndromes by factor analysis of symptoms. *Jama* 1997;277(3):215-22.

22. Giacobini E. Invited review: Cholinesterase inhibitors for Alzheimer's disease therapy: from tacrine to future applications. *Neurochem Int* 1998;32(5-6):413-9.

23. Branciforte D, Martin SL. Developmental and cell type specificity of LINE-1 expression in mouse testis: implications for transposition. *Mol Cell Biol* 1994;14(4):2584-92.

24. Hu X, Worton RG. Partial gene duplication as a cause of human disease [see comments]. *Hum Mutat* 1992;1(1):3-12.

25. Stephenson J, Czepulkowski B, Hirst W, Mufti G. Deletion of the acetylcholinesterase locus at 7q22 associated with myelodysplastic syndromes (MDS) and acute myeloid leukaemia (AML). *Leuk Res* 1996;20(3):235-241.

Figure 1

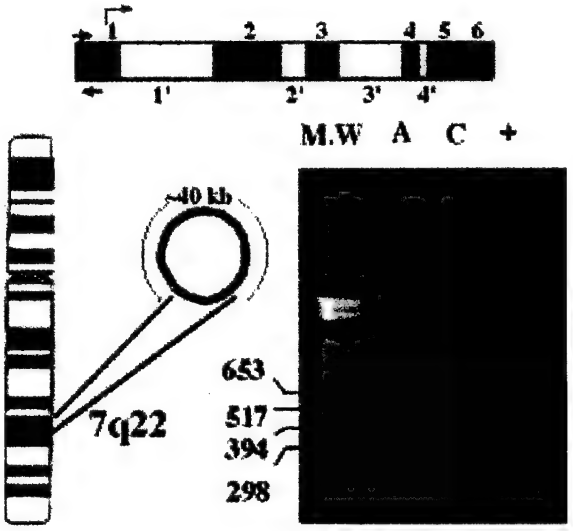

Figure 2

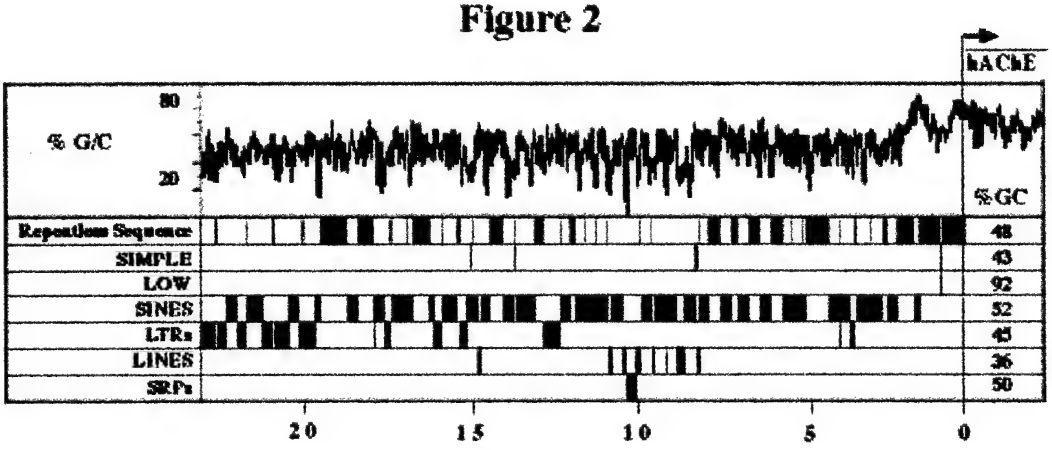

Figure 3

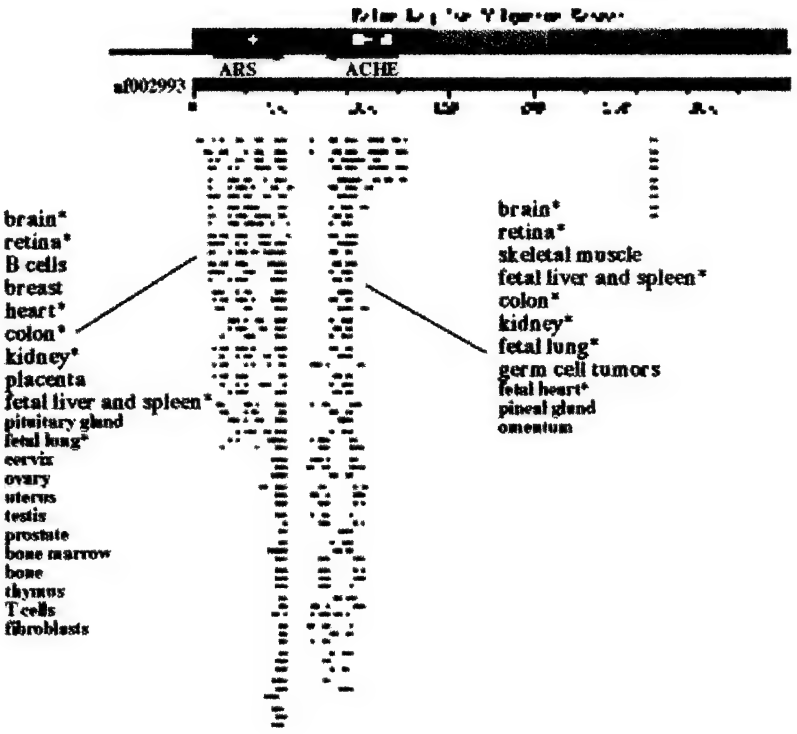

Figure 4

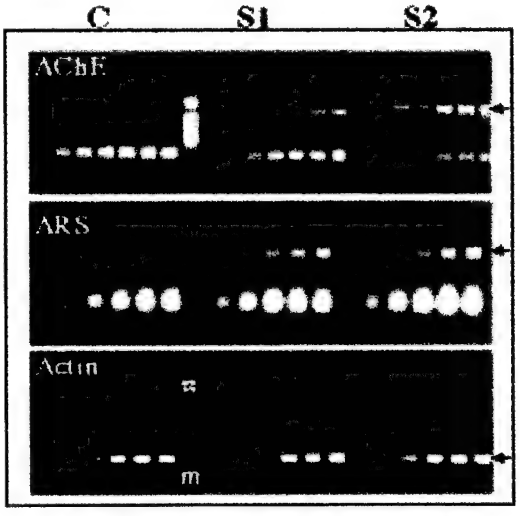

Human acetylcholinesterase gene expression is controlled by an exceptionally long stress-responding promoter

Michael Shapira, Alastair Grant, Mira Korner and Hermona Soreq*

Department of Biological Chemistry, The Life Sciences Institute, The Hebrew University of Jerusalem, Israel 91904
*To whom correspondence should be addressed (Tel 972-2-6585109, Fax 972-2-6520258, email: **soreq@shum.huji.ac.il**)

Running title: the human *ACHE* extended promoter

Abstract

The acetylcholine hydrolyzing enzyme acetylcholinesterase (AChE) is a key element in cholinergic neurotransmission, which is known to be upregulated under acute psychological stress. We have recently reported massive transcriptional activation of *ACHE* gene expression following forced swim stress; however, the genomic origin(s) of this induction and the extent of individual variabilities in its intensity remained obscure. To explore for possible causes for these phenomena, we subjected the mammalian *ACHE* locus, harboring this gene to database searches and transcriptional analyses. Here, we report the properties of an extended promoter domain upstream to the *ACHE* gene. The 22 Kb long *ACHE* upstream region was found to be rich in consensus motifs for binding diverse transcription factors, including the stress-associated glucocorticoid receptor, stat-5 and the interleukin 6 receptor. The mouse database of expressed sequence tags (EST) includes *ACHE* mRNA transcripts from several tissues; ESTs from a yet broader range of tissue sources were found that are derived from an adjacent, inversely-oriented gene, *ARS*. Moreover, high resolution *In situ* hybridization demonstrated that ARS mRNA is expressed in a higher level in hippocampal neurons of human (h)AChE-overexpressing transgenic mice as compared with FVB/N controls. These findings demonstrate genomic stress response elements in the extended *ACHE* promoter and suggest complex multigenic and strain-specific control for this locus.

Introduction

In addition to its known role in terminating cholinergic neurotransmission, the acetylcholine (ACh) hydrolyzing enzyme acetylcholinesterase (AChE) appears to be subject to robust transcriptional activation under acute psychological stress or exposure to AChE inhibitors (anti-AChEs; (Kaufer et al., 1998). Trancriptional activation from the *ACHE* gene was particularly conspicuous in the hippocampus, predicting relevance for cognitive functions. This is of utmost importance in view of the accumulated experience in the use of anti-AChEs as drugs for treating Alzheimer's disease patients (Giacobini, 1998). AChE overproduction following stress insults can be beneficial as it ensures hydrolysis of the excess ACh that is secreted under stress (Kaufer et al., 1999). However, robust AChE accumulation under inhibitor treatment may prevent the intended increase in ACh level, thus limiting the therapeutic efficacy of anti-AChEs. Therefore, individual diversities in the capacity to induce *ACHE* gene expression may be associated both with the effective drug dose required to improve cognition and with variable abilities to adjust to stress insults.

Behavioral stress modifies hippocampal plasticity through N-methyl-D-Aspertate receptor activation (Kim et al., 1996), facilitates classical conditioning processes (Shors et al., 1992) and induces long-term depression in the hippocampus (Xu et al., 1997). The key regulator of all these processes is the glucocorticoid receptor, which activates protein and RNA synthesis-dependant mechanisms underlying modulations in synaptic plasticity (Xu et al., 1998). Therefore, genes that are subject to stress-induced regulation are likely to include in their promoters consensus motifs for binding glucocorticoid hormones.

To search for plausible molecular mechanisms regulating AChE expression under stress, we subjected the extended human (h)*ACHE* promoter to database searches aimed to define its tentative length and the composition of binding motifs included in it. In addition, we tested the expression levels of ARS, a second gene in this locus, in hAChE overespressing transgenic mice as well as in 2 FVB/N and C57bl/6J mice, 2 strains known to differ in the number of cholinergic neurons and in their cognitive performance. Our findings demonstrate potential glucocorticoid hormone regulation and individual diversities in the efficacy for mammalian gene expression from the *ACHE* locus.

Materials and Methods

Sequence analyses. The cosmid clone harboring the human ACHE gene was searched for open reading frames (ORFs), expression sequence tags (ESTs) and consensus motif elments for binding diverse transcription factors using the following software programs: Grail (**http://avalon.epm.ornl.gov/Grail-bin/EmptyGrailForm**) , Blast (**http://www.ncbi.nlm.nih.gov/BLAST/**), FindPatterns (The University of Wisconsin GCG software package) and MatInspector (**http://www.gsf.de/cgi-bin/matsearch.pl**; with core similrity of 1 and matrix similarity of 0.85).

***In situ* hybridization (ISH)** was performed as described elsewhere (Grifman et al., 1998). Briefly, 7 μm thick paraffin-embedded tissue sections were subjected to hybridization with a 50-mer biotinylated, 2'-o-methylated, RNA probe specific for ARS transcripts (complementary for the hARS gene; position 4562 in af002993). After incubation of sections with streptavidin-alkaline phosphatase (AP) conjugate (Amersham Life Sciences Products, Little Chalfont, Buckinghamshire, England) transcripts were detected using the ELF fluorogenic AP substrate (Molecular Probes, Leiden, The Netherlands) and a fluorescent Zeiss Axioplan microscope.

Reverse transcription PCR (RT-PCR). Primers used for PCR amplification were 5'-CAGGTCCCGATATTCCACAAT-3' and 5' GGGCTGACCATAGGGCATCA-3' for mouse (m)ARS, 5'-TGAAACAACATACAATTCCATCATGAAGTGTGAC-3' and 5'-AGGAGCGATAATCTTGATCTTCATGGTGCT-3' for actin and primers complementary to exon 2 of mAChE which is common to all AChE isoforms (Friedman et al., 1996). Samples of PCR products were withdrawn every third cycle starting at cycle 18 for AChE and actin and every second cycle starting at cycle 26 for ARS.

Results

The human *ACHE* gene maps to the long arm of chromosome 7, on 7q22 (Ehrlich et al., 1992; Getman et al., 1992). We obtained the h*ACHE* locus sequence by shotgun-sequencing clones fished out of a chromosome 7 cosmid library (Melmer et al., 1990). Figure 1 depicts the primary characteristics seen in the sequence of one of these cosmid clones. Analysis of 20 Kb of the *ACHE* upstream sequence was performed using the MatInspector and FindPatterns programs. These searches identified a large array of consensus motifs for binding diverse transcription factors. These included motifs known to be involved in neuronal or cellular stress responses, e.g. glucocorticoid response element (GRE; (Tronche et al., 1998)), with a half palindromic site, TGTTCT; interleukin 6 receptor (IL-6 (Hirano, 1998), CTGGG/AAA); EGR1, involved in the muscarinic regulation of

ACHE gene expression (Nitsch et al., 1998) or stat-5 (Lechner et al., 1997) (TTCCCAGAA or TT(C/A)(C/T)N(A/G)(G/T)AA). Of these, stat-5 and the glucocorticoid receptor are known to act synergistically in enhancement of the β-cascin gene expression (Lechner et al., 1997). Other binding motifs, were for osteogenic factors such as the vitamin D receptor, with various binding elemetns (VDREs; (Haussler et al., 1995)) arranged in pairs or, in one case, in a triplet, as found in the vitamin D-regulated promoter of the c-fos gene (Candeliere et al., 1996). In some clusters, CAAT boxes were found to be located close to VDREs where factors of the CTF/NF-1 family were shown to act synergistically with the vitamin D receptor (Liu and Freedman, 1994). Other osteogenic factors include the vitamin D-regulated repressor HES-1 (with CACNAG as the binding element; (Matsue et al., 1997)), Krox-20/24 (GCGGGGGCGGG; (Lemaire et al., 1990)), core-binding factor A1 (Cbfa1; AACCAC (Komori et al., 1997)) and the estrogen receptor, which usually binds as a dimer to a palindromic element but was also shown to activate transcription from such half palindromic elements (GGTCA; (Tora et al., 1988)). Figure 2 presents these transcription factor motifs in a schematic manner. Involvement of some of these factors in AChE expression was demonstrated in tissue culture experiments (Grisaru et al., 1999). These findings suggested that the human *ACHE* promoter extends far beyond the previously estimated ~1 Kb (Ben Aziz Aloya et al., 1993; Getman et al., 1995) and called for exploring the expression regulation from the entire locus.

To find out which mouse (m) tissues express AChE and ARS, we searched the expression sequence tags (EST) database. Mouse ESTs originating from AChE and ARS mRNA transcripts were found in many different tissues. These included both adult tissues (brain and placenta) as well as fetal ones (liver and spleen, lung and heart) (Fig. 3). mARS mRNA was abundant in a considerably larger number of tissues, including brain.

To explore the expression patterns of mARS in the mouse brain, we performed *in situ* hybridization on brain sections from both normal FVB/N mice and from transgenic mice expressing the human AChE under control of its 600 bp proximal promoter (Ben Aziz Aloya et al., 1993). The latter suffer from early cognitive deterioration (Beeri et al., 1995) and from typical neuropathological characteristics of stress in their brain (Sternfeld et al., submitted). m*ARS*, like the mammalian *ACHE* was found to be expressed in hippocampal neurons (Fig. 4A). Moreover, AChE transgenic mice displayed considerable overexpression of neuronal mARS RNA as compared with control, non-transgenic FVB/N mice (Fig. 4B). The mammalian *ACHE* and *ARS* genes thus share both chromosomal localization and neuronal expression capacities.

This overlap in cell type expression of mARS and mAChE raised the possibility of coordinated transcriptional regulation of the entire chromosomal domain. This was supported by their close genomic proximity in both primates and rodents (data not shown). To explore this possibility, we compared brain mAChE and mARS mRNA levels between untreated C57bl/6J mice reported to have lower levels than normal of cortical cholinergic neurons (Bentivoglio et al., 1994; Schwab et al., 1990), to those of FVB/N mice possessing normal cholinergic activities. Kinetic followup of RT-PCR analyses demonstrated higher brain levels of both mAChE and mARS mRNA in the FVB/N mice (data not shown), supporting the notion of strain-specific coordinated regulation of gene expression in the *ACHE* locus.

Discussion

We have subjected the human *ACHE* locus to genomic and transcriptional characterization aimed at explaining the reported diversity in the levels of the AChE protein between individuals and defining the molecular origin(s) for its involvement in stress responses. Our findings demonstrate ubiquitous expression of the m*ACHE* gene and even more so of the adjacent m*ARS* gene. Detection of clusters of consensus motifs for binding various transcription factors further explains the large number of

tissues expressing the *ACHE* gene. The apparent relevance of several of these factors for stress responses as well as the co-regulation of mAChE and mARS expression in the mouse brain points at this entire locus as a stress-responding one. Of special interest was the finding of a glucocorticoid response element 17 Kb upstream from the *ACHE* transcription start site, in a region where a deletion of 4 bp was found to be functionally involved in the regulation of AChE expression (Shapira et al., submitted).

The progressive cognitive failure of transgenic mice overexpressing the h*ACHE* gene (Beeri et al., 1995; Beeri et al., 1997) predicts a causal relationship between AChE overproduction and neurodeterioration. The stress-induced transcriptional activation of the *ACHE* locus (Kaufer et al., 1998; Kaufer et al., 1999; Shapira et al., submitted) suggests that psychological stress insults may therefore increase the risk for neurodeterioration due to AChE overproduction. While susceptibility for adverse responses to mental stress is most likely a complex trait, which involves many different genes, our findings point at the *ACHE* locus as an active participant in such processes. Participation of the *ARS* gene in these transcriptional processes seems very plausible, based on its apparent co-regulation with *ACHE*. However, the function of this gene product and its possible contribution to stress-associated processes is still unknown and remains to be explored. Variable capabilities to respond to stress insults by AChE overproduction would modify the efficacy of anti-AChE treatments or the severity of post-exposure symptoms in a manner related to the glucocorticoid hormone levels in the examined individuals. The *ACHE* locus thus emerges as a complex region subject to both genetic and epigenetic control processes that are relevant to cognition as well as to drug and poison responses.

Acknowledgements

This study was supported by the Medical Research and Development Command of the US Army (DAMD17-99-1-9547), the Israel Science Foundation (590/97), the German-Israel Foundation (I-0512-206.01/96), the Israel Ministry of Science (8433-1-97) and Ester Neuroscience, Ltd. (to H.S.). A.G. is an incumbent of a fellowship by the Friends of the Hebrew University, London.

References

Beeri, R., Andres, C., Lev Lehman, E., Timberg, R., Huberman, T., Shani, M., and Soreq, H. (1995). Transgenic expression of human acetylcholinesterase induces progressive cognitive deterioration in mice. Curr Biol *5*, 1063-71.

Beeri, R., Le Novere, N., Mervis, R., Huberman, T., Grauer, E., Changeux, J. P., and Soreq, H. (1997). Enhanced hemicholinium binding and attenuated dendrite branching in cognitively impaired acetylcholinesterase-transgenic mice. J Neurochem *69*, 2441-51.

Ben Aziz Aloya, R., Sternfeld, M., and Soreq, H. (1993). Promoter elements and alternative splicing in the human ACHE gene. Prog Brain Res *98*, 147-53.

Bentivoglio, A. R., Altavista, M. C., Granata, R., and Albanese, A. (1994). Genetically determined cholinergic deficiency in the forebrain of C57BL/6 mice. Brain Res *637*, 181-9.

Candeliere, G. A., Jurutka, P. W., Haussler, M. R., and St-Arnaud, R. (1996). A composite element binding the vitamin D receptor, retinoid X receptor alpha, and a member of the CTF/NF-1 family of transcription factors mediates the vitamin D responsiveness of the c-fos promoter. Mol Cell Biol *16*, 584-92.

Ehrlich, G., Viegas Pequignot, E., Ginzberg, D., Sindel, L., Soreq, H., and Zakut, H. (1992). Mapping the human acetylcholinesterase gene to chromosome 7q22 by fluorescent in situ hybridization coupled with selective PCR amplification from a somatic hybrid cell panel and chromosome-sorted DNA libraries. Genomics *13*, 1192-7.

Friedman, A., Kaufer, D., Shemer, J., Hendler, I., Soreq, H., and Tur-Kaspa, I. (1996). Pyridostigmine brain penetration under stress enhances neuronal excitability and induces early immediate transcriptional response. Nat Med *2*, 1382-1385.

Getman, D. K., Eubanks, J. H., Camp, S., Evans, G. A., and Taylor, P. (1992). The human gene encoding acetylcholinesterase is located on the long arm of chromosome 7. Am J Hum Genet *51*, 170-7.

Getman, D. K., Mutero, A., Inoue, K., and Taylor, P. (1995). Transcription factor repression and activation of the human acetylcholinesterase gene. J Biol Chem *270*, 23511-9.

Giacobini, E. (1998). Cholinergic foundations of Alzheimer's disease therapy. J Physiol Paris *92*, 283-7.

Grifman, M., Galyam, N., Seidman, S., and Soreq, H. (1998). Functional redundancy of acetylcholinesterase and neuroligin in mammalian neuritogenesis. Proc Natl Acad Sci U S A *95*, 13935-40.

Grisaru, D., Lev-Lehman, E., Shapira, M., Chaikin, E., Lessing, J. B., Eldor, A., Eckstein, F., and Soreq, H. (1999). Human osteogenesis involves differentiation-dependent increases in the morphogenically active 3' alternative splicing variant of acetylcholinesterase. Mol Cell Biol *19*, 788-95.

Haussler, M. R., Jurutka, P. W., Hsieh, J. C., Thompson, P. D., Selznick, S. H., Haussler, C. A., and Whitfield, G. K. (1995). New understanding of the molecular mechanism of receptor-mediated genomic actions of the vitamin D hormone. Bone *17*, 33S-38S.

Hirano, T. (1998). Interleukin 6 and its receptor: ten years later. Int Rev Immunol *16*, 249-84.

Kaufer, D., Friedman, A., Seidman, S., and Soreq, H. (1998). Acute stress facilitates long-lasting changes in cholinergic gene expression. Nature *393*, 373-7.

Kaufer, D., Friedman, A., Seidman, S., and Soreq, S. (1999). Anticholinesterases induce multigenic transcriptional feedback response suppressing cholinergic neurotransmission. Chemico-Biological Interactions.

Kim, J. J., Foy, M. R., and Thompson, R. F. (1996). Behavioral stress modifies hippocampal plasticity through N-methyl-D- aspartate receptor activation. Proc Natl Acad Sci U S A *93*, 4750-3.

Komori, T., Yagi, H., Nomura, S., Yamaguchi, A., Sasaki, K., Deguchi, K., Shimizu, Y., Bronson, R. T., Gao, Y. H., Inada, M., Sato, M., Okamoto, R., Kitamura, Y., Yoshiki, S., and Kishimoto, T. (1997). Targeted disruption of Cbfa1 results in a complete lack of bone formation owing to maturational arrest of osteoblasts [see comments]. Cell *89*, 755-64.

Lechner, J., Welte, T., and Doppler, W. (1997). Mechanism of interaction between the glucocorticoid receptor and Stat5: role of DNA-binding. Immunobiology *198*, 112-23.

Lemaire, P., Vesque, C., Schmitt, J., Stunnenberg, H., Frank, R., and Charnay, P. (1990). The serum-inducible mouse gene Krox-24 encodes a sequence-specific transcriptional activator. Mol Cell Biol *10*, 3456-67.

Liu, M., and Freedman, L. P. (1994). Transcriptional synergism between the vitamin D3 receptor and other nonreceptor transcription factors. Mol Endocrinol *8*, 1593-604.

Matsue, M., Kageyama, R., Denhardt, D. T., and Noda, M. (1997). Helix-loop-helix-type transcription factor (HES-1) is expressed in osteoblastic cells, suppressed by 1,25(OH)2 vitamin D3, and modulates 1,25(OH)2 vitamin D3 enhancement of osteopontin gene expression. Bone *20*, 329-34.

Melmer, G., Sood, R., Rommens, J., Rego, D., Tsui, L. C., and Buchwald, M. (1990). Isolation of clones on chromosome 7 that contain recognition sites for rare-cutting enzymes by oligonucleotide hybridization. Genomics *7*, 173-81.

Nitsch, R. M., Rossner, S., Albrecht, C., Mayhaus, M., Enderich, J., Schliebs, R., Wegner, M., Arendt, T., and von der Kammer, H. (1998). Muscarinic acetylcholine receptors activate the acetylcholinesterase gene promoter. J Physiol Paris *92*, 257-64.

Schwab, C., Bruckner, G., Castellano, C., Oliverio, A., and Biesold, D. (1990). Different levels of acetylcholinesterase and choline acetyltransferase activities in C57Bl/6 and DBA/2 mice are not accompanied with different density of cortical acetylcholinesterase reactive fibers. Neurochem Res *15*, 1127-33.

Shors, T. J., Weiss, C., and Thompson, R. F. (1992). Stress-induced facilitation of classical conditioning. Science *257*, 537-9.

Tora, L., Gaub, M. P., Mader, S., Dierich, A., Bellard, M., and Chambon, P. (1988). Cell-specific activity of a GGTCA half-palindromic oestrogen-responsive element in the chicken ovalbumin gene promoter. Embo J *7*, 3771-8.

Tronche, F., Kellendonk, C., Reichardt, H. M., and Schutz, G. (1998). Genetic dissection of glucocorticoid receptor function in mice. Curr Opin Genet Dev *8*, 532-8.

Xu, L., Anwyl, R., and Rowan, M. J. (1997). Behavioural stress facilitates the induction of long-term depression in the hippocampus. Nature *387*, 497-500.

Xu, L., Holscher, C., Anwyl, R., and Rowan, M. J. (1998). Glucocorticoid receptor and protein/RNA synthesis-dependent mechanisms underlie the control of synaptic plasticity by stress. Proc Natl Acad Sci U S A *95*, 3204-8.

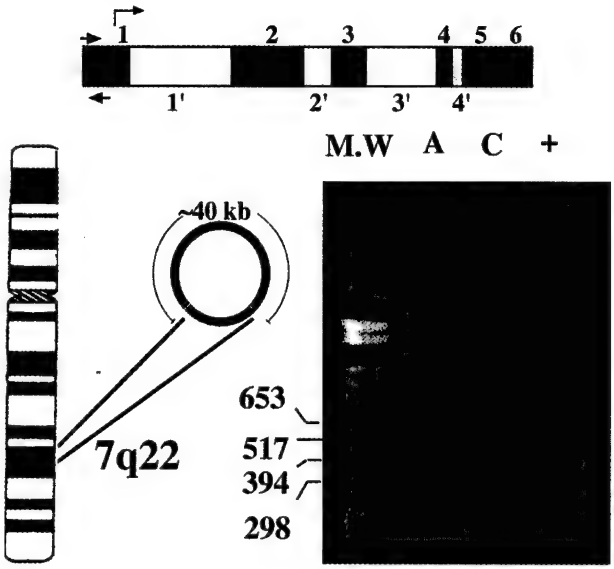

Figure 1. Schematic representation of the fully sequenced 7q22 cosmid. Shown is the output of the Grail program for the af002993 cosmid sequence. The lower strand encodes AChE and contains a 20 Kb upstream sequence. In the upper strand, the hRAS ORF has a strong homology with a Chinese hamster arsenite resistance gene (Genebank accession no. U41500). Other features are part of the Grail program output and include white columns representing predicted exons with different quality of prediction, different repetitive sequences, etc. AChE Transcription start site is nt. 22465 in af002993 reverse sequence.

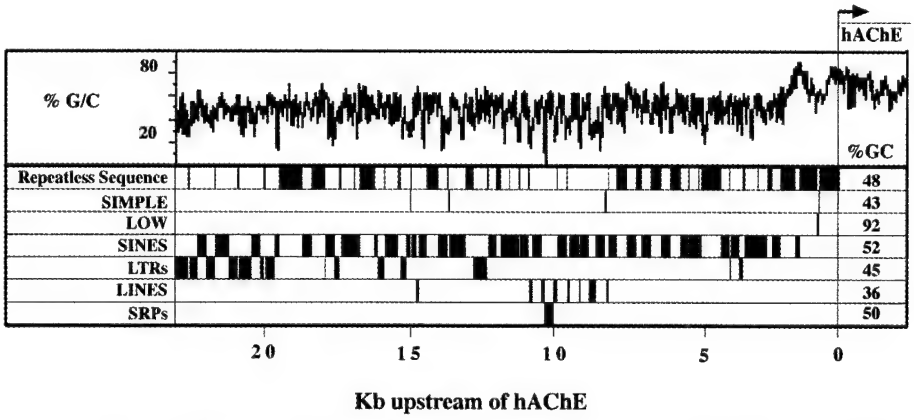

Figure 2. The AChE gene includes several clusters of stress-associated motifs. Depicted is the reverse sequence of the cosmid af002993 insert containing the human *ACHE* gene and its upstream sequence; nucleotide postions are designated accordingly. Arrow represents the transcription start site. Introns are designated with tagged numbers and exons are represented by filled boxes; alternatively spliced exons are filled with bright colors. Shown are regions with a relatively high incidence of consensus motifs for various proteins regulating stress-associated gene expression. Approximate positions are marked by wedges. Positions of various Vitamin D Receptor binding elements (VDREs) are marked by light grey circles: AGGACA; dark grey circles: AGGTCA; open rectangles: ATGCCA; hatched rectangels: GGTTCA; filled circles: GGGTGA; and dark grey rectangles: AGGTGA.

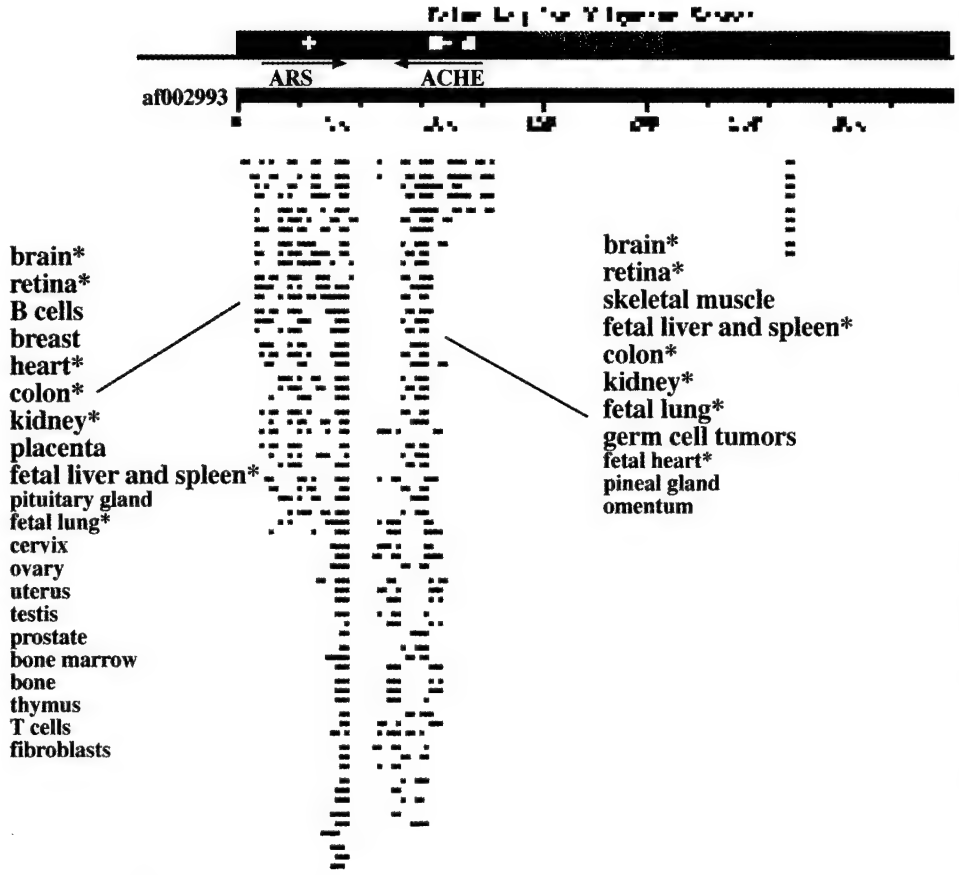

Figure 3. Mouse expression from the ACHE locus as reflected in the EST database. Shown is the graphical output of the Blast program run against the expressed sequence tags database using the af002993 cosmid as a query sequence and restricting the search to mouse clones. The identified ESTs are aligned against the corresponding regions of the query sequence, which is shown in red and scaled in bp, with ESTs colored according to their alignment score as depicted in the color key bar (black-hatched portions represent incontinuities in the alignments and therefore indicate introns). Designated are the *ARS* and *ACHE* gene regions and the tissue origins of the different ESTs. Asterisks designate tissues expressing both genes.

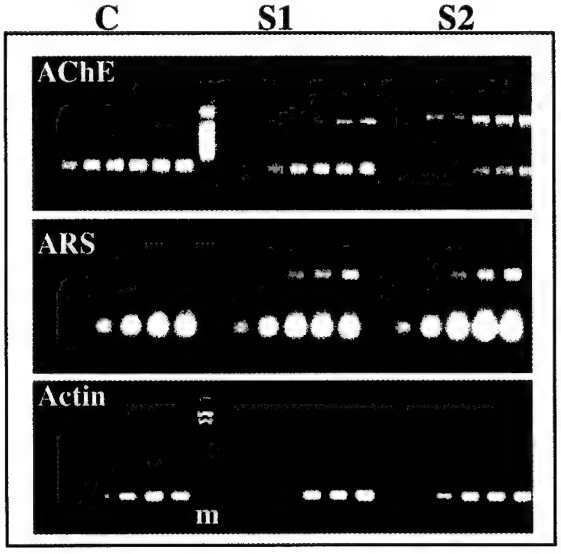

Figure 4. mARS expression is increased in the hippocampus of hAChE-overexpressing transgenic mice. Representative micrographs of ISH experiments performed on FVB/N mouse sagital brain sections obtained from control (A) and hAChE transgenic (B) mice (n=2 for each group). Shown are the CA1, CA2 and the dentate gyrus (DG) hippocampal structures, known to express AChE (Kaufer et al., 1998). Note the increase in ARS mRNA, (yellowish fluorescent signal) in both regions of transgenic mice.

Human Molecular Genetics, 2000, Vol. 9, No. 9 1273–1281

ARTICLE

A transcription-activating polymorphism in the *ACHE* promoter associated with acute sensitivity to anti-acetylcholinesterases

Michael Shapira[1], Ilan Tur-Kaspa[2], Leonard Bosgraaf[1], Nadav Livni[1], Alastair D. Grant[1], Dan Grisaru[1,3], Mira Korner[1], Richard P. Ebstein[4] and Hermona Soreq[1,+]

[1]Department of Biological Chemistry, Institute of Life Sciences, The Hebrew University of Jerusalem, Jerusalem 91904, Israel, [2]The IVF Unit, Department of Obstetrics and Gynecology, Barzilai Medical Center, Ben-Gurion University of the Negev, Ashkelon 78306, Israel, [3]Department of Obstetrics and Gynecology, Sourasky Medical Center, The Sackler School of Medicine, Tel Aviv University, Tel Aviv 64239, Israel and [4]The Research Laboratory, Herzog Hospital, PO Box 35300, Jerusalem 81351, Israel

Received 5 January 2000; Revised and Accepted 27 March 2000

Hypersensitivity to acetylcholinesterase inhibitors (anti-AChEs) causes severe nervous system symptoms under low dose exposure. In search of direct genetic origin(s) for this sensitivity, we studied six regions in the extended 22 kb promoter of the *ACHE* gene in individuals who presented adverse responses to anti-AChEs and in randomly chosen controls. Two contiguous mutations, a T→A substitution, disrupting a putative glucocorticoid response element, and a 4-bp deletion, abolishing one of two adjacent HNF3 binding sites, were identified 17 kb upstream of the transcription start site. Allele frequencies for these mutations were 0.006 and 0.012, respectively, in 333 individuals of various ethnic origins, with a strong linkage between the deletion and the biochemically neutral H322N mutation in the coding region of *ACHE*. Heterozygous carriers of the deletion included a proband who presented with acute hypersensitivity to the anti-AChE pyridostigmine and another with unexplained excessive vomiting during a fourth pregnancy following three spontaneous abortions. Electromobility shift assays, transfection studies and measurements of AChE levels in immortalized lymphocytes as well as in peripheral blood from both carriers and non-carriers, revealed functional relevance for this mutation both *in vitro* and *in vivo* and showed it to increase AChE expression, probably by alleviating competition between the two hepatocyte nuclear factor 3 binding sites. Moreover, AChE-overexpressing transgenic mice, unlike normal FVB/N mice, displayed anti-AChE hypersensitivity and failed to transcriptionally induce AChE production following exposure to anti-AChEs. Our findings point to promoter polymorphism(s) in the *ACHE* gene as the dominant susceptibility factor(s) for adverse responses to exposure or to treatment with anti-AChEs.

INTRODUCTION

Chemical hypersensitivity to xenobiotics causes adverse responses to normally subacute levels of a specific chemical, or a group of chemicals. Affected individuals may suffer from exaggerated immune response manifested as inflammation of epithelial and mucosal tissues (1,2). Alternatively, they may present altered capacity for scavenging, modifying or degrading a relevant chemical (3). The aberrantly processed chemical may cause toxicological stress in target tissues, with symptoms that vary in nature and timing according to the tissue, type of exposure and the permeability of the chemical. Mutations leading to such aberrant chemical metabolism were identified largely within coding regions, thus affecting detoxifying protein properties. However, impaired transcriptional activation of genes responsible for detoxification, due to mutations in their regulatory sequences, may be an equally important cause of chemical hypersensitivity. For example, the metal-chelating metallothioneins (4) and some members of the cytochrome P450 chemical-modifying enzyme family (5) respond to exposure to xenobiotics by transcriptional activation which increases protection. Impaired transcriptional activation due to promoter polymorphisms in such genes would hence cause chemical hypersensitivity.

Organophosphate and carbamate acetylcholinesterase inhibitors (anti-AChEs) are often implicated in chemical hypersensitivity (6,7). These agents impair neurotransmission (8,9)

+To whom correspondence should be addressed. Tel: +972 2 6585109; Fax: +972 2 6520258; Email: soreq@shum.huji.ac.il

and interact with both AChE and its serum homolog, butyrylcholinesterase (BuChE). Their toxicity has led recently to limitation of their use in the USA as agricultural or home-use insecticides (7,8,10). However, agricultural anti-AChEs are prolifically used in developing countries. Other anti-AChEs are employed as Alzheimer's disease drugs (11) or as prophylactic agents under anticipation of chemical warfare (12). Certain cases of anti-AChE hypersensitivity were attributed to decreased scavenging capacity in carriers of the mutant 'atypical' (6) or 'silent' (13) BuChE variants or to polymorphisms in the paraoxonase gene, *PON1* (14,15), encoding an organophosphate-hydrolyzing enzyme. However, many cases appear to have another, yet undefined origin(s) (16). Previous studies have shown that anti-AChEs promote overproduction of the *readthrough* AChE splice variant (AChE-R) in the mouse brain (17). This induction of AChE production, and the consequent increase in scavenging capacity, confer short-term protection during exposure to such chemicals (18). Conversely, we postulated that an impaired ability for such an induction would be associated with hypersensitivity to anti-AChEs. Impaired transcriptional response to chemical stressors may be due to deficient association with specific transcription factors. Functional polymorphisms affecting chemical hypersensitivity to anti-AChEs are therefore likely to be found close to consensus motifs for stress-associated transcription factors, e.g. the glucocorticoid receptor (GR) (19) or hepatocyte nuclear factor 3 (HNF3) (20).

Here, we describe the identification of two adjacent mutations in a distal upstream enhancer domain of the human (h)*ACHE* gene. One of the mutations, identified in a woman who presented with acute hypersensitivity to the anti-AChE pyridostigmine, was found to constitutively increase AChE expression by abolishing one of two adjacent HNF3 binding sites; the other impairs a GR binding site. Increased sensitivity and impaired transcriptional response to anti-AChEs were also observed in transgenic mice overexpressing hAChE. Moreover, these mice presented increased expression of HNF3β in target tissues. Altogether, our findings imply an association of *ACHE* promoter polymorphism(s) with anti-AChE hypersensitivity by way of a mechanism that probably involves both early modulators such as the HNF3β transcription factor and the downstream responding *ACHE* gene.

RESULTS

Genotyping and sequencing of promoter regions in the *ACHE* locus

Genomic DNA from 103 subjects, including several individuals who suffered cholinergic symptoms under anti-cholinesterase exposure, was subjected to length polymorphism analysis at each of the six regions detailed in Materials and Methods. This analysis identified a 4-bp deletion in region I of the *ACHE* promoter in three heterozygous carriers, including proband I, her mother and proband II. Region I, rich in consensus binding sequences for various transcription factors, includes two sites, 19 bp apart, for binding HNF3β or HNF5/HNF3α. The more upstream of these sites partially overlaps a glucocorticoid response element (GRE) half-palindromic site (Fig. 1B, top) and is abolished by the newly identified deletion (Fig. 1B, bottom). Further screening of region I in 230

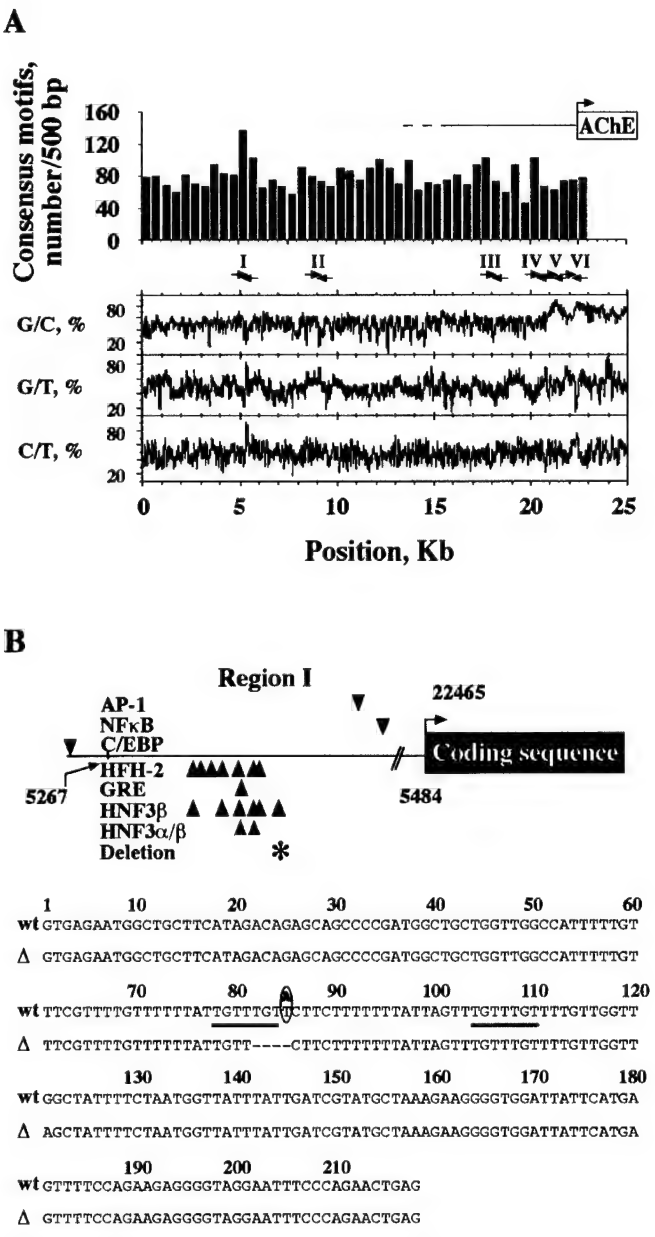

Figure 1. *ACHE* promoter polymorphism in the hypersensitive proband I. (**A**) Selecting domains prone to effective polymorphism in the h*ACHE* upstream region. (Top) Density of consensus motifs. Shown are cumulative numbers of consensus motifs in 500 bp regions along the AF002993 cosmid reverse DNA sequence. Arrow above represents the *ACHE* transcription start site (nt 22465 in the cosmid sequence; 37,38). (Bottom) Nucleotide pair patterns. Shown are percentages of the noted nucleotide pairs counted in 60 bp windows and 3 nt shifts along the AF002993 DNA. Peaks and troughs represent homogeneous sequences; arrow-delineated Roman numerals represent approximate positions of primer pairs designed to amplify the regions of interest. Note the high number of consensus motifs located in region I. (**B**) Characteristics of the polymorphic region I. (Top) Consensus binding sites for transcription factors in region I. Presented (triangles) are approximate positions within region I of binding sites for the transcription factors designated on the left. Sites with complete consensus sequences as well as the GRE half-palindromic site (42), TGTTCT, were located using FindPatterns of the GCG software package and the MatInspector program (34). Gray triangles represent consensus sequences known to bind either HNF3α or HNF3β; the asterisk designates the mutated binding site. The first and last nucleotides of region I as well as the transcription start site are marked. (Bottom) Region I sequence. Presented is the normal region I sequence (wt; the T/A substitution is circled) aligned with the mutant sequence allele carrying the 4-bp deletion (Δ). Nucleotide 1 is 5267 in the AF002993 cosmid reverse sequence. The two HNF3 consensus binding sites are underlined.

Table 1. Allele frequencies of cholinesterases gene mutations

Mutation (position[a])	Allele frequency	Sample size	Genotype	Additional linked *ACHE* mutations
ACHE Δ4 (–17116)	0.012	333	all heterozygous	5× H322/N322[d]
ACHE T→A (–17113)	0.006	333	all heterozygous	none
BCHE	0.025	177[c]	7× heterozygous,	ND
D70G[b]			1× homozygous	

Mutation detection was achieved by length polymorphism analysis (for ACHE Δ4) or by PCR and subsequent sequencing (for *ACHE* T→A, *ACHE* H322N and the *BCHE* D70G mutation).
[a]Positions are relative to *ACHE* transcription start site.
[b]The mutation responsible for the 'atypical' BuChE variant.
[c]This is a subset of the sample used for *ACHE* mutation screening.
[d]The biochemically neutral H322N mutation is responsible for the Yt[b] blood group. Screening was performed in six carriers of *ACHE* Δ4, three carriers of *ACHE* T→A and 16 non-carriers.
ND, not determined.

additional individuals identified a second mutation, a T→A substitution, which impairs the GRE (Fig. 1B, bottom), and established the allele frequencies of the deletion and the substitution as 0.012 and 0.006, respectively (Table 1), in conformity with a Hardy–Weinberg distribution. Although one carrier of the deletion was hospitalized for multi-infarcts, no increase was detected in the prevalence of any of these mutations in 100 patients hospitalized for infarcts. Carriers of both mutations, who were of various ethnic origins, were additionally screened for the H322N mutation in *ACHE* (21). Five of the six screened deletion carriers were found to be heterozygous for this mutation as well (Table 1). This compares with two heterozygous individuals out of 16 screened non-carriers. No linkage was found between the T→A substitution and the H322N mutation.

Of the total 333 individuals, 177 were also screened for the *BCHE* 'atypical' allele. The allele frequency of 0.025 determined for this sample (Table 1) agrees with the reported frequency range of 0.015–0.05 for 'atypical' *BCHE* in different ethnic groups of the Israeli population (21). In the group currently being analyzed, none of the individuals directed to us due to suspected anti-AChE sensitivity, nor the carriers of the *ACHE* promoter mutations, carried the *BCHE* 'atypical' allele.

Increased basal levels of blood AChE in carriers of the 4-bp deletion

Two carriers of the deletion showed symptoms that may be associated with cholinergic excitation (see Materials and Methods). Proband III displayed gastrointestinal distress compatible with peripheral nervous system (PNS) excitation, which could be attributed to pesticide exposure in her home vicinity, a crop-growing area. Proband I suffered characteristic acute anti-AChE intoxication in response to a subacute dose of the carbamate anti-AChE pyridostigmine. Several years after this incident, peripheral blood AChE levels were measured in proband I as well as in her parents and were found to be slightly higher than normal in both the proband and her mother (Fig. 2A). No differences were found in serum BuChE activity levels, in BuChE inhibition by succinylcholine or in the *BCHE* gene sequence (data not shown), excluding BuChE abnormalities and its potential involvement in the proband's phenotype. Epstein–Barr virus (EBV)-transformed lymphoblast cell lines were established from the second carrier (proband II) and from

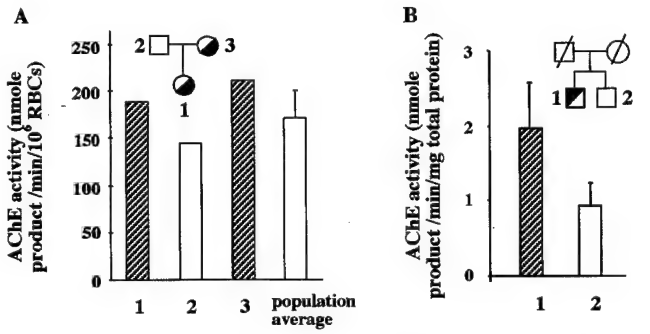

Figure 2. Increased AChE activity levels in blood from carriers of the 4-bp deletion. (**A**) Red blood cell (RBC) AChE levels in proband I, family and control individuals. Shown is the pedigree of proband I, with the proband and her mother heterozygous for the 4-bp deletion (half-filled circles, see below). Columns present means of triplicate measurements of specific AChE activity in RBC fractions from members of the proband's family. For the control population, presented are mean ± standard deviation (n = 20). (**B**) AChE levels in EBV-transformed lymphoblasts from a deletion-carrying individual and his non-carrier brother. Presented are AChE activity levels in homogenates of EBV-transformed lymphoblast cell lines established from peripheral blood of proband II, a carrier of the 4-bp deletion and his non-carrier brother, as depicted in the pedigree. Shown are means and standard deviations of AChE levels in seven separate homogenates normalized to total protein measured with the Bio-Rad $^{D}_{C}$ protein assay kit (Bio-Rad, Hercules, CA).

his non-carrier brother, both negative for the 'atypical' *BCHE* mutation. These cells showed significantly higher AChE activity levels for the deletion carrier than for his brother (Fig. 2A).

HNF3β binding assays

The functionality of the two putative HNF3 binding sites in region I was confirmed by electromobility shift assays (EMSAs). Probes containing either one or both of the normal sites all displayed a mobility shift when incubated with cell extracts from HNF3β-overexpressing COS cells (Fig. 3A). An additional supershift caused by rat HNF3β-specific polyclonal antibodies identified the binding activity as HNF3β. In contrast, the mutated upstream site was unable to bind HNF3β, or to compete with the normal upstream site probe for HNF3β binding. Nevertheless, the deletion did not interfere with HNF3β binding to the intact downstream site in a probe representing the mutant allele (Fig. 3A).

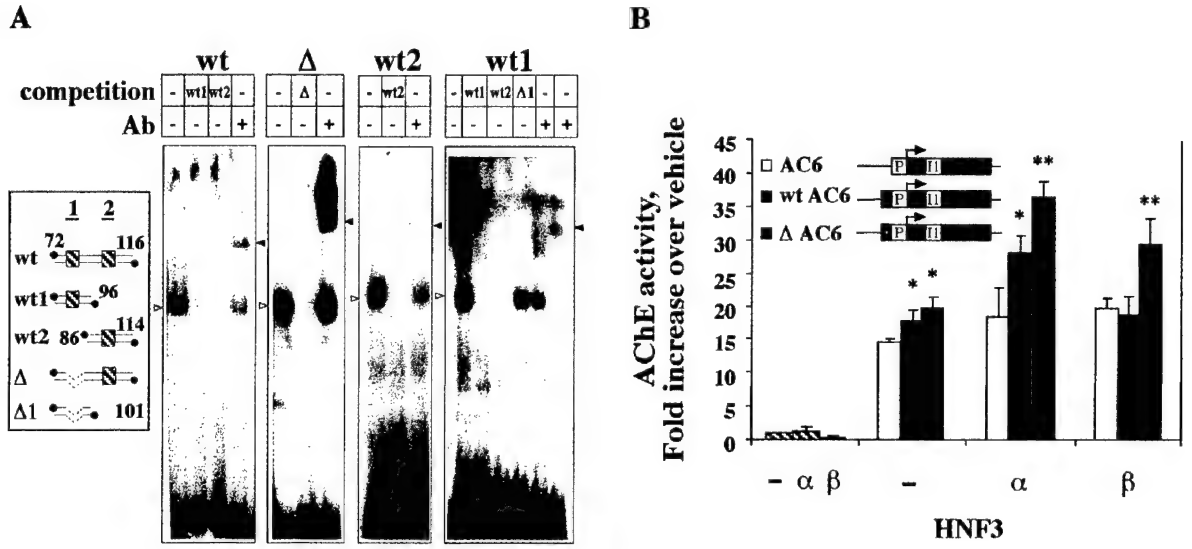

Figure 3. Functional characterization of region I deletion. (**A**) Gel mobility shift assays reveal differential HNF3β affinities for the two normal and one mutant region I sites. EMSA gel images show shifted probe bands (open triangles), as well as supershifted bands (filled triangles; Ab, antibody in a 1:1000 or 1:500 dilution for wt1 in the two right lanes, respectively). Probes used for each assay are designated above the respective table. (Inset) Presented are the 5′ end-labeled (filled circles) double-stranded oligodeoxynucleotides tested for the binding capacities of the normal and mutant domains in region I. Numbers are as in Figure 1B, bottom. Putative HNF3-binding sites on these probes are boxed and numbered. (**B**) Differences in transcription activation abilities of the normal and mutant region I sequences. (Inset) Presented are AChE expression constructs used for transfection experiments. Designated are region I normal and variant fragments (dark gray boxes; deletion dotted), the minimal promoter (P), intron 1 (I1), and numbered exons (E). Columns show fold increase values of AChE activities in COS cells transfected with AC6 (open bars), wtAC6 (closed bars) or the ΔAC6 vector (shaded bars), either alone or together with constructs encoding the designated rat transcription factors, both under control of the rat phosphoglycerate kinase-1 promoter. Cross-hatched columns represent transfections with constructs encoding the transcription factors alone. Shown are average specific AChE activities in cell lysates from five transfection experiments as compared with those of cells treated with Lipofectamine alone, in the same set (–). Asterisks mark activities significantly different ($P < 0.01$, Scheffe's test) from those in lysates of cells transfected with AC6 alone. Double asterisks mark an additional significant difference between the wild-type and mutant groups.

The 4-bp deletion increases HNF3β-induced *ACHE* gene expression

To test whether HNF3 binding to the identified sites can modulate transcription from the h*ACHE* gene, we employed the AC6 AChE promoter–reporter DNA constructs to which we added the normal (wtAC6) or deleted (ΔAC6) region I sequence. When transfected into COS cells, each of these three constructs directed h*ACHE* expression, with both versions of region I slightly enhancing the minimal promoter's effect (Fig. 3B). Co-transfection with a construct encoding rat HNF3α increased AChE expression by 50 and 100% for the normal and mutant versions, respectively, compared with the minimal promoter. Rat HNF3β increased AChE expression by 60% for the mutant, but had no effect on the normal allele. Hence, region I includes a functional HNF3-dependent enhancer and the 4-bp deletion increases its effect on AChE expression.

Inherited increases in AChE basal levels impair its anti-AChE-induced overexpression and increase sensitivity to these inhibitors

To test whether AChE overexpression impairs individual responses to subacute doses of anti-AChEs, we used transgenic mice overexpressing human synaptic AChE (22). Exposure to a subacute dose of pyridostigmine caused severe diarrhea in hAChE-transgenics as compared with mild symptoms in control FVB/N mice. Additionally, average survival time under exposure to a lethal dose of diisopropylfluorophosphate (DFP) was 1.9 ± 0.4 min for hAChE-transgenic mice as compared with 5.5 ± 3.3 min for age- and sex-matched control mice ($n = 4$ for each group; $P < 0.05$, Student's t test). Two hours after exposure to a subacute dose of DFP, intestinal AChE was found to be inhibited to 49 ± 38% and 38 ± 7% of its initial activity in transgenic and normal mice, respectively. *In situ* hybridization revealed ~5-fold increases in the stress-associated AChE-R mRNA transcripts in the small intestine (known to express HNF3β) (23) of normal mice. Labeling was localized primarily to the intestinal epithelium, muscularis mucosa and intestinal gland regions where proliferation of epithelial cells takes place (Fig. 4). In contrast to normal mice, transgenics displayed initially higher levels of intestinal AChE-R mRNA, yet showed no significant difference between DFP- and saline-injected groups (Fig. 4).

HNF3β and AChE are co-expressed in hematopoietic progenitors and in the brain

To contribute to anti-AChE responses, HNF3β would be expected to be expressed in AChE-producing cells, which respond to anti-AChE exposure. To examine whether this basic condition is met, HNF3β mRNA was searched for in brain and blood cells by reverse transcriptase–polymerase chain reaction (RT–PCR) and *in situ* hybridization (ISH) analyses. HNF3β production was identified in cortical, cerebellar and hippocampal neurons in the mouse brain (Fig. 5A and data not shown) as well as in AChE-expressing megakaryocytes, lymphocytes and CD34-positive human blood cell progenitors

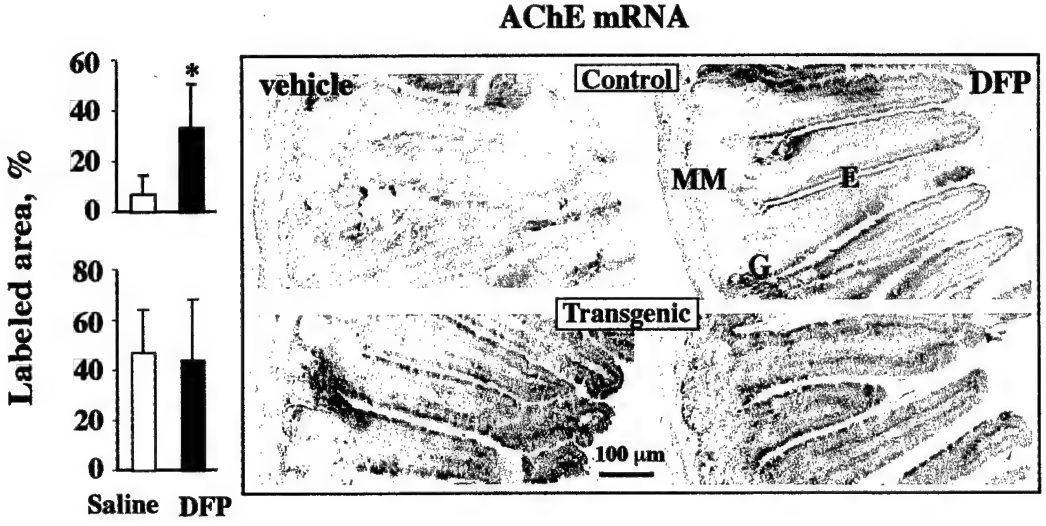

Figure 4. Anti-AChE exposure induces trasncriptional AChE activation in the intestine of normal but not AChE-overexpressing transgenic mice. Presented are representative transverse ileum sections prepared from mice 2 h post-injection (i.p., 1 mg/kg body weight) of DFP or saline. Columns present AChE-R mRNA signal quantified in similar micrographs as percentages of labeled area out of the villus area (means of two to five villi from two to six animals, one to three separate experiments for each animal ± standard deviation). Asterisks denote statistically significant differences ($P < 0.01$, Scheffe's test). Note the drastic increase in AChE-R mRNA levels within the intestinal epithelium (E), the muscularis mucosa (MM) and the intestinal gland (G) regions of DFP-treated normal mice.

(Fig. 5B). Involvement of HNF3β with the impaired transcriptional response to anti-AChE exposure would further predict altered HNF3β expression in AChE-overproducing mice. In keeping with this expectation, brain HNF3β expression, which was barely detectable in normal mice, was conspicuously higher in AChE-overexpressing transgenics (Fig. 5A). Impaired responses to anti-AChE exposure in AChE-overexpressing mammals can therefore include HNF3 contribution in brain, blood and intestinal epithelium alike.

DISCUSSION

We have identified a transcription activating deletion in a distal enhancer domain of the human *ACHE* promoter and demonstrated impairment of the transcriptional activation response to anti-AChE exposure in transgenic mice overproducing AChE. In both mice and humans, AChE overproduction was associated with anti-AChE hypersensitivity. Together, this suggests *ACHE* promoter polymorphisms as novel susceptibility factors for anti-AChE hypersensitivity.

Previously described polymorphisms in the coding regions of *BCHE* (6) and *PON1* (14,15) genes were reported to predispose homozygous carriers to slowly manifested central nervous system (CNS) symptoms of anti-AChE poisoning (6,15). In contrast, the *ACHE* promoter deletion is manifested in dominant and rapidly developing PNS symptoms in heterozygous carriers. The allele frequency of 0.012 defines this deletion as a rare polymorphism in the Israeli population. The other mutation in this region of the *ACHE* promoter, a T→A substitution, was found to be even less abundant, with an allele frequency of 0.006. As carriers of both mutations are of diverse ethnic origin, it is conceivable that these mutations have more than one founder. However, the higher prevalence of the H322N mutation in carriers of the promoter deletion, compared with the reported allele frequency range of 0.06–0.19 in different ethnic groups of the Israeli population (21), suggests a strong linkage between the two mutations.

DNA sequencing, EMSAs and transfection experiments demonstrated that the transcription activation conferred by the 4-bp deletion was due to elimination of a functional binding site for transcription factors of the HNF3 family. HNF3β is known to enhance transcription of several genes through distal enhancer domains (e.g. mouse serum albumin) (24). When included in constructs carrying the normal allele and tranfected into COS cells, the normal HNF3 site hampered transcriptional activation, probably by interfering with HNF3 binding to a second site located 19 bp (~65 Å) downstream. The higher steady-state blood AChE levels in carriers of the mutation and the elevated expression in immortalized lymphoblasts from such a carrier, compared with normal homozygotes, imply that similar activation occurs when the enhancer domain is in its natural context.

That AChE overexpression may hamper anti-AChE responses was shown in transgenic mice, which presented with hypersensitivity to anti-AChEs, accompanied by impairment in the transcriptional activation of AChE production. Such activation was shown previously to occur in the brain, both under inhibition and in response to psychological stress (25). Our current findings suggest that transcriptional AChE overproduction in intestinal endothelium may contribute towards overcoming toxicological stress by offering protection to the peripheral cholinergic systems. While the detailed cause of impairments in the transcriptional activation of AChE remain to be uncovered, one possible factor may be HNF3β which presents increased transcription in the brains of AChE-overexpressing mice.

AChE overproduction was manifested under exposure to both the slowly reversible inhibitor pyridostigmine (17) and the irreversible inhibitor DFP (this report). Such feedback response should be crucial for overcoming exposure to irreversible inhibitors, yet is also important during exposure to slowly reversible

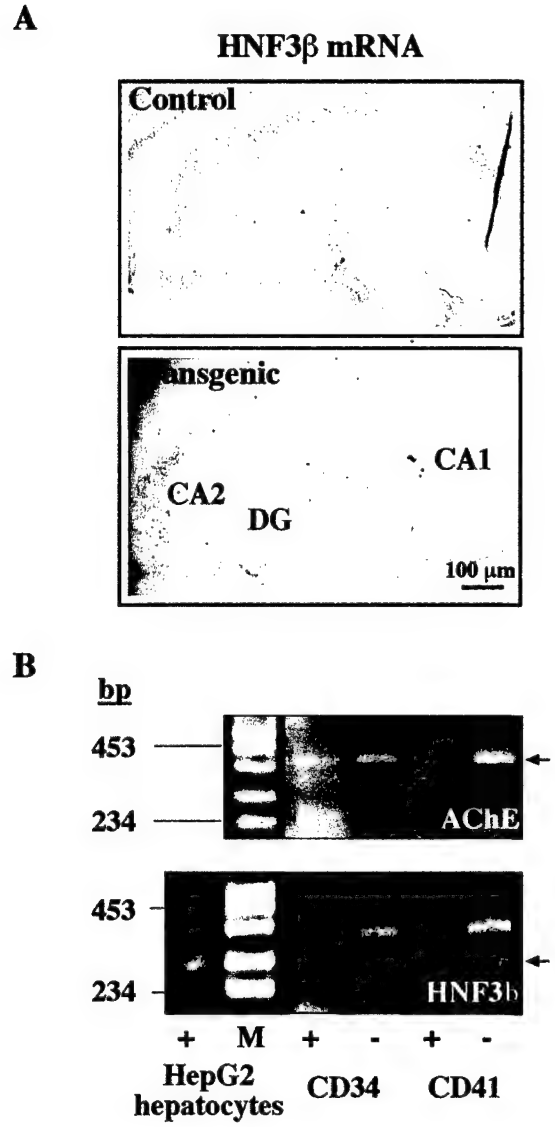

Figure 5. HNF3β is elevated in the brain of hAChE-overexpressing mice and is co-expressed with AChE in diverse human hematopoietic lineages. (**A**) Hippocampal expression of HNF3β increases in transgenic mice. Representative micrographs of ISH experiments performed on FVB/N mouse sagital brain sections obtained from control and transgenic mice (n = 2 for each group). Shown are the CA1, CA2 and the dentate gyrus (DG) hippocampal structures, known to express AChE (17). Note the increase in HNF3β mRNA, (red signal) in both regions of transgenic mice. (**B**) Hematopoietic expression. presented are RT–PCR products amplified using primers specific for the domain common to all hAChE splice variants (top) or for rat HNF3β (bottom), from RNA of human hematopoietic cells, sorted by flow cytometry from umbilical cord blood (43). Shown are products from CD34-positive progenitor cells (CD34$^+$), CD34-negative fully committed white blood cells and megakaryocytes (CD34–), mature megakaryocytes (CD41$^+$) and white blood cells (CD41–). All express AChE and the expected ~300 bp HNF3β product (arrow; also produced in the liver carcinoma HepG2 cell line) accompanied by an ~400 bp unidentified product. M, size marker. No products appeared in control reactions containing no RT (data not shown).

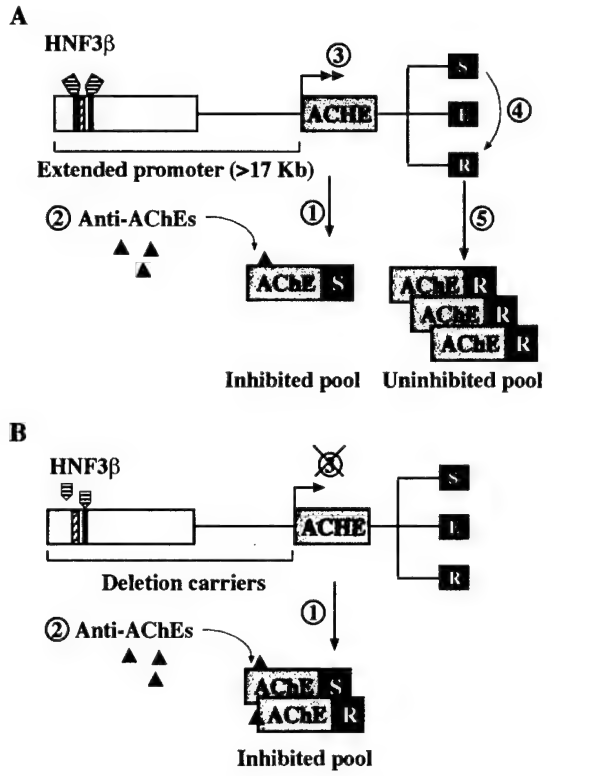

Figure 6. Constitutive AChE overproduction impairs the feedback response to anti-AChEs. (**A**) Transcriptional AChE overproduction and alternative splicing confer protection by increasing scavenging capacity. The scheme shows the *ACHE* gene and its extended promoter, with the two adjacent HNF3β binding sites (black boxes) and an additional binding site for the glucocorticoid receptor (diagonally hatched box). Numbered steps display the tentative pathway of anti-AChEs responses, as follows. (1) Under normal conditions, the major transcript in both the CNS and PNS is the synaptic variant (AChE-S); hematopoietic cells express preferentially the GPI-anchored AChE-E isoform. (2) Anti-AChEs bind to the active site in the core domain common to all AChE isoforms. This elevates acetylcholine levels, causes cholinergic excitation and thus mimics stress conditions (25). (3) Cholinergic excitation causes enhanced transcription, possibly via the c-*fos* transcription factor, which is thought to activate AChE transcription under stress (17). (4) Newly transcribed AChE mRNA is produced. Alternative splicing preference is for production of AChE-R mRNA instead of AChE-S mRNA. (5) Consequently, a new pool of uninhibited, hyper-sensitive AChE-R molecules accumulates in the tissue, increasing its inhibitor scavenging capacity. (**B**) Deletion carriers may fail to respond by transcriptional overproduction due to constitutive AChE accumulation. With one HNF3β site missing, the remaining site is more effectively activated by the transcription factor, causing constitutive AChE overproduction (1). This leads to AChE accumulation of which at least a part comprises AChE-R molecules. Anti-AChEs (2) would therefore inhibit preferentially the more sensitive AChE-R variant, leaving some enzyme (possibly AChE-S, or AChE-E in the case of hematopoietic cells) uninhibited. However, the feedback response (3) is impaired. This is apparently crucial for replenishing the enzyme pool to an extent sufficient to suppress acute post-exposure symptoms.

ones. Thus, *de novo* synthesis of a new pool of uninhibited enzyme, to replace the non-functioning pool offers a major pathway for down-regulating inhibitor-induced hyper-excitation. The feedback response to anti-AChE exposure preferentially produces the alternatively spliced stress-associated AChE-R variant (ref. 17 and this report). AChE-R displays significantly higher inhibition constants for several anti-AChEs as compared with the normally produced 'synaptic' AChE-S variant (A. Salmon and H. Soreq, unpublished data). The increased anti-AChE scavenging capacity of AChE-R supports the notion of its involvement with exposure responses, as it would protect the functionally essential synaptic isoform. However, constitutive AChE overproduction such as that occurring in heterozygous carriers of the upstream deletion may prevent sufficient overpro-

duction of these scavenging AChE molecules (Fig. 6). Under exposure, such carriers would therefore lack a fresh pool of uninhibited enzyme, providing a plausible explanation of their apparent hypersensitivity.

HNF3 has been reported to participate in the acute-phase response of the liver to trauma or inflammation (20). In addition to its known expression patterns (23), we found HNF3β to be expressed in hematopoietic cells and hippocampal neurons, both of which are known for their rapid toxicological stress responses (17,26). Our current findings further demonstrate that overexpression of AChE leads to HNF3β overproduction and creates a predisposition to adverse responses to anti-AChE exposure. The greater sensitivity presented by the hAChE-transgenic mice within minutes of exposure to anti-AChEs, suggests a prior, permanent change in the cholinergic system of these mice which is also attributed to AChE overexpression. This change can be caused by the overexpressed HNF3β; alternatively, it may involve non-catalytic functions of AChE, such as its previously reported roles in proliferation and differentiation of various cell types (27). Altogether, this predicts the participation of HNF3-regulated AChE in toxicological stress responses in many tissues, and points to HNF3β as a more general stress-responsive protein than previously realized. AChE regulation by HNF3β may be further influenced by the ubiquitous stress-related GR (19), known to act with HNF3 either synergistically (28) or competitively (29), plausibly affecting the choice between the two HNF3-binding sites in the *ACHE* promoter.

We identified the polymorphic region in the h*ACHE* upstream sequence by combined search for regions of sequence homogeneity rich in clustered transcription factor binding motifs. Similar screens may be useful for future identification of polymorphisms, especially in individuals with chemical hypersensitivity and in genes that are subject to transcriptional activation under chemical exposure. The deletion identified in the *ACHE* promoter appears particularly interesting for screening in individuals suffering from multiple chemical sensitivity (MCS)—a phenomenon still awaiting a clear case definition—which involves multi-organ adverse responses (e.g. gastrointestinal distress and neurological disorders) to normally subacute levels of diverse chemicals (30,31). This syndrome is believed to be caused by neuronal sensitization in specific regions of the CNS limbic system (32). Both stress and anti-AChEs have been shown to elevate AChE expression and to cause cholinergic excitation in the mouse brain (17). As the limbic system is modulated by cholinergic neurons, among others (33), the anti-AChE hypersensitivity presented by proband I suggests a link between increased AChE levels and such MCS-related sensitization.

To conclude, this polymorphism, located 17 kb upstream of the h*ACHE* transcription start site, identifies a new HNF3-binding enhancer domain important for AChE expression. Heterozygosity for the deletion is manifested as constitutive overproduction of AChE; such overproduction, which increases the susceptibility to acute anti-AChE exposures in mice, is likely to be the cause of the hypersensitivity of proband I to pyridostigmine. The proposed link between this mutation and the hypersensitivity points to carriers of this allele as individuals at risk of developing adverse responses under treatment with or exposure to anti-AChEs, which is important in view of the increasing use of anti-AChEs as Alzheimer's disease drugs (11). Moreover, stress- or anti-AChE-induced increases in AChE levels (17) may cause acquired anti-AChE sensitivity, putting at risk a considerably wider group of individuals (7). This type of chemical hypersensitivity therefore emerges from our study as a complex trait, perhaps involving both early modulators such as transcription factors and downstream responding genes.

MATERIALS AND METHODS

Subjects

A total of 333 individuals were investigated. Of these, 20 were directed to us for investigation of unexplained symptoms with apparent cholinergic involvement, or were family members of such individuals. The majority were randomly selected, with various medical histories and no reported chemical sensitivity. One hundred were older patients hospitalized due to infarcts. The study was approved by the Institutional Review Board of the Herzog Hospital.

Case reports

Proband I, a 30-year-old woman of Ashkenazi Jewish origin and no significant history of adverse drug responses, received a single oral dose of 30 mg pyridostigmine, a dose considered safe, which is given prophylactically under anticipation of chemical warfare (12). Within 1 h, peripheral blood AChE fell to an almost undetectable level, increasingly severe muscle fasciculations developed, accompanied by intense headache, rhinorea, lacrimation and frequent urination. These acute symptoms continued for 3 days, and resolved into a 5-day period of extreme fatigue, muscle weakness and general malaise.

Proband II, a 72-year-old man, was hospitalized due to a multi-infarct dementia, a condition caused by blood flow deprivation during a multi-focal stroke, which damages several brain regions.

Proband III was a 39-year-old woman of Turkish origin with a history of three spontaneous abortions performed under general anesthesia who suffered from excessive unexplained vomiting during a fourth pregnancy.

Selection of screened promoter regions

Promoter regions prone to transcription-modifying polymorphisms were sought in a cosmid clone (GenBank accession no. AF002993) spanning the h*ACHE* gene and ~22 kb of its upstream sequence. Clusters of putative transcription factor binding elements were identified using the MatInspector 2.0 program (34) (core similarity of 1, matrix similarity of 0.85; Fig. 1A, top). Homogeneous sequence regions rich in nucleotide pairs and susceptible to slippage mutation (35) were identified using the Window statistical program of the University of Wisconsin GCG software package (Fig. 1A, bottom). The combined searches yielded six regions of interest: region I, which spans a cluster of putative binding elements (e.g. glucocorticoid response, hepatic and ubiquitous transcription factors such as AP-1) and is G/T-rich; region II, with high C/A content and a 30-nt G/A-rich domain; regions III–V, containing sequence motifs suspected of forming protein-binding DNA secondary structures (36); and region VI, reported to be important for *ACHE* transcription (37,38).

Length polymorphism analysis

Screening involved PCR amplification of assigned genomic DNA regions from peripheral blood lymphocytes, using flanking primer pairs with forward primers 5′-labeled with the fluorophore 6-FAM (Applied Biosystems, Foster City, CA). Electrophoresis (ABI377 automated sequencer, Applied Biosystems) included an internal size marker labeled with a second fluorophore, TAMRA (Applied Biosystems). Fragment length was determined by the ABI GeneScan analysis program. Primers spanned nucleotides 5267–5484 (region I), 9173–9606 (II), 18149–18435 (III), 20709–21029 (IV), 21485–21673 (V) and 22259–22534 (VI), numbered as in the AF002996 reverse sequence.

Genetic screening

DNA samples were subjected to length polymorphism analysis as well as sequencing of region I of the *ACHE* promoter; samples from 177 individuals were also screened for the D70G 'atypical' *BCHE* allele (21) by PCR and subsequent sequencing. All samples positive for mutations in the promoter were also screened for the catalytically neutral H322N polymorphism in the *ACHE* coding region (21).

Cholinesterase assays

AChE and BuChE activity levels were assessed by measuring rates of acetylthiocholine or butyrylthiocholine hydrolysis, respectively, as described previously (6).

Plasmid constructs

Constructs were engineered using amplified DNA fragments from normal (wt) or mutant (Δ) genomic DNA using primers 5267(+) and 5484(–). Ligation upstream of a minimal 600 bp fragment of the h*ACHE* promoter (37) in the AC6 construct yielded wtAC6 and ΔAC6, both encoding human AChE as a reporter.

Cell cultures, transfection and harvesting

COS-1 cells were grown in a humidified chamber in Dulbecco's modified Eagle's medium (Biological Industries, Beit Ha'emek, Israel) supplemented with 10% fetal calf serum (FCS) and 2 mM L-glutamine at 37°C, 5% CO_2. Lymphocytes transformed with EBV were used to create lymphoblast cell lines (39). These were grown similarly to COS-1 with 16% FCS. Transfections of COS cells with 2 μg plasmid DNA per well were carried out using Lipofectamine (Gibco BRL Life Technologies, Bethesda, MD) according to the manufacturer's instructions. Cell homogenates, prepared 2 days post-transfection in phosphate-buffered saline (PBS) containing 1% Triton X-100, were assayed for AChE activity, which is not affected by this detergent. For EMSAs, cells were harvested with cold PBS and homogenized in a buffer containing 10 mM NaH_2PO_4, 400 mM KCl, 10% glycerol, 1 mM dithiothreitol (DTT), 5 μg/ml aprotinin, leupeptin and pepstatin A, and 5 μM NaF. Supernatants, divided into aliquots, were stored at –70°C until use.

Electromobility shift assays

EMSAs were performed using dsDNA probes homologous to restricted parts of region I, essentially as detailed elsewhere (40). Briefly, ~0.5 ng ^{32}P-labeled dsDNA was incubated (2 h on ice) in a total volume of 36 μl of 150 mM KCl, 83 μg/ml poly(dIdC:dIdC), 5 mM DTT, 1 mM EDTA, 5 mM $MgCl_2$, 12% glycerol, 15 mM Tris pH 7.5 and ~20 μg protein from whole cell extracts. Reaction products were electrophoresed in 5% polyacrylamide gels. For competition experiments, a 100-fold molar excess of the corresponding unlabeled probe was used. Pre-incubation of protein extracts (20 min on ice) with anti-HNF3β polyclonal antibodies (1:1000 dilution) was employed for supershift assays.

RT–PCR

Reactions were performed as described elsewhere (37). Primers designed according to rat HNF3β (numbered as in accession no. L09647) were 219(+) and 518(–). Primers for hAChE (numbered as in AF002993) were 25587(+) and 26968(–). Annealing temperatures were 55 and 65°C, respectively. Plus and minus denote forward and reverse primers, respectively.

In situ hybridization

ISH was performed as described elsewhere, using a fluorescent product (41) or the Fast-red product (Boehringer-Mannheim GmbH, Germany) (17) for labeling. Biotinylated, 2′-*O*-methylated cRNA probes were used, complementary to rat HNF3β mRNA (positions 281–330 in sequence accession no. L09647) or to mouse AChE-R (positions 32–81 in M76540). Fluorescent signal quantification involved one to three sections from separate animals and ISH experiments. Intact villi (excluding the cell-shedding villus tips) were selected using the Adobe Photoshop program. Following determination of signal range, the percentage of labeled areas out of the total selected areas was calculated.

Animal experiments

Mice were injected i.p. with either 1 mg/kg body weight (in ISH experiments) or 7 mg/kg (for survival experiments) of the organophosphate anti-AChE DFP (Sigma, St Louis, MO). Pyridostigmine (0.2 mg/kg; Sigma) served for testing sensitivity to anti-AChEs. Mice were killed 2 h after injection. All experiments were approved by the Committee for Animal Experimentation at the Institute of Life Sciences.

ACKNOWLEDGEMENTS

We thank Dr Lap-Chee Tsui, Toronto, for the AF002993 cosmid; Drs A. Rosenthal and B. Hinzmann, Jena, for their help with the cosmid sequencing; Drs N. Benvenisty and M. Levinson, Jerusalem, for HNF3 cDNA constructs and antibodies; Ms Luba Nemanov for help with experiments; and Drs Alon Friedman, Beer Sheva and David Glick, Jerusalem, for assistance in clinical examination of proband I and for critically reviewing this manuscript. This study was supported by the Israel Science Foundation (590/97), the US Army Medical Research and Development Command (DAMD17-99-1-9547), the Israeli Ministry of Science (9433-1-97) and Ester Neuroscience, Ltd (to H.S.).

REFERENCES

1. Kimber, I. and Dearman, R.J. (1997) Cell and molecular biology of chemical allergy. *Clin. Rev. Allergy Immunol.*, **15**, 145–168.
2. Romagnani, S. (1997) Atopic allergy and other hypersensitivities interactions between genetic susceptibility, innocuous and/or microbial antigens and the immune system [editorial]. *Curr. Opin. Immunol.*, **9**, 773–775.
3. Wormhoudt, L.W., Commandeur, J.N. and Vermeulen, N.P. (1999) Genetic polymorphisms of human N-acetyltransferase, cytochrome P450, glutathione-S-transferase, and epoxide hydrolase enzymes: relevance to xenobiotic metabolism and toxicity. *Crit. Rev. Toxicol.*, **29**, 59–124.
4. Thiele, D.J. (1992) Metal-regulated transcription in eukaryotes. *Nucleic Acids Res.*, **20**, 1183–1191.
5. Denison, M.S. and Whitlock Jr, J.P. (1995) Xenobiotic-inducible transcription of cytochrome P450 genes. *J. Biol. Chem.*, **270**, 18175–18178.
6. Loewenstein Lichtenstein, Y., Schwarz, M., Glick, D., Norgaard Pedersen, B., Zakut, H. and Soreq, H. (1995) Genetic predisposition to adverse consequences of anti-cholinesterases in 'atypical' BCHE carriers. *Nature Med.*, **1**, 1082–1085.
7. Miller, C.S. and Mitzel, H.C. (1995) Chemical sensitivity attributed to pesticide exposure versus remodeling. *Arch. Environ. Health*, **50**, 119–129.
8. Soreq, H. and Zakut, H. (1993) *Human Cholinesterases and Anticholinesterases*. Academic Press, San Diego, CA.
9. Taylor, P. and Radic, Z. (1994) The cholinesterases: from genes to proteins. *Ann. Rev. Pharmacol. Toxicol.*, **34**, 281–320.
10. US Environmental Protection Agency (1999) Headquarters press release.
11. Winkler, J., Thal, L.J., Gage, F.H. and Fisher, L.J. (1998) Cholinergic strategies for Alzheimer's disease. *J. Mol. Med.*, **76**, 555–567.
12. Keeler, J.R., Hurst, C.G. and Dunn, M.A. (1991) Pyridostigmine used as a nerve agent pretreatment under wartime conditions [see comments]. *J. Am. Med. Assoc.*, **266**, 693–695.
13. Prody, C.A., Dreyfus, P., Zamir, R., Zakut, H. and Soreq, H. (1989) *De novo* amplification within a 'silent' human cholinesterase gene in a family subjected to prolonged exposure to organophosphorous insecticides. *Proc. Natl Acad. Sci. USA*, **86**, 690–694.
14. Davies, H.G., Richter, R.J., Keifer, M., Broomfield, C.A., Sowalla, J. and Furlong, C.E. (1996) The effect of the human serum paraoxonase polymorphism is reversed with diazoxon, soman and sarin. *Nature Genet.*, **14**, 334–336.
15. Haley, R.W., Billecke, S. and La Du, B.N. (1999) Association of low PON1 type Q (type A) arylesterase activity with neurologic symptom complexes in Gulf War veterans. *Toxicol. Appl. Pharmacol.*, **157**, 227–233.
16. Jensen, F.S. and Viby-Mogensen, J. (1995) Plasma cholinesterase and abnormal reaction to succinylcholine: twenty years' experience with the Danish Cholinesterase Research Unit. *Acta Anaesthesiol. Scand.*, **39**, 150–156.
17. Kaufer, D., Friedman, A., Seidman, S. and Soreq, H. (1998) Acute stress facilitates long-lasting changes in cholinergic gene expression. *Nature*, **393**, 373–377.
18. Kaufer, D., Friedman, A. and Soreq, H. (1999) The vicious circle: long-lasting transcriptional modulation of cholinergic neurotransmission following stress and anticholinesterase exposure. *Neuroscientist*, **5**, 173–183.
19. Tronche, F., Kellendonk, C., Reichardt, H.M. and Schutz, G. (1998) Genetic dissection of glucocorticoid receptor function in mice. *Curr. Opin. Genet. Dev.*, **8**, 532–538.
20. Qian, X., Samadani, U., Porcella, A. and Costa, R.H. (1995) Decreased expression of hepatocyte nuclear factor 3 alpha during the acute-phase response influences transthyretin gene transcription. *Mol. Cell. Biol.*, **15**, 1364–1376.
21. Ehrlich, G., Ginzberg, D., Loewenstein, Y., Glick, D., Kerem, B., Ben Ari, S., Zakut, H. and Soreq, H. (1994) Population diversity and distinct haplotype frequencies associated with ACHE and BCHE genes of Israeli Jews from trans-Caucasian Georgia and from Europe. *Genomics*, **22**, 288–295.
22. Beeri, R., Andres, C., Lev Lehman, E., Timberg, R., Huberman, T., Shani, M. and Soreq, H. (1995) Transgenic expression of human acetylcholinesterase induces progressive cognitive deterioration in mice. *Curr. Biol.*, **5**, 1063–1071.
23. Kaestner, K.H., Hiemisch, H., Luckow, B. and Schutz, G. (1994) The HNF-3 gene family of transcription factors in mice: gene structure, cDNA sequence, and mRNA distribution. *Genomics*, **20**, 377–385.
24. Herbst, R.S., Friedman, N., Darnell Jr, J.E. and Babiss, L.E. (1989) Positive and negative regulatory elements in the mouse albumin enhancer. *Proc. Natl Acad. Sci. USA*, **86**, 1553–1557.
25. Friedman, A., Kaufer, D., Shemer, J., Hendler, I., Soreq, H. and Tur-Kaspa, I. (1996) Pyridostigmine brain penetration under stress enhances neuronal excitability and induces early immediate transcriptional response. *Nature Med.*, **2**, 1382–1385.
26. Jern, C., Manhem, K., Eriksson, E., Tengborn, L., Risberg, B. and Jern, S. (1991) Hemostatic responses to mental stress during the menstrual cycle. *Thromb. Haemost.*, **66**, 614–618.
27. Grisaru, D., Sternfeld, M., Eldor, A., Glick, D. and Soreq, H. (1999) Structural roles of acetylcholinesterase variants in biology and pathology. *Eur. J. Biochem.*, **264**, 672–686.
28. O'Brien, R.M., Noisin, E.L., Suwanichkul, A., Yamasaki, T., Lucas, P.C., Wang, J.C., Powell, D.R. and Granner, D.K. (1995) Hepatic nuclear factor 3- and hormone-regulated expression of the phosphoenolpyruvate carboxykinase and insulin-like growth factor- binding protein 1 genes. *Mol. Cell. Biol.*, **15**, 1747–1758.
29. Wang, D.P., Stroup, D., Marrapodi, M., Crestani, M., Galli, G. and Chiang, J.Y. (1996) Transcriptional regulation of the human cholesterol 7 alpha-hydroxylase gene (CYP7A) in HepG2 cells. *J. Lipid Res.*, **37**, 1831–1841.
30. Bell, I.R., Baldwin, C.M. and Schwartz, G.E. (1998) Illness from low levels of environmental chemicals: relevance to chronic fatigue syndrome and fibromyalgia. *Am. J. Med.*, **105**, 74S–82S.
31. Fiedler, N. and Kipen, H. (1997) Chemical sensitivity: the scientific literature. *Environ. Health Perspect.*, **105** (suppl. 2), 409–415.
32. Bell, I.R., Baldwin, C.M., Fernandez, M. and Schwartz, G.E. (1999) Neural sensitization model for multiple chemical sensitivity: overview of theory and empirical evidence [in process citation]. *Toxicol. Ind. Health*, **15**, 295–304.
33. Baxter, M.G. and Chiba, A.A. (1999) Cognitive functions of the basal forebrain. *Curr. Opin. Neurobiol.*, **9**, 178–183.
34. Quandt, K., Frech, K., Karas, H., Wingender, E. and Werner, T. (1995) MatInd and MatInspector: new fast and versatile tools for detection of consensus matches in nucleotide sequence data. *Nucleic Acids Res.*, **23**, 4878–4884.
35. Richards, R.I. and Sutherland, G.R. (1994) Simple repeat DNA is not replicated simply [news]. *Nature Genet.*, **6**, 114–116.
36. Nadel, Y., Weisman-Shomer, P. and Fry, M. (1995) The fragile X syndrome single strand d(CGG)*n* nucleotide repeats readily fold back to form unimolecular hairpin structures. *J. Biol. Chem.*, **270**, 28970–28977.
37. Ben Aziz Aloya, R., Seidman, S., Timberg, R., Sternfeld, M., Zakut, H. and Soreq, H. (1993) Expression of a human acetylcholinesterase promoter–reporter construct in developing neuromuscular junctions of *Xenopus* embryos. *Proc. Natl Acad. Sci. USA*, **90**, 2471–2475.
38. Getman, D.K., Mutero, A., Inoue, K. and Taylor, P. (1995) Transcription factor repression and activation of the human acetylcholinesterase gene. *J. Biol. Chem.*, **270**, 23511–23519.
39. Bennett, E.R., Yedgar, S., Lerer, B. and Ebstein, R.P. (1991) Phospholipase A2 activity in Epstein–Barr virus-transformed lymphoblast cells from schizophrenic patients [see comments]. *Biol. Psychiatry*, **29**, 1058–1062.
40. Silverman, E., Eimerl, S. and Orly, J. (1999) CCAAT enhancer-binding protein beta and GATA-4 binding regions within the promoter of the steroidogenic acute regulatory protein (StAR) gene are required for transcription in rat ovarian cells. *J. Biol. Chem.*, **274**, 17987–17996.
41. Grifman, M., Galyam, N., Seidman, S. and Soreq, H. (1998) Functional redundancy of acetylcholinesterase and neuroligin in mammalian neuritogenesis. *Proc. Natl Acad. Sci. USA*, **95**, 13935–13940.
42. Lechner, J., Welte, T. and Doppler, W. (1997) Mechanism of interaction between the glucocorticoid receptor and Stat5: role of DNA-binding. *Immunobiology*, **198**, 112–123.
43. Pick, M., Nagler, A., Grisaru, D., Eldor, A. and Deutsch, V. (1998) Expansion of megakaryocyte progenitors from human umbilical cord blood using a new two-step separation procedure. *Br. J. Haematol.*, **103**, 639–650.

J Mol Med (2000) 78:228–236
Digital Object Identifier (DOI) 10.1007/s001090000104

ORIGINAL ARTICLE

E. Shohami · D. Kaufer · Y. Chen · S. Seidman
O. Cohen · D. Ginzberg · N. Melamed-Book
R. Yirmiya · H. Soreq

Antisense prevention of neuronal damages following head injury in mice

Received: 24 January 2000 / Accepted: 3 April 2000 / Published online: 17 May 2000

Abstract Closed head injury (CHI) is an important cause of death among young adults and a prominent risk factor for nonfamilial Alzheimer's disease. Emergency intervention following CHI should therefore strive to improve survival, promote recovery, and prevent delayed neuropathologies. We employed high-resolution nonradioactive in situ hybridization to determine whether a single intracerebroventricular injection of 500 ng 2′-O-methyl RNA-capped antisense oligonucleotide (AS-ODN) against acetylcholinesterase (AChE) mRNA blocks overexpression of the stress-related *readthrough* AChE (AChE-R) mRNA splicing variant in head-injured mice. Silver-based Golgi staining revealed pronounced dendrite outgrowth in somatosensory cortex of traumatized mice 14 days postinjury that was associated with sites of AChE-R mRNA overexpression and suppressed by anti-AChE AS-ODNs. Furthermore, antisense treatment reduced the number of dead CA3 hippocampal neurons in injured mice, and facilitated neurological recovery as determined by performance in tests of neuromotor coordination. In trauma-sensitive transgenic mice overproducing AChE, antisense treatment reduced mortality from 50% to 20%, similar to that displayed by head-injured control mice. These findings demonstrate the potential of antisense therapeutics in treating acute injury, and suggest antisense prevention of AChE-R overproduction to mitigate the detrimental consequences of various traumatic brain insults.

ESTHER SHOHAMI received her Ph.D. in physiology from the Hebrew University of Jerusalem, Israel. She is presently Associate Professor of Pharmacology, Head of the Pharmacology Teaching Unit in the Faculty of Medicine, and member in the Betz Center for Injury Prevention at the Hebrew University of Jerusalem. Her research interests include mechanisms of brain damage and potential repair in traumatic brain injury, using in vivo and in vitro model systems. Special emphasis is given to inflammatory mediators such as cytokines and reactive oxygen specials.

HERMONA SOREQ received her Ph.D. in biochemistry from the Weizmann Institute of Science in Rehovot, Israel. She is presently Professor of Molecular Biology and Head of the Eric Roland Center for Neurodegenerative Diseases at the Hebrew University of Jerusalem. Her research interests include transgenic and antisense approaches for studying stress insults, with special emphasis on the multifaceted involvement of acetylcholinesterase in stress responses.

E. Shohami · Y. Chen
Department of Pharmacology, School of Pharmacy,
Faculty of Social Sciences, Hebrew University of Jerusalem,
Jerusalem 91904, Israel

D. Kaufer · S. Seidman · O. Cohen · D. Ginzberg
N. Melamed-Book · H. Soreq (✉)
Department of Biological Chemistry, Life Sciences Institute,
Faculty of Social Sciences, Hebrew University of Jerusalem,
Jerusalem 91904, Israel
e-mail: soreq@shum.huji.ac.il
Tel.: +972-2-6585109, Fax: +972-2-6520258

O. Cohen · R. Yirmiya
Department of Psychology, Faculty of Social Sciences,
Hebrew University of Jerusalem, Jerusalem 91904, Israel

Key words Antisense · Oligonucleotides · Head injury · Acetylcholinesterase · Emergency medicine

Abbreviations *AChE:* Acetylcholinesterase · *ARP:* Acetylcholinesterase *readthrough* peptide · *AS-ODN:* Antisense oligodeoxynucleotide · *CHI:* Closed head injury · *UTR:* Untranslated region

Introduction

Head trauma is an important cause of death among young adults [1, 2] and among the most significant risk factors known for nonfamilial Alzheimer's disease [3]. Emergency intervention in head injury must therefore consider not only short-term survival and recovery but also potential delayed neurological disorders. Robust production of stress hormones, transcription factors, cytokines, and neurotrophic factors have all been reported to occur in the injured brain [4, 5, 6]. Recently we demonstrated rapid and persistent overexpression of AChE-R in brain following acute psychological and chemical stressors associated with cholinergic excitation [7]. These observations suggested a role for AChE-R in stress responses accompanying various traumatic insults to the central nervous system [8]. Since the early post-CHI response phase includes a burst of released acetylcholine [9], we considered whether AChE-R acts as a stress response element following head injury. While acute stress responses likely promote survival, it has been argued that prolonged activation of stress-related genes initiates cascades of events with pleiotrophic and potentially deleterious effects [10]. Transgenic mice overexpressing human "synaptic" AChE-S in central cholinergic neurons exhibit delayed impairments in learning and memory [11] reminiscent of neuropathologies associated with posttraumatic stress disorder and anticholinesterase intoxication [8]. In this context, trauma-induced AChE-R might represent a candidate molecule contributing to the tight correlation between head injury and accelerated neurodeterioration.

Antisense oligonucleotides (AS-ODNs) eliciting selective destruction of specific messenger RNAs are ideally suited to the need for targeted downregulation of overexpressed proteins [12]. AS-ODNs are short, synthetic strands of DNA designed to hybridize with a specific target messenger RNA based on the rules of complementary Watson-Crick base pairing. Upon hybridization with AS-ODN, duplexed RNA becomes susceptible to RNase-mediated nucleolytic degradation, effectively blocking de novo synthesis of the unwanted protein. AS-ODNs have been used with remarkable success to modulate nervous system gene expression in the laboratory [13]. Nevertheless, restricted transport of oligonucleotides across the blood-brain barrier still poses a formidable obstacle to the application of antisense therapeutics to clinical neurology [14]. Here, we have used direct intracerebroventricular injections to deliver AS-ODNs to the injured brain, effectively suppressing stress-induced overexpression of AChE-R and improving the outcome of CHI.

Materials and methods

Closed head injury

Adult mice were anesthetized with ether to loss of pupillary and corneal reflexes. Closed head injury (CHI) was as described [15], in accordance with NIH guidelines for the use and care of laboratory animals and following approval by the Animal Care Committee of the Hebrew University of Jerusalem. Neurological functioning attesting to the severity of the injury was determined 1 h post-trauma, by recording of successful trials of crossing a 2- or 3-cm wide beam.

Antisense oligonucleotides

AS3 is a 20-mer oligodeoxynucleotide (5′-CTGCAATATTTTCT-TGCACC-3′) complementary to a sequence in exon E2 of mouse AChEmRNA. ASB (5′-GACTTTGCTATGCAT3′) is targeted to mRNA encoding mouse butyrylcholinesterase. In both cases, the last three 3′ nucleotides were replaced with 2'-O-methyl ribonucleotide analogs. Oligonucleotides were synthesized, purified by high-pressure liquid chromatography and tested for purity by mass spectrometry at Hybridon (Rochester, N.Y., USA).

Golgi staining

Brains were fixed in 34 mM (1%) cobalt nitrate (18 h, room temperature), impregnated in 117 mM (2%) silver nitrate (24–48 h, room temperature) and processed in fresh Ramon y Cajal's developer. Paraffin sections were toned in 5 mM (0.2%) gold chloride, washed and counterstained with 2 mM alum carmine.

Results

To test whether AChE-R overproduction takes place under exposure to physical stress we exposed adult FVB/N mice to unilateral CHI [15] and used in situ hybridization to label AChE-R mRNA in brain sections. Consistent with previous findings, AChE-R mRNA was low in brains of uninjured mice ([7] and data not shown). In traumatized mice, however, intense labeling was observed in the contused hemisphere 14 days postinjury, especially close to the site of injury (Fig. 1a). Less prominent labeling was also evident in the contralateral hemisphere (Fig. 1b). Using a probe specific for AChE-S mRNA, we could not detect differences in the levels of this message between the injured and noninjured hemispheres (data not shown). To study the implications of AChE-R mRNA upregulation on the outcome of CHI, we employed AS-ODNs to selectively suppress postinjury AChE-R mRNA overproduction.

In cultured Saos-2 and PC12 cells low doses of AS3, a partially 2'-O-methyl-RNA modified antisense oligonucleotide targeted to the common domain in AChE mRNA, efficiently and selectively reduced AChE-R, but not AChE-S, mRNA levels ([16] and data not shown). Following CHI, a single intracerebroventricular injection of as little as 0.5 μg AS3 (70 pmol in a total volume of 10 μl) 1 h postinjury significantly prevented AChE-R mRNA accumulation in both brain hemispheres of injured mice (Fig. 1c, d). Treated mice displayed no signs of acute cholinergic hypofunction, suggesting that AChE-S levels were not significantly reduced. Confocal microscopy (Fig. 1 e-h) revealed four- to fivefold increased AChE-R mRNA labeling in both somata and apical dendrites of individual somatosensory cortical neurons in the contused versus contralateral hemisphere

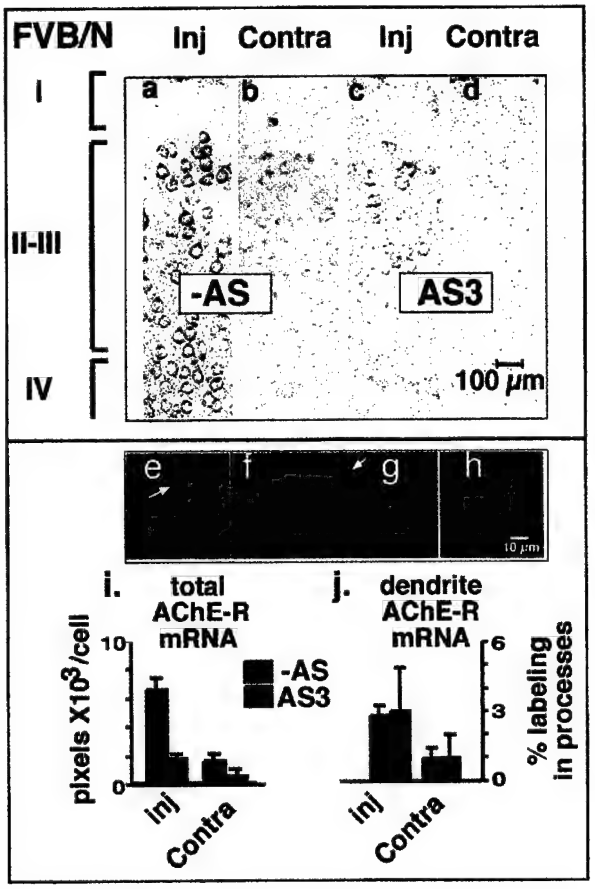

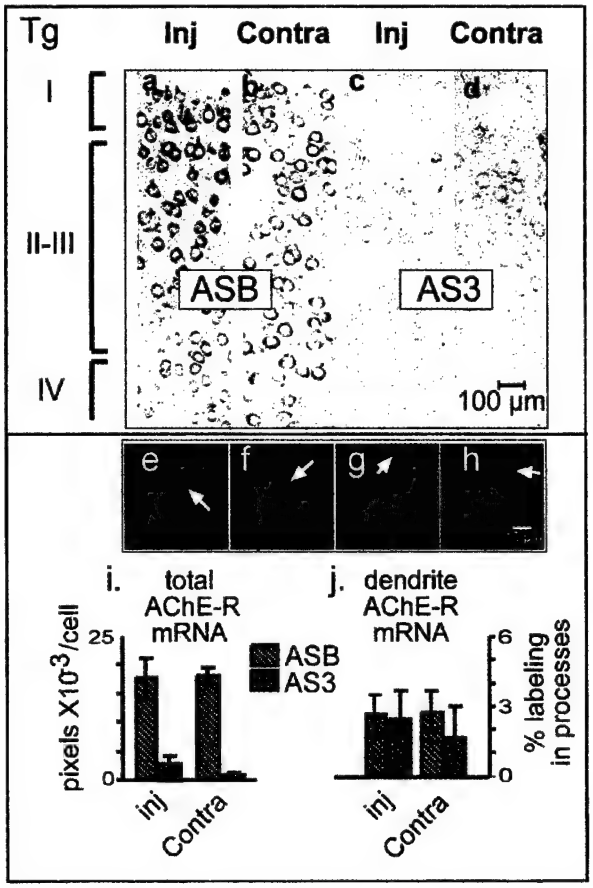

Fig. 1a–j Antisense oligonucleotides suppress trauma-induced accumulation of readthrough AChE-R mRNA in mouse brain. Male adult FVB/N mice were subjected to controlled closed head injury (left side of the head), injected after 1 h into the left ventricle with either saline or 500 ng of the partially 2-O-methyl-protected 20-mer AS-ODN AS3 and killed 14 days later. In situ hybridization was performed on 5-µm paraffin-embedded brain sections using a 50-mer biotinylated 2′-O-methyl cRNA probe targeted to intron I4 in mouse AChE-R mRNA. Staining was with Fast Red (Molecular Probes). **a–d** Brightfield digital photomicroscopy images of cortical layers I–IV from injured (**a, c**) and contralateral (**b, d**) hemispheres. *Red staining* marks sites of AChE-R mRNA accumulation. Note the intense staining of cortical neurons on the injured vs. contralateral side of the brain and the pronounced bilateral reduction in staining following a single unilateral injection of AS3. **e–h** Shown are representative confocal images of neurons from somatosensory cortex. Note the massive accumulation of AChE-R mRNA in both somata and apical dendrites (*white arrows*). AS3 dramatically suppressed the accumulation of AChE-R mRNA in neurons from both the injured (**e** vs. **g**) and contralateral (**f** vs. **h**) hemispheres and in both subcellular compartments. **i,j** Densitometric analysis was performed on confocal images of cortical neurons as depicted in **e–h**. **i** *Columns* Total number and standard deviation of pixels/cell for 10–20 neurons in each group (*left*) or the percentage of total pixels detected within dendrites (*right*) for the injured and contralateral hemispheres of mice injected with saline or AS3. Note the disproportionately high levels of AChE-R mRNA-specific fluorescence in neurons from the injured as compared to contralateral hemisphere, and the four- to sixfold reduced levels of staining in animals treated with AS3. The relative fraction of AChE-R mRNA appearing in dendrites was unmodified by antisense intervention (**j**)

Fig. 2a–j Head trauma elicits pronounced bilateral accumulation of endogenous AChE-R mRNA in AChE transgenic mice. Experimental details were as in Fig. 1 except that saline was replaced with an irrelevant oligonucleotide, ASB (see "Materials and methods"), as control. Note that transgenic mice, as opposed to control FVB/N mice display prominent overexpression of AChE-R mRNA in both the injured and noninjured brain hemispheres following head injury. **a–d** Brightfield microscopy. In brains from traumatized AChE transgenic mice with preexisting AChE excesses, similarly intense red hybridization signals were observed in cell bodies and dendrites of neurons from both the injured and contralateral hemispheres. AS3 effectively suppressed AChE-R mRNA expression in both hemispheres. **e–h** Confocal microscopy as in Fig. 1i–j. Densitometric analysis as in Fig. 1, note the more intense staining and higher dendrite localization of AChE-R mRNA in the contralateral hemisphere of transgenics as compared to FVB/N mice

(quantified in Fig. 1i). AS3 treatment conspicuously suppressed neuronal labeling in both subcellular compartments with approximately equal efficiency (Fig. 1j). Thus, CHI induced a persistent, at least 2-weeks-long overexpression of AChE-R mRNA in mouse brain, that was observed predominantly in the injured hemisphere. Moreover, AChE-R expression was prominently relieved by a single postinjury injection of an AS-ODN directed to a common exon in AChE mRNA.

To explore the molecular and cellular effects of preinjury AChE accumulation we traumatized transgenic mice

expressing up to twofold excesses of AChE-S in cholinergic CNS neurons. Following CHI, transgenic mice were injected with either AS3 or an antisense oligonucleotide targeted to mRNA encoding the nonrelevant, homologous butyrylcholinesterase (ASB; see above and [16]). Following in situ hybridization with an AChE-R mRNA specific probe, intense hybridization signals were observed in cortical neurons from both the injured and contralateral hemispheres of transgenic mice treated with the irrelevant oligonucleotide (Fig. 2a, b). In contrast, a single injection of AS3, effectively blocked AChE-R mRNA accumulation in both hemispheres (Fig. 2c, d). Confocal analysis demonstrated two- to fourfold increased levels of AChE-R mRNA in cells from either hemisphere of transgenic as compared with control mice (Fig. 2e-h). AS3 treatment reduced AChE-R mRNA to similarly low levels in both FVB/N and transgenics without affecting its subcellular distribution (Fig. 2i, j).

To test the effects of these AS-ODNs in noninjured transgenic mice we implanted 2-mm cannulae into the lateral ventricle. Ten days postimplantation we infused 25 ng ODN in a total volume of 1 µl twice at 24 h intervals. Mice were killed 24 h after the second injection and cortical homogenates prepared. An affinity-purified antibody raised against a recombinant fusion protein of glutathione transferase and the acetylcholinesterase *readthrough* peptide (ARP), selective for AChE-R (Fig. 3a) labeled a ladder of bands in denaturing gels run with these homogenates. Based on densitometry of the six most prominent bands, we calculated that animals treated with ASB exhibited elevated levels (approximately 40% above naive mice) of immunoreactive polypeptides, especially the more rapidly migrating ones that likely reflect degradation products of AChE-R (Fig. 3b). This increase in AChE-R immunoreactivity was attributed to the trauma associated with surgical implantation of the cannula and was mostly suppressed by AS3 ($P \leq 0.01$; Fig. 3b). Immunolabeling with monoclonal antibodies targeted at the core domain failed to show suppression of immunoreactive protein by AS3 (data not shown). As these latter antibodies recognize both AChE-S and AChE-R, this analysis was consistent with the selectivity of AS3 effects on AChE-R mRNA. AS3-treated mice functioned well in behavioral tests of social recognition that are dependent on cholinergic function (data not shown), attesting to the integrity of normal cholinergic neurotransmission. Thus, the accumulation of AChE-R mRNA induced by even "mild" head injury appeared to be translated into elevated AChE-R protein levels. Moreover, AS3 blocked accumulation of both AChE-R mRNA and protein following trauma without promoting deleterious cognitive side effects in nonimpaired animals.

Regulated neurite outgrowth is likely an important component in short-term recovery from brain injury [17], but excessive neuronal sprouting following injury might be harmful and could promote posttraumatic epilepsy [18]. Since recent evidence attributes noncatalytic, neurite growth promoting activities to AChE [19], we con-

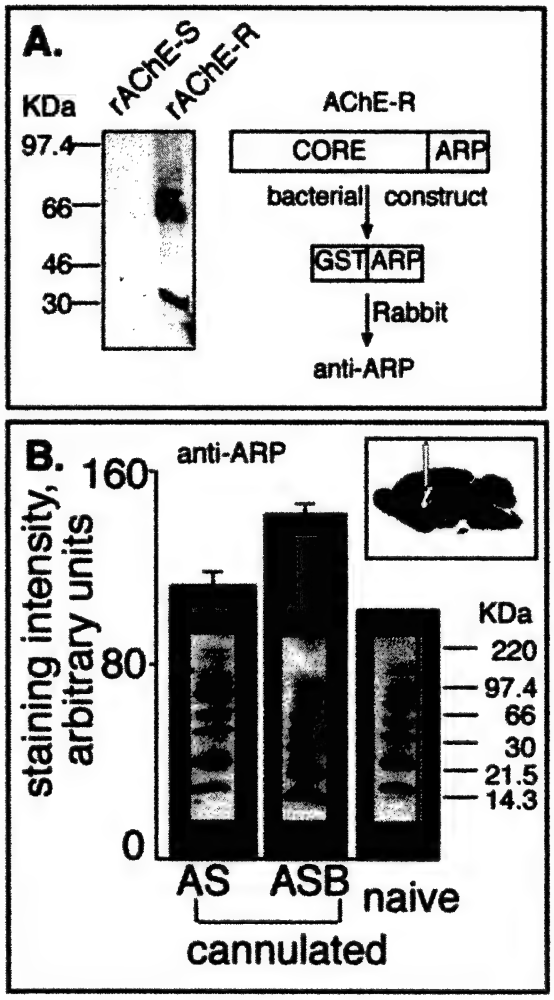

Fig. 3A,B AS3 suppresses trauma-induced overproduction of immunoreactive AChE-R protein. **A** Selective immunodetection of the AChE-R protein. To selectively label the AChE-R variant, rabbits were immunized with a recombinant fusion protein of glutathione transferase (*GST*) with the 26 amino acid C-terminal peptide unique to AChE-R (*ARP*). The resultant antiserum, affinity purified to remove anti-GST antibodies, selectively labeled recombinant (*r*) AChE-R produced in transfected Cos cells (66–67 K_d) and an apparent AChE-R degradation product (approx. 30 K_d), but not purified rAChE-S (Sigma, St. Louis, Mo., USA) in immunoblot analysis. **B** AS3 suppresses AChE-R labeling. Cortical homogenates from AChE transgenic mice injected icv with either AS3 or ASB on two consecutive days were subjected to sodium dodecyl sulfate polyacrylamide gel electrophoresis on a 4–20% reducing gel and probed with anti-ARP antiserum. Shown are the corresponding chemiluminescence-labeled lanes as *insets within a bar graph* representing the summation of densitometric analyses of the six most prominent bands in each lane. *Inset in right-hand corner* illustrates the position of the cannula. *Columns* represent mean±SEM for homogenates from six AS3- and four ASB-treated mice, respectively. A single representative control, untreated, nonoperated animal is shown (naive)

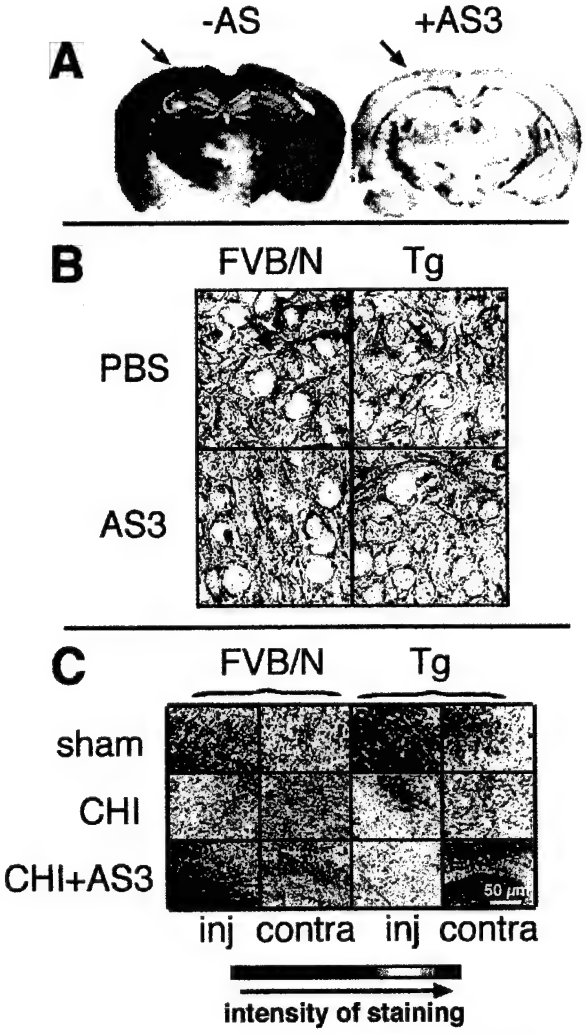

Fig. 4A–C Antisense treatment suppresses AChE-R mRNA and neurite growth and promotes neuron survival following head trauma. **A** Low magnification image of whole brain sections from head-injured FVB/N mice subjected to in situ hybridization as in Fig. 1A. Note that AChE-R mRNA is intensively expressed in the injured hemisphere (*left*), especially in the cortex, close to the site of injury (*arrows*). AS3 significantly suppressed AChE-R mRNA accumulation in both hemispheres. **B** Golgi staining was performed on brain sections from FVB/N or transgenic (*Tg*) mice subjected to CHI and injected intracerebroventricularly with either PBS or AS3. Shown are representative high magnification (×1000) images from layer IV of somatosensory cortex on the injured hemisphere 14 days following head injury. Note that AS3 treatment notably reduced the density of stained neurites in both FVB/N and transgenic mice. **C** Golgi staining performed on brain sections depicted in B was semiquantified in sections from uninjured (*sham*) FVB/N or AChE transgenic (*Tg*) mice and from mice untreated (*CHI*) or treated with AS3 (*CHI+AS3*) following closed head injury. Presented are pseudocolor representations of cortical sections in which stained neurites appear red. Note the intense Golgi staining, representing high neurite density in cortex from the injured hemisphere of FVB/N mice and the higher intensity in transgenic mice. Red signal was significantly reduced in both FVB/N and Tg mice treated with AS3

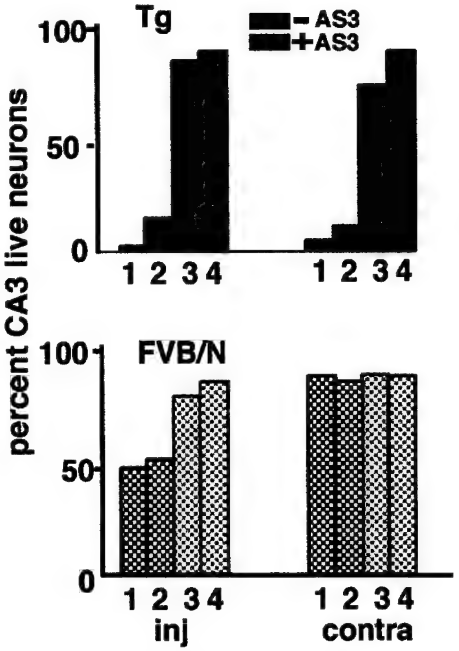

Fig. 5 Live and dead neurons in the CA3 hippocampal region were counted in two consecutive sections from four control and four transgenic mice 14 days following closed head injury with or without antisense treatment. Overt neuronal cell death was identified by the presence of pyknotic black cell bodies. For each mouse 150–200 cells were counted. *Columns* represent the percentage of live neurons counted for individual mice. Note the dramatic bilateral neuron loss suffered by transgenic as compared with FVB/N mice and the minimal neuron loss observed among antisense-treated animals

sidered the possibility that overexpressed AChE-R and/or its degradation products promote a phase of neurite outgrowth following CHI. To assess neuritic growth we performed quantitative image analysis on 100–200 μm² somatosensory cortical fields in Golgi-stained brain sections from mice 14 days posttrauma and searched for a correlation between neurite outgrowth and elevated AChE-R mRNA levels. Following head injury, pronounced increases in AChE-R mRNA labeling were colocalized with sites of intensified Golgi staining, especially in the somatosensory cortex around the site of injury, and particularly in transgenic mice (Fig. 4). AS3 significantly attenuated this increased staining in both FVB/N and transgenic mice, suggesting a correlation between AChE mRNA overproduction and induced neurite growth.

Excessive reinnervation following injury could subject hippocampal cells in the traumatized brain to hyperexcitation and glutamate toxicity. Indeed, hippocampal neurons, especially in the CA3 domain, are highly susceptible to cell death following brain injury [15, 20, 21]. Fourteen days following head injury we observed up to 50% loss of CA3 neurons in the contused hemisphere of FVB/N mice. In striking contrast, transgenic mice displayed up to 90% neuron death in CA3 of both hemi-

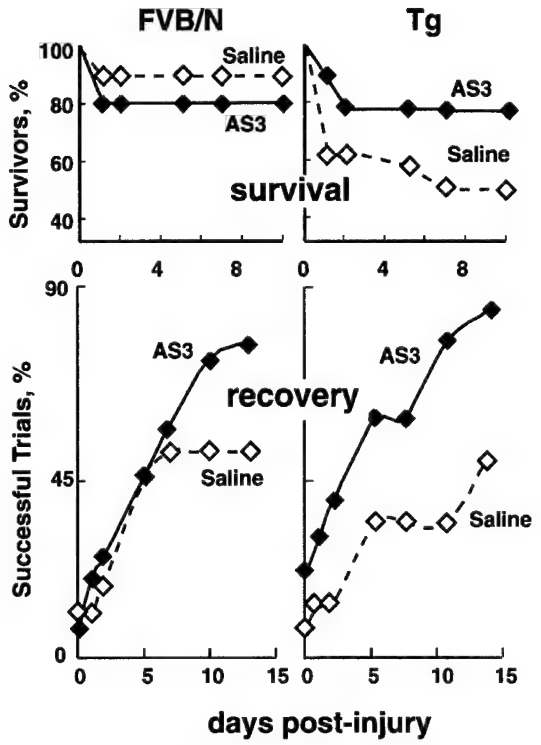

Fig. 6 Antisense treatment rescues survival and neurological recovery of injured mice. Survival and neurological recovery of FVB/N and AChE transgenic mice were monitored following CHI. One hour following trauma a neurological evaluation of the mice was taken using a graded balancing task of 2- and 3-cm-wide beam crossing. Recovery was monitored at various time points posttrauma for each mouse. Presented are percentages of surviving mice (*top*) and average percentage successes for surviving mice in the beam task (*bottom*) on the noted days following trauma. Note the high mortality and slow recovery of transgenic mice compared to controls and the improved outcome following a single AS3 treatment. Starting n=20–24 mice per group

spheres. Thus, overproduction of transgenic AChE appears to prime hippocampal neurons in CA3 for premature death following trauma. AS3 treatment afforded dramatic protection of hippocampal neurons in both control and transgenic animals subjected to CHI (Fig. 5).

The excessive loss of hippocampal neurons in brains of traumatized transgenic mice suggested that this strain would display a genetic vulnerability to CHI as compared to the parental FVB/N line. Indeed, young adult transgenic mice were considerably more vulnerable to unilateral CHI than age and sex-matched controls. Only 12 of 24 transgenics, as compared with 18 out of 20 FVB/N mice survived the first 10 days postinjury (Fig. 6). The 90% survival rate among FVB/N mice was similar to that displayed by other mouse strains subjected to this trauma protocol [15]. No further mortality was observed for the duration of the 30-day follow-up period. As overexpression of AChE was correlated with enhanced neurite outgrowth, the high mortality of AChE transgenic mice following CHI strengthens the idea that hyperinnervation may cause acute toxic effects during a phase of recovery lasting from 24 h up to 1 week posttrauma. Consistent with this conclusion, AS3 treatment retrieved the survival rate of AChE transgenics to 80%, comparable to that of FVB/N mice (Fig. 6).

Increased neuronal vulnerability to trauma implied that surviving transgenic mice would present impaired neurological recovery. To monitor neurological recovery we used a beam test, in which the percentage of mice that are capable of crossing 2- and 3-cm-wide beams is recorded. Success in this test is indicative of balanced and coordinated movement [15]. Although uninjured transgenic mice display some neuromotor impairments at the age of 4 months [22], transgenic and control mice scored very similarly 1 h postinjury (7 and 11%, respectively), indicating similar severity of trauma. Spontaneous recovery of transgenic survivors lagged significantly behind that of control mice throughout the 30 day follow-up period, especially during the first 10 days (Fig. 6 and data not shown). However, single dose AS3 treatment rapidly improved the performance of transgenic mice, to that of controls. Starting 7 days postinjury, AS3-treated FVB/N and transgenics both displayed improved performance as compared to untreated mice, both reaching ca. 80% of success, in comparison to 50% in the untreated groups (Fig. 6).

Discussion

We observed strong and persistent bilateral elevation in AChE-R mRNA levels and dramatic bilateral loss of hippocampal CA3 neurons in brains from AChE transgenic mice subjected to CHI. In comparison, trauma-induced overexpression of AChE-R and hippocampal cell loss in control FVB/N mice were primarily observed in the injured as opposed to contralateral hemispheres. Therefore, increased mortality among head-injured AChE transgenic mice and retarded neurological recovery of transgenic survivors associate robust, bilateral overexpression of AChE-R with poor prognosis following traumatic head injury. Despite progressive late-onset cognitive deficits, transgenic mice function normally until about 2 months of age [23]. This observation attests to the existence of compensatory mechanisms designed to overcome acetylcholine deficits imposed by overexpressed AChE ([24] and unpublished data). Since AChE-R expression is elevated by acute cholinergic stimulation [25], the pronounced bilateral overexpression of AChE-R in injured transgenic mice may therefore reflect heightened cholinergic activation in the noninjured hemisphere of these mice. As neurite growth is notably associated with increases in AChE activity (reviewed under [26]), it is understandable how antisense oligonucleotides blocking the initial postinjury accumulation of AChE-R could spare hippocampal neurons and minimize the morbidity of transgenic mice following CHI by reducing excessive neurite outgrowth. Prevention of this cascade of events also explains how a single, timely, and effective dose of

AS-ODN could provide long-lasting protection to the injured brain.

Head trauma patients may suffer delayed neurological deficits, including increased risk for Alzheimer's disease. The noncatalytic capacity of the AChE protein to induce β-amyloid aggregation [27] may be associated with this risk. The long-term neurological protection afforded by AS3 treatment thus remains to be tested in additional animal models, for example, mice that develop β-amyloid plaques [28]. Nevertheless, our findings provide the first experimental basis for the application of antisense technology to acute gene-oriented intervention in emergency medicine. In this light, AChE-R mRNA emerges as an appropriate target for such intervention where severe trauma to the nervous system is involved. Under psychological stress, AChE-R mRNA accumulation is preceded by an induction of c-fos [7]. Recently, Morrow and coworkers reported the use of AS-ODNs targeted towards c-fos mRNA to suppress central stress responses [29]. The higher ODN doses used in that study could reflect limited diffusion from the intracortical site of injection that was employed.

The increase in AChE-R and the accumulation of its degradation products in noninjured, cannulated transgenic mice most likely reflect surgery-related stress. Following two daily intracerebroventricular injections of 25 ng AS3, AChE-R immunolabeling was decreased to levels similar to those in the naive brain and significantly lower than that in brains of cannulated mice injected with the irrelevant ODN ASB. This experiment therefore provides a tentative time frame (48 h or less) for the AS3 effects, and demonstrates the potency of this ODN in blocking accumulation of AChE-R protein. In this context, it is important to note that AChE-R mRNA includes a 1094 basepair 3′ untranslated region (UTR) with high (66%) G, C content whereas AChE-S mRNA includes a considerably shorter, 219 basepair UTR. A long UTR predicts AChE-R mRNA to be more vulnerable to cellular nucleolytic degradation than AChE-S mRNA, consistent with the observation that AChE-R, but not AChE-S, mRNA is rapidly degraded in PC12 cells treated with actinomycin D [30]. The inherent instability of AChE-R mRNA could explain the preferential suppression of AChE-R over AChE-S mRNA by AS3 and AS1 [16], both of which target exon 2, common to all three alternative AChE mRNA splicing variants [31].

The AChE transcriptional response to stress involves modulation of the regular splicing pattern. It is not yet known whether the shift towards 3′ unspliced *read-through* AChE mRNA represents an active or passive process. However, stress-induced changes in alternative splicing have also been described for potassium channels, where stress hormones favor the splice variant encoding a channel subtype conferring repetitive firing characteristics [32]. Similarly, optic nerve injury induces altered splicing of the retinal NMDAR1 (NR1) receptor mRNA [33]. That active changes in cellular splicing machinery take place following stress is indicated by evidence for hypoxia-induced production of the YT521 splicing-related protein [34] and heat shock-induced splicing arrest [35]. Further studies are required to determine the mechanism(s) regulating stress-related changes in AChE mRNA splicing.

Following either stress or head injury, the subcellular distribution of AChE-R mRNA is altered, appearing also in the proximal domain of dendrites. The somatodendritic localization of this mRNA is not suppressed by AS3 and hence does not depend on mRNA content. Dendritic targeting of mRNAs encoding brain-derived neurotropic factor and TrkB has been reported in hippocampal neurons following activation of glutamate receptors [36]. These studies indicate the existence of neuronal activity dependent mechanisms for the subcellular distribution of neuronal mRNAs and suggest an association between mRNA redistribution and synaptic plasticity. The dendritic localization of AChE mRNA strengthens the notion that AChE contributes directly towards neurite growth in vivo, and suggests a role for this protein in dendrite abnormalities characteristic of the cognitively impaired AChE transgenic mice [11] and aged humans [8].

The prominent protection of hippocampal neurons, as well as improved rate of recovery with respect to regained neuromotor functions in head-injured AS3-treated FVB/N and transgenic mice, demonstrates the value of suppressing AChE-R levels for long-term recovery in terms of neurological functioning, and attributes profound implications for the potential application of antisense therapeutics to a clinical setting. That AChE-R mRNA accumulates under psychological [7], chemical [8], and physical (this report) stressors suggests that this transcript represents a general nervous system stress-response element. In view of our current findings, the grave consequences of AChE-R accumulation in the mammalian brain may extend to a wide range of maladies, including not only Alzheimer's disease but also poststroke depression [37], multiple sclerosis and amyotrophic lateral sclerosis. Moreover, our findings indicate a potentially increased risk for CHI victims with preinjury overexpression of brain AChE (for example, posttraumatic stress patients).

The side effects of repetitive administration of AS-ODNs in the nervous system have not been thoroughly studied, but are not expected to be severe [12, 13, 14]. Indeed, the recent United States Food and Drug Administration approval of the first antisense drug (Fomivirisen, ISIS) for treating a viral infection of the eye marks a milestone in the long-awaited transition of this intriguing technology from the research laboratory to the clinic. However, there are outstanding challenges in antisense therapeutics. Our current work addresses the potential to substantially reduce the dose and toxicity of antisense drugs, and demonstrates successful application of antisense technology to a cellular, rather than viral or oncogenic target. Moreover, they raise the possibility that exploiting injury-associated breaches of the blood-brain barrier [15, 38] to deliver antisense drugs into the brain could place the trauma model in a unique position

to advance the goal of clinical antisense therapeutics for the nervous system.

Acknowledgements The authors are indebted to Dr. Aharon S. Cohen (Boston) for fruitful discussions. This work was supported by grants to H.S. from the United States Army Medical Research and Development Command (DAMD17-99-1-9547), The Israel Science Foundation (590/97), the United States–Israel Binational Science Foundation (96-00110), and Ester Neurosciences, Ltd. E.S. is affiliated with the David R. Bloom Center for Pharmacy, the Hebrew University, Jerusalem.

References

1. McIntosh TK, Juhler M, Wieloch T (1998) Novel pharmacologic strategies in the treatment of experimental traumatic brain injury. J Neurotrauma 15:731–769
2. Siesjo BK (1993) Basic mechanisms of traumatic brain damage. Ann Emerg Med 22:959–969
3. Gennarelli TA, Graham DI (1998) Neuropathology of the head injuries. Semin Clin Neuropsychiatry 3:160–175
4. Yakovlev AG, Faden AI (1995) Molecular biology of CNS injury. J Neurotrauma 12:767–777
5. Roe SY, McGowan EM, Rothwell NJ (1998) Evidence for the involvement of corticotrophin-releasing hormone in the pathogenesis of traumatic brain injury. Eur J Neurosci 10: 553–559
6. Shohami E, Gallily R, Mechoulam R, Bass R, Ben-Hur T (1997) Cytokine production in the brain following closed head injury: dexanabinol (HU-211) is a novel TNF-alpha inhibitor and an effective neuroprotectant. J Neuroimmunol 72:169–177
7. Kaufer D, Friedman A, Seidman S, Soreq H (1998) Acute stress facilitates long-lasting changes in cholinergic gene expression. Nature 393:373–377
8. Kaufer D, Friedman A, Soreq H (1999) The vicious circle: long-lasting transcriptional modulation of cholinergic neurotransmission following stress and anticholinesterase exposure. Neuroscientist 5:173–183
9. Gorman LK, Fu k, Hovda DA, Becker DP, Katayama Y (1989) Analysis of acetylcholine release following concussive brain injury in the rat. J Neurotrauma 6:203
10. Sapolsky RM (1996) Why stress is bad for your brain. Science 273:749–750
11. Beeri R, Le Novere N, Mervis R, Huberman T, Grauer E, Changeux JP, Soreq H (1997) Enhanced hemicholinium binding and attenuated dendrite branching in cognitively impaired acetylcholinesterase-transgenic mice. J Neurochem 69:2441–2451
12. Crooke ST (1998) An overview of progress in antisense therapeutics. Antisense Nucleic Acid Drug Dev 8:115–122
13. McCarthy MM (1998) Use of antisense oligonucleotides in the central nervous system: why such success? In: Stein CAK, Krieg AM (eds) Applied antisense oligonucleotide technology. Willey-Liss, New York, pp 283–296
14. Seidman S, Eckstein F, Grifman M, Soreq H (1999) Antisense technologies have a future fighting neurodegenerative diseases. Antisense Nucleic Acid Drug Dev 9:333–340
15. Chen Y, Constantini S, Trembovler V, Weinstock M, Shohami E (1996) An experimental model of closed head injury in mice: pathophysiology, histopathology, and cognitive deficits. J Neurotrauma 13:557–568
16. Grisaru D, Lev-Lehman E, Shapira M, Chaikin E, Lessing JB, Eldor A, Eckstein F, Soreq H (1999) Human osteogenesis involves differentiation-dependent increases in the morphogenically active 3' alternative splicing variant of acetylcholinesterase. Mol Cell Biol 19:788–795
17. Casceres A, Steward O (1983) Dendritic reorganization in the denervated gyrus of the rat following entorhinal cortical lesions: a Golgi and electron microscopic analysis. J Comp Neurol 214:387–403
18. McKinney RA, Debanne D, Gahwiler BH, Thompson SM (1997) Lesion-induced axonal sprouting and hyperexcitability in the hippocampus in vitro: implications for the genesis of posttraumatic epilepsy. Nat Med 3:990–996
19. Sternfeld M, Ming G, Song H, Sela K, Timberg R, Poo M, Soreq H (1998) Acetylcholinesterase enhances neurite growth and synapse development through alternative contributions of its hydrolytic capacity, core protein, and variable C termini. J Neurosci 18:1240–1249
20. Baldwin SA, Gibson T, Callihan CT, Sullivan PG, Palmer E, Scheff SW (1997) Neuronal cell loss in the CA3 subfield of the hippocampus following cortical contusion utilizing the optical disector method for cell counting. J Neurotrauma 14: 385–398
21. Tang YP, Noda Y, Hasegawa T, Nabeshima T (1997) A concussive-like brain injury model in mice. II. Selective neuronal loss in the cortex and hippocampus. J Neurotrauma 14:863–873
22. Andres C, Beeri R, Friedman A, Lev-Lehman E, Henis S, Timberg R, Shani M, Soreq H (1997) Acetylcholinesterase-transgenic mice display embryonic modulations in spinal cord choline acetyltransferase and neurexin Ibeta gene expression followed by late-onset neuromotor deterioration. Proc Natl Acad Sci U S A 94:8173–8178
23. Beeri R, Andres C, Lev Lehman E, Timberg R, Huberman T, Shani M, Soreq H (1995) Transgenic expression of human acetylcholinesterase induces progressive cognitive deterioration in mice. Curr Biol 5:1063–1071
24. Perry E, Martin-Ruiz C, Lee M, Griffiths M, Johnson M, Piggott M, Haroutunian V, Davis K, Gotti C, Tzartos S, Cohen O, Soreq H, Jaros E, Perry R, Court J (2000) Nictotinic receptor subtypes in human brain ageing and dementia. Eur J Pharmacol (in press)
25. Kaufer D, Friedman A, Seidman S, Soreq H (1998) Acute stress facilitates long-lasting changes in cholinergic gene expression. Nature 393:373–377
26. Grisaru D, Sternfeld M, Eldor A, Glick D, Soreq H (1999) Structural roles of acetylcholinesterase variants in biology and pathology. Eur J Biochem 264:672–686
27. Inestrosa NC, Alvarez A, Perez CA, Moreno RD, Vicente M, Linker C, Casanueva OI, Soto C, Garrido J (1996) Acetylcholinesterase accelerates assembly of amyloid-beta-peptides into Alzheimer's fibrils: possible role of the peripheral site of the enzyme. Neuron 16:881–891
28. Schenk D, Barbour R, Dunn W, Gordon G, Grajeda H, Guido T, Hu K, Huang J, Johnson-Wood K, Khan K, Kholodenko D, Lee M, Liao Z, Lieberburg I, Motter R, Mutter L, Soriano F, Shopp G, Vasquez N, Vandevert C, Walker S, Wogulis M, Yednock T, Games D, Seubert P (1999) Immunization with amyloid-beta attenuates Alzheimer-disease-like pathology in the PDAPP mouse. Nature 400:173–177
29. Morrow BA, Elsworth JD, Inglis FM, Roth RH (1999) An antisense oligonucleotide reverses the footshock-induced expression of fos in the rat medial prefrontal cortex and the subsequent expression of conditioned fear-induced immobility. J Neurosci 19:5666–5673
30. Grifman M, Soreq H (1997) Differentiation intensifies the susceptibility of pheochromocytoma cells to antisense oligodeoxynucleotide-dependent suppression of acetylcholinesterase activity. Antisense Nucleic Acid Drug Dev 7:351–359
31. Soreq H, Seidman S (2000) Antisense approach to isoform specific blockade of acetylcholinesterase. In: Crooke ST (ed) Antisense drug technology: principles, strategies, and applications. Dekker, New York
32. Xie J, McCobb DP (1998) Control of alternative splicing of potassium channels by stress hormones. Science 280:443–446
33. Kreutz MR, Bockers TM, Bockmann J, Seidenbecher CI, Kracht B, Vorwerk CK, Weise J, Sabel BA (1998) Axonal injury alters alternative splicing of the retinal NR1 receptor: the

preferential expression of the NR1b isoforms is crucial for retinal ganglion cell survival. J Neurosci 18:8278–8291
34. Imai Y, Matsuo N, Ogawa S, Tohyama M, Takagi T (1998) Cloning of a gene, YT521, for a novel RNA splicing-related protein induced by hypoxia/reoxygenation. Brain Res Mol Brain Res 53:33–40
35. Gattoni R, Mahe D, Mahl P, Fischer N, Mattei MG, Stevenin J, Fuchs JP (1996) The human hnRNP-M proteins: structure and relation with early heat shock-induced splicing arrest and chromosome mapping. Nucleic Acids Res 24:2535–2542
36. Tongiorgi E, Righi M, Cattaneo A (1997) Activity-dependent dendritic targeting of BDNF and TrkB mRNAs in hippocampal neurons. J Neurosci 17:9492–9505
37. Robinson RG (1997) Neuropsychiatric consequences of stroke. Annu Rev Med 48:217–229
38. Friedman A, Kaufer D, Shemer J, Hendler I, Soreq H, Tur-Kaspa I (1996) Pyridostigmine brain penetration under stress enhances neuronal excitability and induces early immediate transcriptional response. Nat Med 2:1382–1385

Anti-Sense Approach to Anticholinesterase Therapeutics

Hermona Soreq PhD and Shlomo Seidman PhD

Department of Biological Chemistry, Life Sciences Institute, The Hebrew University, Jerusalem, Israel

Key words: anti-sense, acetylcholinesterase, myasthenia gravis, stress, head injury, Alzheimer's disease, cholinesterase inhibitors

Abstract

The acetylcholine-hydrolyzing enzyme, acetylcholinesterase, is the molecular target of approved drugs for Alzhiemer's disease and myasthenia gravis. However, recent data implicate AChE splicing variants in the etiology of complex diseases such as AD and MG. Despite the large arsenal of anti-AChE drugs, therapeutic inhibitors are primarily targeted towards an active site shared by all variants. In contrast, anti-sense oligonucleotides attack unique mRNA sequences rather than tertiary protein structures. AS-ODNs thus offer a means to target gene expression in a highly discriminative manner using very low concentrations of drug. In light of the likely role(s) of specific AChE variants in various diseases affecting cholinergic neurotransmission, the potential contribution that anti-sense technology can make towards improved approaches to anti-AChE therapeutics deserves serious attention.

IMAJ 2000;2(Suppl):81–85

The high specificity of anti-sense oligonucleotides

Anti-sense oligonucleotides are short synthetic DNA chains, usually 15–25 nucleotides long, that have been designed to hybridize with a target messenger RNA according to the rules of Watson-Crick base-pairing [1,2]. The cellular uptake of oligonucleotides is not well understood. However, once inside the cell, the AS-ODN finds its complementary mRNA and forms an RNA-ODN duplex. The action of RNAseH upon the nascent hybrid results in AS-ODN-mediated destruction of the target RNA. To protect AS-ODNs from nucleolytic degradation, chemically modified analogs have been developed that display both prolonged and enhanced anti-sense effects. Common modifications include substitution of a non-bridging oxygen in the phosphodiester backbone with sulfur (phosphorothioate modification), and replacement of the 5' and/or 3' terminal bases of the ODN with 2'-O-methyl ribonucleotides. Since each of these modifications has its own unique advantages and disadvantages, it is becoming accepted to combine variably modified nucleotides into what are known as mixed-base oligonucleotides. AS-ODNs have been used to study a variety of medically relevant nervous system proteins, including ion channels, neurotransmitter receptors, neuropeptides and enzymes [Table 1]. Indeed, remarkable success has been reported using anti-sense technology to dissect the roles of closely related and pharmacologically indistinguishable proteins in the central nervous system [3].

Current anticholinesterase pharmacology

Acetylcholinesterase is responsible for the control of neurotransmission at cholinergic synapses and neuromuscular junctions by hydrolyzing acetylcholine. Rapid hydrolysis of ACh removes excess neurotransmitter from the synapse, preventing overstimulation and tetanic excitation of the postsynaptic cell. For this reason, AChE is the target protein of pesticides and chemical warfare

Table 1. Examples of nervous system proteins studied using anti-sense oligonucleotides

Potassium channels	N. Meiri, et al., *Proc Natl Acad Sci USA* 1997;94:4430–4
	N. Meiri, et al., *Proc Natl Acad Sci USA* 1998;95:15037–42
Dopamine receptors	J.M. Tepper, et al., *J Neurosci* 1997;17:2519–30.
cAMP response element-binding protein (CREB)	S.B. Lane Ladd, et al., *J Neurosci* 1997;17:7890–901
	R. Lamprecht, et al., *J Neurosci* 1997;17:8443–50.
Neuropeptide Y; galanin	P.S. Kalra, et al., *Methods Enzymol* 2000;314:184–200
Opioid receptors	G.W. Pasternak, Y X. Pan, *Methods Enzymol* 2000;2314:51–60
	P. Sanchez-Blazquez, et al., *Antisense Nucleic Acid Drug Dev* 1999;9:253–60
Neuronal nitrous oxide synthetase (nNOS)	Y.A. Kolesnikov, et al., *Proc Natl Acad Sci USA* 1997;94:8220–5
Cyclic nucleotide phosphodiesterases (PDE)	P.M. Epstein, *Methods* 1998;14:21–33

ACh = acetylcholine

AChE = acetylcholinesterase
AD = Alzheimer's disease
MG = myasthenia gravis
AS-ODNs = anti-sense oligonucleotides

agents [4,5]. At the same time, controlled use of AChE inhibitors plays a leading role in therapeutic strategies designed to enhance the cholinergic system. The rationale behind the clinical use of anticholinesterases is that AChE blockade extends the half-life of released ACh, thereby enhancing postsynaptic signals in patients with compromised cholinergic function. Indeed, the extensive use of anticholinesterase therapies highlights their clinical value. Nevertheless, accumulated experience attests to the limited extent and duration of clinical effects achieved with pharmacological AChE inhibitors. Recent advances in molecular and cellular biology suggest several explanations to account for limitations of classic anticholinesterase therapeutics and suggest a novel genome-based approach.

Specificity in anticholinesterase pharmaceuticals

A primary challenge confronting anticholinesterase pharmacology is to overcome the structural and functional homology between AChE and butyrylcholinesterase, also known as "serum cholinesterase" [6,7]. AChE and BChE are carboxylesterase type B serine hydrolases with 52% identity [8]. Both enzymes degrade acetylcholine. However, AChE is very specific in its substrate recognition, while BChE recognizes a broad range of substrates. For this reason, it has been suggested that circulating plasma BChE serves a scavenging function, protecting AChE from naturally occurring inhibitors. At the same time, however, BChE will also scavenge anticholinesterase drugs, elevating the dose necessary to achieve inhibition at the target organ. To complicate the issue, the large number of polymorphic BChE variants with differing affinities for inhibitors was predicted to confer inheritable variations in the sensitivity of individuals to anti-AChE drugs and poisons [9]. The AChE/BChE specificity problem has been partially overcome with the development of AChE inhibitors, demonstrating up to 1,000-fold preference for AChE [10]. Nevertheless, the minimal homology displayed by AChE and BChE at the level of the gene makes these sequences completely non-overlapping targets for an anti-sense-based drug.

AChE variants

A new dimension to the question of specificity with regard to AChE inhibitors emerged as molecular cloning revealed that alternative splicing gives rise to three distinct AChE isoforms [11,12]. The presumed target of all anticholinesterase therapeutics is the "synaptic" AChE-S isoform with its unique 40 amino acid, amphiphilic, C-terminal peptide. A second, erythrocyte-bound form, AChE-E, is presumed to participate with BChE in scavenging blood-borne inhibitors, including drugs of abuse [13]. Until recently, AChE-S and AChE-E were considered the primary factors in the development of anticholinesterase drugs. Recently, the rare *"readthrough "* AChE-R isoform was discovered to undergo dramatic upregulation under some conditions, including acute psychological stress, closed head injury, and exposure to AChE inhibitors [14,15]. This finding suggested that AChE-R plays a role in the body's response to stress [16,17]. In addition, it raised the possibility that the balance between AChE-R and AChE-S carries important implications for health and disease. These studies therefore challenge us to develop inhibitors that selectively target specific AChE variants. However, the differences in the affinities of inhibitors for AChE-S and AChE-R are small (Salmon et al., submitted), suggesting an anti-sense approach to the problem of isoform-specific inhibition of AChE.

Transgenic models of AChE over-expression

The discovery that traumatic insults and AChE inhibitors elicit feedback over-expression of AChE-R highlights the complexity of anticholinesterase therapeutics on the one hand, and the need to understand the physiological role of AChE-R on the other. To examine these issues, we produced transgenic mice over-expressing various AChE isoforms. Mice over-expressing AChE-S in CNS neurons displayed an age-dependent tendency for increased AChE-R that was associated with neuromotor and cognitive impairments that presented features of human neurological diseases [18–20]. In contrast, transgenic mice over-expressing AChE-R from birth were relatively free of age-dependent markers of neuronal stress [21]. These studies indicate that the long-term balance between AChE-S and AChE-R may be a critical element mediating outcomes of AChE responses.

Avoiding feedback

Electrophysiological recordings in hippocampal brain slices indicated that overproduction of AChE-R is initiated by the acute cholinergic stimulation resulting from abrupt pharmacological blockade of AChE [14]. Moreover, novel polymorphisms in the upstream promoter region of the human ACHE gene locus encoding AChE have been associated with acute hypersensitivity to anticholinesterase drugs [22]. Anti-sense technology offers two solutions to this problem. First, the relative instability of AChE-R vs. AChE-S mRNA [23] suggests that AS-ODNs could be aimed primarily at AChE-R, leaving AChE-S and cholinergic neurotransmission intact. Moreover, by blocking production of new AChE rather than neutralizing existing AChE, anti-sense suppression of enzyme activity occurs more slowly than that of conventional drugs. Gradual inhibition allows the target tissue to adapt to graded increases in ACh concentrations. Finally, thanks to the anti-mRNA nature of anti-sense blockade, oligonucleotide doses can be tailored to suppress *de novo* expression of the ACHE gene (N. Galyam and H. Soreq, unpublished data).

BChE = butyrylcholinesterase

Non-catalytic activities of AChE

In addition to its long-recognized role in hydrolyzing acetylcholine, AChE exerts profound effects on neurite outgrowth and cell adhesion [7,24]. These activities were proven to be independent of ACh hydrolysis [25] and were tentatively attributed to homologies between ACHE and cholinesterase-like cell adhesion molecules like *Drosophila* neurotactin and mammalian neuroligins [26–28]. Non-catalytic activities of AChE have been tentatively mapped to the peripheral anionic site, but were not yet shown to be affected by conventional anticholinesterase drugs. Moreover, since damaging effects of over-expressed AChE-R may be related to non-catalytic activities, cholinesterase inhibitors may actually aggravate certain conditions by elevating the levels of catalytically inactivated AChE via the feedback loop. Since anti-sense technology targets production of the protein, rather than the activity of existing enzyme, AS-ODNs offer a potential solution to this problem as well.

Anti-AChE anti-sense oligonucleotides – where do we stand?

AS-ODNs to AChE have been demonstrated effective *in vitro* and *in vivo*, especially in the hematopoietic system [29–31]. First-generation anti-AChE AS-ODNs were prepared in unmodified or fully phosphorothioated forms [32] and then in partially phosphorothioated form. Reducing the phosphorothioate content minimized cytotoxicity without compromising activity [33]. Two AChE AS-ODNs, AS1 and AS3 [23], demonstrated potent inhibition of AChE in rat pheochromocytoma PC12 cells (up to 50%) at extremely low nanomolar concentrations. Substitution of 2'-O-methyl-modified ribonucleotides at the three terminal 3' positions conferred a wide effective window (0.02–200 nM; N. Galyam and H. Soreq, manuscript in preparation) and became the routine configuration for AS-ODN synthesis in our laboratory. In osteosarcoma Saos-2 cells, 2 nM AS-ODN blocked AChE and modified proliferation, reinforcing evidence that AChE plays a role in mammalian osteogenesis [34]. The pronounced effects elicited by such low concentrations of AS-ODN predict reduced costs and minimal non-specific side effects of future anti-sense therapies.

Potential applications

Anticholinesterase exposures

The association between AChE inhibitors, AChE feedback, and neuromuscular impairments [7,35] suggests AChE AS-ODNs for treating anticholinesterase intoxication. During the Persian Gulf War, several hundred thousand soldiers received the carbamate AChE inhibitor pyridostigimine to protect them against threatened chemical warfare. A recent Rand Corporation report (Document no. MR-1018/2-OSD) prompted the U.S. Defense Department to acknowledge that pyridostigmine cannot be ruled out as a possible contributor to various unexplained symptoms experienced by Gulf War veterans, including muscle weakness [36]. In light of our knowledge about the AChE feedback loop, the detrimental effects of over-expressed AChE on muscle [37], and the fact that no clinical protocol has been implemented to treat muscle weakness among Gulf War veterans, we suggest that this may represent an appropriate arena in which to test the utility of anti-sense therapy for neuromuscular impairments. The regrettably high incidence of agricultural anticholinesterse poisoning incidents in Israel alone (about 500 per year) suggests another potential application for anti-AChE ODN drugs.

Neuromuscular disease

Myasthenia gravis is a debilitating neuromuscular disease characterized by muscle weakness and deterioration of neuromotor function [38]. MG results from autoimmune antibody-mediated depletion of acetylcholine receptors from neuromusclular junctions. AChE inhibitors such as Mestinon – a commercial formulation of pyridostigmine – treat the symptoms of MG but do not slow its progression.[39]. Moreover, the pharmacological effects of anticholinesterase drugs are short-lasting, and relatively high doses of these medications must be taken up to six times per day for many years. It has even been suggested that pyridostigmine may contribute to progressive deterioration in muscle function [40]. In this light, it is not surprising that a promising AChE inhibitor for Alzheimer's disease was withdrawn from clinical trials after some patients reported muscle weakness (SCRIP World Pharmaceutical News. 1998, No. 2374. P. 19). We demonstrated that the AChE feedback loop is active in muscle, and that AS3 suppresses inhibitor-induced over-expression of AChE in mice [37]. In that study, 80 μg/kg AS3 blocked anticholinesterase-induced accumulation of catalytically active AChE in muscle by 60%, and suppressed the accompanying increase in motor endplates. These experiments proved that AS-ODNs can suppress both catalytic and morphogenic activities of muscle AChE *in vivo*. Tests in rats with experimental autoimmune myasthenia are in progress (in collaboration with T. Brenner).

Head trauma

Closed head injury is a major cause of death among young adults [41,42] and a risk factor in non-familial Alzheimer's disease [43]. Effective treatment should therefore consider survival, recovery, and prevention of delayed neurological disorders. We observed elevated AChE-R mRNA in brains of mice subjected to CHI [14]. A single intracerebroventricular administration of 0.5 μg AS3 within one hour of injury blocked the accumulation of AChE-R mRNA and the excessive dendritic growth accompanying it. In AChE transgenic mice, anti-sense treatment reduced mortality, facilitated recovery and protected CA3 hippocampal neurons. These findings demonstrated the potential of anti-sense therapeutics in emergency medicine and

suggest the application of AChE AS-ODN to protect against the long-term consequences of traumatic insults to the nervous system.

Neurodegenerative disease

Alzheimer's disease is a debilitating neurodegenerative disease characterized by progressive deterioration of cognitive faculties including learning, memory, problem solving and abstract thinking. The cholinergic theory of AD suggests that loss of cholinergic neurons leaves a relative deficit of acetylcholine in the brain regions that mediate learning and memory [44]. The only approved drugs for AD are potent AChE inhibitors [45]. Nevertheless, the cognitive improvement afforded by conventional anticholinesterase therapy is limited. Moreover, recent studies suggest that AChE plays a role in AD that goes beyond the cholinergic theory [46,47]. Indeed, the putative role of AChE as an active component in the progress of AD may explain the disappointing performance of AChE inhibitors in providing effective long-term improvement. Using surgically implanted cannulae to deliver nanomolar quantities of AS3 to the cerebrospinal fluid of cognitively impaired transgenic mice, we are testing the effects of anti-sense therapy on performance in behavior models such as social exploration and spatial navigation (O. Cohen et al., Abstract to the Israel Society of Neuroscience, Eilat, 1999). Nevertheless, the challenge of bringing AS-ODN technology to CNS therapeutics faces yet unresolved technical limitations. Among the most difficult issues to resolve is the poor transport of oligonucleotides across the blood-brain-barrier [2]

Conclusions

Advances in our understanding of the molecular and cellular mechanisms of action of AChE allow us to postulate mechanisms explaining the limitations of conventional anticholinesterase pharmacology. These limitations are likely based on non-catalytic activities of AChE isoforms and a feedback loop leading to over-expression of AChE following acute blockade of enzymatic activity. At the same time, cloning of the human ACHE gene opened the door to novel strategies to suppress AChE biosynthesis using antisense technology. These advances in basic research allow us to think ahead to the application of AS-ODN-based drugs to future anticholinesterase therapeutics.

Acknowledgements: The work presented here was supported by Israel Ministry of Health, the U.S. Army Medical Research and Development Command, the Israel Science Foundation, the U.S.-Israel Binational Science Foundation, the Eric Roland Center for Neurodegenerative Diseases, and Ester Neurosciences, Ltd., Tel Aviv.

References

1. Agrawal S, Kandimalla ER. Antisense therapeutics: is it as simple as complementary base recognition? *Mol Med Today* 2000;6:72–81.
2. Seidman S, Eckstein F, Grifman M, Soreq H. Antisense technologies have a future fighting neurodegenerative diseases. *Antisense Nucleic Acid Drug Dev* 1999;9:333–40.
3. McCarthy MM. Use of antisense oligonucleotides in the central nervous system: why such success? In: Stein CA, Krieg AM. eds. Allied Antisense Oligonucleotide Technology. New York Wiley-Liss, Inc., 1998:283–96.
4. Soreq H, Zakut H, eds. In: Human Cholinesterases and Anticholinesterases. San Diego: Academic Press, 1993.
5. Taylor P. Agents acting at the neuromuscular junction and autonomic ganglia. In: Hardman JG, Limbird LE, Molinoff PB, Ruddon RW, eds Goodman and Gilman's The Pharmacological Basis of Therapeutics. Ninth edition. New York: McGraw-Hill. 1996:177–197.
6. Schwarz M, Glick D, Loewenstein Y, Soreq H. Engineering of human cholinesterases explains and predicts diverse consequences of administration of various drugs and poisons. *Pharmacol Ther* 1995;67:283–322.
7. Soreq H, Glick D. Novel roles for cholinesterases in stress and inhibitor responses. In: Giacobini E ed. Cholinesterases and Cholinesterase Inhibitors. London: Martin Dunitz, 2000:47–61.
8. Soreq H, Ben-Aziz R, Prody CA, Seidman S, Gnatt A, Neville L, Lieman-Hurwitz J, Lev-Lehman, Ginzberg D, Lapidot-Lifson Y, et al. Molecular cloning and construction of the coding region for human acetylcholinesterase reveals a G + C-rich attenuating structure. *Proc Natl Acad Sci USA* 1990;87:9688–92.
9. Loewenstein Lichtenstein Y, Schwarz M, Glick D, Norgaard Pedersen B, Zakut H, Soreq H. Genetic predisposition to adverse consequences of anti-cholinesterases in 'atypical' BCHE carriers. *Nat Med* 1995;1:1082–5.
10. Bryson HM, Benfield P. Donepezil. *Drugs Aging* 1997;10:234–9; discussion 240–1.
11. Ben Aziz Aloya R, Sternfeld M, Soreq H. Promoter elements and alternative splicing in the human ACHE gene. *Prog Brain Res* 1993;98:147–53.
12. Li Y, Camp S, Rachinsky TL, Getman D, Taylor P. Gene structure of mammalian acetylcholinesterase. Alternative exons dictate tissue-specific expression. *J Biol Chem* 1991;266:23083–90.
13. Salmon AY, Goren Z, Avissar Y, Soreq H. Human erythrocyte but not brain acetylcholinesterase hydrolyses heroin to morphine. *Clin Exp Pharmacol Physiol* 1999;26:596–600.
14. Friedman A, Kaufer D, Shemer J, Hendler I, Soreq H, Tur Kaspa I. Pyridostigmine brain penetration under stress enhances neuronal excitability and induces early immediate transcriptional response. *Nat Med* 1996;2:1382–5.
15. Shohami E, Kaufer D, Chen Y, Seidman S, Cohen O, Ginzberg D, Melamed-Book N, Yirmiya R, Soreq H. Antisense prevention of neuronal damages following head injury in mice. *J Mol Med* 2000.In press.
16. Kaufer D, Soreq H. Tracking cholinergic pathways from psychlogical and chemical stressors to variable neurodegeneration paradigms. *Curr Opin Neurol* 1999;12:739–43.
17. Kaufer D, Friedman A, Soreq H. The vicious circle: long-lasting transcriptional modulation of cholinergic neurotransmission following stress and anticholinesterase exposure. *The Neuroscientist* 1999;5:173–83.
18. Beeri R, Le Novere N, Mervis R, Huberman T, Grauer E, Changeux JP, Soreq H. Enhanced hemicholinium binding and attenuated dendrite branching in cognitively impaired acetylcholinesterase-transgenic mice. *J Neurochem* 1997;69:2441–51.
19. Beeri R, Andres C, Lev Lehman E, Timberg R, Huberman T, Shani M, Soreq H. Transgenic expression of human acetylcholinesterase induces progressive cognitive deterioration in mice. *Curr Biol* 1995;5:1063–71.
20. Andres C, Beeri R, Friedman A, Lev-Lehman E, Henis S, Timberg R, Shani M, Soreq H. Acetylcholinesterase-transgenic mice display embryonic modulations in spinal cord choline acetyltransferase and neurexin 1beta gene expression followed by late-onset neuromotor deterioration. *Proc Natl Acad Sci USA* 1997;94:8173–8.
21. Sternfeld M, Shoham S, Klein O, Flores-Flores C, Evron T, Idelson GH, Kirsberg D, Patrick JW, Soreq H. Excess "readthrough" acetylcholinesterase attenuates but the "synaptic" variant intensifies neurodeterioration correlates. *Proc Natl Acad Sci USA* 2000: (in press).
22. Shapira M, Tur-Kaspa I, Bosgraaf L, Livni N, Grant AD, Grisaru D, Korner M, Ebstein RP, Soreq H. A transcription-activating polymorphism in the ACHE promoter associated with acute sensitivity to anticholinesterases. *Hum Mol Genet* 2000;9:1273–81.
23. Grifman M, Soreq H. Differentiation intensifies the susceptibility of pheochromocytoma cells to antisense oligodeoxynucleotide-dependent suppression of acetylcholinesterase activity. *Antisense Nucleic Acid Drug Dev* 1997;7:351–9.

24. Grisaru D, Sternfeld M, Eldor A, Glick D, Soreq H. Structural roles of acetylcholinesterase variants in biology and pathology. *Eur J Biochem* 1999;264:672–86.

25. Sternfeld M, Ming G, Song H, Sela K, Timberg R, Poo M, Soreq H. Acetylcholinesterase enhances neurite growth and synapse development through alternative contributions of its hydrolytic capacity, core protein, and variable C termini. *J Neurosci* 1998;18:1240–9.

26. Darboux I, Barthalay Y, Piovant M, Hipeau Jacquotte R. The structure-function relationships in Drosophila neurotactin show that cholinesterasic domains may have adhesive properties. *EMBO J* 1996;15:4835–43.

27. Ichtchenko K, Nguyen T, Sudhof TC. Structures, alternative splicing, and neurexin binding of multiple neuroligins. *J Biol Chem* 1996;271:2676–82.

28. Grifman M, Galyam N, Seidman S, Soreq H. Functional redundancy of acetylcholinesterase and neuroligin in mammalian neuritogenesis. *Proc Natl Acad Sci USA* 1998;95:13935–40.

29. Soreq H, Patinkin D, Lev-Lehman E, Grifman M, Ginzberg D, Eckstein F, Zakut H. Antisense oligonucleotide inhibition of acetylcholinesterase gene expression induces progenitor cell expansion and suppresses hematopoietic apoptosis ex vivo. *Proc Natl Acad Sci USA* 1994;91:7907–11.

30. Lev Lehman E, Ginzberg D, Hornreich G, Ehrlich G, Meshorer A, Eckstein F, Soreq H, Zakut H. Antisense inhibition of acetylcholinesterase gene expression causes transient hematopoietic alterations in vivo. *Gene Ther* 1994;1:127–35.

31. Lev-Lehman E, Deutsch V, Eldor A, Soreq H. Immature human megakaryocytes produce nuclear-associated acetylcholinesterase. *Blood* 1997;89:3644–53.

32. Patinkin D, Seidman S, Eckstein F, Benseler F, Zakut H, Soreq H. Manipulations of cholinesterase gene expression modulate murine megakaryocytopoiesis in vitro. *Mol Cell Biol* 1990;10:6046–50.

33. Ehrlich G, Patinkin D, Ginzberg D, Zakut H, Eckstein F, Soreq H. Use of partially phosphorothioated "antisense" oligodeoxynucleotides for sequence-dependent modulation of hematopoiesis in culture. *Antisense Res Dev* 1994;4:173–83.

34. Grisaru D, Lev-Lehman E, Shapira M, Chaikin E, Lessing JB, Eldor A, Eckstein F, Soreq H. Human osteogenesis involves differentiation-dependent increases in the morphogenically active 3' alternative splicing variant of acetylcholinesterase. *Mol Cell Biol* 1999;19:788–95.

35. Glick D, Shapira M, Soreq H. Molecular neurotoxicity implications of acetylcholinesterase inhibition, In: Lazarovici P, Lester D, eds. Site-Specific Neurotoxicology, New York: Plenum Press. In press .

36. Haley RW, Kurt TL, Hom J. Is there a Gulf War Syndrome? Searching for syndromes by factor analysis of symptoms. *JAMA* 1997;277:215–22.

37. Lev-Lehman E, Evron T, Broide RS, Meshorer E, Ariel I, Seidman S, Soreq H. Synaptogenesis and Myopathy under Acetylcholinesterase Overexpression. *J Molec Neurosci* 2000;14:93–105.

38. Schonbeck S, Chrestel S, Hohlfeld R. Myasthenia gravis: prototype of the antireceptor autoimmune diseases. *Int Rev Neurobiol* 1990;32:175–200.

39. Evoli A, Batocchi AP, Tonali P. A practical guide to the recognition and management of myasthenia gravis. *Drugs* 1996;52:662–70.

40. Swash M.: Motor innervation of myasthenic muscles [Letter]. *Lancet* 1975;ii:663.

41. Siesjo BK. Basic mechanisms of traumatic brain damage. *Ann Emerg Med* 1993;22:959–69.

42. Yakovlev AG, Faden AI. Molecular biology of CNS injury. *J Neurotrauma* 1995;12:767–77.

43. Gennarelli TA, Graham DI. Neuropathology of the Head Injuries. *Semin Clin Neuropsychiatry* 1998;3:160–75.

44. Coyle JT, Price DL, DeLong MR. Alzheimer's disease: a disorder of cortical cholinergic innervation. *Science* 1983;219:1184–90.

45. Giacobini E. Cholinesterase inhibitors for Alzheimer's disease therapy: from tacrine to future applications [Invited review]. *Neurochem Int* 1998;32:413–19.

46. Inestrosa NC, Alvarez A, Perez CA, Moreno RD, Vicente M, Linker C, Casanueva OI, Soto C, Garrido J. Acetylcholinesterase accelerates assembly of amyloid-beta-peptides into Alzheimer's fibrils: possible role of the peripheral site of the enzyme. *Neuron* 1996;16:881–91.

47. Campos EO, Alvarez A, Inestrosa NC. Brain acetylcholinesterase promotes amyloid-beta-peptide aggregation but does not hydrolyze amyloid precursor protein peptides. *Neurochem Res* 1998;23:135–40.

Correspondence: Dr. S. Soreq, Dept. of Biological Chemistry, Life Sciences Institute, The Hebrew University, Jerusalem 91904, Israel. Tel: (972-2) 658 5109; Fax: (972-2) 652 0258; email: soreq@cc.huji.ac.il.

Excess "read-through" acetylcholinesterase attenuates but the "synaptic" variant intensifies neurodeterioration correlates

Meira Sternfeld*†, Shai Shoham‡, Omer Klein*, Cesar Flores-Flores*, Tamah Evron*, Gregory H. Idelson§, Dani Kitsberg§, James W. Patrick¶, and Hermona Soreq*‖

*The Eric Roland Center for Neurodegenerative Diseases, Department of Biological Chemistry, Hebrew University of Jerusalem, Jerusalem 91904, Israel; ‡Research Department, Herzog Hospital, Jerusalem 91351, Israel; §Alomone Labs, P.O. Box 4287, Jerusalem 91042, Israel; and ¶Baylor College of Medicine, Division of Neuroscience, One Baylor Plaza, Houston, TX 77030-3498

Edited by Tomas Hökfelt, Karolinska Institute, Stockholm, Sweden, and approved May 10, 2000 (received for review January 6, 2000)

Acute stress increases the risk for neurodegeneration, but the molecular signals regulating the shift from transient stress responses to progressive disease are not yet known. The "read-through" variant of acetylcholinesterase (AChE-R) accumulates in the mammalian brain under acute stress. Therefore, markers of neurodeterioration were examined in transgenic mice overexpressing either AChE-R or the "synaptic" AChE variant, AChE-S. Several observations demonstrate that excess AChE-R attenuates, whereas AChE-S intensifies, neurodeterioration. In the somatosensory cortex, AChE-S transgenics, but not AChE-R or control FVB/N mice, displayed a high density of curled neuronal processes indicative of hyperexcitation. In the hippocampus, AChE-S and control mice, but not AChE-R transgenics, presented progressive accumulation of clustered, heat shock protein 70–immunopositive neuronal fragments and displayed a high incidence of reactive astrocytes. Our findings suggest that AChE-R serves as a modulator that may play a role in preventing the shift from transient, acute stress to progressive neurological disease.

Both chronic stress and acute stress promote neuroanatomic changes in brains of evolutionarily diverse species, including higher vertebrates and humans (1). Some of these changes likely reflect normal physiological adaptation to injury, environmental challenge, traumatic experience, or even standard maintenance conditions of laboratory animals (2). However, stress may also precipitate delayed or prolonged neuropsychiatric dysfunction, the etiology of which is yet poorly defined. For example, up to 30% of individuals exposed to an acute traumatic experience develop posttraumatic stress disorder, a syndrome characterized by progressively worsening personality disturbances and cognitive impairments (3). The cellular and molecular factors mediating the switch between physiological accommodation of stress and progressive disease are unknown but likely reflect complex interactions between the genetic background of the challenged individual and the nature of the stress insult (3–5). The accepted notion is that physiological stress responses are beneficial in the short run but detrimental if overactivated or prolonged (6). This concept suggests the existence of stress modulators designed to regulate the extent, duration, and long-term impact of acute stress responses.

We recently reported massive induction of a unique mRNA species encoding the rare "read-through" variant of acetylcholinesterase (AChE-R) in brains of mice subjected to forced swimming stress (7). AChE-R differs from the dominant "synaptic" variant, AChE-S, in the composition of its C-terminal sequence (8). Both enzymes effectively hydrolyze acetylcholine. However, AChE-S can form multimeric complexes and associate with membranes through interactions with structural subunits, whereas AChE-R is monomeric and soluble (9). In hippocampal brain slices, induced AChE-R seemed to play a role in delimiting a state of enhanced neuronal excitation observed after acute cholinergic stimulation (7). This observation suggested that AChE-R acts as a stress modulator in mammalian brain.

Transgenic mice overexpressing human AChE-S in central cholinergic neurons exhibited progressive impairments in learning and memory, diminished dendritic branching, and reduced numbers of spines in cortical neurons (10). Similar behavioral and morphological characteristics were reported in senile dementia (11), a murine model of chronic stress (12), and delayed consequences of anticholinesterase intoxication (7).

The up-regulation of AChE-R under stress, the unique biochemical characteristics of AChE-R compared with AChE-S, and the characteristics of neurodegenerative disease manifested in AChE-S transgenic mice, together raised the question of whether AChE-R is involved in the shift from acute stress response to neurodegenerative state. To study this issue, we compared two lines of transgenic mice overexpressing human AChE-R (13) with AChE-S transgenic and control FVB/N mice. We hypothesized that if AChE-R promotes neurodegeneration, transgenic animals with chronic overexpression of this protein would display neuroanatomical markers of neuronal pathology even when confronted only with the mild stresses of daily life. On the other hand, if AChE-R works against the slide into neurodegeneration, AChE-R transgenics should display markers of neuroprotection. Herein, we report that AChE-R transgenic mice are indeed relatively free of some neuronal stress correlates compared with controls, whereas AChE-S transgenics display accelerated, age-dependent accumulation of neuroanatomical features indicative of neuronal stress responses. This study points at AChE-R as a stress-induced modulator of delayed neural stress response processes that can protect the mammalian brain from neurodegenerative disease, perhaps by preventing AChE-S from causing such deterioration.

Methods

Animals. Mice were killed by cervical dislocation, and tissues were rapidly excised and frozen. Homogenates were prepared in nine volumes of 0.01 M Na-phosphate buffer, pH 7.4/1% Triton X-100 (wt/wt), incubated on ice (1 h), and centrifuged (at 14,000

This paper was submitted directly (Track II) to the PNAS office.

Abbreviations: AChE, acetylcholinesterase; AChE-R, read-through AChE variant; AChE-S, synaptic AChE variant; ARP, AChE read-through peptide; GST, glutathione *S*-transferase; GFAP, glial fibrillary acidic protein; NFT200, neurofilament 200; HSP, heat shock protein; GABA, γ-aminobutyric acid; PCP, phencyclidine.

†Present address: Department of Evolution Systematics and Ecology, Institute of Life Sciences, Hebrew University of Jerusalem, 91904, Israel.

‖To whom reprint requests should be addressed. E-mail: soreq@cc.huji.ac.il.

The publication costs of this article were defrayed in part by page charge payment. This article must therefore be hereby marked "*advertisement*" in accordance with 18 U.S.C. §1734 solely to indicate this fact.

Article published online before print: *Proc. Natl. Acad. Sci. USA*, 10.1073/pnas.140004597. Article and publication date are at www.pnas.org/cgi/doi/10.1073/pnas.140004597

rpm for 45 min in an Eppendorf model 5417R centrifuge); supernatants were then collected.

AChE Activity and Protein Concentration. AChE activity and protein concentration determinations were performed as described (13). Sucrose gradient centrifugation was performed as detailed elsewhere (14), except that 0.5% Triton X-100 was used as detergent.

Immunoblotting. Immunoblot analysis was performed essentially as detailed (15). Immunodetection was performed with pooled goat anti-mouse and anti-human AChE antibodies directed at an N-terminal peptide common to the different variants (N-19 and E-19; Santa Cruz Biotechnology). Signals were quantified with IMAGE-PRO software (Media Cybernetics, Silver Spring, MD).

Preparation of Antibodies Directed at the AChE Read-Through Peptide (ARP). A glutathione *S*-transferase (GST)-ARP (GMQGPAGS-GWEEGSGSPPGVTPLFSP) fusion protein was expressed in *Escherichia coli* and purified by affinity chromatography. Female New Zealand rabbits were immunized with 0.3 mg of ARP-GST in Freund's complete adjuvant and reimmunized monthly with 0.2 mg of ARP-GST in Freund's incomplete adjuvant. Specific serum antibodies were detected by ELISA by using immobilized ARP-GST with excess soluble GST. Crude IgG fraction was prepared by $(NH_4)_2SO_4$ precipitation. IgG fractions were incubated repeatedly with immobilized GST or heat-shocked *E. coli* lysate and eluted with 4.5 M $MgCl_2$. Unbound fractions were incubated with ARP-GST beads, eluted, and dialyzed.

Preparation of Brain Sections. Mice were deeply anesthetized with Fluothane (Zenaca, Macclesfield Cheshire, U.K.) and transcardially perfused with 4% (vol/vol) paraformaldehyde. Brains were postfixed in 4% (vol/vol) paraformaldehyde (overnight, 2–8°C) and incubated in 15% (vol/vol) sucrose/0.1 M PBS. Coronal cryostat sections (30 μm) were floated in PBS and kept at −20°C in 40% (vol/vol) ethylene glycol/1% polyvinylpyrrolidone/0.1 M potassium acetate (pH 6.5) until staining.

Immunohistochemistry. Immunohistochemistry was performed as described (16). Staining was with extravidin-peroxidase (Sigma) reacted with diaminobenzidine and nickel ammonium sulfate. Silver impregnation to detect degenerating argyrophilic neurons was performed by using kit PK301 (FD Neurotechnologies, Ellicott City, MD). Antibody dilutions were mouse anti-neurofilament 200 (NFT200; clone N52, Sigma; 1:200); mouse anti-heat shock protein 70 (HSP70; clone BRM22, Sigma; 1:125); mouse anti-glial fibrillary acidic protein (GFAP; clone GA5, Sigma; 1:500); mouse anti-calbindin D28K (clone CL-300, Sigma, 1:500); mouse anti-parvalbumin (clone P19, Sigma 1:500); mouse anti-human erythrocyte AChE (Chemicon; 1:500); and the above described rabbit anti-ARP antiserum (1:100).

Results

AChE-R and AChE-S Are Moderately Overexpressed in Brains of Transgenic Mice. Catalytic activity measurements showed moderately elevated AChE activity in cortex, hippocampus, and basal nuclei of mice from two independent AChE-R transgenic lines (lines 45 and 70; ref. 13) and a single line of AChE-S transgenics (10), as compared with controls (Fig. 1*A*). Immunoblot analysis of cortex homogenates with antibodies directed at the N-terminal domain common to all AChE variants revealed two to three immunoreactive bands, probably reflecting posttranslational processing. The top two bands appeared more intense in transgenics. Cumulative densitometry of all three bands revealed that AChE immunoreactivity was modestly elevated in cortex of both AChE-R and AChE-S transgenics as compared with controls (Fig. 1*B*). In contrast, sucrose gradient centrifugation

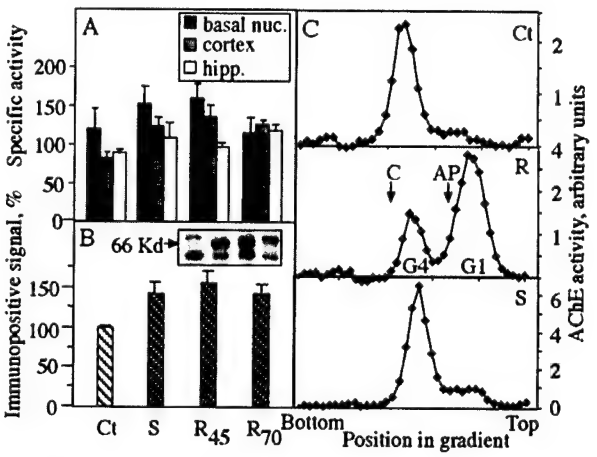

Fig. 1. Overexpression of AChE in transgenic brain. (*A*) AChE activity in brain regions of transgenic mice. Shown are rates of acetylthiocholine hydrolysis per min per mg of protein in homogenates of basal nuclei (basal nuc.), cortex, and hippocampus (hipp.) of AChE-S (S), AChE-R of line 45 (R_{45}), AChE-R of line 70 (R_{70}) transgenics, and control (Ct) mice, all from the FVB/N strain. Bars present averages ± SEM for homogenates from four or five mice of each pedigree. Note that elevation in catalytic AChE activity, although nonsignificant, is common to all transgenic lines. (*B*) AChE immunoreactivity in cortex of transgenic mice. Shown are average intensities ± SEM of immunopositive bands after SDS/PAGE, immunoblot, and densitometric analyses of cortical homogenates from transgenic and control mice. The antibody used was targeted against the common N-terminal domain of AChE; the positive signal obtained with this antibody in control mouse samples (see *Inset*) demonstrates massive cross reactivity with the mouse enzyme. Intensities were determined for the three main immunopositive bands (see *Inset*) from five to eight lanes loaded with protein from individual mice of each strain and are presented as percentage of control values within the same gel. Note that elevation in immunoreactivity, although nonsignificant, is common to all transgenic lines. (*B Inset*) An example of an immunoblot film, showing the main bands in each lane for each of the transgenics and controls at the same order as in the bar graph. Kd, kilodalton. (*C*) Altered multimeric assembly. Shown are sucrose gradient profiles for AChE in the cortex of control (Ct), AChE-S (S), and AChE-R (R; line 45) mice. Arrows denote the sedimentation of bovine catalase (C; 11.4 S) and alkaline phosphatase (AP; 6.1 S). Note elevation in AChE tetramers (G4; ≈10 S) or monomers (G1; ≈4.4 S) and the altered ratio between these isoforms in the different transgenics.

demonstrated a large increase of AChE monomers in the cortex of AChE-R mice (Fig. 1*C*). The ratio between tetramers and monomers was 11.0, 7.4, and 0.4 in cortices of control, AChE-S transgenic, and AChE-R transgenic mice, respectively. That the ratio between tetramers and monomers was altered more substantially than the absolute elevation of enzyme activity in AChE-R mice suggested that the multimeric assembly of AChE in brain depends on the ratio of AChE-S to AChE-R monomers.

Immunological Detection of AChE-R in Mammalian Brain. An antiserum directed at human ARP unique to the AChE-R isoform was used to immunostain frozen coronal brain sections. Anti-ARP antiserum stained neurons, but not glia, from both control and transgenic mice (Fig. 2). In sections from AChE-R transgenic mice, intense neuronal staining, apparent both in soma and dendrites, was noted in somatosensory and piriform cortex, dentate gyrus, and basolateral amygdala (Fig. 2 *Right*), presumably reflecting prominent expression of human AChE-R in these regions. Dendritic staining was limited to proximal regions, except for dentate gyrus neurons, where distal dendritic regions (at least 70 μm in length) were stained as well. Many additional neurons in these brain regions exhibited weak to moderate staining of the cytoplasm, leaving the nucleus completely pale. In addition, prominent staining of some neurons was observed in the hypothalamus, thalamus, and nucleus basalis magnocel-

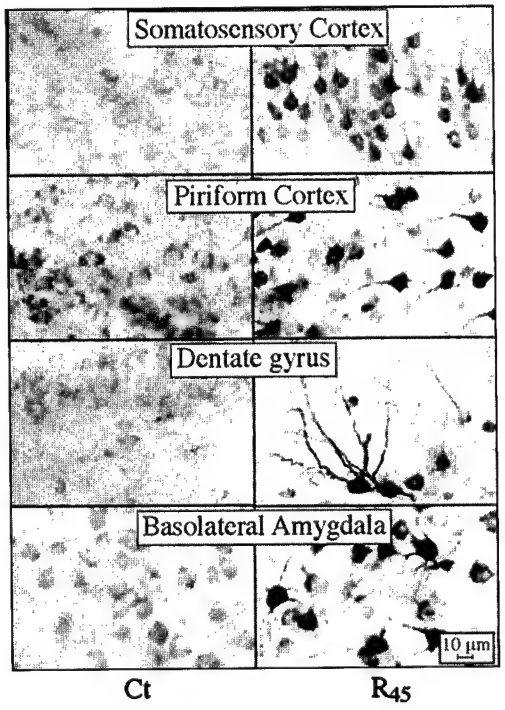

Fig. 2. AChE-R immunoreactivity in transgenic brain. Shown is AChE-R immunoreactivity in high-magnification photomicrographs of coronal sections 1.2 mm posterior to bregma from the brains of control (Ct) mice and the AChE-R line 45 transgenics (R_{45}). Note that ARP immunostaining is apparent only in neurons, that both somata and processes are stained, and that the intensity of neuronal staining is highly variable between the different brain regions.

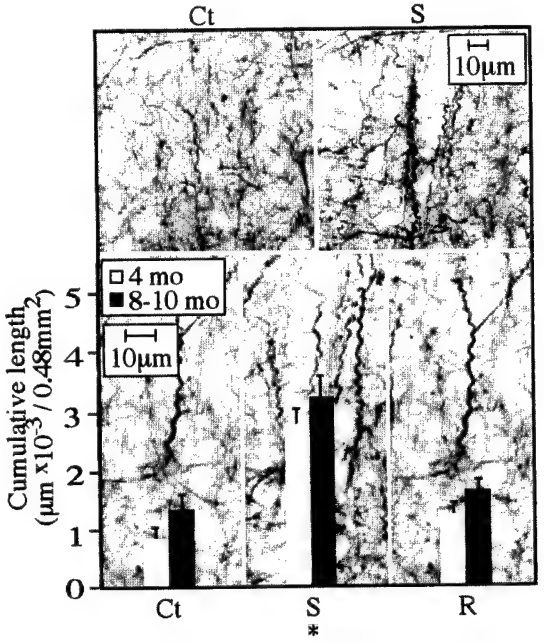

Fig. 3. Evidence for neuronal process malformation in AChE-S transgenic mice. (*Upper*) Example micrographs from control (Ct) and AChE-S transgenics (S) immunolabeled for NFT200. (*Lower*) Cumulative lengths (averages ± SEM) of all axonal or dendritic segments displaying a corkscrew-like pattern are displayed on high-magnification micrographs from the parietal cortex of 4-month-old or 8- to 10-month-old AChE-S (S) and AChE-R (R) transgenics and control (Ct) mice. Numbers were derived from three coronal sections containing the somatosensory cortex, 1–2 mm posterior to bregma, from each of six male mice per group. Analysis with the Seescan Image Analysis system (Seescan plc, Cambridge, U.K.) was performed on 32 subfields of 150 μm (width) × 100 μm (height; total area of 0.48 mm^2). *, $P < 0.001$.

lularis neurons (data not shown). Both staining intensity and numbers of stained neurons were higher in line 45 than in line 70 mice. Weak, diffuse staining was also observed in many brain regions of control and AChE-S transgenic mice (Fig. 2 and data not shown). In control mice, however, somewhat pronounced AChE-R accumulation was noted in piriform cortex and basolateral amygdala. Control sections exposed to antiserum preadsorbed with synthetic ARP (10 μM) were completely negative (data not shown), demonstrating specificity of the staining. With antiserum directed at the common domain of the enzyme, only AChE-S transgenic mice displayed immunopositive signals. In this case, the antibody labeled neurons in the nuclei of the basal ganglia, including striatum, globus pallidus, nucleus basalis magnocellularis, entopeduncular nucleus, and substantia nigra pars reticulata. Overall, the immunodetection of AChE-R and AChE-S in transgenic mice was consistent with *in situ* hybridization data localizing expression of the various mRNAs to the same brain regions (ref. 10 and data not shown). Thus, the failure of anti-common-domain antiserum to stain AChE-R overexpressing neurons may reflect differential folding properties of AChE-S (17) and AChE-R monomers.

Indication for AChE-S-Induced Neuronal Hyperexcitation. Because AChE overexpression in mammalian and amphibian systems affected neuronal processes (10, 15), we compared process morphology in control and AChE transgenic mice. Immunostaining with a monoclonal antibody to the cytoskeletal protein NFT200 revealed a curled "corkscrew"-like deformation of cortical, but not hippocampal, processes in all mouse lines (Fig. 3). Corkscrew processes, which are indicative of neuronal hyperexcitation (18), exhibited an invariant sinusoid-like regularity and did not stain for HSP70. To quantify the extent of corkscrew formation, we measured the cumulative length of neurites with corkscrew morphology in 500-μm^2 regions. The cumulative length of corkscrew-shaped neurites progressed with age from 4 to 8–10 months, in all pedigrees. However, at both 4 months and 8–10 months of age, AChE-S mice displayed significantly greater extents of corkscrew morphology than either control or AChE-R transgenic mice. In striking contrast, both lines of AChE-R transgenic mice displayed a degree of corkscrew morphology comparable with that of control mice (Fig. 3 and Table 1). Because deterioration of cortical inhibitory GABAergic interneurons was suggested to be the cause of the corkscrew phenomenon (18), we characterized GABAergic neurons in the somatosensory cortex of transgenic mice. No cell loss or shrinkage and no morphological aberrations were observed among any of the transgenic pedigrees as compared with controls (Table 1). Moreover, average thickness of the parietal cortex and neuronal density were similar between the different lines. Furthermore, silver impregnation did not stain parietal cortex neurons in any of these pedigrees, showing no evidence for terminal neurodegeneration (not shown).

AChE-R Protects Hippocampal Neurons from Stress-Related Morphologies. In all pedigrees, some clusters of NFT200-immunoreactive neuronal fragments were observed in the stratum radiatum layer of the hippocampal CA1–3 regions (Fig. 4 *Top*), increasing in number with advancing age (Fig. 4 and Table 1). AChE-S transgenic mice exhibited a significant extent of cluster formation already at 4 months of age, which was approximately doubled in 8- to 10-month-old mice. In contrast, only about one-third of 4-month-old control FVB/N and AChE-R mice exhibited clustered neural fragments, and then, not more than one cluster per mouse was observed. The 8- to 10-month-old

Table 1. Suppressed stress-associated morphological features in AChE-R transgenics

Morphological Abnormality	Measurement	AChE-S	AChE-R	Control	Statistical test
Curled processes, (NFT200)	Cumulative length in 0.48 mm² (μm)	3,080 ± 210; $P < 0.0001$	1,410 ± 150	1,070 ± 170	Newman–Keuls
Cortex thickness μm		230 ± 7	240 ± 8	230 ± 5	*F* test
GABAergic interneurons	Cell number in cortical layers 1–3	210 ± 4	190 ± 14	190 ± 19	*F* test
(parvalbumin)	Cell number in cortical layers 4–6	250 ± 12	270 ± 14	250 ± 10	*F* test
	Cell area, μm²	68 ± 3	66 ± 3	60 ± 3	*F* test
GABAergic interneurons	Cell number in cortical layers 1–3	290 ± 10	300 ± 6	260 ± 15	*F* test
(calbindin D28K)	Cell number in cortical layers 4–6	67 ± 5	73 ± 2	76 ± 5	*F* test
	Cell area, μm²	57 ± 2	55 ± 1.5	54 ± 2	*F* test
Neuronal fragment	Number of clusters per section	3.3 ± 0.8	0.4 ± 0.2; $P < 0.02$	1.7 ± 0.4	Mann–Whitney
clusters (NFT200)	Cluster area, μm²	3,470 ± 370	2,090 ± 500*	2,060 ± 230	*T* test
	Number of fragments per cluster	110 ± 16; $P < 0.002$	70 ± 15*	46 ± 4	*T* test
	Fragment density in cluster	0.032 ± 0.002; $P < 0.03$	0.035 ± 0.008*	0.023 ± 0.002	*T* test
Neuronal fragment	Number of clusters per section	6.2 ± 2.1; $P < 0.005$	0.4 ± 0.3	1.7 ± 0.7	Mann–Whitney
clusters (HSP70)	Cluster area, μm²	2,690 ± 380; $P < 0.03$	1,370 ± 280*	1,690 ± 240	*T* test
	Number of fragments per cluster	50 ± 6; $P < 0.02$	30 ± 7*	31 ± 4	*T* test
	Fragment density in cluster	0.020 ± 0.001	0.022 ± 0.004*	0.019 ± 0.001	*T* test
Astrocytes (GFAP)	Total number of cells	270 ± 9	250 ± 10	270 ± 10	*F* test
	Percentage of hypertrophic cells	24 ± 2	16 ± 3; $P < 0.03$	24 ± 2	Newman–Keuls

Presented are average values ± SEM for the measurements of morphological features noted in the text. The antibody used for staining is noted in parentheses. Age groups of 4-month-old and 8- to 10-month-old mice were combined for calculations, except for the clustering phenomenon, which increased with age, and for which, the data presented (pooled from three mice) is for the 8- to 10-month-old group. A normal distribution could not be assumed, and nonparametric tests were used: Kruskal–Wallis's for the main effects of transgenic line or age and Mann–Whitney's for multiple comparisons of transgenic lines. Significant *P* values (in comparison with control mice) are noted where appropriate. GABA; γ-aminobutyric acid.

*In AChE-R transgenics, the small number of clusters found precluded any statistical comparison of cluster area and number of fragments per cluster.

control mice displayed approximately half the number of fragment clusters as age-matched AChE-S mice. In 10-month-old AChE-R mice, clustered neuronal fragments were very rare. Cluster size, the number of fragments per cluster, and fragment density were all significantly greater in 8- to 10-month-old AChE-S mice than in age-matched controls or AChE-R transgenics (Table 1).

Neuronal fragment clusters have been observed in posttraumatic states, for example after head injury (19–21). Therefore, we stained sections for HSP70, which stains degenerating processes in acute head trauma (19, 20) and Alzheimer's disease (22). Anti-HSP70 antibodies revealed clusters in hippocampus resembling those observed with anti-NFT200, with similar patterns and incidence (Fig. 4 and Table 1). As with NFT200-stained clusters, HSP70-positive clusters were more abundant in AChE-S and more sparse in AChE-R mice than in controls. Progression with age, from 4 to 8 months, was observed both in control and AChE-S mice ($P = 0.05$) but not AChE-R mice. In no case were hippocampal neurons stained by silver impregnation, demonstrating sustained cell viability.

Suppressed Astrocyte Reactivity in AChE-R Transgenic Mice. Immunostaining for GFAP was performed to test whether the neuroanatomic changes in cortical and hippocampal neurons overexpressing the different AChE variants involve morphological changes in glial cells. Modified astrocyte morphology was observed in the stratum lacunosum moleculare of the hippocampal CA3 subregion, where a subset of reactive astrocytes presented highly immunoreactive soma and enhanced dendritic staining (Fig. 5) as compared with normal astrocytes in which the soma were pale or invisible. Only minor differences were discerned in the average total numbers of astrocytes. However, the percentage of reactive astrocytes was significantly lower in the AChE-R transgenics than in controls or AChE-S transgenics (Table 1 and Fig. 5).

Discussion

After acute stress, the ratio between AChE-R and AChE-S increases dramatically, probably by a combination of transcriptional and posttranscriptional mechanisms (7). To test whether prolonged modulation of AChE expression could influence neuroanatomic features in the mammalian brain, we generated transgenic mice with subtle overexpression of either AChE-S or AChE-R in brain neurons. The 30–50% elevated expression of AChE in these transgenic models resembles that observed by us for FVB/N mice subjected to forced swim stress. We therefore hypothesized that if excess AChE-R exacerbates the cumulative neurological consequences of stress, AChE-R transgenics would display exaggerated histopathological features characteristic of stress response processes. In fact, we observed reduced numbers and sizes of clustered neuronal fragments and decreased numbers of reactive astrocytes in 8- to 10-month-old AChE-R transgenic mice compared with controls. Therefore, our data indicate that AChE-R works to protect the brain against neurodegeneration. The inverse pattern of morphological correlates in AChE-S transgenic mice points to AChE-S as a potential accelerator of stress-promoted neurodeterioration.

The predominance of 3′ unspliced AChE-R mRNA in brain after stress represents a diversion of alternative splicing that was also observed in stress responses for the retinal *N*-methyl-D-aspartate receptor I, clathrin light chain B, and transformer-2 β (23). Similarly, stress hormone-induced shifts in alternative splicing were reported to favor the repetitive firing variants of K^+ channels in adrenal chromafin tissue (24). The primary differences between AChE isoforms are reflected in the enzyme's oligomeric assembly, hydrodynamic properties, and subcellular distribution (9). These features will affect the sites of potential action of the enzyme, both with respect to catalytic and noncatalytic activities. That AChE-S, but not AChE-R, accelerates the corkscrew phenomenon attributes a previously unperceived role in neurite degeneration to this AChE variant. Several observations support the notion that AChE-S activates a unique

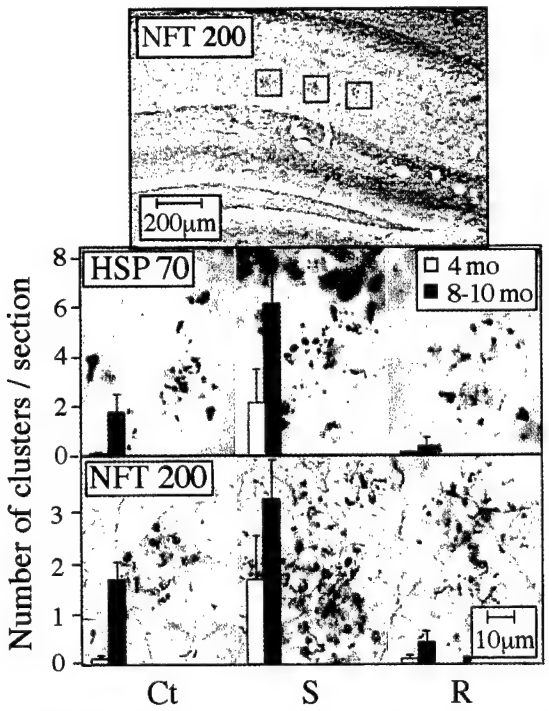

Fig. 4. Clustered neuronal fragments. Shown are coronal brain sections from 8- to 10-month-old control and transgenic mice after immunostaining of NFT200 or HSP70 with cresyl violet counter staining. (*Top*) Low-magnification image, in which gray-black clusters of neuronal fragments immunopositive for NFT200 (surrounded by red frames) are apparent in the stratum radiatum layer of hippocampal CA1–3 regions (1.6–2.8 mm posterior to bregma). (*Middle and Bottom*) High-magnification images of the framed regions, stained for HSP70 and NFT200, respectively. Clusters including over 10 neuronal fragments were counted in three sections from each mouse, 2 to 4 mm posterior to bregma. Bars present counted clusters per section as average ± SEM for six mice from each strain and age group (4-month-old and 8- to 10-month-old). Ct, control FVB/N mouse; S, AChE-S transgenic mouse; R, AChE-R transgenic mouse.

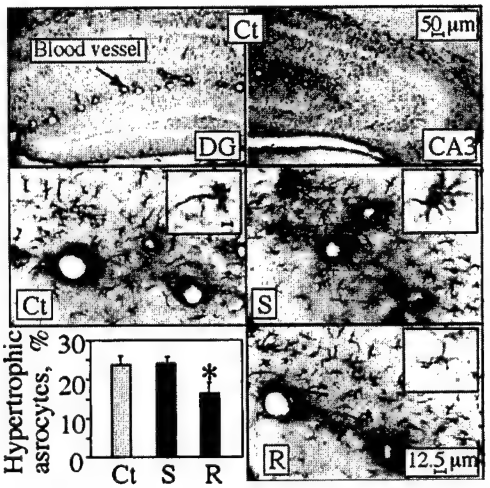

Fig. 5. Astrocyte reactivity. Normal and reactive astrocytes were counted in the stratum lacunosum moleculare in hippocampal sections 2 to 4 mm posterior to bregma (three from each of six mice in each strain). Shown is GFAP astrocyte labeling in coronal brain sections from 4-month-old transgenic and control mice. Note that in normal astrocytes, only dendrites are stained, and soma are pale or invisible, whereas reactive cells display highly immunoreactive soma and enhanced dendritic staining. (*Top*) Example low-magnification micrographs of dentate gyrus (DG; *Left*) and CA3 (*Right*) hippocampal regions of control (Ct) mice. (*Middle and Bottom*) High-magnification images of stratum lacunosum moleculare from the hippocampal CA3 subregion from control (Ct), AChE-S (S), and AChE-R (R) mice. (*Insets*) Individual astrocytes stained for GFAP (Bar = 1 μm). (*Bottom Left*) Percentage of reactive astrocytes of the total counted astrocytes (average ± SEM of $n = 6$ mice for each group). *, $P < 0.05$.

cell-signaling cascade or cascades. For example, in the embryonic spinal cord, AChE-S overexpression was shown to enhance the production of choline acetyl transferase (25). The difference between AChE-S and AChE-R transgenics in this respect probably includes a component related to noncatalytic properties of the two variants. Interestingly, increased ratios between AChE monomers and tetramers, perhaps reflecting AChE-R overproduction, were reported for Alzheimer's disease (26) and after anticholinesterase exposure (reviewed in ref. 27).

We previously reported that chronic overexpression of AChE-S causes progressively impaired memory and decreased dendritic branching in cortical neurons (10), as in senile dementia (11). Our current work demonstrates that AChE-S transgenics manifest additional features of neuronal stress, such as corkscrew processes, neuronal retraction balls, and reactive gliosis. NFT200-positive structures are subject to morphological changes in both the normal and the pathological ranges of plasticity (19, 20, 28). Sinusoidal corkscrew processes were shown after chemical [e.g., phencyclidine (PCP); "angel dust"] intoxication, head trauma, and ischemic/hypoxic stress and in brains of patients with Alzheimer's disease (19–21, 29). This deformity often precedes process degeneration and neuronal death but may also be reversible. The pathway that creates the corkscrew phenotype is considered to be associated with hyperexcitation. For example, PCP, an antagonist of *N*-methyl-D-aspartate receptors on inhibitory GABAergic interneurons, causes hyperactivation of cortical pyramidal neurons with which these interneurons communicate (18). Because muscarinic receptor blockers prevent formation of PCP-induced corkscrew structures (21), this hyperactivation is apparently caused by the excitatory inputs to cortical pyramidal neurons, which include a cholinergic element.

AChE-R transgenics displayed relatively prominent overexpression of the AChE-R protein in precisely those neurons that are notably associated with stress responses in the dentate gyrus, amygdala (30), and piriform cortex (31). Corkscrew structures were increased significantly in AChE-S but not in AChE-R transgenics as compared with control mice, supporting the notion of a protective role for AChE-R. Based on the PCP model, we expected to find pathology among GABAergic neurons and/or increased cholinergic input in AChE-S mice. Because we found no evidence of pathology to GABAergic neurons, there remains the possibility of excessive cholinergic input. Elevated high-affinity choline transport in these mice (10) and elevated acetylcholine levels as measured by microdialysis (C. Erb, unpublished work) indeed indicate cholinergic hyperexcitation.

Clustered neuronal fragments reflecting axonal and dendritic "retraction balls," depict advanced neurite changes (19–21). Elevated HSP70 reported after head injury and in Alzheimer's disease (19, 22) highlights the importance of these clustered neural fragments as markers of neurodeterioration. Although these fragments often predict subsequent neuronal death (20), silver impregnation excluded exceptional rates of neuronal death among AChE-S transgenics, both in the parietal cortex where corkscrew-like processes appeared and in the hippocampus where the process retraction balls were seen. Cluster numbers and sizes and fragment numbers and density within clusters were significantly elevated in 8- to 10-month-old versus 4-month-old control mice and in AChE-S transgenics versus controls in both ages. Thus, AChE-S seemed to accelerate a normal age-

dependent neuropathological process. In contrast, AChE-R prominently attenuated cluster formation in both age categories. The possibility that the protective effects of AChE-R derive from a direct interaction or competition with AChE-S or its putative cell surface ligands remains to be studied. One way to approach this question would be to establish transgenic mice overexpressing both transcripts. In cultured glioma cells coexpressing AChE-S and AChE–R mRNAs, AChE-R exerted a dominant phenotype (32).

GFAP overproduction in astrocytes is considered to reflect neuronal changes such as synaptic remodeling (33). Reactive astrocytes, significantly reduced in the hippocampus of AChE-R transgenics as compared with controls or AChE-S transgenic mice, are the hallmark of "reactive gliosis," reflecting the reaction of glial cells to trauma. Reactive gliosis occurs in acute brain injury, in neurodegenerating regions within the brain of patients with Alzheimer's, during viral infections, after chemical intoxication (34), and even in normal aging (35). The low incidence of reactive glia in AChE-R transgenic mice further reinforces the notion that chronic presence of AChE-R acts to protect the brain against long-term stress-related damage.

In this study, mice were not subjected to experimental stress but were exposed to mildly stressful daily handling (2). However, they developed features associated with stress in numerous species and various stress paradigms (18–22, 29, 33–37). However, genetic background may have a significant effect on the rate and extent of stress-induced neurodeterioration. Different strains of mice may vary in fearfulness and response to stress (38). FVB/N mice were shown to be highly susceptible to the widespread neurodegeneration that follows kainic acid seizures (39) but not to the selective loss of midbrain dopaminergic neurons induced by 1-methyl-4-phenyl-1,2,3,6-tetrahydropyridine (40) as compared with the C57BL/6 mice. No evidence for neuronal loss was found in AChE-S transgenic mice with the FVB/N background up to 10 months of age. Nevertheless, these animals can live up to 2 years, and neuronal death may occur only at truly advanced ages.

Chronic overexpression of AChE-R was consistently associated with reduction in several morphological correlates of neurodegeneration in transgenic mice. Demonstration of such association in two distinct transgenic lines shows that this phenotype did not depend on the integration site of the transgene but probably on a certain threshold of AChE-R overexpression. Our current findings therefore demonstrate that AChE-R, most likely with another modulator or modulators, may be beneficial in the response to acute stress at two levels: (*i*) by dampening the acute cholinergic hyperactivation that accompanies stress (7) and (*ii*) by protecting the brain from entering the downward spiral into progressive neurodegeneration through an as-yet unidentified mechanism, which could involve noncatalytic activities and/or direct competition with AChE-S. In that case, the diversion of up-regulated AChE expression after insults to the central nervous system from production of the usual AChE-S to the unusual AChE-R isoform (7) would reflect an elegant evolutionary mechanism to avoid the dangers of overexpressed AChE-S. These findings imply that mutations conferring heritable up-regulation of AChE-R would protect the mammalian central nervous system from some age-dependent neuropathologies. The definitive role of AChE-R after transient stress or drug-induced overexpression remains to be examined in additional animal models permitting conditional regulation of AChE gene expression.

We thank Dr. S. Seidman (Jerusalem) for critically reviewing this manuscript. This study was supported by U.S.–Israel Binational Science Foundation Grant 96-00110 to H.S. and J.W.P. and by grants to H.S. from the Israel Science Fund (number 590/97), Ester Neurosciences, the U.S. Army Medical Research and Materiel Command (DAMD 17-99-1-9547), and the research fund in memory of Leopold, Sara, and Norman Israel. C.F.-F. was the incumbent of a FEBS Long-Term Fellowship.

1. McEwen, B. S. (1999) *Annu. Rev. Neurosci.* **22,** 105–122.
2. Riley, V. (1981) *Science* **212,** 1100–1109.
3. Turnbull, G. J. (1998) *Injury* **29,** 169–175.
4. True, W. R., Rice, J., Eisen, S. A., Heath, A. C., Goldberg, J., Lyons, M. J. & Nowak, J. (1993) *Arch. Gen. Psychiatry* **50,** 257–264.
5. Graham, D. I., Gentleman, S. M., Nicoll, J. A., Royston, M. C., McKenzie, J. E., Roberts, G. W., Mrak, R. E. & Griffin, W. S. (1999) *Cell. Mol. Neurobiol.* **19,** 19–30.
6. Sapolsky, R. M. (1996) *Science* **273,** 749–750.
7. Kaufer, D., Friedman, A., Seidman, S. & Soreq, H. (1998) *Nature (London)* **393,** 373–377.
8. Grisaru, D., Sternfeld, M., Eldor, A., Glick, D. & Soreq, H. (1999) *Eur. J. Biochem.* **264,** 672–686.
9. Seidman, S., Sternfeld, M., Ben Aziz-Aloya, R., Timberg, R., Kaufer-Nachum, D. & Soreq, H. (1995) *Mol. Cell. Biol.* **15,** 2993–3002.
10. Beeri, R., Le Novere, N., Mervis, R., Huberman, T., Grauer, E., Changeux, J. P. & Soreq, H. (1997) *J. Neurochem.* **69,** 2441–2451.
11. Buell, S. J. & Coleman, P. D. (1981) *Brain Res.* **214,** 23–41.
12. Sakic, B., Szechtman, H., Denburg, J. A., Gorny, G., Kolb, B. & Whishaw, I. Q. (1998) *J. Neuroimmunol.* **87,** 162–170.
13. Sternfeld, M., Patrick, J. D. & Soreq, H. (1998) *J. Physiol. (Paris)* **92,** 249–255.
14. Flores-Flores, C., Martinez-Martinez, A., Munoz-Delgado, E. & Vidal, C. J. (1996) *Biochem Biophys. Res. Commun.* **219,** 53–58.
15. Sternfeld, M., Ming, G., Song, H., Sela, K., Timberg, R., Poo, M. & Soreq, H. (1998) *J. Neurosci.* **18,** 1240–1249.
16. Shoham, S. & Ebstein, R. P. (1997) *Exp. Neurol.* **147,** 361–376.
17. Bourne, Y., Grassi, J., Bougis, P. E. & Marchot, P. (1999) *J. Biol. Chem.* **274,** 30370–30376.
18. Olney, J. W. & Farber, N. B. (1995) *Arch. Gen. Psychiatry* **52,** 998–1007.
19. Li, R., Fujitani, N., Jia, J. T. & Kimura, H. (1998) *Am. J. Forensic Med. Pathol.* **19,** 129–136.
20. Kubo, S., Kitamura, O., Orihara, Y., Ogata, M., Tokunaga, I. & Nakasono, I. (1998) *J. Med. Invest.* **44,** 109–119.
21. Corso, T. D., Sesma, M. A., Tenkova, T. I., Der, T. C., Wozniak, D. F., Farber, N. B. & Olney, J. W. (1997) *Brain Res.* **752,** 1–14.
22. Hamos, J. E., Oblas, B., Pulaski-Salo, D., Welch, W. J., Bole, D. G. & Drachman, D. A. (1991) *Neurology* **41,** 345–350.
23. Daoud, R., Da Penha Berzaghi, M., Siedler, F., Hubener, M. & Stamm, S. (1999) *Eur. J. Neurosci.* **11,** 788–802.
24. Xie, J. & McCobb, D. P. (1998) *Science* **280,** 443–446.
25. Andres, C., Beeri, R., Friedman, A., Lev-Lehman, E., Henis, S., Timberg, R., Shani, M. & Soreq, H. (1997) *Proc. Natl. Acad. Sci. USA* **94,** 8173–8178.
26. Saez-Valero, J., Sberna, G., McLean, C. A. & Small, D. H. (1999) *J. Neurochem.* **72,** 1600–1608.
27. Kaufer, D., Friedman, A. & Soreq, H. (1999) *The Neuroscientist* **5,** 173–183.
28. Trojanowski, J. Q., Walkenstein, N. & Lee, V. M. (1986) *J. Neurosci.* **6,** 650–660.
29. Braak, E., Braak, H. & Mandelkow, E. M. (1994) *Acta Neuropathol.* **87,** 554–567.
30. Herman, J. P. & Cullinan, W. E. (1997) *Trends Neurosci.* **20,** 78–84.
31. Imaki, T., Shibasaki, T., Hotta, M. & Demura, H. (1993) *Brain Res.* **616,** 114–125.
32. Karpel, R., Sternfeld, M., Ginzberg, D., Guhl, E., Graessmann, A. & Soreq, H. (1996) *J. Neurochem.* **66,** 114–123.
33. Laping, N. J., Teter, B., Nichols, N. R., Rozovsky, I. & Finch, C. E. (1994) *Brain Pathol.* **4,** 259–275.
34. Wu, V. W. & Schwartz, J. P. (1998) *J Neurosci. Res.* **51,** 675–681.
35. Unger, J. W. (1998) *Microsc. Res. Tech.* **43,** 24–28.
36. Faden, A. I. (1993) *Crit. Rev. Neurobiol.* **7,** 175–186.
37. Ma, K. C., Nie, X. J., Hoog, A., Olsson, Y. & Zhang, W. W. (1994) *J. Neurol. Sci.* **126,** 184–192.
38. Francis, D. D. & Meaney, M. J. (1999) *Curr. Opin. Neurobiol.* **9,** 128–134.
39. Schauwecker, P. E. & Steward, O. (1997) *Proc. Natl. Acad. Sci. USA* **94,** 4103–4108.
40. German, D. C., Nelson, E. L., Liang, C. L., Speciale, S. G., Sinton, C. M. & Sonsalla, P. K. (1996) *Neurodegeneration* **5,** 299–312.

Antisense approach to isoform specific blockade of acetylcholinesterase

Hermona Soreq and Shlomo Seidman

[1]Department of Biological Chemistry, The Life Sciences Institute, The Hebrew University of Jerusalem, Jerusalem, Israel 91904

Tel. 972 2 658 5109/ fax. 972 2 652 0258

email: soreq@cc.huji.ac.il

Overview:

Specific inhibition of nervous system enzymes or receptors is often difficult to achieve pharmacologically, especially where the target protein is a particular subtype within a family of closely related gene products. Antisense oligonucleotides attack unique nucleotide sequences rather than 3- dimensional protein structures. Thus, they offer a powerful tool to discriminate between closely related proteins derived from homologous genes, polymorphic alleles, or alternative splicing products. The acetylcholine-hydrolyzing enzyme, acetylcholinesterase (AChE), is the molecular target of approved drugs for Alzhiemer's disease (AD) and myasthenia gravis (MG). However, novel findings implicate alternative splicing variants of AChE in the complex etiology of diseases such as AD and MG. Despite the large arsenal of anti-AChE drugs, AChE inhibitors are targeted towards an active site shared by all isoforms. Therefore, isoform specific inhibtors are not likely to become available in the near future. Thus, the putative roles of different AChE isoforms in health and disease emphasize the potential contribution that antisense technology can make towards improved understanding and strategic approaches to anti-AChE therapeutics.

The need for subtype-specific protein targeting:

The vast complexity of the mammalian central nervous system (CNS) is facilitated by the large variety of neurotransmitters and neurotransmitter receptors in the brain (Barnard, 1988). Molecular heterogeneity in the CNS is generated, in part, by homologous genes, alternative splicing, and combinations of non-identical subunits that generate heterooligomeric complexes. Thus, closely related receptor isoforms may possess diverse properties with regard to ligand affinity, channel kinetics, or spatio-temporal expression. Moreover, alternative isoforms may be preferentially expressed under various physiological conditions or states of disease (Xie and McCobb, 1998). The same is true for enzyme isoforms catalyzing the various biochemical reactions allowing the brain to maintain homeostasis and respond to external stimuli. The role that specific neurotransmitter or receptor subtypes, or isozymes play in behavior, health, and disease, emphasizes the importance of selective drug targeting. Nevertheless, isoform-specific pharmacological inhibitors are often elusive. For that reason, antisense oligonucleotides have become an attractive alternative to classic pharmacology for both basic brain reseaerch and drug development.

Exploiting the High Specificity of Antisense Oligonucleotides

Antisense oligonucleotides have been used to study various families of CNS proteins, including ion channels, neurotransmitter receptors, neuropeptides, and enzymes. Many of these studies have been performed *in vivo*, using stereotaxic injections or infusions through a surgically implanted cannula. For example, over 40 different potassium channels have been identified in the

mammalian CNS. Despite their diverse electrophysiological characteristics, the channel domain of potassium channels has been highly conserved through evolution, making the various subtypes difficult to distinguish pharmacologically. Using multiple intracerebroventricular administrations of isoform-specific antisense oligonucleotides, the ATP-dependent A-type potassium channel Kv1.4 was selectively inactivated in rats, and its role in long-term potentiation and spatial memory distinguished from that of the late-rectifying K+ channel Kv1.1 (Meiri et al., 1997; Meiri et al., 1998). Similarly, antisense oligonucleotides were used to distinguish between members of the D2 class of dopamine receptors. Since the K_Ds for most agonists and antagonists towards different members of this receptor family are within one order of magnitude, pharmacological discrimination between them is poor. On the other hand, antisense oligonucleotides elicited selective, physiologically-significant reductions in either D_2 or D_3 autoreceptors in dopaminergic neurons in the substantia nigra of treated rats (Tepper et al., 1997). An interesting suggestion made in that study was that the limited diffusion of oligonucleotides following intraparenchymal injection can be exploited to specifically target either presynaptic or postsynaptic neurons, an options not afforded by conventional drugs. Indeed, highly specific regional targeting of antisense oligonucleotide effects in the brain has been observed by others (Lamprecht et al., 1997; Lane Ladd et al., 1997). Nevertheless, it should be noted that distant transport of a minor fraction of injected oligonucleotides along projection pathways has been reported (Sommer et al., 1998). In the case of the peptide neurotransmitters neuropeptide Y and galanin, antisense oligonucleotides have been used to down regulate both the neurotransmitters themselves and specific receptor subtypes (Kalra et al., 2000).

Classification and characterization of the opioid receptors mu, delta, and kappa has been greatly assisted by antisense technology (Pasternak and Pan, 2000). Selective oligonucleotides blocking behavioral or analgesic responses helped map the separate opiate receptors, while oligonucleotides targeting specific exons within a subtype have provided evidence for alternative splicing and additional levels of subtype complexity. For example, oligonucleotides targeting 5 different exons in the mu opioid receptor were able to differentiate between analgesic effects mediated by endomorphin-1 and morphine (Sanchez-Blazquez et al., 1999). Antisense oligonucleotides targeting specific exons in the neuronal nitrous oxide synthetase gene were similarly employed to differentiate the actions of 2 isozymes derived by alternative splicing (nNOS-1 and nNOS-2) on morphine analgesia (Kolesnikov et al., 1997). Cyclic nucleotide phosphodiesterases (PDE), some families of which may generate as many as 15 splice variants, have been suggested as another potential area for applied antisense technology (Epstein, 1998). The high specificity of antisense oligonucleotides and the ability to discriminate between closely related gene products made antisense technology a natural tool in approaching the complex biology and therapeutic centrality of acetylcholinesterase.

Current anticholinesterase pharmacology

Acetylcholinesterase (EC 3.1.1.7) is the enzyme responsible for maintaining tight regulation of neurotransmission at cholinergic synapses by hydrolyzing spent acetylcholine (ACh). Rapid hydrolysis of ACh acts to reduce the concentration of neurotransmitter at the synapse, preventing overstimulation and tetanic excitation of the postsynaptic nerve or muscle. For this reason, AChE is the target protein of numerous agricultural pesticides and chemical warfare agents (Soreq and Zakut, 1993; Taylor, 1996). For the same reason, however, controlled use of AChE inhibitors has come to play a leading role in therapeutic strategies designed to augment the cholinergic system. The rationale behind clinical use of AChE inhibitors is that

inactivation of AChE prolongs the half-life of released ACh, thereby enhancing postsynaptic signals. Indeed, anticholinesterase therapies have served the medical community relatively well. Nevertheless, inherent limitations restrict the therapeutic utility of pharmacological AChE inhibitors.

Limitations of AChE pharmacology

1. Specificity

One of the principle challenges of classical anticholinesterase pharmacology was to overcome the structural and functional homology between AChE and the closely related enzyme butyrylcholinesterase (BChE, EC 3.1.1.8) in designing specific inhibitors (Schwarz et al., 1995; Taylor et al., 1995). AChE and BChE are carboxylesterase type B serine hydrolases sharing 52% identical amino acids (Soreq et al., 1990). Although both enzymes hydrolyze acetylcholine, AChE is very specific in its substrate recognition, while BChE is much more permissive. Due to its relaxed substrate specificity, BChE interacts to some extent or another with most AChE inhibitors. Thus, the high concentration of plasma BChE has been suggested to serve a scavenging function, protecting AChE from various naturally occurring AChE inhibitors (Loewenstein Lichtenstein et al., 1995). By the same token, however, BChE will act to scavenge therapeutic anti-AChE drugs, elevating the dose necessary to achieve inhibition at the target organ. Moreover, as BChE is characterized by a large number of allelic polymorphisms with different affinities for anticholinesterase compounds, genetic variation was predicted to introduce individual differences in sensitivity to anti-AChE drugs and poisons (Loewenstein Lichtenstein et al., 1995). The AChE/BChE specificity problem has been partially, but not completely overcome with the development of AChE inhibitors demonstrating up to 1000-fold preference for AChE over BChE (Bryson and Benfield, 1997). Nonetheless, the insignificant sequence homology displayed by AChE and BChE at the level of the gene makes these proteins completely distinguishable, non-overlapping targets using antisense technology. Furthermore, the question of specificity with regard to AChE inhibitors took an unforseen leap in complexity as molecular data describing the nature and potential consequences of 3' altenative splicing of AChE mRNA became available (Grisaru et al., 1999).

Cloning of the mammalian ACHE gene revealed 3 forms of mature mRNA encoding AChE, together accounting for the multitude of known AChE isoforms (Ben Aziz Aloya et al., 1993; Li et al., 1991) (figure1). The presumed target of all AChE inhibitors is the "synaptic" AChE-S isoform bearing a unique, 40 amino acid C-terminal peptide encoded by exon 6. A second, erythrocyte-bound form, AChE-E, is encoded by mRNA carrying alternative exon 5. AChE-E presumably participates, together with BChE, in scavenging blood-borne inhibitors, including drugs of abuse (Salmon et al., 1999). Until recently, AChE-S and AChE-R were considered the primary players in the development of anticholinesterase therapies. The big surprise came with the discovery that a rare "*readthrough* " mRNA retaining intron 4 in the open reading frame encodes a novel AChE isoform, AChE-R, that is dramatically upregulated under some physiological conditions, including acute traumatic stress and exposure to AChE inhibitors (Friedman et al., 1996; Kaufer et al., 1998). Using heterologous expression in microinjected *Xenopus* oocytes and embryos, AChE-R was shown to represent a monomeric, hydrophilic, soluble form of catalytically active AChE (Seidman et al., 1995) (figure 2). In hippocampal brain slices, elevated AChE-R was associated with suppressed electrophysiological activity 3 hrs. following treatment with the potent AChE inhibitor physostigmine (Kaufer et al., 1998). These studies raised the possibility that AChE-R plays a unique role in the physiological response to

stress (Kaufer et al., 1999; Kaufer and Soreq, 1999). In addition, it raised the possibility that the balance between AChE variants carries important implications for health and disease. These studies therefore challenge the pharmaceutical industry to develop isoform-specific AChE inhibitors. Although small differences were found in the affinity of some inhibitors for AChE-S and AChE-R (A. Salmon and H. Soreq, unpublished data), it is yet unclear whether a pharmacological solution to the problem of isoform-specific inhibition is attainable. In contrast, antisense technology offers potential solutions. One approach would be to design exon-specific oligonucleotides to preferentially target exon 6 (AChE-S) or intron 4 (AChE-R). Another option is to exploit the inherent instability of AChE-R mRNA to selectively target this RNA species. The rapid degradation of AChE-R mRNA under treatment of rat phaeochromocytoma (PC12) cells with actinomycin D supported the validity of this latter approach (Grifman and Soreq, 1997).

2. Feedback overexpression of AChE alters the balance and levels of AChE isoforms

The discovery that stress and AChE inhibitors elicit pronounced and prolonged feedback expression of AChE-R highlights the complexity of anticholinesterase therapeutics on the one hand, and the need to understand the role of AChE-R in long-term responses to stress on the other. To study this issue, we generated transgenic mice overexpressing various AChE isoforms. Mice overexpressing AChE-S in CNS neurons display late-onset cognitive and neuromotor impairments with features reminiscent of human neurological diseases (Andres et al., 1997; Beeri et al., 1995; Beeri et al., 1997). More recent studies of transgenic mice overexpressing AChE-R suggest that the balance between AChE-S and AChE-R, and the interplay between them, is itself important in mediating long-term effects (M. Sternfeld, submitted for publication).

These studies raise the question of whether or not it is possible to devise an anticholinesterase strategy that does not promote the feedback loop. Inhibitor-mediated enzyme overproduction appears to be activated by the acute cholinergic stimulation resulting from an abrupt pharmacological blockade of AChE (Kaufer et al., 1998). The inherent instability of AChE-R mRNA suggests that antisense technology could be aimed primarily at AChE-R, leaving AChE-S, and cholinergic neurotransmission intact. However, even if the desired target will be AChE-S, it is likely that the pharmacokinetics of antisense inhibition would be less acute and occur over a longer period of time than that of anticholinesterase drugs. By preventing only *de novo* synthesis, an antisense oligonucleotide inhibitor would be slower-acting in its depletion of ACh hydrolyzing potential. In contrast to the abrupt inactivation of catalytic sites taking place with pharmacological inhibitors, the slow action of an antisense inhibitor would conceivably allow the target cell to adapt to gradually increasing concentrations of ACh. Graded inhibition could therefore be expected to minimize or eliminate the feedback response. Furthermore, even if antisense inhibition would elicit a feedback response, the anti-mRNA nature of antisense blockade is such that careful titration of the oligonucleotide dose could be fine-tuned to suppress *de novo* feedback expression of the ACHE gene.

3. Non-Catalytic activities of AChE

A final issue to contend with when addressing pharmacological inhibition of AChE relates to recently described non-catalytic morphogenic activities of the protein. Data accumulated over the past decade demonstrated that in addition to its long-recognized role in hydrolyzing acetylcholine, AChE possesses profound morphogenic effects on neuronal and synaptic architecture—especially with respect to neurite outgrowth and cell adhesion properties

(Reviewed by Grisaru et al., 1999; Soreq and Glick, 2000). These activities were proven to be independent of ACh hydrolysis (Sternfeld et al., 1998) and tentatively attributed to sequence homologies between ACHE and a family of cholinesterase-like neuronal cell adhesion molecules that includes *Drosophila* neurotactin and mammalian neuroligins (Darboux et al., 1996; Grifman et al., 1998; Ichtchenko et al., 1996). To validate the concept of using antisense technologies to control morphogenetic processes in the nervous system, we established a model in PC12 cells (Grifman et al., 1998). PC12 cells were stably transfected with a plasmid carrying a 132 base pair fragment encoding antisense cRNA corresponding to a sequence in exon 6 of the rat ACHE gene. Transfected cells displayed pronounced loss of AChE-R mRNA and significant, but less dramatic, decreases in mRNA encoding AChE-S. Antisense depletion of AChE mRNA was accompanied by a marked reduction in the processes extension normally accompanying nerve growth factor (NGF)-induced differentiation (Figure 3). Thus, these studies demonstrated pronounced antisense-mediated effects on the cytoarchitecture of these cholinergic neuron-like cells. The abnormal antisense phenotype was partially rescued with exogenous AChE, and by transfection with plasmids directing the expression of either AChE (catalytically active or inactive) or neuroligin, stressing the overlapping functional significance of the cholinesterase-like domain shared by these proteins.

Non-catalytic morphogenic activities of AChE have been tentatively mapped to the peripheral anionic site, and were not yet shown to be affected by the current anticholinesterase therapeutics. Thus, pharmacological inhibitors of AChE block the catalytic activity of the enzyme, but do not necessarily interfere with other biological activities of the protein. On the contrary, since damaging effects of overexpressed AChE may be related to non-catalytic activities, these drugs may actually aggravate certain conditions by elevating the levels of catalytically inactivated AChE via the feedback loop. In that case, antisense technology would be the only approach to offer a potential solution by blocking production of the protein. Figure 4 summarizes the fundamental differences between pharmacological and antisense-based anti-AChE drugs.

Anti-AChE antisense oligonucleotides—The state of the art

The lure of highly specific AChE and BChE inhibitors prompted the initiation of an antisense program in our laboratory shortly after the mammalian genes were cloned and sequenced. AChE targeted antisense oligonucleotides have been shown effective in both *in vitro* and *in vivo* paradigms, especially in their effects on the hematopoietic system (Lev Lehman et al., 1994; Soreq et al., 1994). Indeed, antisense oligonucleotides have played an important part in establishing an active role for AChE in hematopoiesis, especially in the genesis of erythroid, lymphocytic, and megakaryocytic lineages. Initially, anti-AChE antisense oligonucleotides were prepared in unmodified phosphodiester or fully phosphorothioated forms (Patinkin et al., 1990); then in partially phosphorothioated form. By restricting phosphorothioate modification to the three terminal 3' nucleotides, cytotoxicity was minimized without loss of activity (Ehrlich et al., 1994). Subsequently, 2'-O-methyl modified RNA replaced phosphorothioate modification as the formulation of choice for 3'-capping of AChE targeted oligonucleotides (Grisaru et al., 1999).

In a screen of 7 antisense oligonucleotides targeted to various regions in rodent AChE mRNA, PC12 cells were shown to be significantly more vulnerable to antisense effects following NGF-mediated differentiation than naïve PC12 cells (Grifman and Soreq, 1997). Using partially phosphorothioate-protected oligonucleotides and a working concentration of 1 μM

oligonucleotide, a maximum inhibition of approximately 30% was achieved. Following that study, two oligonucleotides—AS1 and AS3—were selected as the primary antisense agents in our laboratory. Recent experiments using these two oligonucleotides demonstrated even greater inhibition of AChE (up to 50%) at 100-1000-fold lower concentrations of oligonucleotide. Moreover, 2'-O-methyl protected AS1 and AS3 displayed a wide window of effective concentrations (0.02-200 nM) as compared to the phosphorothioate-protected oligos (N. Galyam and H. Soreq, manuscript in preparation). In osteosarcoma Saos-2 cells, 2nM 2'-O-methyl capped antisense oligonucleotides achieved pronounced blockade of AChE expression that was accompanied by suppressed cellular proliferation, reinforcing evidence that AChE plays an active role in mammalian osteogenesis (figure 5 and Grisaru et al., 1999). The strong antisense effects elicited by extremely low concentrations of oligonucleotide in these variable systems greatly reduces the cost of antisense experiments, and can be expected to significantly reduce potential, unwanted side effects. We have therefore extrapolated these *in vitro* studies to test low dose administration of anti-AChE oligonucleotides *in vivo* in animal models of acute psychological stress, chronic low-dose anticholinesterase intoxication, myasthenia gravis, Alzheimer's disease, and closed head injury.

Potential applications of AChE antisense technologies

Anticholinesterase poisoning:

The association between AChE inhibitors and neuromuscular impairments (Soreq and Glick, 2000; Glick et al., 2000) suggests a potential application for AChE-targeted antisense oligonucleotides in treating victims of anticholinesterase intoxication. Estimates of illness associated with occupational exposure to organophosphate (OP) anticholinesterase pesticides range from 150,000-300,000 annually in the United States alone (Feldman, 1999). Accidental ingestion and food contamination are additional sources of OP intoxication with potential long-range health implications. During the Persian Gulf War, several hundred thousand American soldiers received prophylactic doses of pyridostigimine to protect them against the threated use of chemical warfare by Iraq. Although no definitive association has been made between unexplained Gulf War Illness and anticholinesterases, a recent Rand Corporation report (Document no.MR-1018/2-OSD) prompted the Defense Department to acknowledge that pyridostigmine cannot be ruled out as a possible contributor to some symptoms experienced by Gulf War veterans. Notably, muscle weakness is prominent among the complaints of some Gulf War vets (Haley et al., 1997). In view of what we know about the AChE feedback loop, the detrimental effects of overexpressed AChE on muscle, and the fact that no coherent approach has been taken to treating muscle weakness among Gulf War veterans, this may represent an appropriate forum in which to examine the utility of antisense therapy for neuromuscular impairments.

Neuromuscular disease

Myasthenia gravis (MG) is a debilitating autoimmune neuromuscular disease characterized by fluctuating muscle weakness and progressive deterioration of neuromotor function (Schonbeck et al., 1990). Symptoms affecting MG patients include drooping eyelids, double vision, difficulty eating or talking, and chronic fatigue. Episodic, life-threatening, "myasthenic crisis" causes respiratory distress which usually requires intensive care hospitalization. MG is reported to affect approximately 36,000 individuals in the United States (statistics from the Myasthenia Gravis Foundation of America, http://www.myasthenia.org). It has been suggested however, that MG is underdiagnosed and that the incidence is probably

higher. Myasthenia gravis results from autoimmune antibody-mediated depletion of acetylcholine receptors from the neuromusclular junctions. As myasthenia is characterized by understimulation of the muscles, AChE inhibitors have proven an effective palliative treatment for this disease (Evoli et al., 1996). The most commonly used AChE inhibitor for the treatment of myasthenia gravis today is Mestinon. Mestinon is the trade name for the carbamate AChE inhibitor pyridostigmine. Anticholinesterase inhibitors address the symptoms of myasthenia gravis, but do not slow its progression. On the contrary, it has been suggested that pyridostigmine may actually contribute to progressive deterioration in muscle function (Swash, 1975). In this light, it is noteworthy that a promising AChE inhibitor for Alzheimer's disease was recently withdrawn from clinical trials after some patients reported muscle weakness (SCRIP World Pharmaceutical News. No. 2374. P. 19 (1998)). In any case, the relief offered by current anticholinesterase drugs is short-lived, and relatively high doses of these medications must be taken up to 6 times per day for many years.

Recently, we demonstrated that the AChE feedback loop active in brain is similarly active in muscle, and that AS3 oligonucleotide acts to suppress inhibitor-induced overexpression of AChE in mice (Lev-Lehman et al., 2000). In those experiements, 80 μg/kg AS3 blocked anticholinesterase-induced accumulation of catalytically active AChE in muscle by 60%, and largely suppressed the accompanying increase in motor endplates (Figure 6). This experiment proved that antisense oligonucleotides to AChE can suppress non-catalytic morphogenic activities of the enzyme *in vivo*. In transgenic mice overproducing AChE in motoneurons, we observed severe deterioration of muscle structure and function (Andres et al., 1997), suggesting that excess acetylcholinesterase may be a factor in the deterioration of muscle function in myasthenic patients. As AChE inhibitors may exacerbate AChE imbalances in the muscle, the potential long-term effects of chronically administered AChE inhibitors should not be ignored. Although continued administration of the inhibitory drug masks the added acetylcholine-degrading activity, it will not necessarily prevent the ill effects of excess non-catalytically active AChE on muscle. Thus, the feedback loop and the role of acetylcholinesterase as a catalytically inert, but biologically active element must be seriously considered in the development of new drugs for myasthenia gravis. In that case, antisense oligonucleotide technology offers a novel approach.

Head trauma:

Closed head injury (CHI) is an important cause of death among young adults (Siesjo, 1993; Yakovlev and Faden, 1995) and a prominent risk factor in non-familial Alzheimer's disease (Gennarelli and Graham, 1998). Effective emergency strategies must be developed to improve survival, promote recovery, and prevent delayed neurological disorders. Recently, we observed pronounced accumulation of AChE-R mRNA in cortex of mice subjected to controlled head injury (Chen et al., 1996). A single post-injury intracerebroventricular administration of only 0.5 μg AS3 abolished the post-injury accumulation of AChE-R mRNA and the excessive dendritic growth accompanying it (E. Shohami et al., submitted). In trauma-sensitive AChE transgenic mice, antisense treatment minimized mortality, facilitated neurological recovery and protected CA3 hippocampal neurons. These findings demonstrate the potential of antisense therapeutics in treating acute injury and suggest antisense blockade of AChE-R for limiting the detrimental consequences of various traumatic insults to the nervous system.

Neurodegenerative disease

Alzheimer's Disease (AD) is a debilitating neurodegenerative disease characterized by progressive deterioration of cognitive faculties including learning, short-term memory, problem solving and abstract thinking. The average lifetime cost approaches $175,000 per patient and total AD patient care amounts to approximately $100 billion per year. AD currently affects 4 million Americans and is currently considered the fourth leading cause of death in the United States (Statistics from the Alzheimer's Association—http://alz.org). The cholinergic theory of Alzheimer's disease suggests that the selective destruction of cholinergic neurons in Alzheimer's disease results in a relative deficit of acetylcholine in brain regions that mediate learning and memory functions (Coyle et al., 1983). The primary approach to treating Alzheimer's disease has therefore aimed to augment the cholinergic system with anticholinesterases. Indeed, the only currently approved drugs for Alzheimer's disease are potent AChE inhibitors (Giacobini, 1998). Nevertheless, the value of cholinesterase therapy is limited to about one year, and to mildly affected patients.

The discovery of a role for AChE in neurite growth is particularly significant in view of the fact that abnormal neurite projections are characteristic features of the Alzheimer's brain, as are abnormal deposits of AChE at sites of senile plaque formation--the principal histopathological hallmark of Alzheimer's disease (Wright et al., 1993). *In vitro*, AChE was even shown to mediate the aggregation of β-amyloid protein, the major component of AD plaques (Campos et al., 1998; Inestrosa et al., 1996). Thus, emerging evidence suggests that acetylcholinesterase may play a role in the etiology of Alzheimer's disease that goes beyond the scope of the cholinergic theory. Taking the feedback loop and non-catalytic activities of AChE into consideration, AChE as an active player in the progress of AD may explain the overall disappointing performance of AChE inhibitors in providing effective long-term relief. Using surgically implanted cannulae to deliver nanomolar quantities of AS3 to the cerebrospinal fluid of cognitively impaired transgenic mice (Beeri et al. 1995), we are testing the effects of antisense therapy on performance in behavioral models such as social exploration and conditioned taste aversion. Indeed, the potential applications of antisense technology to treating diseases of the central nervous system are enticing (McCarthy, 1998; Seidman et al., 1999). Nevertheless, the challenge of bringing oligonucleotide therapeutics to AD in particular, and to neurodegenerative disease in general faces yet unresolved technical limitations. Among the most difficult issues to resolve is the poor transport of oligonucleotides across the blood-brain-barrier (Soreq et al., manuscript in preparation).

Summary

Developments in our knowledge of the molecular and cellular mechanisms of action of AChE have allowed us to identify the inherent limitations of conventional pharmacological blockade of AChE catalytic activity. These limitations are based on the discovery of non-catalytic activities of AChE isoforms, and on the existence of a feedback loop leading to overexpression of AChE following acute inhibition of enzymatic activity. At the same time, cloning of the ACHE gene opened the door to novel strategies to contain undesired AChE activities based on antisense technology. These hand-in-hand advances in AChE basic research afford us the opportunity to think ahead to the application of antisense oligonucleotides to future anticholinesterase therapeutics. An antisense approach to the control of AChE expression promises to address the heretofore unappreciated role of AChE variants in the etiology of disease, something which

pharmacological approaches have not yet begun to explore. Given the unique challenges of AChE-based therapeutics and the highly relevant answers that antisense technology offers to these challenges, AChE represents a promising target with which to promote the development of therapeutic antisense for the central and peripheral nervous systems.

Acknowledgements

The authors would like to acknowledge the contributions of Dr. D. Glick, Dr. D. Grisaru, Dr. M. Grifman and Ms. Tama Evron to the work described in this review. The work presented here was supported by the US Army Medical Research and Development Command (DAMD17-99-1-9547), The Israel Science Foundation (96-00110), the US-Israel Binational Science Foundation (590/97), The Eric Roland Center for Neurodegenerative Diseases and Ester Neuroscience, Ltd., Tel Aviv.

Bibliography

1. Andres, C., Beeri, R., Friedman, A., Lev-Lehman, E., Henis, S., Timberg, R., Shani, M., and Soreq, H. (1997). Acetylcholinesterase-transgenic mice display embryonic modulations in spinal cord choline acetyltransferase and neurexin Ibeta gene expression followed by late-onset neuromotor deterioration. Proc Natl Acad Sci U S A *94*, 8173-8.

2. Barnard, E. A. (1988). Molecular neurobiology. Separating receptor subtypes from their shadows [news]. Nature *335*, 301-2.

3. Beeri, R., Andres, C., Lev Lehman, E., Timberg, R., Huberman, T., Shani, M., and Soreq, H. (1995). Transgenic expression of human acetylcholinesterase induces progressive cognitive deterioration in mice. Curr Biol *5*, 1063-71.

4. Beeri, R., Le Novere, N., Mervis, R., Huberman, T., Grauer, E., Changeux, J. P., and Soreq, H. (1997). Enhanced hemicholinium binding and attenuated dendrite branching in cognitively impaired acetylcholinesterase-transgenic mice. J Neurochem *69*, 2441-51.

5. Ben Aziz Aloya, R., Sternfeld, M., and Soreq, H. (1993). Promoter elements and alternative splicing in the human ACHE gene. Prog Brain Res *98*, 147-53.

6. Bryson, H. M., and Benfield, P. (1997). Donepezil. Drugs Aging *10*, 234-9; discussion 240-1.

7. Campos, E. O., Alvarez, A., and Inestrosa, N. C. (1998). Brain acetylcholinesterase promotes amyloid-beta-peptide aggregation but does not hydrolyze amyloid precursor protein peptides. Neurochem Res *23*, 135-40.

8. Chen, Y., Constantini, S., Trembovler, V., Weinstock, M., and Shohami, E. (1996). An experimental model of closed head injury in mice: pathophysiology, histopathology, and cognitive deficits. J Neurotrauma *13*, 557-68.

9. Coyle, J. T., Price, D. L., and DeLong, M. R. (1983). Alzheimer's disease: a disorder of cortical cholinergic innervation. Science *219*, 1184-1190.

10. Darboux, I., Barthalay, Y., Piovant, M., and Hipeau Jacquotte, R. (1996). The structure-function relationships in Drosophila neurotactin show that cholinesterasic domains may have adhesive properties. EMBO J *15*, 4835-43.

11. Ehrlich, G., Patinkin, D., Ginzberg, D., Zakut, H., Eckstein, F., and Soreq, H. (1994). Use of partially phosphorothioated "antisense" oligodeoxynucleotides for sequence-dependent modulation of hematopoiesis in culture. Antisense Res Dev *4*, 173-83.

12. Epstein, P. M. (1998). Antisense inhibition of phosphodiesterase expression. Methods *14*, 21-33.

13. Evoli, A., Batocchi, A. P., and Tonali, P. (1996). A practical guide to the recognition and management of myasthenia gravis. Drugs *52*, 662-70.

14. Feldman, R. G. (1999). Occupational and Environmental Neurotoxicity (Philadelphia: Lippincott-Raven Publishers).

15. Friedman, A., Kaufer, D., Shemer, J., Hendler, I., Soreq, H., and Tur Kaspa, I. (1996). Pyridostigmine brain penetration under stress enhances neuronal excitability and induces early immediate transcriptional response. Nat Med *2*, 1382-5.

16. Gennarelli, T. A., and Graham, D. I. (1998). Neuropathology of the Head Injuries. Semin Clin Neuropsychiatry *3*, 160-175.

17. Giacobini, E. (1998). Invited review: Cholinesterase inhibitors for Alzheimer's disease therapy: from tacrine to future applications. Neurochem Int *32*, 413-9.

18. Glick, D., Shapira, M., and Soreq, H. (2000). Molecular neurotoxicology implications of acetylcholinesterase inhibition. In Site-Specific Neurotoxicology, P. Glazarovici and D. Lester, eds. (New York: Plenum Press), pp. (in press).

19. Grifman, M., Galyam, N., Seidman, S., and Soreq, H. (1998). Functional redundancy of acetylcholinesterase and neuroligin in mammalian neuritogenesis. Proc Natl Acad Sci U S A *95*, 13935-40.

20. Grifman, M., and Soreq, H. (1997). Differentiation intensifies the susceptibility of pheochromocytoma cells to antisense oligodeoxynucleotide-dependent suppression of acetylcholinesterase activity. Antisense Nucleic Acid Drug Dev *7*, 351-9.

21. Grisaru, D., Lev-Lehman, E., Shapira, M., Chaikin, E., Lessing, J. B., Eldor, A., Eckstein, F., and Soreq, H. (1999). Human osteogenesis involves differentiation-dependent increases in the morphogenically active 3' alternative splicing variant of acetylcholinesterase. Mol Cell Biol *19*, 788-95.

22. Grisaru, D., Sternfeld, M., Eldor, A., Glick, D., and Soreq, H. (1999). Structural roles of acetylcholinesterase variants in biology and pathology. Eur J Biochem *264*, 672-86.

23. Haley, R. W., Kurt, T. L., and Hom, J. (1997). Is there a Gulf War Syndrome? Searching for syndromes by factor analysis of symptoms. Jama *277*, 215-22.

24. Ichtchenko, K., Nguyen, T., and Sudhof, T. C. (1996). Structures, alternative splicing, and neurexin binding of multiple neuroligins. J Biol Chem *271*, 2676-82.

25. Inestrosa, N. C., Alvarez, A., Perez, C. A., Moreno, R. D., Vicente, M., Linker, C., Casanueva, O. I., Soto, C., and Garrido, J. (1996). Acetylcholinesterase accelerates assembly of amyloid-beta-peptides into Alzheimer's fibrils: possible role of the peripheral site of the enzyme. Neuron *16*, 881-91.

26. Kalra, P. S., Dube, M. G., and Kalra, S. P. (2000). Effects of centrally administered antisense oligodeoxynucleotides on feeding behavior and hormone secretion. Methods Enzymol *314*, 184-200.

27. Kaufer, D., Friedman, A., Seidman, S., and Soreq, H. (1998). Acute stress facilitates long-lasting changes in cholinergic gene expression. Nature *393*, 373-7.

28. Kaufer, D., Friedman, A., and Soreq, H. (1999). The vicious circle: long-lasting transcriptional modulation of cholinergic neurotransmission following stress and anticholinesterase exposure. The Neuroscientist *5*, 173-183.

29. Kaufer, D., and Soreq, H. (1999). Tracking cholinergic pathways from psychlogical and chemical stressors to variable neurodegeneration paradigms. Neurodegeneration *Curr. Opin. Neurol.*, 739-743.

30. Kolesnikov, Y. A., Pan, Y. X., Babey, A. M., Jain, S., Wilson, R., and Pasternak, G. W. (1997). Functionally differentiating two neuronal nitric oxide synthase isoforms through antisense mapping: evidence for opposing NO actions on morphine analgesia and tolerance. Proc Natl Acad Sci U S A *94*, 8220-5.

31. Lamprecht, R., Hazvi, S., and Dudai, Y. (1997). cAMP response element-binding protein in the amygdala is required for long- but not short-term conditioned taste aversion memory. J Neurosci *17*, 8443-50.

32. Lane Ladd, S. B., Pineda, J., Boundy, V. A., Pfeuffer, T., Krupinski, J., Aghajanian, G. K., and Nestler, E. J. (1997). CREB (cAMP response element-binding protein) in the locus coeruleus: biochemical, physiological, and behavioral evidence for a role in opiate dependence. J Neurosci *17*, 7890-901.

33. Lev-Lehman, E., Evron, T., Broide, R. S., Meshorer, E., Ariel, I., Seidman, S., and Soreq, H. (2000). Synaptogenesis and Myopathy under Acetylcholinesterase Overexpression. J. Molec. Neurosci., In press.

34. Lev Lehman, E., Ginzberg, D., Hornreich, G., Ehrlich, G., Meshorer, A., Eckstein, F., Soreq, H., and Zakut, H. (1994). Antisense inhibition of acetylcholinesterase gene expression causes transient hematopoietic alterations in vivo. Gene Ther *1*, 127-35.

35. Li, Y., Camp, S., Rachinsky, T. L., Getman, D., and Taylor, P. (1991). Gene structure of mammalian acetylcholinesterase. Alternative exons dictate tissue-specific expression. J Biol Chem *266*, 23083-90.

36. Loewenstein Lichtenstein, Y., Schwarz, M., Glick, D., Norgaard Pedersen, B., Zakut, H., and Soreq, H. (1995). Genetic predisposition to adverse consequences of anti-cholinesterases in 'atypical' BCHE carriers. Nat Med *1*, 1082-5.

37. Massoulie, J., Anselmet, A., Bon, S., Krejci, E., Legay, C., Morel, N., and Simon, S. (1998). Acetylcholinesterase: C-terminal domains, molecular forms and functional localization. J Physiol Paris *92*, 183-90.

38. McCarthy, M. M. (1998). Use of antisense oligonucleotides in the central nervous system: Why such success? In Allied Antisense Oligonucleotide Technology, C. A. Stein and A. M. Krief, eds.: Wiley-Liss, Inc), pp. 283-296.

39. Meiri, N., Ghelardini, C., Tesco, G., Galeotti, N., Dahl, D., Tomsic, D., Cavallaro, S., Quattrone, A., Capaccioli, S., Bartolini, A., and Alkon, D. L. (1997). Reversible antisense inhibition of Shaker-like Kv1.1 potassium channel expression impairs associative memory in mouse and rat. Proc Natl Acad Sci U S A *94*, 4430-4.

40. Meiri, N., Sun, M. K., Segal, Z., and Alkon, D. L. (1998). Memory and long-term potentiation (LTP) dissociated: normal spatial memory despite CA1 LTP elimination with Kv1.4 antisense. Proc Natl Acad Sci U S A *95*, 15037-42.

41. Pasternak, G. W., and Pan, Y. X. (2000). Antisense mapping: assessing functional significance of genes and splice variants. Methods Enzymol *314*, 51-60.

42. Patinkin, D., Seidman, S., Eckstein, F., Benseler, F., Zakut, H., and Soreq, H. (1990). Manipulations of cholinesterase gene expression modulate murine megakaryocytopoiesis in vitro. Mol Cell Biol *10*, 6046-6050.

43. Salmon, A. Y., Goren, Z., Avissar, Y., and Soreq, H. (1999). Human erythrocyte but not brain acetylcholinesterase hydrolyses heroin to morphine [In Process Citation]. Clin Exp Pharmacol Physiol 26, 596-600.

44. Sanchez-Blazquez, P., DeAntoio, I., Rodriguez-Diaz, M., and Garzon, J. (1999). Antisense oligodeoxynucleotide targeting distinct exons of the cloned mu-opioid receptor distinguish between endomorphin-1 and morphine supraspinal antinociception in mice. Antisense Nucleic Acid Drug Dev *9*, 253-60.

45. Schonbeck, S., Chrestel, S., and Hohlfeld, R. (1990). Myasthenia gravis: prototype of the antireceptor autoimmune diseases. Int Rev Neurobiol *32*, 175-200.

46. Schwarz, M., Glick, D., Loewenstein, Y., and Soreq, H. (1995). Engineering of human cholinesterases explains and predicts diverse consequences of administration of various drugs and poisons. Pharmacol Ther *67*, 283-322.

47. Seidman, S., Eckstein, F., Grifman, M., and Soreq, H. (1999). Antisense technologies have a future fighting neurodegenerative diseases. Antisense Nucleic Acid Drug Dev *(in press)*.

48. Seidman, S., Sternfeld, M., Ben Aziz Aloya, R., Timberg, R., Kaufer Nachum, D., and Soreq, H. (1995). Synaptic and epidermal accumulations of human acetylcholinesterase are encoded by alternative 3'-terminal exons. Mol Cell Biol *15*, 2993-3002.

49. Siesjo, B. K. (1993). Basic mechanisms of traumatic brain damage. Ann Emerg Med *22*, 959-69.

50. Sommer, W., Cui, X., Erdmann, B., Wiklund, L., Bricca, G., Heilig, M., and Fuxe, K. (1998). The spread and uptake pattern of intracerebrally administered oligonucleotides in nerve and glial cell populations of the rat brain. Antisense Nucleic Acid Drug Dev *8*, 75-85.

51. Soreq, H., Ben-Aziz, R., Prody, C. A., Seidman, S., Gnatt, A., Neville, L., Lieman-Hurwitz, J., Lev-Lehman, E., Ginzberg, D., Lapidot-Lifson, Y., and et al. (1990). Molecular cloning and construction of the coding region for human acetylcholinesterase reveals a G + C-rich attenuating structure. Proc Natl Acad Sci U S A *87*, 9688-92.

52. Soreq, H., and Glick, D. (2000). Novel roles for cholinesterases in stress and inhibitor responses. In Cholinesterases and Cholinesterase Inhibitors, E. Giacobini, ed. (London: Martin Dunitz), pp. (in press).

53. Soreq, H., Patinkin, D., Lev-Lehman, E., Grifman, M., Ginzberg, D., Eckstein, F., and Zakut, H. (1994). Antisense oligonucleotide inhibition of acetylcholinesterase gene expression induces progenitor cell expansion and suppresses hematopoietic apoptosis ex vivo. Proc Natl Acad Sci USA *91*, 7907-11.

54. Soreq, H., and Zakut, H. (1993). Human Cholinesterases and Anticholinesterases (San Diego: Academic Press).

55. Sternfeld, M., Ming, G., Song, H., Sela, K., Timberg, R., Poo, M., and Soreq, H. (1998). Acetylcholinesterase enhances neurite growth and synapse development through alternative

contributions of its hydrolytic capacity, core protein, and variable C termini. J Neurosci *18*, 1240-9.

56. Swash, M. (1975). Letter: Motor innervation of myasthenic muscles. Lancet *2*, 663.

57. Taylor, P. (1996). Agents acting at the neuromuscular junction and autonomic ganglia. In Goodman and Gilman's The Pharmacological Basis of Therapeutics, J. G. Hardman, L. E. Limbird, P. B. Molinoff and R. W. Ruddon, eds. (New York: McGraw-Hill), pp. 177-197.

58. Taylor, P., Radic, Z., Hosea, N. A., Camp, S., Marchot, P., and Berman, H. A. (1995). Structural bases for the specificity of cholinesterase catalysis and inhibition. Toxicol Lett *82-83*, 453-8.

59. Tepper, J. M., Sun, B. C., Martin, L. P., and Creese, I. (1997). Functional roles of dopamine D2 and D3 autoreceptors on nigrostriatal neurons analyzed by antisense knockdown in vivo. J Neurosci *17*, 2519-30.

60. Wright, C. I., Geula, C., and Mesulam, M. M. (1993). Neurological cholinesterases in the normal brain and in Alzheimer's disease: relationship to plaques, tangles, and patterns of selective vulnerability. Ann Neurol *34*, 373-84.

61. Xie, J., and McCobb, D. P. (1998). Control of alternative splicing of potassium channels by stress hormones. Science *280*, 443-6.

62. Yakovlev, A. G., and Faden, A. I. (1995). Molecular biology of CNS injury. J Neurotrauma *12*, 767-77.

Legends to Figures

Figure 1. Alternative splicing generates AChE variants. Depicted is the exon/intron structure of the 7 Kb human ACHE gene at chromosomal locus 7q22. Exons are indicated by shaded boxes, introns by white boxes, and the pseudo-intron I4 (4') by a hatched box. The extended ACHE promoter (Pr) extends over 17 Kb upstream of the transcription initiation site and includes, among others, consensus regulatory sites for expression in nervous tissue, muscle, hematopoietic cells and bone. In addition, the ACHE promoter includes stress and steroid hormone response elements. Alternative splicing yields mRNA transcripts carrying the common coding exons 2-3-4, together with exon 6, intron 4', or exon 5 encoding the synaptic (S), *readthrough* (R) or erythrocyte (E) AChE variants, respectively. The dotted lines under the RNA schemes indicate the open reading frame of each alternative transcript. The catalytically active core domain of all AChE isoforms is derived from the common exons, resulting in only very small differences between the variants in their affinities for both substrates and inhibitors. In contrast, the alternative C-terminal peptides impose diverse biophysical properties upon the various isoforms that determine hydrophobicity, modes of oligomeric assembly, interactions with non-catalytic subunits and subcellular localization (Reviewed by Massoulie et al., 1998).

Figure 2. Unique properties of the stress-related *readthrough* AChE. The C-terminal domain of AChE-R, encoded by pseudo-intron 4', is a 26 amino acid, hydrophilic peptide lacking a cysteine residue necessary for oligomeric assembly (1). When expressed in microinjected *Xenopus* tadpoles, cDNA encoding AChE-R gave rise to a catalytically active enzyme that fractionated almost completely (ca 90%) into the low-salt (LS) as opposed to detergent-containing (LSD) or high-salt (HS) buffer fraction (2), was secreted in large quantities into the external medium (3), and accumulated into epidermal secretory cells rather that muscle (4) (Seidman et al., 1995). Following both acute stress and exposure to AChE inhibitors, AChE-R is dramatically overexpressed in brain and muscle where its unique properties are presumed to mediate both long and short term physiological stress responses.

Figure 3. Antisense AChE cRNA arrests neurite extension--Proof of Concept. PC12 cells stably expressing a 132 bp fragment from the rat ACHE gene in the antisense orientation display dramatically reduced levels of AChE mRNA as determined by RT-PCR (A) and 80% suppression of AChE catalytic activity (B). Note the extreme sensitivity of AChE-R mRNA to antisense-mediated downregulation compared to AChE-S mRNA. NGF-Process extension is prominently blocked by antisense AChE cRNA (C), attributing a morphogenic role to AChE in differentiating PC12. When grown on a collagen matrix infused with purified recombinant human AChE (rhAChE), the neurite-deficient phenotype was partially reversed (D). When re-transfected with DNA encoding either catalytically active or inactive AChE-S, or neuroligin, partial recovery was also observed (E). These studies reinforced the notion that AChE shares overlapping, non-catalytic activities with neuroligin-related cell adhesion proteins, and suggest that antisense oligonucleotides may one day be used to intervene in stress or AChE inhibitor-induced changes in neuronal architecture. Figure after Grifman et al., 1998.

Figure 4. Antisense oligonucleotide approach to anti-AChE drug therapy. AChE displays two independent types of biological activities. Some activities depend on the hydrolysis of acetylcholine; others, on non-enzymatic features of the protein that are presumed to mediate cell adhesion processes. Conventional pharmacology targets the enzyme's catalytic activity by either blocking access of substrate to the active site, or by inactivating the catalytic triad through the

formation of non-regenerating enzyme intermediates. Commonly used therapeutic AChE inhibitors do not differentiate between AChE isozymes and do not inhibit the non-catalytic activities of the protein. In contrast, antisense oligonucleotides targeting AChE mRNA block *de novo* synthesis of AChE protein, thereby blocking both its catalytic and non-catalytic activities. The low cellular abundance AChE mRNA, the high specificity of antisense agents, and the differential stabilities of the various alternative AChE-encoding mRNAs, allows the use of very low doses of oligonucleotides to target specific AChE isoforms.

Figure 5. Antisense oligonucleotides suppress AChE activity in osteogenic Saos-2 cells. Human osteosarcoma Saos-2 cells were grown in the presence of anti-AChE oligonucleotides for 12 hrs and subjected to either histocytochemical staining for catalytically active AChE (middle panel) or *in situ* hybridization(right panel) with a probe detecting all AChE mRNAs. DAPI was used to mark the nuclei of cells stained for AChE activity (left panel). Confocal microscopy was used to document and quantify the *in situ* hybridization data as represented in the bar graph to the right. AS1 and AS3 denote 20-mer antisense oligonucleotides with a 3', 2'-O-methyl cap (last 3 nucleotides) targeting different regions within exon 2 in the ACHE gene (Grifman et al., 1997; Grisaru et al., 1999). ASB is a control, 15-mer antisense oligonucleotide targeting the homologous enzyme butyrylcholinesterase. Proliferation of Saos-2 cells, as determined by BrdU incorporation was increased by 25% under AS1 treatment, supporting a role for AChE in osteogenic development.

Figure 6. Antisense blockade of anticholinesterase-induced synaptic proliferation. Adult FVB/N mice received 4 consecutive daily i.p. injections with diisopropylfluorophosphonate (DFP), a potent irreversible AChE inhibitor, with or without co-administration of AS3 (80 μg/Kg). Two weeks later, diaphragm muscles were excised and histochemically stained for AChE as a marker of motor endplates. DFP alone promoted feedback elevations in AChE activity as determined in homogenates, neurite outgrowth (not shown) and proliferation of small endplates. Coadministration of partially 2'-O-methyl protected AS3 restrained feedback overexpression of AChE and partially blocked proliferation of motor endplates. These experiments suggest the application of antisense technology to diseases of the neuromuscular junction such as myasthenia gravis and for the prevention of delayed muscle weakness associated with accidental or occupational exposure to AChE inhibitors. Figure after Lev-Lehman et al., 2000, In press.

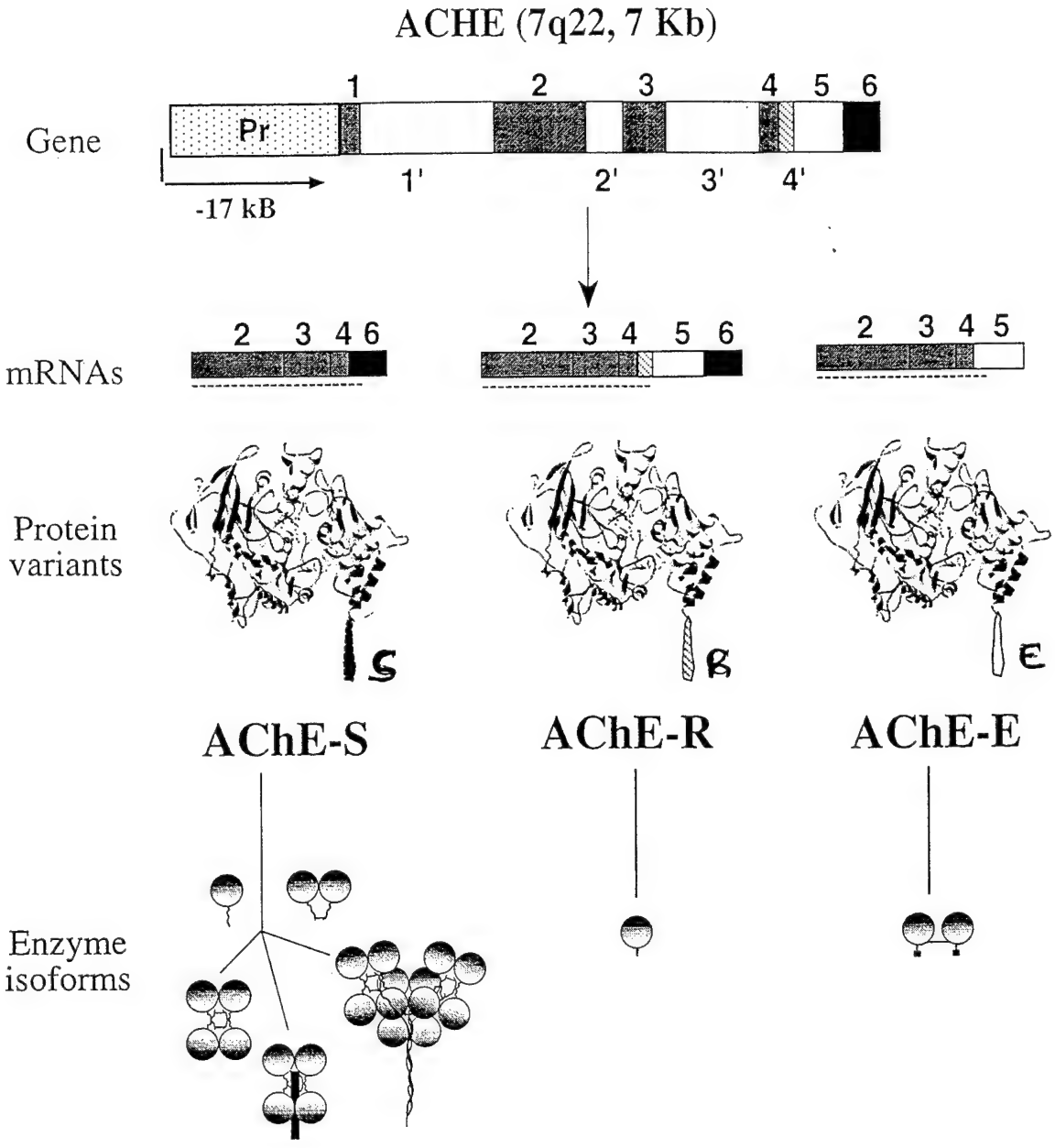
ACHE (7q22, 7 Kb)
Gene
Pr
1
2
3
4
5
6
1'
2'
3'
4'
-17 kB
mRNAs
2 3 4 6
2 3 4 5 6
2 3 4 5
Protein variants
AChE-S
AChE-R
AChE-E
Enzyme isoforms

FIGURE 1

FIGURE 2

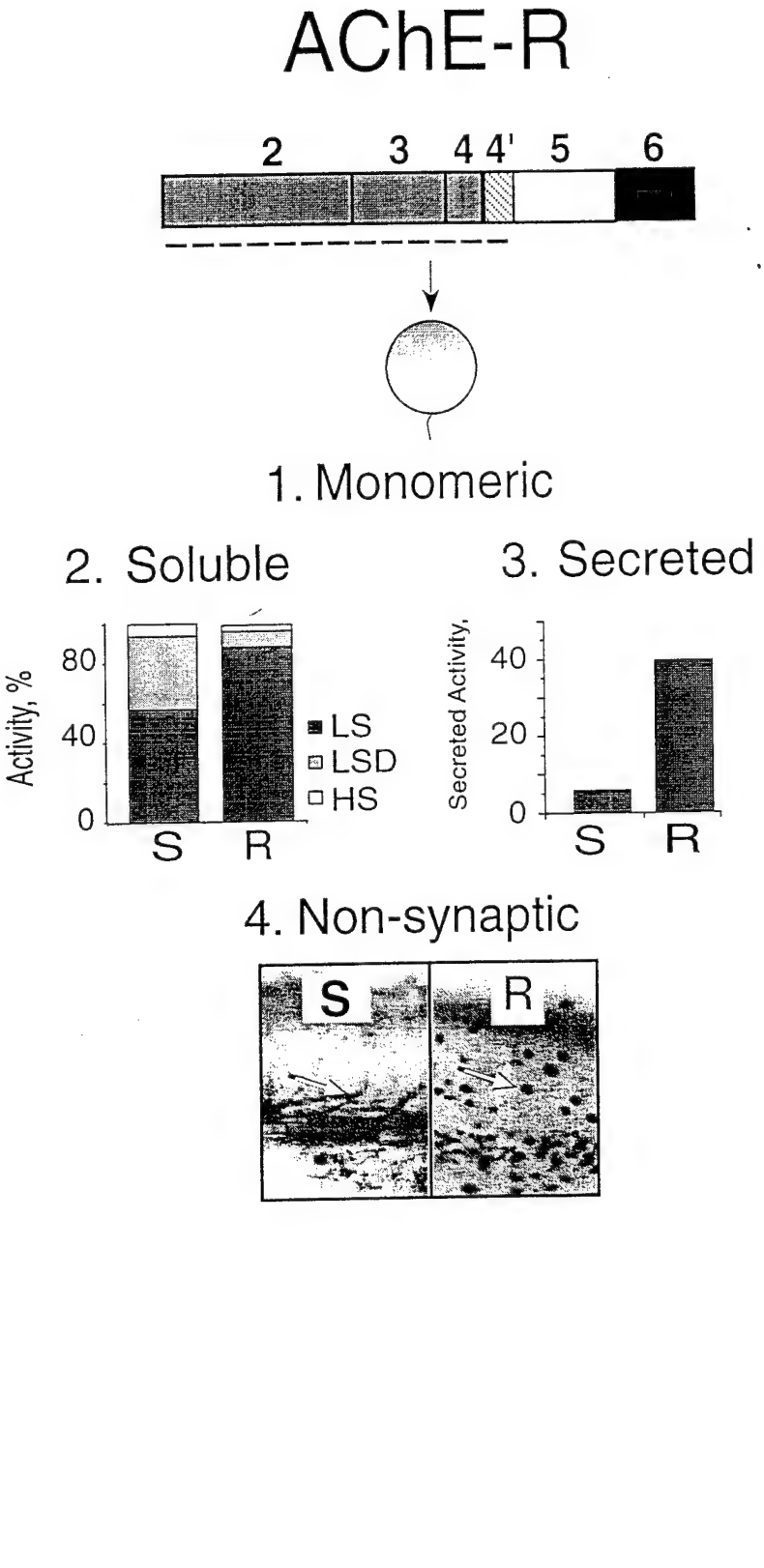
AChE-R
2
3
4
4'
5
6
1. Monomeric
2. Soluble
3. Secreted
Activity, %
80
40
0
LS
LSD
HS
S
R
Secreted Activity,
40
20
0
S
R
4. Non-synaptic
S
R

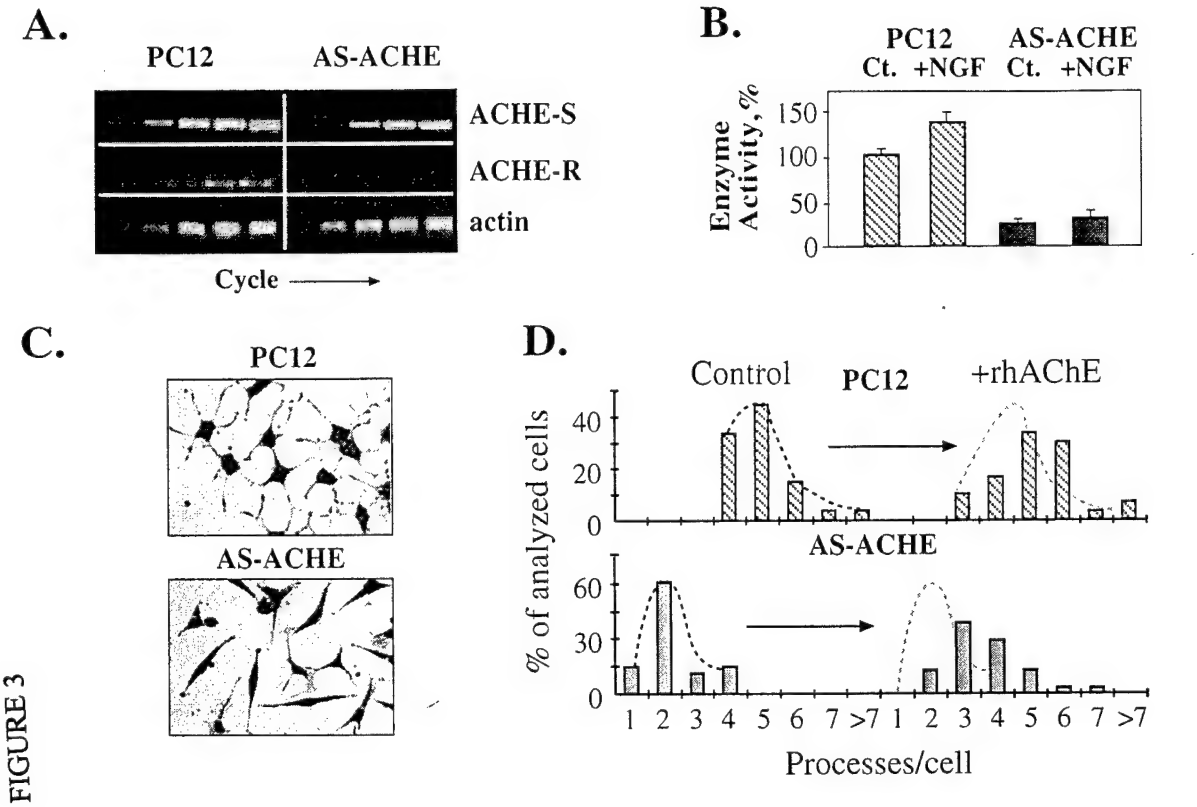
A.
PC12
AS-ACHE
ACHE-S
ACHE-R
actin
Cycle
B.
PC12
AS-ACHE
Ct. +NGF Ct. +NGF
Enzyme Activity, %
150
100
50
0
C.
PC12
AS-ACHE
D.
Control
PC12
+rhAChE
AS-ACHE
% of analyzed cells
40
20
0
60
30
0
1 2 3 4 5 6 7 >7 1 2 3 4 5 6 7 >7
Processes/cell
E.
PC12
AS+E6
AS
AS+In
AS+ctr
AS+Nrl
% of analyzed cells
% of analyzed cells
40
20
0
60
40
20
0
1 2 3 4 5 6 7 1 2 3 4 5 6 7
Processes/cell

FIGURE 3

FIGURE 4

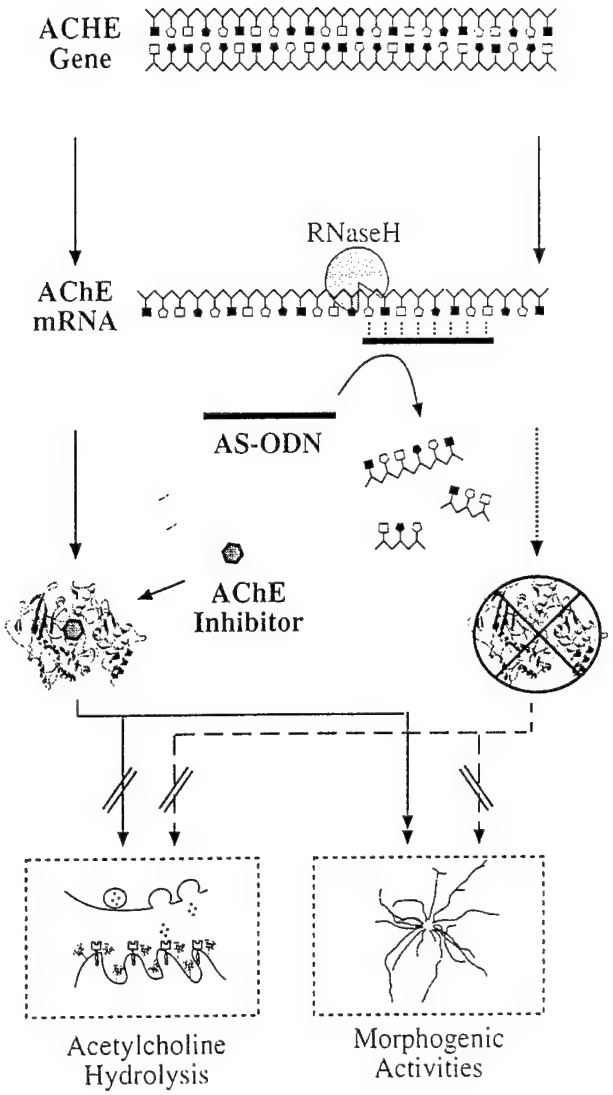
ACHE
Gene
RNaseH
AChE
mRNA
AS-ODN
AChE
Inhibitor
Acetylcholine
Hydrolysis
Morphogenic
Activities

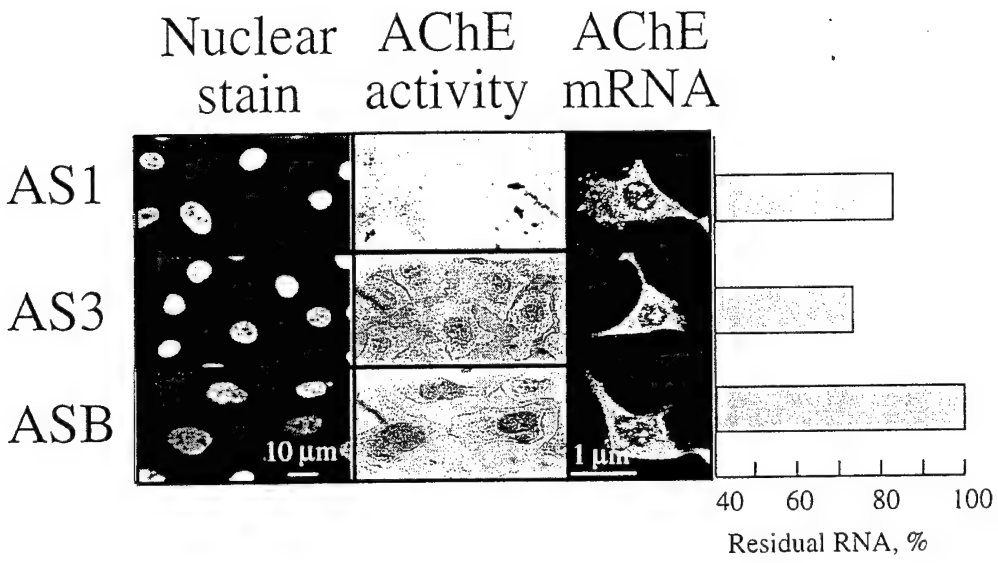
Nuclear stain
AChE activity
AChE mRNA
AS1
AS3
ASB
10 µm
1 µm
40
60
80
100
Residual RNA, %

FIGURE 5

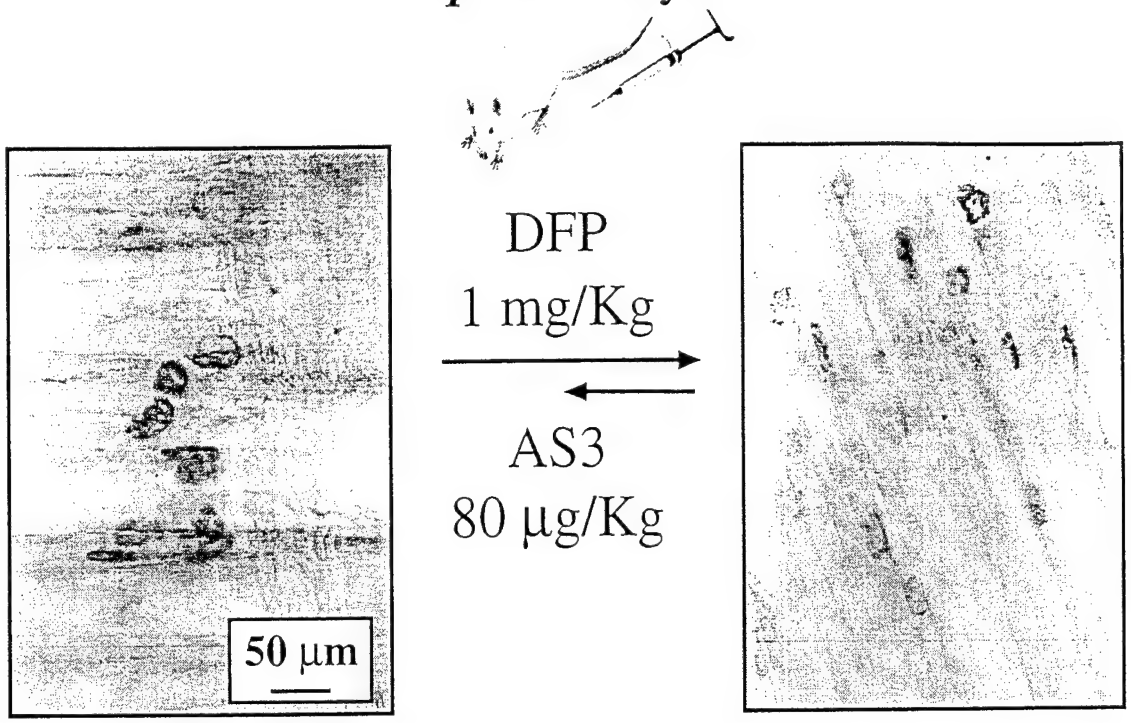
i.p. X 4 days
DFP
1 mg/Kg
AS3
80 µg/Kg
50 µm

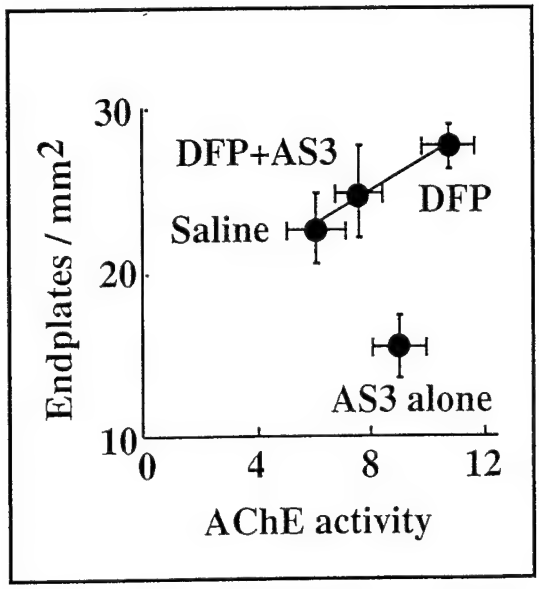
30
20
10
Endplates / mm2
DFP+AS3
DFP
Saline
AS3 alone
0
4
8
12
AChE activity

FIGURE 6

Acetylcholinesterase variants in mammalian stress: catalytic short-term and structural long-term roles

Meira Sternfeld and Hermona Soreq

Dept. of Biological Chemistry, The Life Sciences Institute
The Hebrew University of Jerusalem, Israel 91904
Tel No: 972-2-6585109; Fax No: 972-2-6520258; email: soreq@shum.huji.ac.il

Overview

The acetylcholine (ACh) hydrolysing enzyme acetylcholinesterase (acetylcholine acetyl hydrolase, EC 3.1.1.7, AChE) has long been known for its catalytic role in terminating cholinergic neurotransmission. Over the past few years, molecular cloning, genetic engineering and antisense studies have widened the scope of AChE's involvement in the development, maintenance and decline of mammalian brain functioning beyond the cholinergic system. Alternative splicing at the 3' end of AChEmRNA transcripts was found to modify the C-terminal peptides of their protein products, define their multimeric assembly and determine their subcellular localization. In addition to ACh hydrolysis, each of the two main brain AChE variants was shown to possess distinct, catalytically-independent structural functions: the synaptic variant AChE-S induces process extension from neurons and glia and affects synapse properties whereas the synaptically-inert "readthrough" AChE-R variant dominantly arrests glial process extension. Dramatic increases occur in the AChE-R: AChE-S ratio following stress. At the short-term range (minutes to hours) this assists in down-tuning excessive cholinergic hyperexcitation through the catalytic activity and accessibility of AChE-R; at the long range (months) AChE-R attenuates neurodeterioration, most likely through its structural capacity to compete with the neurodeterioration-accelerating role(s) of AChE-S. AChE's transcriptional regulation and alternative splicing therefore provide both immediate and long-lasting balancing functions which protect the mammalian brain from the adverse consequences of acute traumatic stress.

Heterologous expression studies demonstrate structural functions of AChE Variants

Early studies reported that externally added AChE enhances neurite growth (for a recent review see Grisaru et al.[1]). Findings obtained through use of AChE inhibitors further suggested a mechanism for this morphogenic function that does not involve catalytic activity of AChE. However, it remained unclear whether each and every one of the variant AChE enzyme forms could promote neurite process extension. These difficulties were overcome in studies of several groups, including ours, which employed cells or organisms overexpressing the various forms of AChE and/or exposed to antisense sequences designed to reduce the levels of particular AChE variants.

In murine neuroblastoma, transfection with murine AChE cDNA induced neurite growth and increased the percentage of neurite-bearing cells. Both phenomena were reversed by addition of a polyclonal AChE antiserum or by transfection with an antisense AChE cDNA[2]. In rat glioma, both DNA microinjections and stable transfections[3] demonstrated distinct effects for the individual AChE isoforms on

cellular development and astrocyte morphology. C6 glioma cells transfected with human AChE-S, displayed enhanced process growth and branching as compared with control cells. In contrast, stable transfections with human AChE-R induced dominant appearance of small, round cells with no processes.

Together, these studies suggested that variable expression levels and alternative splicing of the ACHE gene could affect both neuronal and glial development in a manner dependent on the expressed variant. The capacity of AChE-S to affect neurite growth was further demonstrated in cultured spinal neurons of *Xenopus laevis* embryos. Different variants of human AChE[4], were transiently expressed from microinjected human AChE cDNA vectors during the blastula stage. Spinal neurons cultured one day later and overexpressing AChE-S displayed significantly faster growth rate. However, neurons overexpressing AChE-R or a truncated AChE from which the natural C-termini were depleted displayed no growth changes. The *Xenopus* system was also used to test a mutated form of AChE-S, incapable of hydrolyzing ACh. This catalytically inactive AChE displayed similar neuritogenic effect as the active enzyme, directly demonstrating that the effect of AChE on neurite outgrowth is unrelated to its catalytic activity. In phaeochromocytoma PC12 cells, antisense suppression of AChE resulted in impaired neurite growth upon differentiation mediated by nerve growth factor[5]. This phenomenon could be reversed, at least partially, by heterologous expression of active or inactive human AChE-S. Moreover, the AChE-homologous and catalytically inactive protein neuroligin-1[6] also rescued neurite growth from antisense oligonucleotide-treated PC12 cells, showing again that this function of AChE does not require ability to hydrolyze AChE. Fig. 1 illustrates the corresponding structural hypothesis, based on the homology of AChE with known cell-cell adhesion proteins and explaining its previously surprising capacity to transduce growth signals through competition with these proteins.

Another structural function of AChE refers to its effects on neuromuscular junction (NMJ) development *in vivo*. Electron micrographs of myotome NMJs of AChE-S overexpressing *Xenopus* embryos showed significant NMJ enlargement. Both post-synaptic length measurements and elevated cytochemical AChE staining were increased as compared to controls[7,8]. In this case, embryos expressing a C-terminally truncated variant of human AChE (E4) also had larger NMJs. However, NMJs of inactive-AChE-S expressing embryos were not different in size from control NMJs, showing that catalytic activity but not the variant C-terminus is necessary for this function of AChE in NMJ development[4]. Human AChE-R overexpression did not lead to AChE accumulation in the NMJ, neither did it cause its enlargement[9]. This suggested that the physical association with synaptic membrane was a necessary prerequisite for this NMJ morphogenic function. These experimental results are summarized in Table 1.

The structural functions of AChE variants involve protein-protein interactions

The differentiation and proliferation effects of AChE variants have been demonstrated in numerous experimental systems and by many laboratories. By now, they are considered firmly established functions[1]. However, the mechanism(s) by which the C-terminal variants of AChE signal their morphogenic functions remain to be elucidated. Genome database analyses demonstrate significant sequence identity between the core

domain of AChE and several non-catalytic proteins that have well-defined cell-cell adhesion roles. These include mammalian thyroglobulin and neuroligins[10] and *Drosophila* gliotactin, glutactin and neurotactins[11-13]. This suggested that the structural effects of AChE variants could potentially reflect competition between the variants themselves or between them and their homologs on the binding partners demonstrated for these homologs. It further seemed plausible that the variant-specific C-termini of AChE can modulate such competitive interactions.

At the extracellular sites, the binding partners of AChE can possibly interact with transmembrane proteins of the neurexin family like the partners of gliotactin and neurotactins[14]. Intracellularly, such partner proteins can interact and transduce intracellular signals through their PDZ motifs[15]. Cytoskeletal elements, such as proteins of the band 4.1 family could serve as the downstream targets for these signals[16]. Proteolytic removal of competitors could also be involved: a recent review[17] suggests that control of many morphogenic functions may be effected via proteolysis by matrix metalloproteins (MMPs). These are known to regulate cell-cell adhesion, and can convert proteolytically susceptible ectoproteins into cell adhesion elements. Both secretory and membrane-associated AChE variants should be considered ectoproteins, their cell adhesion activity being determined by their characteristic C-termini and perhaps modulated by an MMP. It is therefore tempting to speculate that cell adhesion properties are regulated by these actions of MMPs on AChE variants and/or their structural homologs. The fact that truncated AChE has been detected *in vivo*[4] and the most recently discovered activities for the C-terminal peptides cleaved off AChE (Grisaru D. et al., unpublished observations) suggest that this hypothesis may have a basis in reality.

The link of AChE variants to the shift from acute stress to neurodegeneration

Acute traumatic stress increases the risk for neurodegeneration in the mammalian brain[18,19], due to both inherited and acquired origins[20,21]. The accepted notion is that responses to acute stress are beneficial in the short term. However, in some cases, acute stress leads to long range neurodegeneration[22]. For example, the physical stress of closed head injury is the largest risk factor known for non-familial Alzheimer's disease[19,21]. Another example is post-traumatic stress disorder (PTSD), in which exposure to acute stress initiates neurodegeneration in certain individuals through a yet unknown cascade of events[18]. The transition from acute stress to neurodegeneration is not understood and should involve an interplay between factors which are constitutively expressed, such as AChE-S and modulator(s) which are upregulated following stress. An intriguing candidate for such modulators is AChE-R, which is upregulated following acute psychological or chemical stress[23,24] and is involved both in AD an in PTSD.

<u>AChE involvement in Alzheimer's disease</u>

The primary site for mammalian AChE-S are cholinergic neurons. This may explain why changes in AChE levels and properties have been reported to be associated with several neurodegenerative diseases. These include AD, a devastating degenerative disorder of the central nervous system (CNS) that results in a progressive deterioration of cognitive function and severe alteration of personality. Degeneration of cholinergic neurons primarily takes place in the nucleus basalis of Meynert (NBM), the origin of the major cholinergic projections to the neocortex. This occurs early in the course of

AD, and parallels both the cognitive decline[25] and neuronal and synaptic loss. However, appearance in the AD brain of amyloid-containing plaques and neurofibrillary tangles[26] cannot be accounted for by cholinergic deficiencies alone and the deficits observed in AD undoubtedly include damages in other neurotransmitter systems. Since complex interactions between such diverse systems play a vital role in maintaining cognitive processing, a wider view of AD has, in the past decade, justly diverted interest from the catalytic role of AChE in this disease. However, the recently established structural role(s) of AChE extend beyond cholinergic neurons alone and should be relevant to many different types of neurons. For example, neuroligin has recently been identified in excitatory, most likely glutamatergic synapses[27]. Therefore, viewing AChE as a multifaceted protein with cell-cell interaction capacities, calls for a reconsideration of our understanding of the involvement of specific AChE variants in the neurodegenerative processes of AD.

Particular emphasis has been directed toward the involvement of cholinesterases (AChE and butyrylcholinesterase; BuChE) during the early stages of AD plaque formation[28]. Catalytically active AChE protein was also found in the neurofibrillary tangles and in the amyloid-positive vessels[29] where it presents a laminar distribution[30]. However, none of these studies addressed the distinction between the various AChE variants in the disease process, primarily because no tools were yet available for that. Moreover, the cellular origin of AD has remained unclear. Neuronal, as opposed to glial, distribution of cholinesterases has been reported in AD brains[31]. Yet, the substrate and inhibitor specificities of AChE found in plaques and tangles resemble those of glial cholinesterases. It was therefore suggested that glial cells are the main source of AD plaque cholinesterases and that amyloid precursor plaques by themselves do not contain the cholinesterase activity[32]. More recently, Inestrosa and co-workers have demonstrated *in vitro* AChE-promoted aggregation of amyloid plaques that was not associated with the active site of the enzyme[33]. This raised the possibility that catalytically inactive AChE, which could not be detected by the employed techniques, could also be involved.

The intriguing link between cholinergic dysfunction in the basal-cortical system, AChE accumulation in amyloid plaques and cognitive deficits, have initiated multiple efforts to elucidate the role of AChE in cognition and neurodegeneration[25]. Most effort was centered on the use of AChE inhibitors to facilitate what remained in the AD brain of cholinergic function. In animal experiments, systemic administration of anticholinesterases partially and temporarily reversed cognitive deficits (see, for example[34]). Clinical trials have therefore been carried out using quaternary, carbamate and organophosphate cholinesterase inhibitors. Multicenter clinical trials of tetrahydroaminoacridine (tacrine)[35], donepezil[36], physostigmine[37], and rivastigmine[38] provided evidence for limited, temporary improvement in cognition of AD patients treated with these drugs. At present, palliative anticholinesterases are the only drugs approved for use in treating AD patients. However, their effects are limited at best and relatively short-lived. Some drugs (e.g. tacrine), further, cause adverse outcome. Therefore, exploration of the molecular mechanism(s) which underlie anti-cholinesterase responses can yield important information also at the clinical level.

Involvement of AChE and anti-cholinesterases in stress responses

PTSD is a clinically recognized syndrom reflecting a highly variable array of neuropsychiatric and physical symptoms[22]. PTSD includes both neuropathological and cognitive characteristics, among them delayed cognitive deterioration, depression, irritability, persistent deficits in short-term memory and even reduced hippocampal volume[39]. The similarity in symptoms suggested that common mechanism(s) may be involved in PTSD and anti-AChE responses[23]. Because anticholinesterases interact with the core domain of AChE, there was initially no indication that alternative splicing could be involved. However, that early impression changed rapidly.

Both anticholinesterase exposure and acute psychological stress of forced swimming disrupt the blood-brain barrier, inducing efficient brain penetrance of anti-AChEs[40]. The consequent inhibition of AChE facilitates a rise in ACh levels and induces a cascade of *c-fos*-mediated transcriptional responses which are dependent on intracellular accumulation of Ca^{++}[23]. These responses involve the "cholinergic locus"[41], where the genes for choline acetyltransferase and the vesicular ACh transporter are located. The expression of these genes is repressed in parallel to ACHE overproduction, leading to decreased ACh levels. This suppression, seen both *in vivo* and in brain slices, down-tunes the excessive cholinergic neurotransmission that is characteristic of stress. This is accompanied by drastic changes in neurophysiological and neuroanatomical properties considered to be associated with memory (reviewed by Kaufer and Soreq[42]). In numerous animal models, suppression of long-term potentiation, enhancement of long-term depression, and changes in dendrite morphology were all observed following exposure to anti-cholinesterases[43]. AChE overexpression may therefore take part in this process and protect the brain from sustained hyperexcitability and from increased susceptibility to seizure activity and neuronal toxicity. However, the consequences of prolonged AChE overexpression on cholinergic neurotransmission remained unclear. Also, the pattern of this overexpression dictated a change in the AChE-R: AChE-S ratio which called for exploration.

Within 30 min post-exposure to an anticholinesterase or to acute psychological stress, alternative splicing specifically leads to the accumulation of the AChE-R isoform. This secretory form of the enzyme would not be expected to accumulate at synapses[9] or alter their structure[4]. Unlike the usually abundant AChE-S variant, overproduction of AChE-R would be expected to reduce process formation, at least from astrocytes[3]. This suggested distinct structural roles for the "synaptic" AChE-S isoform and the soluble AChE-R variant in post-traumatic stress. A soluble form of AChE is best suited to reduce the excessive ACh accumulation associated with the stress-characteristic hyperexcitation. This pointed at this isoform as most appropriate for the immediate needs of the acutely stressed brain, but left the issue of its potential long-term effects unanswered.

To address this subject, transgenic mice were created which overexpress either AChE-S or AChE-R. Higher than normal levels of AChE-S in brain neurons, achieved under control of the minimal 600 bp authentic human ACHE promoter, lead to progressive deterioration in cognitive[44,45] and neuromotor faculties[46]. In contrast, AChE-R accumulation left NMJ functioning intact (Soreq H. et al., unpublished observations) and protected the mouse brain from the appearance of age-dependent

neurodeterioration phenomenae (Sternfeld M. et al., unpublished observations). This highlights the benefits of the elevation of AChE-R levels post-stress for long-term protection. Neuropsychiatric stress-induced symptoms are often reported years after acute[47] or chronic[48] exposure to anticholinesterases. This raises a concern that the AChE-S isoform may be involved in other human mental disorders as well. The extensive and growing use of several FDA-approved anticholinesterases for the treatment of AD[49], the arguable use of the anticholinesterase pyridostigmine, for prophylactic protection under the threat of chemical warfare[40], and the recent withdrawal of investigational anti AChEs from further development due to adverse symptoms (SCRIP World Pharmaceutical News No. 2374, pg. 19; 1998) emphasize the importance of this issue.

AChE-R involvement in preventing neurodegeneration

Two major phases in post-stress responses may require AChE-dependent modulation. These are the short-term phase (minutes to hours), when cholinergic neurotransmission should be suppressed, and the long-term phase (months to years), when the risk for neurodegeneration materializes. It is interesting to note that AChE-R can answer at least part of the brain's needs for balancing at both these phases, and that both its catalytic and structural properties match these purposes. In this context, the rapid accumulation and easy accessibility of the soluble AChE-R provide the means for immediate down-regulation of hyperexitation, whereas its competent competitiveness with AChE-S on its structural functions protects the brain from neurodeterioration. That most neurons produce AChE during development but not during adulthood[50] and the stress-induced increases in ACHE gene expression, together may suggest an association of AChE with neuronal plasticity. Thus, AChE may take part not only in the normal development of mammalian neurons but also in controlling their capacity to respond to external insults.

Alternative splicing and stress induced neuronal activity

The dramatic modulation of AChE variants under acute stress raises a more general question, namely, to what extent does alternative splicing change under stress induced alterations of neuronal activity and are such changes functionally relevant. Search of the recent literature demonstrates that neuronal activity does have a considerable effect over alternative splicing, which is perhaps due to the rapid fluctuation in the concentration of intracellular ions that is induced during neurotransmission. Altogether, alternative splicing emerges over the past decade as a major mechanism of neuronal response to external stimuli. Neurons are especially adapted for rapid modulations in alternative splicing and include several families of neuron-specific RNA binding proteins, for example ELAV and ELAV-related proteins[51] and Sm/N proteins[52]. The potential contribution of neuronal activity-dependent alternative splicing toward plasticity-related properties such as learning and memory has been reviewed by Bailey et al.[53].

In several cases, neuronal activity-dependent changes in alternative splicing can introduce C-terminal changes in the produced proteins. This can occur, as it does in the case of ACHE-R, through the insertion of a "readthrough" pseudointron thereby changing the sequence encoding the C-terminus and/or introducing stop codons. Modified C-termini have been shown to create altered partially functional receptors[54],

change ligand affinity[55] or produce inactive, truncated variants[56]. In addition, neuronal activity-dependent alternative splicing has been shown to modify signalling peptides [57] and change the properties of vesicle coat proteins[58] and ion channels[59]. In conjunction with the alternative splicing of many transcription factors[60], this yields an intricate picture of complex, multileveled control of neuronal gene expression under modified excitability.

Alternative splicing under changes in cholinergic neurotransmission was subject to special attention. For example, the muscarinic cholinergic agonist pilocarpine, which induces seizures when systemically administered, modulates the splicing patterns of the tra2-β splicing factor, NMDAR1 and clathrin B genes[58,59]. These cholinergic excitation-dependent changes are brain-region specific, transient and reversible within 48 hours[59]. In principle, alternative splicing is at least partially modulated by SR or SR-like proteins[61]. The SR family includes serine-arginine RNA-binding proteins that recognize purine-rich exon-enhancer motifs[62] surrounding relatively weak splice sites. Other RNA binding factors may also be involved, for example ASF [63] or SF2[64]. The modulations in alternative splicing are quite specific, as NMDA1R is selectively modified by pilocarpine induced seizures[59].

Many of the splicing changes induced by neuronal activity appear to be functionally relevant. Thus the neuron-specific exon of clathrin light chain B, involved in the intracellular transport of coated vesicles, is influenced by the splicing factor htra2-β 1 which is itself modulated by neuronal activity[58]. Also, the KV3.1a potassium channel transcript, which changes the K^+ rectifier currents, is subject to bEGF and protein kinase C regulation, and thus affects neuronal response to external stimuli[65].

Recent genetic screening unraveled significant association between mutations that prevent alternative splicing options and neurodegenerative disease, which emphasizes these splices options as essential for attenuating neurodegeneration. For example, 5' splice site mutations in the microtubuli-associated tau gene are associated with fronto-temporal dementia and parkinsonism linked to chromosome 17[66,67]. Another example involves the Ataxia-telangiectasia ATM gene, which increases the risk for neurodegeneration. The ATM gene is subject to complex modulation of 5' and 3' alternative exons under environmental stimuli and various changes in cellular physiology[68], suggesting involvement of these changes with ATM-induced neurodeterioration. Also, overexpression of specific splice variants of human tyrosine hydroxylase mRNA is associated with progressive supranuclear palsy[69], and chronic exposure to the neurodegenerration inducer ethanol induces differential changes in the alternative splicing pattern of AMPA receptors[70]. Altogether, these studies demonstrate tight involvement of alternative splicing and consequent signal transduction processes in neuronal placticity following stress.

Roles of AChE variants in neuronal development and deterioration

Our findings indicate causal involvement of specific AChE variants in neuronal plasticity and the factors that influence it. Interestingly, several observations differentiate between the potential effects of these variants in neuronal development and deterioration. Thus, AChE-S, but not AChE-R promotes neurite growth[4] and glial process extension[3]. However, when persistently overexpressed, AChE-S also induces

progressive dendrite depletion and spine loss[45]. In the mouse brain, AChE-S facilitates corkscrew deformities, neurite retraction balls and reactive gliosis whereas AChE-R attenuates the appearance of all these deterioration characteristics (Sternfeld M. et al., unpublished observations). This dual effect is not exceptional, as several key proteins display such seemingly opposing effects. For example, NGF induces both excessive axon outgrowth and decreased terminal innervation[71]. Likewise, NF-KB modulates both neurodeterioration and neuroprotection[72]. These distinctions call for exploring the effects of AChE variants on neuronal plasticity, which would be relevant both in the CNS and the peripheral nervous system.

In both developing and adult neurons, enhanced activity induces rapid yet long-lasting changes in gene expression[73,74]. However, the nature and the extent of such induction may differ substantially. Rapidly affected genes include activity-inducible transcription factors, which turn on cascades of downstream target genes[75] as well as neurotrophic factors and signalling molecules [76]. These are presumably involved in stabilizing both long-term potentiation (LTP[77]) and long-term depression (LTD[78]) in the hippocampus. As indicated from the apparently opposing nature of these physiological processes, many of the induced genes (e.g. c-Jun) display intricate balance roles between protective and damaging effects[79]. While the detailed signalling pathways have not yet been defined, several key elements have been identified (e.g. trkB[80] cAMP-dependent kinase[81], BDNF and NT3[82]).

The apparent distinction between development and neurodeterioration processes is emphesized under acute conditions. Thus, adult neurons undergo extensive and continual adaptation in response to external insults; they also confront conditions that are quite different from those of early development[83]. In view of the cumulative information on AChE gene expression and its morphogenic effects, involvement of AChE variants may be explained in the survival, growth and neurotransmission capacity of both developing and adult neurons in both the central and peripheral systems. This refers especially to simpathetic neurons, since adrenergic and cholinergic neurons in the sympathetic system are considered to share a common progenitor[84].

Despite the contrasting needs of different phases in neuronal life, common elements are involved in the mechanisms of plasticity in both phases. In both cases, for example, dendrite morphology is affected[85]. Interactions between neurons and their targets, whether effector cells (e.g. astrocytes, microglia), other neurons or target tissues (e.g. muscle) are vital to all of these aspects of neural plasticity, which extends to the level of neurotransmitter plasticity[85].

Developing neurons require access to target-derived diffusible neurotrophic factors (e.g. NGF, NT3 and GDNF for sympathetic neurons) as well as to bound elements of the extracellular matrix such as laminin or agrin. The recent establishment of AChE-R as a diffusible protein that is expressed both in developing neurons and in many of their target cells (e.g. muscle) calls for testing its capacity as a neurotrophic factor and for searching for the target protein(s) with which it interacts. Based on our findings, it appears that both AChE-R and AChE-S (and, possibly, the ratio between these two proteins) affect plasticity throughout life. At the adult phase, this primarily relates to neuronal maintenance, growth and neurotransmitter expression. Failure to maintain

satisfactory neuronal function in old age, for example in the breakdown of homeostasis due to external insults, may result partly from the disturbance of the dynamic, trophic relationship between neurons and their targets. The AChE variants are excellent candidates for modulating such processes due to their ubiquitous expression in the corresponding cells, their rapid yet long-lasting modulation in response to variable stressors and their cholinergic and morphogenic effects. Altered expression of these variants may, in turn, underlie the selective vulnerability of some individuals for age-dependent neurodeterioration.

By carrying the transgenes in inherited forms, our transgenic animals inevitably experience both developmental and adult changes in the brain's structure and function. Synaptic reorganization has been shown to be induced in the hippocampus by abnormal cholinergic hyperexcitation[86]. In the adult state, such changes are primarily mediated by NMDA receptors[87]. Because of its non-catalytic properties, overexpression of AChE during development not only induces a chronic hypocholinergic state but may also alter neuronal circuitry. The localization of the AChE-homologous protein neuroligin to glutamatergic synapses[27] and the redundant neuritogenic functions of AChE and neuroligin[5] further suggest glutamatergic effects. Excess AChE at the key sites where it exerts its role(s) could hence affect the brain's structure and function through several separate ways:

(1) Due to its role as a neurotransmitter hydrolysing enzyme, excess AChE would induce a hypocholinergic state that may cause secondary feedback response to enable minimal cholinergic neurotransmission.

(2) Because of its non-catalytic activity and its shared morphogenic functions with neurexin ligands such as neuroligin[14] or gliotactin[12], AChE overexpression may alter neuron-neuron or neuron-glia interactions and modify the PDZ-signalling processes of these AChE homologues and their protein partners.

(3) Since the elements in which these two distinct functions are involved are constituents of one system, one should expect the cholinergic and structural function(s) of AChE to affect each other in a complex manner.

The structural and catalytic unctions of AChE would therefore be expected to mutually influence each other. Thus, altered structural signalling in cholinergic neurons would modulate cholinergic neurotransmission and modulated acetylcholine hydrolysis can be expected to affect neuron-neuron and neuron-glia structural interactions. Changes in AChE variants can hence initiate a self-fed loop of events that includes multilple structural and physiological components in both cholinergic and other neurotransmission pathways.

AChE variants may modulate neuron-glia interactions under stress

Apart from their complex neuronal and synaptic roles, alternative AChE variants emerge as relevant to glial-glial and neuron-glial interactions. Our AChE transfection studies unraveled distinct effects for the AChE-S and the AChE-R variants on glial process extension and general morphology[3]. This predicts changes in glial properties under acute stress, when the AChE-R to AChE-S ratio is drastically increased. Modified glia, in turn, can affect neuronal activity and synaptic neurotransmission[88]. Furthermore, neuron activity-induced elevation of internal Ca^{+} concentration in glia can potentially activate the Ca^{++} response element in the ACHE promoter, inducing AChE production from glia themselves and escalating the neuronal response[89] .

The implications of AChE variants to neuron-glial interactions may become particularly relevant in neurodegenerative disease. Reactive astrocytes, the hallmark of injured brain, display altered cell adhesion molecules and are currently considered involved in the recovery of neurotransmission following injury[90]. That persistent AChE-R overproduction attenuates reactive gliosis (Sternfeld M. et al., unpublished observations) may hence point at this protein as characteristic of a certain early phase in the post-stress response, before reactive gliosis is allowed to take place.

The general view of reactive gliosis during neurodegenerative disease associates this process with inflammatory responses[91]. The intimate interaction between reactive astrocytes and neuritic AD plaques with their elevated AChE[32,91] further points at the potential relationship between AChE and activated glia. Reports of the non-catalytic involvement of AChE in amyloid precipitation[33,92] focus our attention at these plaques as dynamic sites of the disease process, but it is not yet known whether specific AChE variants differ in their capacity for such activity.

Unlike neurons, glia do not express the Neurexin I-III genes, which implies that conservative neurexin-neuroligin interactions[10] cannot be relevant for neuron-glia contacts. However, mammalian glia do express Caspr, the mammalian neurexin IV homologue[15], as well as homologues to *Drosophila* gliotactin[12,93]. Genomic disruption of either gliotactin or neurexin IV induces similar abnormalities in glial-neuron interactions in insect larvae. This suggests potential interaction between the AChE-homologous gliotactin and Neurexin IV, extending the neuronal paradigm of neurexin-neuroligin interaction to glia. New possibilities of neuron-glia interactions are thus indicated through additional, yet unproven links between neuronal and glial cell surface proteins carrying AChE and neurexin modules. Such putative interactions can be relevant to blood brain barrier functioning[24,40], CNS and PNS development and even brain tumor growth.

From brain to blood: the pluripotent stem cell effects of AChE variants

The distinct morphogenic effects of AChE variants on neurons and glia, coupled with the known expression of these variants in hematopoietic cells, raised the question whether these variants are morphogenically effective in blood cell progenitors too. In a recent study, we have demonstrated that this is indeed the case (Grisaru D. et al., unpublished observations). This study further raises the question whether the AChE variants we studied, or fragments thereof, can modulate the commitment, proliferation and/or differentiation of pluripotent stem cells in a multi-tissue manner (see Scheffler et al.[94] for a recent review of neuropoiesis/hematopoiesis similarities). A detailed study of the involvement of AChE variants in the creation of neurons, astrocytes and supportive brain tissue can yield important insights both on the origin of the corresponding cells and the molecular mechanisms through which AChE exerts its numerous morphogenic effects. Additionally, such studies can contribute substantially towards the new and rapidly developing field of human stem cell therapy in the nervous system [95].

General considerations and future prospects

Using a combination of molecular, cellular, biochemical and transgenic approaches, we initiated a study aimed at defining and characterizing the structural properties of alternative AChE variants. In spite of the relatively limited differences in the sequence of these variants (26 or 40 residues out of 560-574), we found striking differences in their roles with regards to neuritogenesis, synaptogenesis and neurodeterioration. Having set up the experimental model systems and DNA and antibody tools, we uncovered what seems to be the tip of an iceberg. These findings therefore call for future dissection of these new phenomena that were outlined in our current work.

Recent developments in molecular biology now offer improved, more powerful techniques for pursuing these goals. The yeast two hybrid system [96] seems ideally suited for screening for those protein partners that presumably interact with the different AChE variants and their C-terminal peptides; tetracycline control [97] could offer the opportunity to induce or suppress their expression at will in an *in vivo* context; and DNA microarrays [98] can define detailed profiles of the changes in gene expression that are induced by the modulation of these variants under modified conditions. These techniques should be coupled with genetic studies of the evolutionary conservation of the AChE variants and their functions and the investigation of these functions could be extended into other tissues and organs. Now established, the morphogenic roles of AChE variants offer a wealth of research opportunities with basic and applied implications.

Acknowledgements:

This study was supported by grants to H.S. by the Israel Science , the U.S.- Israel Binational Science Foundation ,the German-Israeli Foundation, the U.S. Army Medical Research and Development Command and Ester Neurosciences Ltd.

References:

1. Grisaru D, Sternfeld M, Eldor A et al. Structural roles of acetylcholinesterase variants in biology and pathology. *Eur J Biochem* 1999; **264**: 672-686.
2. Koenigsberger C, Chiappa S , Brimijoin S. Neurite differentiation is modulated in neuroblastoma cells engineered for altered acetylcholinesterase expression. *J Neurochem* 1997; **69 (4)**: 1389-1397.
3. Karpel R, Sternfeld M, Ginzberg D et al. Overexpression of alternative human acetylcholinesterase forms modulates process extensions in cultured glioma cells. *J Neurochem* 1996; **66**: 114-123.
4. Sternfeld M, Ming G, Song H et al. Acetylcholinesterase enhances neurite growth and synapse development through alternative contributions of its hydrolytic capacity, core protein, and variable C termini. *J Neurosci* 1998a; **18**: 1240-1249.
5. Grifman M, Galyam N, Seidman S et al. Functional redundancy of acetylcholinesterase and neuroligin in mammalian neuritogenesis. *Proc Natl Acad Sci U S A* 1998; **95**: 13935-13940.
6. Ichtchenko K, Hata Y, Nguyen T et al. Neuroligin 1: a splice site-specific ligand for beta-neurexins. *Cell* 1995; **81**: 435-443.
7. Shapira M, Seidman S, Sternfeld M et al. Transgenic engineering of neuromuscular junctions in Xenopus laevis embryos transiently overexpressing key cholinergic proteins. *Proc Natl Acad Sci U S A* 1994; **91**: 9072-9076.

8. Seidman S, Aziz Aloya RB, Timberg R et al. Overexpressed monomeric human acetylcholinesterase induces subtle ultrastructural modifications in developing neuromuscular junctions of Xenopus laevis embryos. *J Neurochem* 1994; **62**: 1670-1681.
9. Seidman S, Sternfeld M, Ben Aziz Aloya R et al. Synaptic and epidermal accumulations of human acetylcholinesterase are encoded by alternative 3'-terminal exons. *Mol Cell Biol* 1995; **15**: 2993-3002.
10. Ichtchenko K, Nguyen T , Sudhof TC. Structures, alternative splicing, and neurexin binding of multiple neuroligins. *J Biol Chem* 1996; **271**: 2676-2682.
11. Olson PF, Fessler LI, Nelson RE et al. Glutactin, a novel Drosophila basement membrane-related glycoprotein with sequence similarity to serine esterases. *EMBO J* 1990; **9**: 1219-1227.
12. Auld VJ, Fetter RD, Broadie K et al. Gliotactin, a novel transmembrane protein on peripheral glia, is required to form the blood-nerve barrier in Drosophila. *Cell* 1995; **81**: 757-767.
13. Darboux I, Barthalay Y, Piovant M et al. The structure-function relationships in Drosophila neurotactin show that cholinesterasic domains may have adhesive properties. *EMBO J* 1996; **15**: 4835-4843.
14. Nguyen T , Sudhof TC. Binding properties of neuroligin 1 and neurexin 1 beta reveal function as heterophilic cell adhesion molecules. *J Biol Chem* 1997; **272 (41)**: 26032-26039.
15. Bellen HJ, Lu Y, Beckstead R et al. Neurexin IV, caspr and paranodin--novel members of the neurexin family: encounters of axons and glia. *Trends Neurosci* 1998; **21**: 444-449.
16. Takeuchi K, Kawashima A, Nagafuchi A et al. Structural diversity of band 4.1 superfamily members. *J Cell Sci* 1994; **107**: 1921-1928.
17. Werb Z , Yan Y. A cellular striptease act. *Science* 1998; **282**: 1279-1280.
18. Turnbull GJ. A review of post-traumatic stress disorder. Part II: Treatment. *Injury* 1998; **29**: 169-175.
19. Graham DI, Gentleman SM, Nicoll JA et al. Is there a genetic basis for the deposition of beta-amyloid after fatal head injury? *Cell Mol Neurobiol* 1999; **19**: 19-30.
20. True WR, Rice J, Eisen SA et al. A twin study of genetic and environmental contributions to liability for posttraumatic stress symptoms. *Arch Gen Psychiatry* 1993; **50**: 257-264.
21. Roses AD , Saunders AM. ApoE, Alzheimer's disease, and recovery from brain stress. *Ann N Y Acad Sci* 1997; **826**: 200-212.
22. Sapolsky RM. Why stress is bad for your brain. *Science* 1996; **273**: 749-750.
23. Kaufer D, Friedman A, Seidman S et al. Acute stress facilitates long-lasting changes in cholinergic gene expression. *Nature* 1998; **393**: 373-377.
24. Kaufer D, Friedman A , Soreq H. The vicious circle: long-lasting transcriptional modulation of cholinergic neurotransmission following stress and anticholinesterase exposure. *The Neuroscientist* 1999; **5**: 173-183.
25. Coyle JT, Price DL , DeLong MR. Alzheimer's disease: a disorder of cortical cholinergic innervation. *Science* 1983; **219**: 1184-1190.
26. Katzman R. Alzheimer's disease. *N Engl J Med* 1986; **314**: 964-973.

27. Song JY, Ichtchenko K, Sudhof TC et al. Neuroligin 1 is a postsynaptic cell-adhesion molecule of excitatory synapses. *Proc Natl Acad Sci U S A* 1999; **96**: 1100-1105.
28. Moran MA, Mufson EJ , Gomez-Ramos P. Colocalization of cholinesterases with beta amyloid protein in aged and Alzheimer's brains. *Acta Neuropathol* 1993; **85**: 362-369.
29. Mesulam M, Carson K, Price B et al. Cholinesterases in the amyloid angiopathy of Alzheimer's disease. *Ann Neurol* 1992; **31**: 565-569.
30. Coleman AE, Geula C, Price BH et al. Differential laminar distribution of acetylcholinesterase and butyrylcholinesterase containing tangles in the cerebral cortex of Alzheimer's disease. *Brain Res* 1992; **596**: 340-344.
31. Wright CI, Guela C , Mesulam MM. Protease inhibitors and indoleamines selectively inhibit cholinesterases in the histopathologic structures of Alzheimer disease. *Proc Natl Acad Sci U S A* 1993; **90**: 683-686.
32. Geula C, Greenberg BD , Mesulam MM. Cholinesterase activity in the plaques, tangles and angiopathy of Alzheimer's disease does not emanate from amyloid. *Brain Res* 1994; **644**: 327-330.
33. Inestrosa NC, Alvarez A, Perez CA et al. Acetylcholinesterase accelerates assembly of amyloid-beta-peptides into Alzheimer's fibrils: possible role of the peripheral site of the enzyme. *Neuron* 1996; **16**: 881-891.
34. Murray CL , Fibiger HC. Pilocarpine and physostigmine attenuate spatial memory impairments produced by lesions of the nucleus basalis magnocellularis. *Behav Neurosci* 1986; **100**: 23-32.
35. Winkler J, Thal LJ, Gage FH et al. Cholinergic strategies for Alzheimer's disease. *J Mol Med* 1998; **76**: 555-567.
36. Rogers SL , Friedhoff LT. The efficacy and safety of donepezil in patients with Alzheimer's disease: results of a US Multicentre, Randomized, Double-Blind, Placebo- Controlled Trial. The Donepezil Study Group. *Dementia* 1996; **7**: 293-303.
37. Thal LJ, Schwartz G, Sano M et al. A multicenter double-blind study of controlled-release physostigmine for the treatment of symptoms secondary to Alzheimer's disease. Physostigmine Study Group. *Neurology* 1996; **47**: 1389-1395.
38. Anand R, Gharabawi G , Enz A. Efficacy and safety results of the early phase studies with exelon (ENA-713) in Alzheimer's disease: an overview. *J Drug Dev Clin Pract* 1996; **8**: 106-116.
39. McEwen BS. Stress and hippocampal plasticity. *Annu Rev Neurosci* 1999; **22**: 105-122.
40. Friedman A, Kaufer D, Shemer J et al. Pyridostigmine brain penetration under stress enhances neuronal excitability and induces early immediate transcriptional response. *Nat Med* 1996; **2**: 1382-1385.
41. Bejanin S, Cervini R, Mallet J et al. A unique gene organization for two cholinergic markers, choline acetyltransferase and a putative vesicular transporter of acetylcholine. *J Biol Chem* 1994; **269**: 21944-21947.
42. Kaufer D , Soreq H. Tracking cholinergic pathways from psychological and chemical stressors to variable neurodeterioration paradigms. *Curr. Opin. Neurol.* 1999; In press.

43. Magarinos AM, McEwen BS, Flugge G et al. Chronic psychosocial stress causes apical dendritic atrophy of hippocampal CA3 pyramidal neurons in subordinate tree shrews. *J Neurosci* 1996; **16**: 3534-3540.
44. Beeri R, Andres C, Lev Lehman E et al. Transgenic expression of human acetylcholinesterase induces progressive cognitive deterioration in mice. *Curr Biol* 1995; **5**: 1063-1071.
45. Beeri R, Le Novere N, Mervis R et al. Enhanced hemicholinium binding and attenuated dendrite branching in cognitively impaired acetylcholinesterase-transgenic mice. *J Neurochem* 1997; **69**: 2441-2451.
46. Andres C, Beeri R, Friedman A et al. Acetylcholinesterase-transgenic mice display embryonic modulations in spinal cord choline acetyltransferase and neurexin Ibeta gene expression followed by late-onset neuromotor deterioration. *Proc Natl Acad Sci U S A* 1997; **94**: 8173-8178.
47. Wickelgren I. Rat model for Gulf War syndrome? *Science* 1997; **278**: 1404.
48. Rosenstock L, Keifer M, Daniell W et al. Chronic central nervous system effects of acute organophosphate pesticide intoxication. The Pesticide Health Effects Study Group. *Lancet* 1991; **338**: 223-227.
49. Winker MA. Tacrine for Alzheimer's disease. Which patient, what dose? *JAMA* 1994; **271**: 1023-1024.
50. Massoulie J, Anselmet A, Bon S et al. Acetylcholinesterase: C-terminal domains, molecular forms and functional localization. *J Physiol Paris* 1998; **92**: 183-190.
51. King PH, Levine TD, Fremeau RT, Jr. et al. Mammalian homologs of Drosophila ELAV localized to a neuronal subset can bind in vitro to the 3' UTR of mRNA encoding the Id transcriptional repressor. *J Neurosci* 1994; **14**: 1943-1952.
52. Schmauss C, McAllister G, Ohosone Y et al. A comparison of snRNP-associated Sm-autoantigens: human N, rat N and human B/B'. *Nucleic Acids Res* 1989; **17**: 1733-1743.
53. Bailey CH, Bartsch D , Kandel ER. Toward a molecular definition of long-term memory storage. *Proc Natl Acad Sci U S A* 1996; **93**: 13445-13452.
54. Wang J , Ross EM. The carboxyl-terminal anchorage domain of the turkey beta 1-adrenergic receptor is encoded by an alternatively spliced exon. *J Biol Chem* 1995; **270**: 6488-6495.
55. Miki T, Bottaro DP, Fleming TP et al. Determination of ligand-binding specificity by alternative splicing: two distinct growth factor receptors encoded by a single gene. *Proc Natl Acad Sci U S A* 1992; **89**: 246-250.
56. Duncan PI, Howell BW, Marius RM et al. Alternative splicing of STY, a nuclear dual specificity kinase. *J Biol Chem* 1995; **270**: 21524-21531.
57. Amara SG, Jonas V, Rosenfeld MG et al. Alternative RNA processing in calcitonin gene expression generates mRNAs encoding different polypeptide products. *Nature* 1982; **298**: 240-244.
58. Stamm S, Casper D, Hanson V et al. Regulation of the neuron-specific exon of clathrin light chain B. *Brain Res Mol Brain Res* 1999; **64**: 108-118.
59. Daoud R, Da Penha Berzaghi M, Siedler F et al. Activity-dependent regulation of alternative splicing patterns in the rat brain. *Eur J Neurosci* 1999; **11**: 788-802.
60. Lopez AJ. Developmental role of transcription factor isoforms generated by alternative splicing. *Dev Biol* 1995; **172**: 396-411.
61. Fu XD. The superfamily of arginine/serine-rich splicing factors. *Rna* 1995; **1**: 663-680.

62. Tacke R, Tohyama M, Ogawa S et al. Human Tra2 proteins are sequence-specific activators of pre-mRNA splicing. *Cell* 1998; **93**: 139-148.
63. Ge H , Manley JL. A protein factor, ASF, controls cell-specific alternative splicing of SV40 early pre-mRNA in vitro. *Cell* 1990; **62**: 25-34.
64. Caceres JF, Stamm S, Helfman DM et al. Regulation of alternative splicing in vivo by overexpression of antagonistic splicing factors. *Science* 1994; **265**: 1706-1709.
65. Liu SJ , Kaczmarek LK. The expression of two splice variants of the Kv3.1 potassium channel gene is regulated by different signaling pathways. *J Neurosci* 1998; **18**: 2881-2890.
66. Hutton M, Lendon CL, Rizzu P et al. Association of missense and 5'-splice-site mutations in tau with the inherited dementia FTDP-17. *Nature* 1998; **393**: 702-705.
67. Spillantini MG, Murrell JR, Goedert M et al. Mutation in the tau gene in familial multiple system tauopathy with presenile dementia. *Proc Natl Acad Sci U S A* 1998; **95**: 7737-7741.
68. Savitsky K, Platzer M, Uziel T et al. Ataxia-telangiectasia: structural diversity of untranslated sequences suggests complex post-transcriptional regulation of ATM gene expression. *Nucleic Acids Res* 1997; **25**: 1678-1684.
69. Dumas S, Le Hir H, Bodeau-Pean S et al. New species of human tyrosine hydroxylase mRNA are produced in variable amounts in adrenal medulla and are overexpressed in progressive supranuclear palsy. *J Neurochem* 1996; **67**: 19-25.
70. Bruckner MK, Rossner S , Arendt T. Differential changes in the expression of AMPA receptors genes in rat brain after chronic exposure to ethanol: an in situ hybridization study. *J Hirnforsch* 1997; **38**: 369-376.
71. Hoyle GW, Mercer EH, Palmiter RD et al. Expression of NGF in sympathetic neurons leads to excessive axon outgrowth from ganglia but decreased terminal innervation within tissues. *Neuron* 1993; **10**: 1019-1034.
72. Lipton SA. Janus faces of NF-kappa B: neurodestruction versus neuroprotection. *Nat Med* 1997; **3**: 20-22.
73. Kaufer D, Friedman A, Seidman S et al. Anticholinesterases induce multigenic transcriptional feedback response suppressing cholinergic neurotransmission. *Chem Biol Interact* 1999; **119-120**: 349-360.
74. Hughes PE, Alexi T, Walton M et al. Activity and injury-dependent expression of inducible transcription factors, growth factors and apoptosis-related genes within the central nervous system. *Prog Neurobiology* 1998; **57**: 421-450.
75. Kang H , Schuman EM. A requirement for local protein synthesis in neurotrophin-induced hippocampal synaptic plasticity. *Science* 1996; **273**: 1402-1406.
76. Cohen-Cory S , Fraser SE. Effects of brain-derived neurotrophic factor on optic axon branching and remodelling in vivo. *Nature* 1995; **378**: 192-196.
77. Bliss TV , Collingridge GL. A synaptic model of memory: long-term potentiation in the hippocampus. *Nature* 1993; **361**: 31-39.
78. Malenka RC , Nicoll RA. Long-term depression with a flash. *Nat Neurosci* 1998; **1**: 89-90.
79. Herdegen T, Skene P , Bahr M. The c-Jun transcription factor--bipotential mediator of neuronal death, survival and regeneration. *Trends Neurosci* 1997; **20**: 227-231.
80. Kang H, Welcher AA, Shelton D et al. Neurotrophins and time: different roles for TrkB signaling in hippocampal long-term potentiation. *Neuron* 1997; **19**: 653-664.

81. Huang YY, Li XC , Kandel ER. cAMP contributes to mossy fiber LTP by initiating both a covalently mediated early phase and macromolecular synthesis-dependent late phase. *Cell* 1994; **79**: 69-79.
82. Klein R, Nanduri V, Jing SA et al. The trkB tyrosine protein kinase is a receptor for brain-derived neurotrophic factor and neurotrophin-3. *Cell* 1991; **66**: 395-403.
83. Cowen T , Gavazzi I. Plasticity in adult and ageing sympathetic neurons. *Prog Neurobiology* 1997; **54**: 249-288.
84. Anderson DJ. Cell fate determination in the peripheral nervous system: the sympathoadrenal progenitor. *J Neurobiol* 1993; **24**: 185-198.
85. Andrews TJ, Thrasivoulou C, Nesbit W et al. Target-specific differences in the dendritic morphology and neuropeptide content of neurons in the rat SCG during development and aging. *J Comp Neurol* 1996; **368**: 33-44.
86. Sutula T, He XX, Cavazos J et al. Synaptic reorganization in the hippocampus induced by abnormal functional activity. *Science* 1988; **239**: 1147-1150.
87. Sutula T, Koch J, Golarai G et al. NMDA receptor dependence of kindling and mossy fiber sprouting: evidence that the NMDA receptor regulates patterning of hippocampal circuits in the adult brain. *J Neurosci* 1996; **16**: 7398-7406.
88. Araque A, Parpura V, Sanzgiri RP et al. Tripartite synapses: glia, the unacknowledged partner. *Trends Neurosci* 1999; **22**: 208-215.
89. Cornell-Bell AH, Finkbeiner SM, Cooper MS et al. Glutamate induces calcium waves in cultured astrocytes: long-range glial signaling. *Science* 1990; **247**: 470-473.
90. Ridet JL, Malhotra SK, Privat A et al. Reactive astrocytes: cellular and molecular cues to biological function. *Trends Neurosci* 1997; **20**: 570-577.
91. Unger JW. Glial reaction in aging and Alzheimer's disease. *Microsc Res Tech* 1998; **43**: 24-28.
92. Inestrosa NC , Alarcon R. Molecular interactions of acetylcholinesterase with senile plaques. *J Physiol Paris* 1998; **92**: 341-344.
93. Baumgartner S, Littleton JT, Broadie K et al. A Drosophila neurexin is required for septate junction and blood-nerve barrier formation and function. *Cell* 1996; **87**: 1059-1068.
94. Scheffler B, Horn M, Blumcke I et al. Marrow-mindedness: a perspective on neuropoiesis. *Trends Neurosci* 1999; **22**: 348-357.
95. Moore MA. "Turning brain into blood"--clinical applications of stem-cell research in neurobiology and hematology. *N Engl J Med* 1999; **341**: 605-607.
96. Fields S , Sternglanz R. The two-hybrid system: an assay for protein-protein interactions. *Trends Genet* 1994; **10**: 286-292.
97. Gossen M, Freundlieb S, Bender G et al. Transcriptional activation by tetracyclines in mammalian cells. *Science* 1995; **268**: 1766-1769.
98. Goffeau A. DNA technology: Molecular fish on chips. *Nature* 1997; **385**: 202-203.

Table 1. Experimental evidence for structural roles of AChE

	Species	Experimental approach	Affected structures	Demonstrated role	Ref.
1	Frog	Transiently transgenic embryos to human AChE variants/cell culture	Spinal neurons/ Myotomes	Neurite outgrowth/ NMJ development	4
2	Frog	Transiently transgenic embryos overexpressing human AChE-S	Myotomes	NMJ development	7
3	Frog	Transiently transgenic embryos overexpressing human AChE variants	Myotomes	NMJ development	9
4	Chick	Cholinesterase inhibitors/ cell culture	Tectal and retinal neurons	Neurite outgrowth	a
5	Chick	Cholinesterase inhibitors/ACh agonists, antagonists/AChE to substratum, medium/cell culture	Sympathetic neurons	Neurite outgrowth	a
6	Rat	Substratum/cell culture	DRG neurons	Neurite outgrowth	a
7	Rat	Substratum/cholinesterase inhibitors/cell culture	DRG neurons	Neurite outgrowth	a
8	Rat	Cholinesterase inhibitors/ organotypic slice culture	Substantia nigra and ventral tegmental neurons	Neurite outgrowth	a
9	Rat	Cholinesterase inhibitors/cAMP analog/ cell culture	DRG neurons	Neurite outgrowth	a
10	Rat	Transfected human AChE variants/ cell culture	C6 glioma cells	Neurite outgrowth	3
11	Rat	AChE monomers, tetramers to medium/organotypic slice culture	Substantia nigra and ventral tegmental neurons	Neurite outgrowth	a
12	Rat	Cholinesterase inhibitors/AChE to medium or substratum/cell culture	Spinal motoneurons	Neurite outgrowth	a
13	Rat	Transfection with antisense-AChE and cDNAs of AChE variants or neuroligin-1/ cell culture	Phaeochromocytoma PC12 cells	Neurite outgrowth	5
14	Mouse	Cholinesterase inhibitors/ transfected with AChE cDNA, antisense-AChE/AChE antiserum/cell culture	Neuroblastoma cells	Neurite outgrowth	2
15	Mouse	Stably transfected transgenic mice	Spinal neurons and	Adult NMJ	46

		overexpressing human AChE	NMJ	structure	
16	Mouse	Golgi staining in transgenics	parietal cortex	dendrite loss	45
17	Mouse	Immunocytochemical NFT200, HSP70 detection in transgenic mice overexpressing AChE-S	Cortical axons; hippocampal retraction balls	Accelerated neurodeterioration	b
18	Mouse	Immunocytochemical NFT200, HSP70 detection in transgenic mice overexpressing AChE-R	Cortical axons; hippocampal retraction balls	Attenuated neurodeterioration	b
19	Human	Aggregation of human β-amyloid peptides influence of mammalian AChE-S	in vitro study	Assembly of senile plaques	33

a Quoted in [1].

b Strenfeld M. et al., unpublished observations.

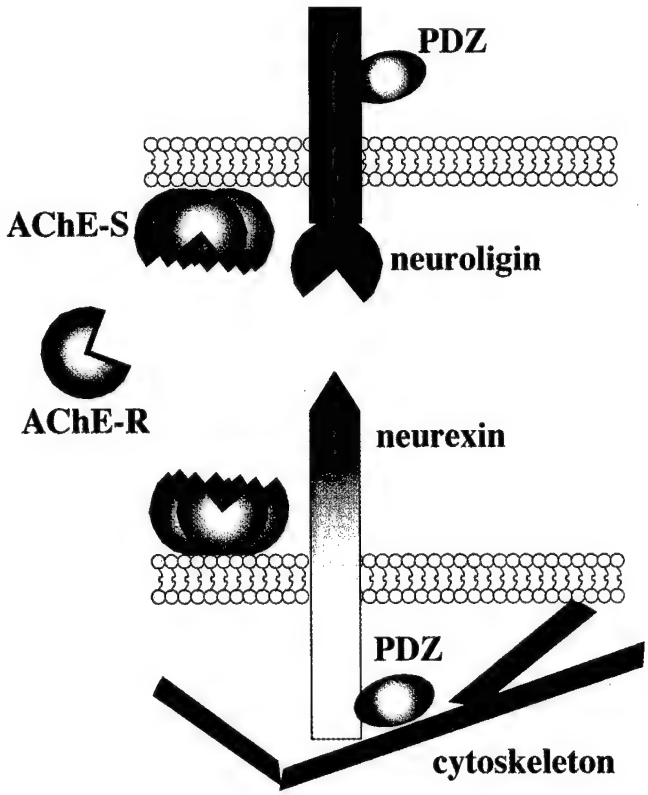

Fig. 1 The potential molecular basis for AChE's morphogenic capacity. Around growing or insulted neurites, AChE may replace or compete with the homologous neuroligins for binding to neurexins. Both neuroligins and neurexins are transmembrane proteins with a signaling capacity at their cytoplasmic domains, mediated by PDZ motifs, including Membrane-Associated Guanylate cyclase Kinase (MAGUK) homologs, which can form bridges between neurexins and neuroligins to band 4.1 cytoskeletal proteins. Therefore, AChE can affect intracellular events by changing the manner through which its structural homologs transduce their own signals into the corresponding cells. (Reproduced with permission from Grisaru et al., 1999 [1]).

Sunday, July 9, 2000

ARP, a peptide derived from the stress-associated acetylcholinesterase variant has hematopoietic growth promoting activities

Running title: A stress-induced hematopoietic growth factor

Dan Grisaru[1,2], Varda Deutsch[2], Michael Shapira[1], Marjory Pick[2], Meira Sternfeld[1], Naomi Melamed-Book[1], Daniela Kaufer[1], Nilly Galyam[1], Michael J. Gait[3], David Owen[3], Joseph B. Lessing[4], Amiram Eldor[2] and Hermona Soreq[1,5]

[1]Dept. of Biological Chemistry, Life Sciences Institute, Hebrew University of Jerusalem, Israel 91904

Depts. of [2]Hematology and [4]Obstetrics-Gynecology, Sourasky Medical Center, Sackler Faculty of Medicine, Tel Aviv University, Israel

[3] Medical Research Council, Laboratory of Molecular Biology, Hills Road, Cambridge CB2 2QH, U.K.

[5]To whom correspondence should be addressed (tel. 972-2-6585109, fax. 972-2-6520258, e-mail: soreq@shum.huji.ac.il)

Abstract

Background: Psychological stress induces rapid and long-lasting changes in blood cell composition implying the existence of stress-induced factors that modulate hematopoiesis. Here, we report the involvement of stress-associated readthrough acetylcholinesterase (AChE-R) in hematopoietic stress responses.

Materials and Methods: We have studied the effects of stress, cortisol, antisense oligonucleotides to AChE and a synthetic peptide derived from AChE-R upon peripheral blood cell composition and clonogenic progenitor status in various normal and AChE transgenic mice, and purified CD34+ cells of murine and human origin. We employed *in situ* hybridization and immunocytochemical staining to monitor changes in *ACHE* gene expression in hematopoietic progenitors. BrdU incorporation together with liquid cultures and clonogenic progenitor assays was performed to correlate AChE-R expression with stimulated proliferation and differentiation of myeloid and megakaryocyte lineages in vivo and ex vivo.

Results: We demonstrate a spatiotemporal correlation between expression of AChE-R and myeloidogenesis during ontogeny of the blood forming organs. Transgenic mice overexpressing AChE-R displayed up to 2-fold elevated white blood cell and platelet counts. In human CD34+ hematopoietic progenitor cells 0.6 μM cortisol elevated AChE-R mRNA150% above control levels and promoted hematopoietic expansion *ex vivo*. ARP, a synthetic peptide corresponding to the unique 26 C-terminal amino acids of AChE-R, was more effective than cortisol and equally as effective as stem cell factor in promoting expansion and differentiation of early hematopoietic progenitor cells into myeloid and megakaryocyte lineages, and in supporting hematon body formations.

Conclusions: Our findings attribute a role to AChE-R and a small AChE-R-derived peptide in hematopoietic homeostasis following stress and suggest the use of ARP in clinical settings where *ex vivo* expansion of progenitor cells is required.

Introduction

Stress insults are associated with rapid and significant changes in blood cell composition [1]. For example, following massive blood loss, or after surgery, the hematopoietic system responds within hours, by an elevation of the white blood cell (WBC) and platelet counts [2]. However, the molecular mechanisms regulating this adjustment are not yet fully understood. Glucocorticoid hormones play a leading role in the adaptive reaction of the bone marrow to stress [3] inducing absolute increases in all hematopoietic lineages, especially myeloid cells [4], and release of WBC to the periphery [5]. Glucocorticoids evoke cascades culminating in the proliferation, differentiation and apoptotic events characteristic of each of the hematopoietic cell lineages (for review see [6]). In addition, glucocorticoid hormones mediate changes in the levels of hematopoietic growth factors that control the proliferation of hematopoietic stem cells [7,8]

Hematopoietic stem cells are pluripotent in that they give rise to all blood cell lineages. During ontogeny, they migrate from the fetal liver to permanently reside in the bone-marrow where they provide a life-long, self-renewing source of blood cells [9]. Under normal conditions the vast majority of these stem cells are nondividing. However, under conditions of development or stress they can undergo clonal expansion and self-renewal[10]. A large number of early-acting cytokines and growth factors, such as stem cell factor (SCF), thrombopoietin (TPO) and FLT-3 ligand, are thought to mediate the proliferative capacity of hematopoietic stem cells, through specific receptors -- c-kit, c-mpl and flt3/flk-2, respectively [11-14]. Alone, their capacity to stimulate proliferation is limited. For example, SCF can maintain survival of stem cells for a few days *in vitro*, but not self-renewal [15]. In combination, however these growth factors acquire a potent co-stimulatory effect [16-18]. The early phase of adaptation of the hematopoietic system to stress (first 24 hr), requires coordinator(s), such as leu-enkephalin [19] which modulate the effects of growth factors on stem cells. However, leu-enkephalin is present in the circulation only immediately following the stress insult, whereas the modulation of hematopoiesis continues long after. Therefore, additional long-acting modulators remain to be identified.

An intriguing, previously unpredicted candidate for a role(s) in hematopoietic stress responses is the acetylcholine hydrolyzing enzyme, acetylcholinesterase (AChE). In addition to its well-known localization at sites of cholinergic neurotransmission, AChE is also expressed in multiple embryonic and tumor tissues [20,21], including those producing blood and bone cells [22,23], shown to share common progenitors [24]. In hematopoietic cells, AChE has been proposed to exert a growth regulatory role [25,26]. In humans, AChE gene expression was demonstrated in early 2N megakaryocytes and observed to decrease with cellular development and differentiation [22]. However, it was not possible until recently to assign hematopoietic activities to any specific AChE variant. In the brain, the readthrough AChE-R splicing variant was shown to be significantly and persistently overexpressed following acute trauma, and was implicated in stress-induced changes in neuronal structure and function [27,28]. Together, these observations suggested a possible role for AChE-R in hematopoietic stress responses.

Here, we demonstrate induction of AChE-R mRNA in human CD34+ hematopoietic progenitor cells by cortisol, and associate elevated AChE-R with enhanced hematopoietic activity in transgenic mice. We trace the *in vivo* hematopoietic activities of AChE-R to a small stress-

induced peptide apparently cleaved from the C-terminal of domain of the "readthrough" AChE variant. Furthermore, we demonstrate potent *in vivo* and *ex vivo* hematopoietic activities for ARP, a synthetic 26 amino acid peptide based on the unique AChE-R C-terminal sequence. Surprisingly, ARP was more effective than cortisol and equally as effective as stem cell factor in promoting expansion and differentiation of bone marrow cells into myeloid and megakaryocyte lineages. Our findings indicate that AChE-R participates in hematopoietic homeostasis following stress, and suggest the use of ARP to facilitate *ex vivo* expansion of hematopoietic stem cells.

Materials and Methods

Cell and tissue sources: Use of all human material in this study was approved by the ethics committee of the Tel Aviv Medical Center according to the regulations of the Helsinki accords. Fresh samples of umbilical cord blood cells were obtained following normal deliveries following informed consent of the mothers, as previously described [29]. Human embryos from terminated normal pregnancies were obtained from the Pathology Department of the Tel Aviv Medical Center.

Isolation and expansion of human umbilical cord blood hematopoietic progenitors. Cord blood was collected and $CD34^+$ cells separated by immune magnetic beads (Dyna, Oslo, Norway). cells were grown as detailed elsewhere in the presence of 10% autologous cord blood plasma, supplemented every 4 days with the noted agents [23,30,31]. Cell proliferation was evaluated by 5-bromo-2'-deoxyuridine (BrdU) incorporation, as previously described [23].Viable cells were counted by trypan blue dye exclusion. Cortisol sodium succinate (Abic Ltd., Netania, Israel) and antisense oligonucleotides were added for the noted periods.

In situ hybridization: *In situ* hybridization procedures, were performed on cultured cells and human fetal tissues, as detailed elsewhere [23,27].Cultured cells were spun down at 300g and fixed, using 4% paraformaldehyde, to collagen-coated cover slips placed on the bottom of the culture well. Tissues from hematopoietic fetal organs (aorta-gonad-mesonephric, liver, spleen and bone marrow) were obtained in each of the selected gestational stages, from 2-3 normal aborted human fetuses. The project was approved by the Sourasky Medical Center Ethics Committee, and written informed consent was obtained from the parents. 50-mer, 5'-biotinylated, fully 2'-O-methylated AChE cRNA probes complementary to 3'-alternative human ACHE exons were purchased from Microsynth GmbH (Switzerland). Detection and quantification of the various AChEmRNA transcripts in fetal tissues were performed as previously described . Confocal scans of the culture-derived cells were obtained using a MRC-1024 Bio-Rad confocal microscope. A projection was built from each cell and specific criteria was set for size and intensity of the Fast Red fluorescence. Image-Pro 3.0 software (Media Cybernetics, Silver Spring, MD, USA) was used to analyze the signal obtained.

Transgenic mice and biochemical AChE measurements are described elsewhere [32]. Confined swim stress was as detailed [27]. WBC and platelet counts were determined using an Ac. T diff coulter (Beckman Coulter. Inc. Fullerton, CA) in heparin- and EDTA- treated blood.

Bone marrow was collected from mouse femurs, and smears prepared and fixed with 4% paraformaldehyde (10 min., room temp.). Immuocytochemical staining was as detailed elsewhere [22] using the ABC Elite kit (Vector Labs, Burlingame, CA) and diaminobenzidine-hydrogen

peroxide (Sigma Chemical Co., 10 min) with Meyer's hematoxylin for counterstaining. *In situ* hybridization and confocal microscopy were as detailed elsewhere [33], as were DNA sequence analyses [34].

Human AChE C-terminal peptides: The peptides ASP and ARP were synthesized on a PerSeptive Biosystems Pioneer Synthesizer on 0.1mmol PEG-polystyrene resin using N-a-Fmoc protected amino acids with the following side-chain protection: Arg(Pbf), Asn(Trt), Asp(OtBu), Cys(Trt), Gln(Trt), Glu(OtBu), His(Trt), Lys(Boc), Ser(tBu), Thr(tBu), Trp(Boc), Tyr(OtBu). Couplings were for 30 minutes using a 4-fold excess of Fmoc-amino-acid in the presence of 0.98 equivalents of HATU and 1.96 equivalents of Hünig's base. Peptides were cleaved from the resins with 91:3:3:3 (v/v/v/w) TFA/EDT/Et3SiH/PhOH for 5 hours and products were purified by preparative reverse-phase HPLC on a Vydac 208TP1022 C8 200x20 mm column using gradients of acetonitrile in 0.1% aqueous TFA. Purified products were analyzed by a) amino-acid analysis on a Pharmacia-Biochrom 20 amino-acid analyser following hydrolysis in 6M HCl for 18 hours at 110° C and b) MALDI-TOF mass spectrometry on a PerSeptive Biosystems Voyager Mass Spectrometer using CHCA matrix to confirm the correct mass. The sequences employed were as follows:

ASP (1-DTLDEAERQWKAEFHRWSSYMVHWKNQFDHYSKQDRCSDL-40)

ARP (1-GMQGPAGSGWEEGSGSPPGVTPLFSP-26)

PBAN was as published (Raina et al., 1989)

Antisense oligonucleotides: To suppress AChE expression, a 20-mer antisense oligonucleotide, AS1 targeted to exon 2 of mammalian AChE mRNAs were used [23]. A 15-mer oligonucleotide targeted to butyrylcholinesterase (BChE) mRNA, previously shown to be inert with regard to AChE mRNA, served as control [28,35]. To protect against nuclease degradation, all oligonucleotides were end-capped at their three 3' terminal positions by 2'-O-methyl ribonucleotides.

Expansion of multipotent and committed human hematopoietic progenitor cells ex-vivo. CD34+ cells were expanded in liquid cultures in the presence of recombinant human cytokines and ARP and the phenotypic properties of the in vitro expanded cell populations were studied by three and four color flow cytometry. In addition, the number of lineage committed clonogenic progenitors was analyzed over time. Liquid cultures were initiated in 96 flat bottom microtiter plates (Nunc, Sweden) at a concentration of 104 cells /well in a volume of 200µl or in 24 well tissue culture plates at a concentration of 1- 2 x 105 cell/well in a volume of 1 mL and grown in Iscove's modified Dulbecco's medium - IMDM (Beit Haemek, Israel) supplemented with 10% autologous plasma. Single cytokines or their combinations were added immediately after seeding. Proliferating cells were demi-depleted and fresh cytokines were added every 4-7 days depending on the cell density in each culture. The cytokines employed included interleukin-3 (IL-3) 10ng/mL, interleukin 6 (IL-6) 50ng/mL, thrombopoietin (TPO) 10ng/mL , flt-3 ligand 10ng/mL, and stem cell factor (SCF) 10 ng/mL, and were all purchased from R&D systems (USA). Synthetic ARP was added to 2nM where noted. Cells were incubated for up to 28 days at 37^0C in 5% CO2 in fully humidified atmosphere. Viability was assessed by trypan blue dye exclusion.

Human clonogenic progenitors were cultured in the presence of various growth factors and colony forming progenitors were assessed at weekly intervals in secondary colony assays. CFU-GM and blast cell colonies were grown in IMDM containing 0.9% methylcellulose containing 10% fetal calf serum (FCS), IL-3 5ng/ml and GM-CSF 10ng/ml and counted after 12-14 days. CFU-MK were grown in plasma clots containing 15% AB plasma, TPO 10n/ml and SCF 10ng/ml and identified and counted by immunofluorescence after 12-14 days in culture as previously described (Deutsch et al 1998). The absolute number of CFU-GM, CFU-MK and CFU-blast colonies grown at each time point during the culture was calculated by multiplying their incidence (per cells seeded in colony assay) by the number of viable nucleated cells present in each liquid culture.

Murine clonogenic progenitors were cultured at 2 x 10^5 cells per 35 mm tissue culture dishes (Corning Glass Works, Corning, NY). Myeloid colonies were grown in supplemented Iscove's modified Dulbecco's medium (Beit Haemek, Israel) supplemented with 0.8% methylcellulose (Sigma, Chemical Co., St. Louis, Md), 10% fetal calf serum (FCS) (Beit Haemek, Israel) and 5 x 10^{-4} M β-mercaptoethanol (2-ME) (Sigma, Chemical Co.). Myeloid colony formation was stimulated with recombinant-mouse granulocyte-macrophage colony stimulating factor (r-m GM-CSF, 5 ng/ml), r-mSCF (10 ng/ml) and r-m interleukin 3 (IL3; 10 ng/ml), all from R & D Systems (Minneapolis, MN), in 5% CO_2 at 37°C, in a fully humidified atmosphere. Colonies were counted in triplicate cultures after 7 days. MK colonies were grown in supplemented McCoy's medium (Beit Haemek) supplemented with 0.3% agar (Difco, Detroit, MI), 10% FCS and 1 x 10^{-4} M 2-ME. Colony formation was stimulated with r-m thrombopoietin (2 ng/ml) and r-mSCF (10 ng/ml) (R & D Systems) in 5% CO_2 at 37°C in a fully humidified atmosphere. CFU-MK identified by specific cytochemical staining as described [22] were counted after 7 days.

Flow cytometric analysis of cultured CD34+ cord blood cells: To determine the type of cells that were expanded in the presence of the different cytokines three color flow cytometry was performed at weekly intervals. For FACS analysis of hematopoietic cells the following antibodies were employed; perCP conjugated anti-CD34, HPCA-2 (Becton-Dickinson, B-D, Immunocytochemistry Systems Inc, San Jose CA., USA), phycoerythrin (PE) conjugated - anti-CD38 (BD), PE anti-CD33 (BD), PE-anti-CD41 (BD)or FITC conjugated anti-CD41 (P2) (Immnunotech/Coulter, England), FITC conjugated anti-CD15 (BD). Multiparameter flow cytometry was performed using a FACScalibur (BD) and Cellquest software (BD) on a minimum of 10,000 events analyzed per sample. Non specific labeling was excluded using the appropriate isotype antibodies conjugated with the same fluorochrome (BD). The actual number of cells expanded of each lineage was calculated by multiplying their relative proportion by the number of viable cells in each culture.

Western blots: Serum proteins (40 µg) were separated on 4-20% polyacrylamide gels (Bio Rad Laboratories, Hercules, CA), blotted to nitrocellulose filters, incubated with rabbit anti -GST-ARP antibodies [32] and peroxidase-conjugated anti-rabbit immunoglobulins, and subjected to ECL™ detection (Amersham Pharmacia Biotech, UK).

Results

Readthrough AChE is overproduced in the myeloidogenic mid-gestation liver:

To study the relevance of AChE expression during development of the hematopoietic system, *in situ* hybridization was performed on paraffin-embedded sections of the aorta-gonad-mesonephric region (AGM), liver, spleen, and bone marrow taken from human fetuses at different gestational ages. Using probes specific for the "synaptic" AChE-S, "erythrocytic" AChE-E, and "readthrough" AChE-R mRNA splicing variants [36], we observed tissue-specific fluctuations in AChE mRNA levels that were consistent with known spatiotemporal shifts in hematopoietic activity among these blood-forming tissues (Figure 1). For example, AChE-E and AChE-S expression were both high in mid-gestation liver and spleen when the principal hematopoietic activity is erythropoiesis, but decreased steadily from the 9^{th}-16^{th} week, as hematopoiesis shifts to the bone marrow. In contrast, AChE-R mRNA was transiently expressed in fetal liver at 16 weeks gestation. This coincides with accelerated myelopoiesis in the liver at this stage [39] but not in the spleen. This unique expression pattern of AChE-R mRNA stimulated our interest in examining its apparent correlation with myeloidogenesis.

Congenital AChE-R overproduction modulates bone marrow expansion and blood cell composition:

To study the role of AChE-R in mammalian hematopoiesis, we studied transgenic mice overexpressing AChE-S or AChE-R [32,40]. In peripheral blood of AChE-R transgenic mice, we observed increases of 2.5- and 130-fold in catalytic AChE activities in 2 pedigrees (line 45 and line 70, respectively) (Figure 2). Platelets were significantly elevated in both lines. In contrast, WBCs were increased only in the highly overexpressing line 70. Transgenic mice expressing AChE-S variants displayed neither increased blood AChE activity nor significant deviations from normal blood cell composition. These observations indicated that AChE-R exerts specific, dose-dependent effects on hematopoietic homeostasis, particularly affecting megakaryocytopoiesis and myeloidogenesis.

To evaluate the status of multipotent hematopoietic progenitors in the bone marrow of transgenic mice, we performed clonogenic progenitor assays where primary bone marrow cells are plated under conditions supporting the growth of specific hematopoietic lineages. Following one week in culture, colonies were classified as granulocyte/erythrocyte/myeloid/macrophage (GEMM), granulocyte/macrophage (GM), megakaryocyte (MK) or adherent cell foci (Ad) colonies and counted. In this assay, each colony is taken to represent a single plated progenitor or colony forming unit (CFU). CFU-MK and CFU-GM were significantly elevated in bone marrow from AChE transgenic mice compared to controls ($p \leq 0.001$, Student's t test; Figure 2). Both early mixed CFU-GEMM colonies and CFU-Ad colonies resembling endothelial or stroma cells were also elevated in AChE transgenics, especially in line 70. However, these latter differences were much less pronounced in colonies grown from mice expressing catalytically inactive AChE-S (AChE-SIn). The facilitated capacity of bone marrow progenitors from these transgenic lines to proliferate and differentiate into myeloid, megakaryocyte and adherent colonies supports the notion that AChE-R plays a role in the proliferation of hematopoietic progenitors without compromising their ability to differentiate into the various hematopoietic lineages. The

clonogenic capacity of bone marrow cells from AChE-SIn mice was reduced compared to those from other transgenics, possibly suggesting that cholinergic activities may be involved.

Hematopoietic and stress-responsive elements in the extended ACHE gene promoter

In the mammalian nervous system, AChE-R is upregulated in response to acute cholinergic stimulation such as that accompanying traumatic stress [27], anticholinesterase intoxication [41], and closed head injury [28]. To explore the possibility that AChE-R operates as a stress-response element in the hematopoietic system as well, we searched the extended promoter of the human *ACHE* gene (cosmid accession no. AF002993) for consensus motifs encoding cis-acting binding sites for stress-associated and hematopoietic transcription factors. Two such clusters, one a functional promoter domain located 17 Kb upstream from the transcription start site [34] and another positioned within the first intron, were found to include glucocorticoid responsive element (GRE) half-palindromic sites TGTTCT, as well as motifs for AP1, NFκB, EGR-1 (as identified by a matrix search against the TransFac database), HNF3β, with the consensus sequence TGTTGT, and Stat-5, TTCCCAGAA or TT(C/A)(C/T)N(A/G)(G/T)AA (Figure3A). Of these, GRE, HNF3, and Stat-5 are known to be actively involved in hematopoiesis [42,43] and cellular stress responses [44,45]. GRE and Stat-5 act synergistically to enhance β-casein gene expression in mammary tissue [46], but have not yet been studied in the context of AChE involvement in hematopoiesis.

Cortisol elevates *ACHE* gene expression in hematopoietic progenitors:

The functional effects of glucocorticoids on hematopoietic *ACHE* expression were investigated in early human progenitors enriched from umbilical cord blood using immune magnetic beads for CD34 to yield a 85 ± 3% pure population of $CD34^+$ cells, as confirmed by flow cytometry (Figure 3B). CD34+ cells were cultured for 24 hr with increasing doses of cortisol and subjected to *in situ* hybridization, confocal microscopy, and semi-quantitative image analysis. This approach provided an accurate and credible tool for the quantification of transcriptional responses in the heterogeneous population of primary $CD34^+$ cells pooled from different individuals. Figure 3C presents representative images of cells analyzed for AChE-S and AChE-R transcripts, and the quantified changes in these transcripts under treatment with different cortisol concentrations. A subtle elevation of cortisol concentration from a basal level of 0.1 μM [47] to 0.6 μM induced a selective 130 ± 30% increase in the area labeled by the AChE-R mRNA probe. In contrast, 1.2 μM stress-associated cortisol concentrations increased the areas labeled by both AChE mRNA transcripts. Cytochemical staining revealed the presence of active enzyme only under the highest cortisol concentrations at which the membrane associated enzyme forms AChE-E and AChE–R were expressed (Figure 3C. top panel and data not shown). This observation is consistent with the secretory nature of AChE-R. Together, these observations demonstrated cortisol-inducible expression of AChE-R in hematopoietic progenitors (Figure 3D), and suggested that stress-promoted modulation of ACHE gene expression and alternative splicing may play an active role in mediating hematopoietic stress responses.

A bioactive peptide derived from AChE-R evokes potent hematopoietic effects

To determine whether AChE-R is present in the blood and whether its level is regulated by stress, we employed antibodies raised against a recombinant fusion protein of glutathione transferase (GST) and ARP, the C-terminal domain unique to AChE-R. Anti GST-ARP antiserum specifically detected AChE-R, but not AChE-S in Western blots (Figure 4A). We therefore subjected FVB/N mice to confined swim stress, collected blood 24 hr later, and performed denaturing gel electrophoresis on serum proteins. Immunodetection with anti-GST-ARP antibodies failed to detect major changes in circulating levels of AChE-R following stress. However, the GST-ARP antibody reacted with a novel short immunoreactive peptide with an apparent molecular weight of approximately 5.0 Kd in serum of stressed mice. The appearance of a short, ARP-related peptide comigrating with synthetic ARP following forced swim suggested that cleavage of AChE-R generates a peptide with a role in hematopoietic stress responses.

To explore the idea that ARP promotes stress-induced hematopoiesis, we employed synthetic ARP peptide. Mice subjected to confined swim stress were injected intravenously with 100 μg/Kg ARP or 30 ng/Kg AS1, an antisense oligonucleotide preferentially suppressing AChE-R [23]. Twenty-four hrs later, bone marrow smears were immunostained with anti-GST-ARP antibodies and peripheral WBC counts performed. In non-stressed mice, ARP did not significantly change bone-marrow labeling or WBC counts. In stressed mice, however, ARP both elevated the number of ARP-positive cells and intensified the immunolabeling in small bone marrow cells with morphological features of stem cells (Figure 4B). AS1 reduced the number of cells labeled with anti-ARP antibodies, indicating that injected ARP amplified endogenous ARP production under stress. Consistent with this hypothesis, AS1 also suppressed WBC counts, suggesting that induced AChE-R and/or cleaved ARP participate in the characteristic stress-related release of WBC from the bone marrow to the periphery.

To examine longer-lasting influences of ARP on stress-induced modulation of hematopoiesis, we performed clonogenic progenitor assays on bone marrow cells collected from mice 24 hrs after stress, with or without ARP or AS1 treatment. Significant increases were noted in CFU-GEMM and CFU-MK from all stressed, as compared with non-stressed, animals (Figure 4C). ARP potentiated stress effects with regard to CFU-MK, and exerted profound effects on both CFU-MK and CFU-GEMM when administered to non-stressed animals (Figure 4C). In contrast, no significant changes were found in the more differentiated granulocyte macrophage CFU-GM progenitors 7 days after plating (data not shown). Together with the bone marrow immunolabeling, these data indicate a dual role for ARP in the expansion of both megakaryocyte and myeloid progenitors.

ARP promotes *ex vivo* progenitor cell proliferation under antisense suppression of AChE-R mRNA

To selectively suppress AChE-R mRNA in hematopoietic cells, we employed very low concentrations of AS1. At picomolar concentrations, AS1 demonstrated highly discriminative preference for AChE-R versus AChE-S mRNA (Figure 5A). At this concentration, an irrelevant oligonucleotide targeted to BChE mRNA (ASB) exerted a very limited effect on AChE mRNA and activity levels ([23]) and data not shown). The antisense strategy allowed us to demonstrate a

specific role for this variant of AChE and/or its peptide derivative ARP in hematopoietic processes. To identify the mechanism(s) accounting for the hematopoietic expansion promoted by ARP, DNA synthesis was studied by following the incorporation of bromodeoxyuracil (BrdU) into CD34+ cells to monitor stem cell proliferation in short-term cultures. Addition of 50 ng/ml (approx. 2nM) ARP together with GM-CSF induced a linear increase in BrdU incorporation from 16 to 36 hrs compared to GM-SCF alone (Figure 5B and data not shown). No such effect on proliferation was observed when synthetic AChE-S C-terminal peptide, ASP, was substituted for ARP (data not shown). BrdU incorporation was partially suppressed by 20 pM AS1, but antisense suppression was completely overridden by ARP (Figure 5B). The observation that antisense blockade of mRNA encoding full-length AChE-R failed to inhibit the proliferative effects of ARP reinforced the notion that ARP peptide is sufficient, in the absence of intact AChE-R to promote expansion of CD34+ hematopoietic progenitor cells.

ARP potentiates myelopoiesis and megakaryocytopoiesis *ex vivo*:

To further demonstrate the hematopoietic potency of ARP, we studied $CD34^+$ progenitor cell development over 2 weeks in liquid culture in the presence of synthetic ARP, cortisol or stem cell factor (SCF). ASP, PBAN (an irrelevant insect peptide of similar size [48]), or AS1 served as controls. Early and late myeloid and megakaryocyte (MK) progenitor cells were labeled with fluorescent monoclonal antibodies detecting commitment- and maturation-specific cell surface markers, and flow cytometry revealed the distinct cell populations generated under the different growth conditions. *Ex vivo*, micromolar cortisol concentrations exerted significant enhancement of both myeloid and megakaryocyte progenitor populations (Table I and figure 6). Thus, cells positive for early and mature myeloid cell markers (Figure 6, top row) as well as proliferating megakaryocyte progenitors positive for both CD34 and CD41 (Figure 6, bottom row) increased in numbers in the analyzed cell populations. At 1000-fold lower concentrations, ARP proved to be an even more powerful stimulator of $CD34^+$ cell expansion than either cortisol or SCF. The antigenic profiles and the relative proportions of the distinct progenitor populations that emerged with ARP or cortisol appeared similar, indicating a common pathway through which ARP or cortisol stimulate hematopoiesis. In contrast, ASP and PBAN had few or none of these effects. SCF, as expected, potentiated expansion of both MK and myeloid progenitors [30]. However, far fewer early CD34+ progenitors were detected. In contrast, AS1 suppressed myelopoiesis and proliferating megakaryocyte progenitors (Table I). These findings further supported the notion that ARP or an ARP-related peptide derived from AChE-R exerts potent, physiologically relevant effects on mammalian hematopoiesis. Furthermore, they lent credence to the idea that ARP may be applied to therapeutic protocols involving *ex vivo* expansion of hematopoietic stem cells.

ARP can substitute for SCF *ex vivo*:

To determine whether ARP could replace any of the known growth factors in a longer *ex vivo* context, we tested ARP alone or combined with known growth factors, on 4 week $CD34^+$ cell cultures. To enable long-term expansion of early progenitors, a cocktail of early-acting cytokines ("GFC": IL3, IL6, TPO and FLT3) was used. These conditions supported expansion of $CD34^+$ cells for up to 28 days in liquid culture (Figure 7A). In the absence of cytokines, however, there was no cell proliferation and the number of viable cells progressively declined. SCF, devoid

of proliferative activity alone, enhanced the proliferation induced by early-acting cytokines. ARP supported proliferation similar to that achieved with SCF. Moreover, the proliferative effects of SCF and ARP together led to a greater than 10-100-fold expansion of viable cells within 28 days (Figure 7A). These data demonstrated that the activity of ARP is additive to those of both the early-acting cytokines and that it could replace SCF in supporting progenitor cell proliferation. To evaluate the capacity of progenitors expanded under the various liquid culture conditions to differentiate into different hematopoietic lineages, we sampled the cultures weekly and performed clonogenic assays in the presence of specific growth factors. In the presence of GFC, both ARP and SCF exerted a minimal 2-3 fold elevation in the formation of colonies containing undifferentiated blast cells (CFU-blast) (Figure 7B). Together, ARP and SCF displayed a potent, synergistic enhancement in CFU-blast formed from cells seeded after 14 days in liquid culture. ARP demonstrated an equal or superior potency in promoting CFU-GM and CFU–MK compared to SCF (Figures 7C,D) and no synergistic effects between ARP and SCF were observed under these conditions. In $CD34^+$ liquid cultures grown without growth factors for 28 days, cells displayed a typical fibroblast morphology (Figure 7E). In contrast, a dense population of small round cells with characteristic stem cell morphology was observed in cultures supplemented with early-acting cytokines and SCF (Figure 7F). This stem cell morphology was also observed when ARP was either combined with or substituted for SCF in the cultures (Figures 7G,H). Notably, floating "hematons", which are independent hematopoietic units rich in myeloid, erythroid, and megakaryocyte progenitors [49] were observed only in ARP-containing cultures (Figure 7G,H insets). The presence of hematons in the cultures further reinforces the differentiation-promoting potential of this peptide.

Discussion

ARP potentiates cortisol effects:

We found that ARP, like cortisol, accumulates in the serum following acute stress and facilitates the cytokine-induced proliferation of human $CD34^+$ hematopoietic progenitors along the myeloid and MK lineages. ARP accumulation may involve stress-induced transcriptional activation [50] modulation of alternative splicing [51,52], changes in the lifespan of AChE-R mRNA [53], enhanced proteolytic activity [54], or a combination of all these processes. Our current findings demonstrate that the cortisol-induced accumulation of ARP can potentiate and extend its hematopoietic effects long after cortisol itself ceases to be produced, as will be required from long-lasting modulators of blood cell composition. Likewise, the effects of ARP on adherent cell foci suggest its involvement in the proliferation and differentiation of stroma and/or endothelial cells, both of which influence cytokine production and hematopoietic homeostasis through a cross-talk with $CD34^+$ progenitors [55,56].

ARP joins a family of hematopoietically active short peptides.

In X-ray crystallography models of *Torpedo* AChE, the C-terminus was unresolved [57]. C-terminal sequencing of highly purified fetal bovine serum AChE-S (B.P. Doctor, personal communication) demonstrated cleavage at, or near, the splice site. Together, these findings indicate a loose structure that may be susceptible to cellular proteases, and a flexibility that may enable binding to other proteins. The apparent natural cleavage of AChE-R and AChE-S invites a

search for morphogenic effects attributable to ARP, ASP, or related peptides. Studies are under way to determine the exact cleavage site giving rise to circulating ARP-related peptide and to identify the protease responsible for this activity.

ARP does not display homology to any known hematopoietic growth factor. Nevertheless, other short peptides were shown to exert growth-factor-like activities. Several synthetic hematopoietically active short peptides are known, some of which are homologous to natural peptides or protein domains (e.g. the CC' surface loop of CD4 [58]). Others share biological function, but not sequence, with natural larger proteins. For example, a synthetic 20-residue cyclic peptide [59] and its 13-residue derivative [60] mimic the interaction of the 166-residue hematopoietic growth hormone, erythropoietin (EPO). Similarly, a 14-a.a. peptide was discovered which is equipotent to the 332 amino acid cytokine TPO [61]. ARP displayed an independent survival effect on hematopoietic progenitors equipotent to that of SCF. ARP was further found to promote megakaryocytopoiesis and myelopoiesis and to potentiate the hematopoietic effects of early-acting cytokines and SCF *ex vivo*. Further studies will be required to define the ARP domains which are necessary and sufficient for these growth-related activities.

SCF-ARP similarities predict mutual receptors.

ARP replaced SCF in long-term cultures, and supported the formation of floating "hematons", indicating the preserved pluripotential nature of the $CD34^+$ cells. Thus, ARP may be useful in conjunction with early-acting cytokines for the *ex vivo* expansion of hematopoietic cells, which may be beneficial in bone marrow transplantation [62]. The antisense inhibition of $CD34^+$ proliferation by selective disabling of AChE-R mRNA suggests that SCF requires AChE-R to drive cell proliferation. The molecular basis for the selective action of low concentrations of antisense oligonucleotides on AChE-R mRNA is likely attributable to intrinsic differences in the stability of this splicing variant (as suggested by its long, G,C-rich 3' untranslated region), and feedback regulation of the gene under antisense suppression (Galyam et al., manuscript in preparation). In any case, the complete rescue achieved with ARP proved that the short ARP and not the entire AChE-R protein is sufficient to support the proliferative effect of SCF. Several cytokine receptors (e.g. GM-CSF) mediate signals through cascades involving Janus and Src-related tyrosine kinases [63]. Such kinases activate and phosphorylate tyrosine residues in their intracellular target proteins, including signal transducers and transcription factors (e.g. stat) [42]. Therefore, ARP-induced potentiation of early-acting cytokine activities, in conjugation with the presence of a Stat-5 binding site in the *ACHE* promoter, suggests that ARP may autoregulate its own levels. This, or similar mechanism(s), may explain both the prolonged effect of ARP on cultured CD34+ progenitors, its accumulation in the blood of stressed mice, and its pronounced *in vivo* effect on AChE mRNA levels in bone marrow stem cells. The high sensitivity of AChE-R mRNA to low levels of AS1 may be due to its 1,094 bp 3'-untranslated region (UTR), with 62% G,C content. This marks it as being more vulnerable to nucleolytic degradation (Jacobson and Peltz, 1996) than AChE-S mRNA, which includes a considerably shorter, 219 bp, UTR with 66% G,C.

ARP potentiates *in vivo* hematopoietic stress responses .

The *in vivo* accumulation of ARP following forced swim raises the possibility that the reported increased risk for brain infarcts following acute stress, exposure to anticholinesterases [64,65] and Alzheimer's disease [66,67] is associated with increased platelet counts due to AChE-R overproduction. Similarly, the increased risk for leukemias in farmers exposed to agricultural insecticides [68] may be related to AChE-R/ARP overproduction under chronic or repeated cholinesterase blockade. Anti-ARP antibodies provide a novel diagnostic tool for testing this option (and possibly for risk assessment) and antisense treatment may offer an attractive protocol for prevention of such adverse responses.

The mechanism(s) of ARP action on hematopoietic progenitors is unknown. However, there is evidence for cross-talk between hematopoietic cells at different stages of differentiation and bone-marrow stromal or endothelial cells. Stroma influences cytokine production and is responsible for maintaining steady-state hematopoiesis and its adjustment under stress [55]. It has been proposed that primitive $CD34^+$ progenitors provide a soluble positive feedback signal to induce cytokine production [56] and it is therefore tempting to speculate that ARP may play such a role. If so, the discovery of ARP would carry important implications for *ex vivo* stem cell expansion, cancer treatment, and gene therapy. Experiments to determine the cellular and molecular sites of action of ARP are currently underway.

AChE-R/ARP as ubiquitous growth-promoting factors

The stem cell survival and proliferative effects of ARP denote a previously unforeseen activity that is particular to the AChE-R protein yet distinct from the ACh hydrolysis and adhesion properties characteristic of the core domain common to all AChE isoforms. Thus, the significance of ARP may extend beyond the hematopoietic system. For example, the multi-organ expression AChE-R predicts roles for ARP during embryogenesis and may explain at least some of the elusive developmental function(s) of AChE. In the mammalian brain, ARP may affect the stress-associated plasticity of neuronal and glial properties, perhaps explaining the morphogenic activities of AChE-R in transfected glia [69]. In the realm of applied biotechnology, it is important to note the significant recent advances in stem cell biology. For example, pluripotent stem cells can now be derived *in vitro* from cultured human primordial germ cells [70,71]. Moreover, neural stem cells were shown to produce a variety of blood cell types *in vivo* [72]. Our current findings present ARP as a potential cue that may be involved in the induction of such growth and expansion capacities of pluripotent stem cells from multi-tissue origins. If so, the unique properties of this peptide can contribute toward the development of diverse human differentiating cell sources for biomedical and research purposes.

Acknowledgements: The authors are grateful to Dr. Haim Gilon (Jerusalem) for early peptide synthesis, to Drs. David Glick and Shlomo Seidman (Jerusalem) and to Dr. Roger Kornberg (Palo Alto) for reviewing this manuscript, and to Ms. Shoshana Baron for her assistance. Support was by the Israel Science Fund and the U.S.-Israel Binational Science Foundation (to H.S.) and the B. Adler Fund, the Israel Ministry of Health (to V.D.). D.G. was the incumbent of a research fellowship from the Tel-Aviv Sourasky Medical Center and of a Meirbaum Award, from Tel-Aviv University.

Table I. The effect of various conditions on cultured cell counts[a]

Treatment	total viable cells	$CD34^+$ (early progenitors)	$CD33^+$ (early myeloids)	$CD33^+$ and $CD15^+$ (total myeloids)	$CD41^+$ (megakaryocytes)
control	61.0	1.0	7.2	12.3	30.9
ARP, 2 nM	570.0	87.2	329.0	530.0	42.3[b]
cortisol, 1.2 μM	80.0	13.0	45.0	73.0	10.1[b]
ASP, 2 nM	100.0	7.2	10.0	13.0	4.6[b]
SCF, 50 ng/ml	118.0	6.3	69.0	72.0	2.6[b]
AS1, 20 pM	81.2	1.4	2.4	5.0	30.9
PBAN, 2 nM	105.0	1.7	1.6	3.1	52.9

[a]Cultures were seeded at 50,000 cells/well. Shown are cells per culture x 10^{-3} on day 14; 1 of 3 reproducible experiments

[b]These are also $CD34^+$ positive early cells with expansion potential.

Legends to Figures

Figure. 1. Spatiotemporal shifts in the level of embryonic AChEmRNA transcripts in blood cell forming tissues during embryogenesis.

Top left: A sagittal section of a human embryo showing the hematopoietic organs - AGM (aorta-gonad-mesonephros), LIV (liver), SPL (spleen), and BM (bone marrow). Top right: Scheme of gestational shifts in hematopoietic processes shows the relative intensity of blood cell formation in the various hematopoietic organs throughout human gestation. (according to [37,38]). Ages of embryos on which in situ hybridization was performed are marked by grey columns. Lower panels: ACHE gene expression: Shown are representative *in situ* hybridization micrographs from the tissues of human fetuses at the noted gestational ages, using probes selective for each of the alternative human AChEmRNA transcripts. Lower right: spatiotemporal changes in labeling intensity for each probe and organ. Note that AChEmRNA expression increases in parallel to active hematopoiesis in the examined organs.

Fig. 2 Potentiated hematopoiesis in ACHE-transgenic mice

A. **Congenital and persistent AChE-R overproduction increases platelet and WBC counts in a dose-dependent manner**. Shown are intra-cardiac blood AChE levels, platelet and WBC counts determined in FVB/N mice (control, n=22) as compared to transgenic FVB/N mice carrying the AChE-S (TG-S, n=12), AChE-R (TG-R70 and TG-R45, n=9 and 6, respectively) or inactivated AChE-S (AChE-SIn, n=3) transgenes. Results are expressed as average ± SEM. Note that increases of 2.5 and 130-fold catalytic AChE activities in TG-R45 and TG-R70, respectively, conferred AChE platelet increases in both these pedigrees, but that WBC counts only increased in TG-R70.

B. **Enhanced clonogenic activities** following 1 week in culture are pronounced for AChE-R (line 70) transgenics, less prominent for AChE-S and negligible for AChE-Sin mice. Shown are fold-increases over the following control values: serum activity, 7.49 nmol substrate hydrolyzed/min/mg protein; 4.77 x 105 platelets/μl; 6.65 x 103 WBCs/μl; 9.02 GEMM colonies; 58.8 GM colonies; 18.87 MK colonies; and 12.72 adherent cell foci. Sample sizes were control, n=22; AChE-S, =12; AChE-R, =9; and AChE-Sin, =3. Asterisks denote statistically significant difference from the control ($p<0.01$, Student's t test), for which experimental groups the standard deviations ranged up to 22% (AChE activity, platelets) of the average.

Fig. 3. Cortisol up-regulates AChE-R expression in human CD34+ cells:

A. **The upstream human ACHE sequence** includes clusters of hematopoietic and stress-related motifs. Depicted is the reverse sequence of the cosmid insert (accession no. AF002993) of the human *ACHE* promoter. The arrow represents the position of a transcription start site. Two potentially relevant regions are shown, one beginning at nucleotide 5267 and one following the first exon (black box). Fully conserved consensus sequences are marked by triangles, and the scale in base pairs (bp) is shown below. Note the presence of a glucocorticoid response element (GRE) half site and two functionally interdependent sites for binding of hepatic nuclear factor (HNF_3) (based on [34]

B. **Enrichment of umbilical cord blood (UCB) CD34+ cells**: CD34+ cells were enriched from human umbilical cord blood cells using bead-attached antibodies to the CD34 protein. Shown is a representative flow cytometry of the recovered cells, demonstrating that 89% express the CD34 antigen. Inset: Example photograph of enriched CD34+ cells stained by May-Grünwald-Giemsa. Note the large nuclei surrounded by thin rims of cytoplasm, characteristic of stem cells.

C,D. **Cortisol stimulates expression of AChE mRNA splicing variants**: Shown are CD34+ cells treated with the noted concentrations of cortisol equivalent to physiologically normal (0.1 μM), mild stress (0.6 μM) and acute stress conditions (1.2 μM). **C.** Presented are cytochemically stained cells (top) and pseudocolor representations of 3-dimensional projections created from confocal scanned images of CD34+ cells following *in situ* hybridization with the noted 5'-biotinylated 2'O-methyl cRNA probes selective for the "synaptic"AChE-S and "readthrough" AChE-R mRNA variants. Note increasing red cytoplasmic labeling under high cortisol levels. Each photograph represents one of 10-20 analyzed cells with deviations in labeling of less than 6%. **D.** Shown are the results of semi-quantitative image analysis of in situ hybridization for each AChE mRNA transcript under stress-relevant concentrations. Note that only AChE-R mRNA accumulated under moderate cortisol concentrations. Asterisks denote statistical significance ($p < 0.05$, ANOVA).

Fig. 4. ARP has short and long term hematological effects *in vivo*

A. **ARP accumulates in the serum under stress.** Top: Shown are Ponceau-stained lanes of gradient polyacrylamide gels (4-20%, Bio-Rad) loaded with: (1) protein extract from COS cells transfected with AChE-R encoding plasmid and mixed with synthetic ARP; (2) recombinant human AChE-S (Sigma) mixed with synthetic ASP; (3) 2 μl serum from a mouse injected with saline or (4) a mouse subjected to confined-swim stress 24 hr post-treatment. Positions of molecular weight markers are shown on the left. Bottom: The above shown gel was electroblotted and probed with affinity-purified rabbit antibodies elicited toward a recombinant GST-ARP fusion protein. Note labeling in the serum of a 67 KDa protein, consistent with the expected size of AChE-R; also note selective labeling of synthetic ARP (but not AChE-S or ASP) by this antibody and the appearance of a novel immunoreactive band of approx. 5 Kd in serum of the stressed mouse.

B. ARP facilitates stress-induced hematopoietic responses i*n vivo*. Top panel: Shown are bone marrow smears immunostained with anti-GST-ARP antibodies. Note that AS1 reduced and ARP intensified Immunolabeling (brown precipitates) and increased the number of small ARP-positive cells in stressed mice. Middle panel: Number of ARP-immunopositive cells in bone marrow from the noted groups of FVB/N mice; Graph represents an average of 5 different fields counted at x1000 magnification for bone marrow. Bottom panel: Peripheral white blood cell counts; Note that both bone marrow immunostaining and white cell counts revealed ARP-dependent elevations and AS1 suppression. N=12 mice per ARP and AS1 treated stress groups. Control, non-stressed FVB/N mice were injected intraperitoneally with normal saline (n=6) or ARP (n=4).

C. 1 week clonogenic cultures. Bone marrow cells from the noted groups of mice were subjected to clonogenic progenitor assays as described in methods. Top: myeloid CFU-GEMM; bottom: CFU-MK. Asterisks denote statistical significance ($p< 0.05$, ANOVA). Increased numbers of CFU reflects increased numbers of viable progenitors able to give rise to each of the assayed cell lineages.

Fig. 5. ARP facilitates, and AS1 suppresses proliferation of $CD34^+$ progenitors.

A. Low concentrations of AS1 selectively suppress AChE-R in human $CD34^+$ progenitors: Human $CD34^+$ cells were incubated for 24 hr with the noted concentrations of AS1, an antisense oligodeoxynucleotide targeted to exon 2 in AChE mRNA. Shown are confocal images taken following *in situ* hybridization with cRNA probes for the noted transcripts. Graph shows an inverted, sequence-specific, dose-dependent suppression of AChE-R mRNA in $CD34^+$ cells by AS1. Shown are average fluorescent signals ± S.D. measured in confocal projections (20 cells per group) of $CD34^+$ cells treated with AS1 and subjected to *in situ* hybridization with AChE-S and -R specific probes. Asterisks note statistically significant differences from control ($p<0.001$), Student's t test).

B. ARP enhances cell proliferation. Cell proliferation was evaluated by measuring BrdU incorporation following 16 hr incubation in the presence of GM-CSF with or without 50 ng/ml ARP and 20 pM of AS1. Presented are average results of 3-6 reproducible experiments ± SEM. Note that ARP enhances GM-CSF-supported increases in cell proliferation, that AS1 attenuates this enhancement and that ARP overrides antisense-suppressed proliferation.

Fig. 6. Cortisol and ARP support myeloidogenic and megakaryocytic expansion *ex vivo*.

Flow cytometric analysis of CD34+ derived hematopoietic cells was performed after two weeks in liquid culture. Each analysis included 10,000 events and regions were set according to the appropriate isotype controls to exclude non specific labeling (first column). The percentage of myeloid (top row) and megakaryocytic (bottom row) cells that developed in the presence of each growth supplement is indicated by numbers on the relevant dot plots. Unlabeled cells appear as black dots, double labeled, as blue dots.

Fig. 7. Potent activity of ARP on progenitor cell expansion and differentiation.

A. Effects on cultured cell viability and proliferation in liquid cultures. Human CD34+ cells were cultured (10^5 cells/ml) in 24-well tissue culture plates and grown in IMDM containing 10% autologous plasma and early-acting cytokines: interleukin-3 (IL-3, 5 ng), interleukin-6 (IL-6, 50 ng), thrombopoietin (TPO, 10 ng), flt-3 ligand (flt-3, 10 ng), to which stem cell factor (SCF, 10 ng) and/or the synthetic AChE-R peptide (ARP, 2 nM) were added. Proliferating cells were demi-depleted and fresh cytokines added every 4 to 7 days, depending on the cell density in each culture. The viability of cells was assessed by trypan blue exclusion. Note that ARP can replace SCF in indücing hematopoietic cell proliferation and that ARP+SCF exert synergistic effects under prolong culture conditions. Average ± S.D. of 4 experiments.

B-D. Progenitor cell assays. The presence of CFU progenitors was assessed at weekly intervals in secondary colony assays. CD34+ progenitors were grown in primary liquid cultures as in Figure 7A for the noted time and plated. Colonies were counted after 12 to 14 days. All cultures contained a combination of growth factors (GFC: IL-3, IL-6, TPO and flt3) to which were added ARP and/or SCF, as noted. containing 10% fetal calf serum, IL-3 (5 mg/ml) and GM-CSF (10 ng/ml). CFU-MK (megakaryocytes) were grown in plasma clots containing 15% AB plasma, TPO (10 ng/ml) and SCF (10 ng/ml). The absolute number of CFU-GM, CFU-MK and CFU-blast grown at each time point during the culture was calculated by multiplying their incidence (per cells seeded) by the number of living nucleated cells present in each liquid culture. Note that ARP can replace SCF in proliferating progenitors for MK and GM, but not blast colonies. Nevertheless, ARP and SCF together exert synergistic effects on CFU-blast. Data are averages of 4 experiments ± SEM.

E.-H. **ARP facilitates development of hematon bodies**. Shown are representative photographs of the 28-day liquid cultures detailed in Fig. 7A: In the absence of stem cell growth factor, and in the presence of GFC, sparse hematopoietic cells and many fibroblasts are seen. (E), either ARP or SCF increases the density of small, round hematopoietic stem cells and sparse MKs (white arrows). GFC + ARP facilitate the formation of hematon bodies (insets) without (H) or with SCF (G).

References

1. Jern, C., Manhem, K., Eriksson, E. *et al.* Hemostatic responses to mental stress during the menstrual cycle. *Thromb Haemost* **66**, 614-618 (1991).

2. Sutor, A. H. Thrombocytosis in childhood. *Semin Thromb Hemost* **21**, 330-339 (1995).

3. McEwen, B. S. Protective and damaging effects of stress mediators. *N Engl J Med* **338**, 171-179 (1998).

4. Dygai, A. M., Shakhov, V. P., Mikhlenko, A. V. & Goldberg, E. D. Role of glucocorticoids in the regulation of bone marrow hemopoiesis in stress reaction. *Biomed Pharmacother* **45**, 9-14 (1991).

5. Maruyama, S., Minagawa, M., Shimizu, T. *et al.* Administration of glucocorticoids markedly increases the numbers of granulocytes and extrathymic T cells in the bone marrow. *Cell Immunol* **194**, 28-35 (1999).

6. Lansdorp, P. M. Telomere length and proliferation potential of hematopoietic stem cells. *J Cell Sci* **108**, 1-6 (1995).

7. Burdach, S. The granulocyte/macrophage-colony stimulating factor (GM-CSF): basic science and clinical application. *Klin Padiatr* **203**, 302-310 (1991).

8. Lord, K. A., Abdollahi, A., Hoffman-Liebermann, B. & Liebermann, D. A. Proto-oncogenes of the fos/jun family of transcription factors are positive regulators of myeloid differentiation. *Mol Cell Biol* **13**, 841-851 (1993).

9. Dieterlen-Lievre, F., Godin, I. & Pardanaud, L. Where do hematopoietic stem cells come from? *Int Arch Allergy Immunol* **112**, 3-8 (1997).

10. Keller, G. & Snodgrass, R. Life span of multipotential hematopoietic stem cells in vivo. *J Exp Med* **171**, 1407-1418 (1990).

11. Kaushansky, K. Thrombopoietin and the hematopoietic stem cell. *Blood* **92**, 1-3 (1998).

12. Metcalf, D. The cellular basis for enhancement interactions between stem cell factor and the colony stimulating factors. *Stem Cells (Dayt)* **11 Suppl 2**, 1-11 (1993).

13. Matthews, W., Jordan, C. T., Gavin, M. *et al.* A receptor tyrosine kinase cDNA isolated from a population of enriched primitive hematopoietic cells and exhibiting close genetic linkage to c- kit. *Proc Natl Acad Sci U S A* **88**, 9026-9030 (1991).

14. Small, D., Levenstein, M., Kim, E. *et al.* STK-1, the human homolog of Flk-2/Flt-3, is selectively expressed in CD34+ human bone marrow cells and is involved in the proliferation of early progenitor/stem cells. *Proc Natl Acad Sci U S A* **91**, 459-463 (1994).

15. Li, C. L. & Johnson, G. R. Stem cell factor enhances the survival but not the self-renewal of murine hematopoietic long-term repopulating cells. *Blood* **84**, 408-414 (1994).

16. Jacobsen, S. E., Okkenhaug, C., Myklebust, J., Veiby, O. P. & Lyman, S. D. The FLT3 ligand potently and directly stimulates the growth and expansion of primitive murine bone marrow progenitor cells in vitro: synergistic interactions with interleukin (IL) 11, IL-12, and other hematopoietic growth factors. *J Exp Med* **181**, 1357-1363 (1995).

17. McNiece, I. K., Langley, K. E. & Zsebo, K. M. Recombinant human stem cell factor synergises with GM-CSF, G-CSF, IL-3 and epo to stimulate human progenitor cells of the myeloid and erythroid lineages. *Exp Hematol* **19**, 226-231 (1991).

18. Bernstein, I. D., Andrews, R. G. & Zsebo, K. M. Recombinant human stem cell factor enhances the formation of colonies by CD34+ and CD34+lin- cells, and the generation of

colony-forming cell progeny from CD34+lin- cells cultured with interleukin-3, granulocyte colony-stimulating factor, or granulocyte-macrophage colony-stimulating factor. *Blood* **77**, 2316-2321 (1991).

19. Goldberg, E. D., Dygai, A. M., Zakharova, O. & Shakhov, V. P. The modulating influence of enkephalins on the bone marrow haemopoiesis in stress. *Folia Biol* **36**, 319-331 (1990).

20. Karpel, R., Ben Aziz-Aloya, R., Sternfeld, M. *et al.* Expression of three alternative acetylcholinesterase messenger RNAs in human tumor cell lines of different tissue origins. *Exp Cell Res* **210**, 268-277 (1994).

21. Massoulie, J., Pezzementi, L., Bon, S., Krejci, E. & Vallette, F. M. Molecular and cellular biology of cholinesterases. *Prog Neurobiol* **41**, 31-91 (1993).

22. Lev-Lehman, E., Deutsch, V., Eldor, A. & Soreq, H. Immature human megakaryocytes produce nuclear-associated acetylcholinesterase. *Blood* **89**, 3644-3653 (1997).

23. Grisaru, D., Lev-Lehman, E., Shapira, M. *et al.* Human osteogenesis involves differentiation-dependent increases in the morphogenically active 3' alternative splicing variant of acetylcholinesterase. *Mol Cell Biol* **19**, 788-795 (1999).

24. Majumdar, M. K., Thiede, M. A., Mosca, J. D., Moorman, M. & Gerson, S. L. Phenotypic and functional comparison of cultures of marrow-derived mesenchymal stem cells (MSCs) and stromal cells. *J Cell Physiol* **176**, 57-66 (1998).

25. Burstein, S. A., Adamson, J. W. & Harker, L. A. Megakaryocytopoiesis in culture: Modulation by cholinergic mechanisms. *J Cell Physiol* **54**, 201-208 (1980).

26. Paoletti, F., Mocali, A. & Vannucchi, A. M. Acetylcholinesterase in murine erythroleukemia (Friend) cells: evidence for megakaryocyte-like expression and potential growth-regulatory role of enzyme activity. *Blood* **79**, 2873-2879 (1992).

27. Kaufer, D., Friedman, A., Seidman, S. & Soreq, H. Acute stress facilitates long-lasting changes in cholinergic gene expression [see comments]. *Nature* **393**, 373-377 (1998).

28. Shohami, E., Kaufer, D., Chen, Y. *et al.* Antisense prevention of neuronal damages following head injury in mice. *J. Mol. Med.* **78**, 228-236 (2000).

29. Grisaru, D., Deutsch, V., Pick, M. *et al.* Placing the newborn on the maternal abdomen after delivery increases the volume and CD34+ cell content in the umbilical cord blood collected – an old manèuver with new applications. *Am J Obstet Gynecol* **(in press)** (1999).

30. Deutsch, V. R., Eldor, A., Olson, T. *et al.* Stem cell factor (SCF) synergizes with megakaryocyte colony stimulating activity in post-irradiated aplastic plasma in stimulating human megakaryocytopoiesis. *Med Oncol* **13**, 31-42 (1996).

31. Pick, M., Nagler, A., Grisaru, D., Eldor, A. & Deutsch, V. Expansion of megakaryocyte progenitors from human umbilical cord blood using a new two-step separation procedure [In Process Citation]. *Br J Haematol* **103**, 639-650 (1998).

32. Sternfeld, M., Shoham, S., Klein, O. *et al.* Excess "readthrough" acetylcholinesterase attenuates but the "synaptic" variant intensifies neurodeterioration correlates. *Proc. Natl. Acad. Sci. USA*, (in press) (2000).

33. Broide, R. S., Grifman, M., Loewenstein, A. *et al.* Manipulations of ACHE gene expression suggest non-catalytic involvement of acetylcholinesterase in the functioning of mammalian photoreceptors but not in retinal degeneration. *Brain Res Mol Brain Res* **71**, 137-148 (1999).

34. Shapira, M., Tur-Kaspa, I., Bosgraaf, L. *et al.* A transcription-activating polymorphism in the ACHE promoter associated with acute sensitivity to anti-acetylcholinesterases. *Hum Mol Genet* **9**, 1273-1281 (2000).

35. Grifman, M. & Soreq, H. Differentiation intensifies the susceptibility of pheochromocytoma cells to antisense oligodeoxynucleotide-dependent suppression of acetylcholinesterase activity. *Antisense Nucleic Acid Drug Dev* **7**, 351-359 (1997).

36. Grisaru, D., Sternfeld, M., Eldor, A., Glick, D. & Soreq, H. Structural roles of acetylcholinesterase variants in biology and pathology. *Eur J Biochem* **264**, 672-686 (1999).

37. Tavassoli, M. Embryonic and fetal hemopoiesis: an overview. *Blood Cells* **17**, 269-281 (1991).

38. Tavian, M., Hallais, M. F. & Peault, B. Emergence of intraembryonic hematopoietic precursors in the pre-liver human embryo. *Development* **126**, 793-803 (1999).

39. Porcellini, A., Manna, A., Manna, M. *et al.* Ontogeny of granulocyte-macrophage progenitor cells in the human fetus. *Int J Cell Cloning* **1**, 92-104 (1983).

40. Beeri, R., Andres, C., Lev-Lehman, E. *et al.* Transgenic expression of human acetylcholinesterase induces progressive cognitive deterioration in mice. *Curr Biol* **5**, 1063-1071 (1995).

41. Kaufer, D. & Soreq, H. Tracking cholinergic pathways from psychological and chemical stressors to variable neurodeterioration paradigms. *Curr Opin Neurol* **12**, 739-743 (1999).

42. Darnell, J. E., Jr., Kerr, I. M. & Stark, G. R. Jak-STAT pathways and transcriptional activation in response to IFNs and other extracellular signaling proteins. *Science* **264**, 11415-11421 (1994).

43. Peters, M., Muller, A. M. & Rose-John, S. Interleukin-6 and soluble interleukin-6 receptor: direct stimulation of gp130 and hematopoiesis. *Blood* **92**, 3495-3504 (1998).

44. McMahon, A. & Sabban, E. L. Regulation of expression of dopamine beta-hydroxylase in PC12 cells by glucocorticoids and cyclic AMP analogues. *J Neurochem* **59**, 2040-2047 (1992).

45. Tronche, F., Kellendonk, C., Kretz, O. *et al.* Disruption of the glucocorticoid receptor gene in the nervous system results in reduced anxiety. *Nat Genet* **23**, 99-103 (1999).

46. Cella, N., Groner, B. & Hynes, N. E. Characterization of Stat5a and Stat5b homodimers and heterodimers and their association with the glucocortiocoid receptor in mammary cells. *Mol Cell Biol* **18**, 1783-1792 (1998).

47. De Vroede, M., Beukering, R., Spit, M. & Jansen, M. Rectal hydrocortisone during stress in patients with adrenal insufficiency. *Arch Dis Child* **78**, 544-547 (1998).

48. Raina, A. K. & Menn, J. J. Pheromone biosynthesis activating neuropeptide: from discovery to current status. *Arch Insect Biochem Physiol* **22**, 141-151 (1993).

49. Blazsek, I., Liu, X. H., Anjo, A. *et al.* The hematon, a morphogenetic functional complex in mammalian bone marrow, involves erythroblastic islands and granulocytic cobblestones. *Exp Hematol* **23**, 309-319 (1995).

50. Ross, M. E., Evinger, M. J., Hyman, S. E. *et al.* Identification of a functional glucocorticoid response element in the phenylethanolamine N-methyltransferase promoter using fusion genes introduced into chromaffin cells in primary culture. *J Neurosci* **10**, 520-530 (1990).

51. Lopez, A. J. Alternative splicing of pre-mRNA: developmental consequences and mechanisms of regulation [In Process Citation]. *Annu Rev Genet* **32**, 279-305 (1998).

52. Xie, J. & McCobb, D. P. Control of alternative splicing of potassium channels by stress hormones. *Science* **280**, 443-446 (1998).

53. Chan, R. Y., Adatia, F. A., Krupa, A. M. & Jasmin, B. J. Increased expression of acetylcholinesterase T and R transcripts during hematopoietic differentiation is accompanied by parallel elevations in the levels of their respective molecular forms. *J Biol Chem* **273**, 9727-9733 (1998).

54. Tarasenko, L. M., Grebennikova, V. F., Tarasenko, V. V. *et al.* [The proteinase and alpha 1-antitrypsin activities in the tissues during emotional stress in rabbits]. *Fiziol Zh* **38**, 115-117 (1992).

55. Gupta, P., Blazar, B. R., Gupta, K. & Verfaillie, C. M. Human CD34(+) bone marrow cells regulate stromal production of interleukin-6 and granulocyte colony-stimulating factor and increase the colony-stimulating activity of stroma. *Blood* **91**, 3724-3733 (1998).

56. Jazwiec, B., Solanilla, A., Grosset, C. *et al.* Endothelial cell support of hematopoiesis is differentially altered by IL-1 and glucocorticoids. *Leukemia* **12**, 1210-1220 (1998).

57. Sussman, J. L., Harel, M. & Silman, I. Three-dimensional structure of acetylcholinesterase and of its complexes with anticholinesterase drugs. *Chem Biol Interact* **87**, 187-197 (1993).

58. Satoh, T., Aramini, J. M., Li, S. *et al.* Bioactive peptide design based on protein surface epitopes. A cyclic heptapeptide mimics CD4 domain 1 CC' loop and inhibits CD4 biological function. *J Biol Chem* **272**, 12175-12180 (1997).

59. Livnah, O., Stura, E. A., Johnson, D. L. *et al.* Functional mimicry of a protein hormone by a peptide agonist: the EPO receptor complex at 2.8 A [see comments]. *Science* **273**, 464-471 (1996).

60. Johnson, D. L., Farrell, F. X., Barbone, F. P. *et al.* Identification of a 13 amino acid peptide mimetic of erythropoietin and description of amino acids critical for the mimetic activity of EMP1. *Biochemistry* **37**, 7699-7710 (1998).

61. Cwirla, S. E., Balasubramanian, P., Duffin, D. J. *et al.* Peptide agonist of the thrombopoietin receptor as potent as the natural cytokine. *Science* **276**, 1696-1699 (1997).

62. Conrad, P. D. & Emerson, S. G. Ex vivo expansion of hematopoietic cells from umbilical cord blood for clinical transplantation. *J Leukoc Biol* **64**, 147-155 (1998).

63. Taniguchi, T. Cytokine signaling through nonreceptor protein tyrosine kinases. *Science* **268**, 251-255 (1995).

64. Schultz, J. A., Hoffman, W. E. & Albrecht, R. F. Sympathetic stimulation with physostigmine worsens outcome from incomplete brain ischemia in rats. *Anesthesiology* **79**, 114-121 (1993).

65. Harmsen, P., Rosengren, A., Tsipogianni, A. & Wilhelmsen, L. Risk factors for stroke in middle-aged men in Goteborg, Sweden. *Stroke* **21**, 223-229 (1990).

66. Inestrosa, N. C., Alarcon, R., Arriagada, J., Donoso, A. & Alvarez, J. Platelets of Alzheimer patients: increased counts and subnormal uptake and accumulation of [14C]5-hydroxytryptamine. *Neurosci Lett* **163**, 8-10 (1993).

67. Snowdon, D. A., Greiner, L. H., Mortimer, J. A. *et al.* Brain infarction and the clinical expression of Alzheimer disease. The Nun Study. *Jama* **277**, 813-817 (1997).

68. Brown, L. M., Blair, A., Gibson, R. *et al.* Pesticide exposure and other agricultural risk factors for leukemia among man in Iowa and Minnesota. *Cancer Res* **50**, 6585-6591 (1990).

69. Karpel, R., Sternfeld, M., Ginzberg, D. *et al.* Overexpression of alternative human acetylcholinesterase forms modulates process extensions in cultured glioma cells. *J Neurochem* **66**, 114-123 (1996).

70. Solter, D. & Gearhart, J. Putting stem cells to work [see comments]. *Science* **283**, 1468-1470 (1999).

71. Shamblott, M. J., Axelman, J., Wang, S. *et al.* Derivation of pluripotent stem cells from cultured human primordial germ cells. *Proc Natl Acad Sci U S A* **95**, 13726-13731 (1998).

72. Bjornson, C. R., Rietze, R. L., Reynolds, B. A., Magli, M. C. & Vescovi, A. L. Turning brain into blood: a hematopoietic fate adopted by adult neural stem cells in vivo [see comments]. *Science* **283**, 534-537 (1999).

FIGURE 1

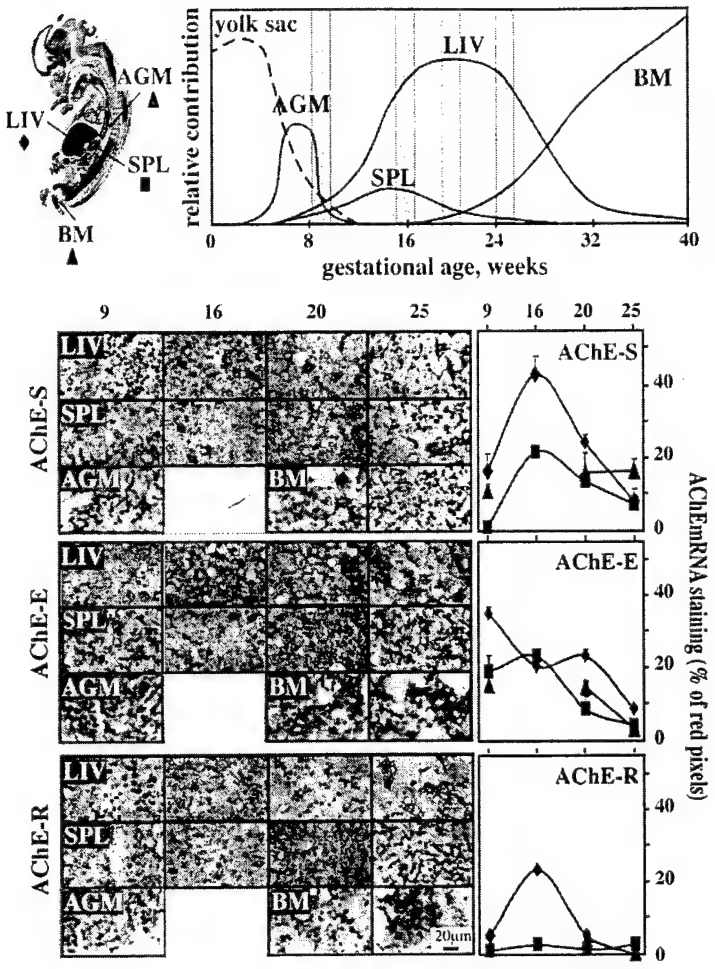
AGM
LIV
SPL
BM
yolk sac
relative contribution
LIV
AGM
SPL
BM
0
8
16
24
32
40
gestational age, weeks
9
16
20
25
AChE-S
AChE-E
AChE-R
LIV
SPL
AGM
BM
40
20
0
AChEmRNA staining (% of red pixels)
20μm

FIGURE 2

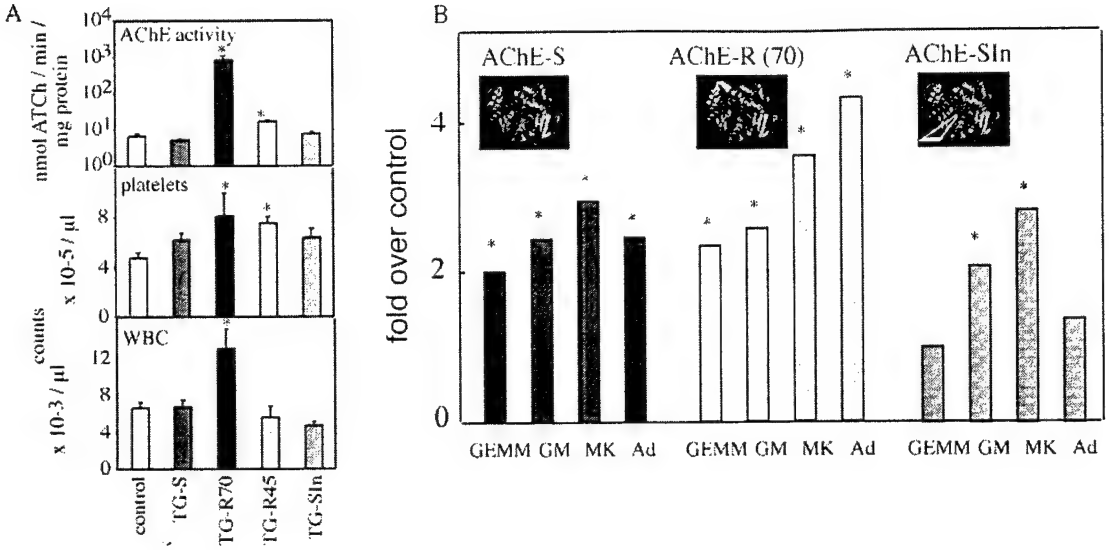

FIGURE 3

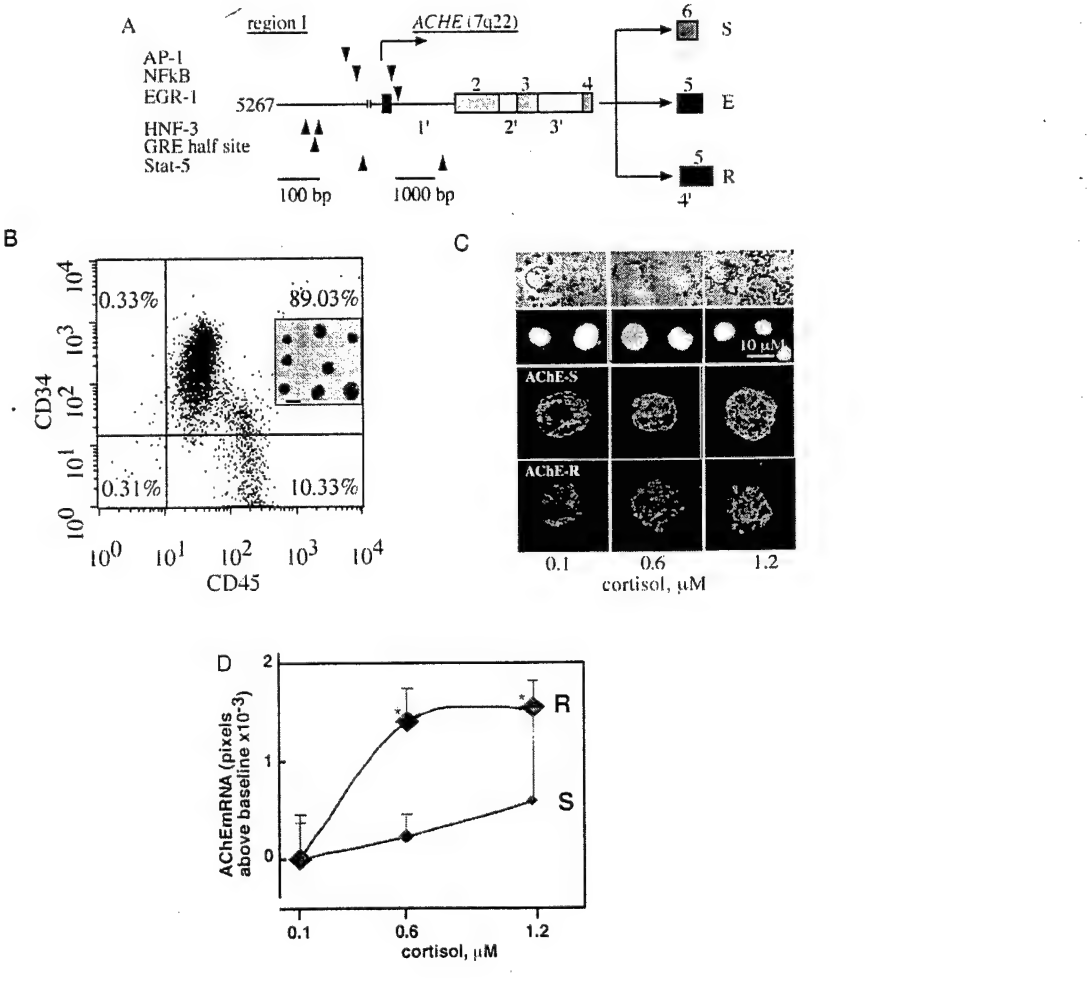

FIGURE 4

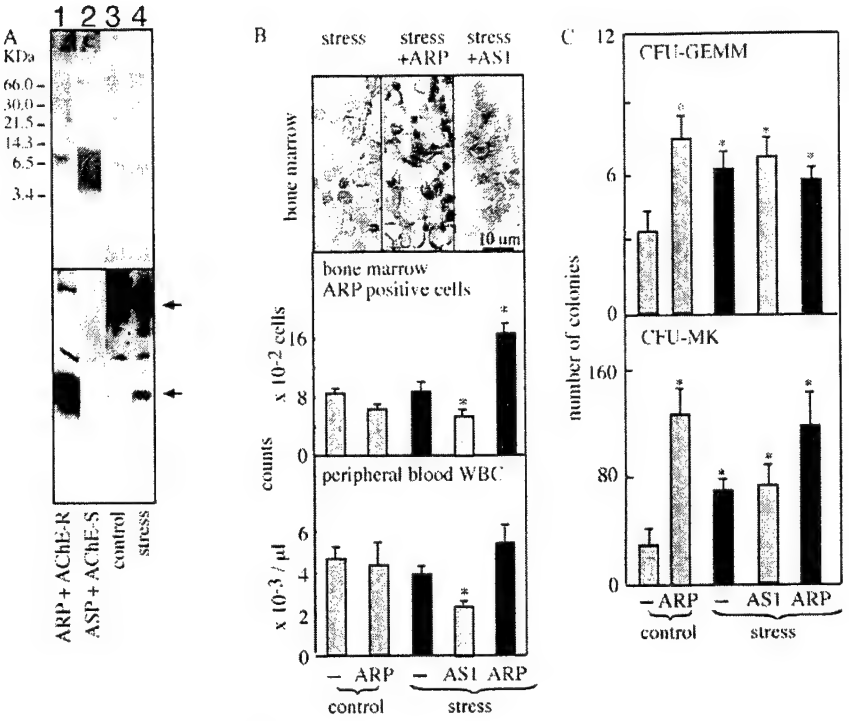

FIGURE 5

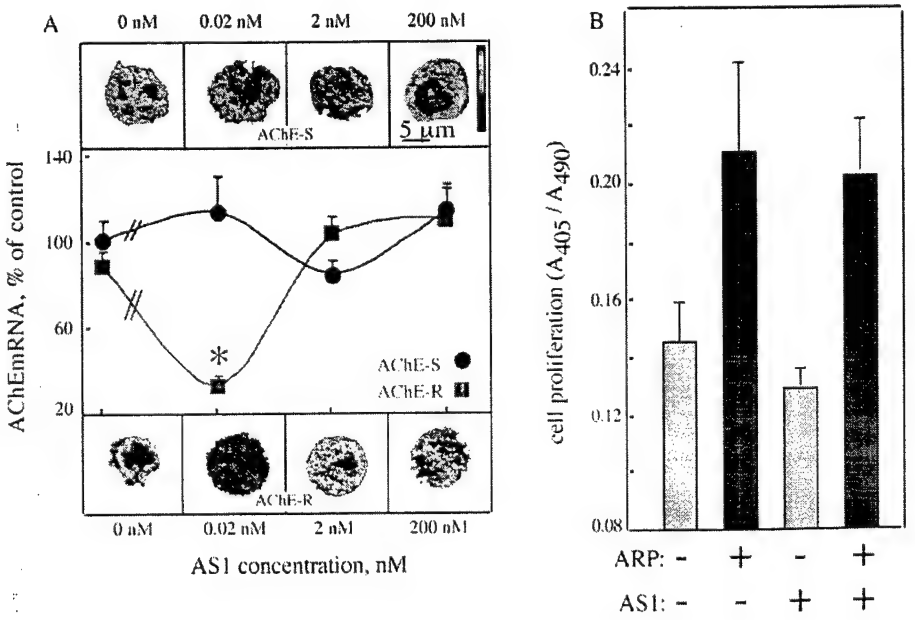

FIGURE 6

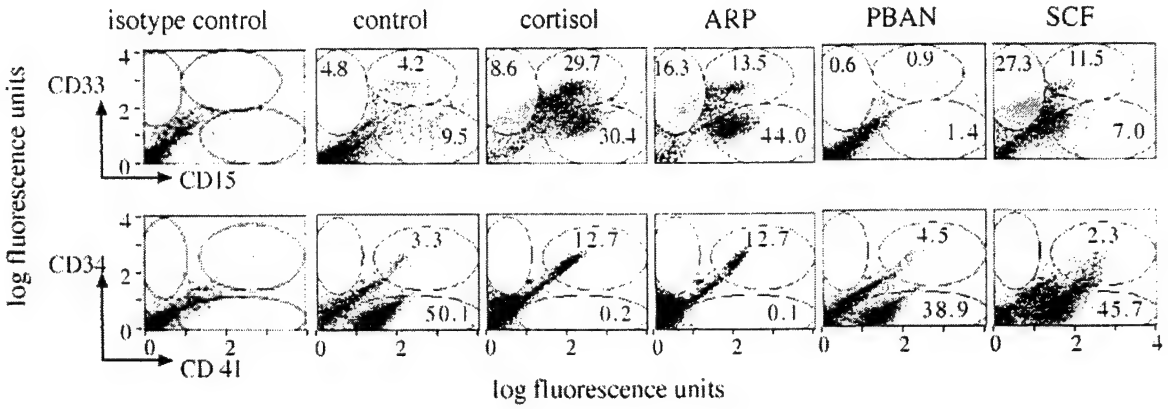

FIGURE 7

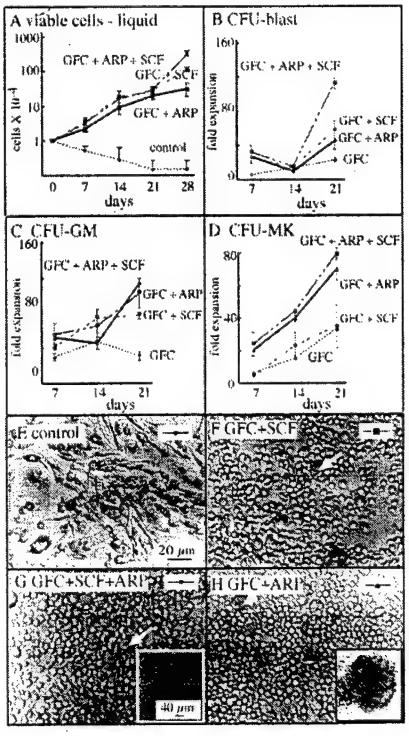

THE STRESS-ASSOCIATED "READTHROUGH" ACETYLCHOLINESTERASE VARIANT DISPLAYS DISTINCT INHIBITOR SENSITIVITIES[a]

Asher Y. Salmon, Dalia Ginzberg, Meira Sternfeld, Inbal Mor, David Glick and Hermona Soreq[†]

Department of Biological Chemistry, Institute of Life Sciences, The Hebrew University, Safra Campus, Jerusalem, Israel, 91904.

Running title:
Anticholinesterase sensitivities of stress-associated AChE-R

Corresponding author:
Hermona Soreq, Department of Biological Chemistry, Institute of Life Sciences, Hebrew University of Jerusalem, 91904 Israel; tel. 972-2-6585109; fax. 972-2-6520258; e-mail soreq@shum.huji.ac.il.

Text pages: 17 (Introduction, Materials and Methods, Results, Discussion, Acknowdedgements, double-spaced)
Tables: 3
Figures: 4
References: 48
Words:

Abstract	246
Introduction	797
Discussion	715

Abbreviations:
ACHE, the acetylcholinesterase gene
AChE, acetylcholinesterase
AChE-C, core AChE, encoded by exons E2, E3 and E4
AChE-E, erythrocytic AChE, encoded by E2, E3, E4 and E5
AChE-R, "readthrough" AChE, encoded by E2, E3, E4 and I4
AChE-S, synaptic AChE, encoded by E2, E3, E4 and E6
ARP, AChE-R peptide, an oligopeptide with the sequence of the 26 C-terminal residues of AChE-R
ATCh, acetylthiocholine
BuChE, butyrylcholinesterase
ChE, cholinesterase
CMV, cytomegalovirus
cmv, cytomegalovirus promoter
DFP, diisopropylfluorphosphonate
EDTA, ethylenediaminetetraacetate
GST, glutathione S-transferase
hp, human promoter sequence
iso-OMPA, tetraisopropylpyrophosphoramide
G1, globular monomer (of AChE)
G2, globular dimer (of AChE)
G4, globular tetramer (of AChE)
PAGE, polyacrylamide gel electrophoresis
SDS, sodium dodecyl sulfate

ABSTRACT

Establishment of anti-cholinesterase therapies for Alzheimer's disease revealed several levels of responsiveness, but the molecular origin of such diversity is unclear. Here, we report differences between the anti-cholinesterase sensitivities of the 3 C-terminally distinct human acetylcholinesterase (AChE) isoforms produced by alternative splicing from the original transcript of the single *ACHE* gene: the major "synaptic" AChE-S, the "erythrocytic" AChE-E and the stress-associated "readthrough" AChE-R. The 3 AChE variants display distinct electrophoretic mobilities and are immunochemically distinguishable by region-specific antibodies. Unlike AChE-S and AChE-E, the C-terminal sequence of AChE-R does not support dimerization or coupling to a glycophosphatidoinositide moiety. When produced in transgenic mice, AChE-R remained low salt-soluble and monomeric. *In vitro* inhibition curves indicated significantly higher sensitivities of AChE-R than those of recombinant AChE-S or purified AChE-E for the organophosphates diisopropylfluorophosphonate and paraoxon, as well as for the pseudo-irreversible carbamate, rivastigmine (Exelon™). In contrast, all AChE isoforms were similarly sensitive to tacrine (Cognex™) and donepezil (Aricept™); and AChE-R was 4-fold less sensitive than AChE-S to the peripheral site inhibitor, propidium. Transgenic C-terminally truncated "core" AChE-C protein presented similar inhibitor sensitivities to those of AChE-R. *In vivo*, somatosensory cortex extracts from AChE-R transgenics and acutely stressed mice had larger proportions of monomeric enzyme and displayed higher sensitivity to rivastigmine, but not donepezil, as compared to strain- and age-matched control mice and AChE-S transgenics. Our findings demonstrate previously unsuspected differences among drug responses of alternative AChE isoforms and predict stress-related and drug-induced changes in the responsiveness to certain anti-cholinesterases.

INTRODUCTION

The uses of, and exposure to inhibitors of the acetylcholine hydrolyzing enzyme acetylcholinesterase (AChE, EC 3.1.1.7) have rapidly grown over the past few years. The anti-AChEs tacrine (Cognex™), donepezil (Aricept™) and rivastigmine (Exelon™) are, to date, the only drugs approved for treatment of Alzheimer's disease patients (Anand, et al., 1996, Giacobini, 1998). These drugs have proven to be useful for short-term improvement of memory failure (Davis, et al., 1992) and are used for a growing number of patients worldwide. Other anti-AChE drugs include neostigmine, used for treating patients with myasthenia gravis (Engel, et al., 1998) and pyridostigmine as a prophylactic in anticipation of chemical warfare (Friedman, et al., 1996), muscle relaxants under surgery (e.g. succinylcholine, (Friedman, et al., 1996, Loewenstein Lichtenstein, et al., 1995), and several other inhibitors of less frequent usage. In addition to drugs, exposure to anti-AChE insecticides is known for industrial and agricultural workers and domestic users (reviewed by Feldman 1999a, 1999b). Altogether, such an extensive exposure to anti-AChEs calls for in-depth examination of the human responses to these agents.

In vivo, most anti-AChEs interact first with the AChE in peripheral organ systems: AChE-E in the blood, where it is associated with the membrane of erythrocytes (Dutta-Choudhury and Rosenberry, 1984) and AChE-S in muscle, where it is embedded in neuromuscular junctions. The AChE-homologous protein butyrylcholinesterase (BuChE, EC 3.1.1.8) resides in the plasma and liver. BuChE, too, binds most anti-AChEs, protecting the CNS by serving as a scavenger that

reduces the amount of inhibitor reaching the brain (Jbilo, et al., 1994, Soreq and Glick, 2000). Therefore, variations in peripheral AChE and BuChE levels would inevitably change the sensitivity to anti-AChEs. This can explain the adverse responses to such drugs in carriers of "atypical" (Loewenstein Lichtenstein, et al., 1995) or "silent" BuChE (Prody, et al., 1989) or in individuals with polymorphisms in the *ACHE* promoter (Shapira, et al., 2000). However, the incidence of these mutations is too low to account for the spectrum of sensitivities to anti-AChEs. This calls for an explanation focussed on the AChE protein itself.

What has not yet been addressed in previous considerations is that there are 3 target AChEs, which result from alternative splicing of the pre-mRNA transcript of the single *ACHE* gene (Li, et al., 1991, Ben Aziz Aloya, et al., 1993). All isoforms share the N-terminal 543-amino acid residue core (AChE-C), and *in vitro*, have indistinguishable specificities and specific activities (Soreq and Glick, 2000, Schwarz, et al., 1995, Glick, et al., 2000). The "synaptic" isoform, AChE-S, is C-terminated by a unique 40-residue sequence, the cysteine residue of which enables dimerization. Up to to three tetramers can interact with the collagen triple helix-like ColQ structural subunit characteristic of the neuromuscular junction (reviewed by Massoulie et al. 1998). "Erythrocytic" AChE-E is C-terminated by its unique 14-residue peptide which enables linkage to the erythrocyte membrane through glycophosphatidoinositide groups (Futerman, et al., 1985). Finally, the "readthrough" AChE-R soluble monomer (Seidman, et al., 1995) C-terminates with a hydrophilic, cysteine-free 26-residue sequence. Most drug testing on human AChE has been done with AChE-E purified from blood (Giacobini, 1998) or recombinant AChE-S produced in stably transfected cells (Shafferman, et al., 1994). In contrast, drug sensitivity testing for AChE-R was limited to crude homogenates of injected *Xenopus* oocytes with low signal to noise ratios that prevented calculation of inhibition constants (Schwarz, et al., 1995). Subsequent studies have emphasized the importance of AChE-R responses, as AChE-R mRNA levels were shown to drastically increase in the mammalian brain shortly after psychological stress (Kaufer, et al., 1998), exposure to anti-AChEs (Kaufer, et al., 1999), or head injury (Shohami, et al., 2000). Moreover, anticholinesterase exposure also modifies the fraction of AChE represented by AChE-R in muscle (Lev-Lehman, et al., 2000) and intestinal epithelium (Shapira, et al., 2000). Therefore more detailed testing of its inhibitor sensitivity profile is required.

To determine whether AChE-R properties differ from those of the other AChE isoforms, we employed milk and muscle homogenates from transgenic mice with massive human AChE-R overproduction (Sternfeld, et al., 2000). In comparison, we used highly purified recombinant AChE-S and AChE-E as well as C-terminally truncated AChE-C, produced in another pedigree of transgenic mice. Truncated AChE has been used in the past to evaluate the role of residues in the C-terminal sequence in multimerization (Cousin, et al., 1996, Gough and Randall, 1995, Gibney and Taylor, 1990), but no effect had been noted on catalytic properties. To investigate the physiological relevance of our findings, we used brain homogenates from stressed or transgenic mice for inhibitor sensitivities and sedimentation studies and immunolabeled the examined AChE-R protein with an antibody targeted to its unique C-terminal sequence. Our findings demonstrate a distinct inhibitor-sensitivity profile for AChE-R; stress-related and/or drug-induced up-regulation of the level of this particular AChE variant may, therefore, modulate the inhibitor responses of brain AChE.

MATERIALS AND METHODS

Chemicals: Human erythrocyte AChE-E, human recombinant AChE-S, tetraisopropylpyrophosphoramide (iso-OMPA), acetylthiocholine (ATCh), pyridostigmine, tacrine (Cognex™, Parke Davis/Warner-Lambert), diisopropylfluorophosphonate (DFP), diethyl-*p*-nitrophenylphosphonate (paraoxon), oxytocin and other basic chemicals were all purchased from Sigma Chemical Co. (St. Louis, MO, USA). Rivastigmine (Exelon™, Novartis) was gratefully received from Dr. M. Weinstock (Jerusalem, Israel). Donepezil (Aricept™, Pfizer) was purchased commercially. Monoclonal mouse anti-human AChE antibodies were provided by Dr. Norgaard-Pedersen (Copenhagen, Denmark). Polyclonal rabbit antibodies against the human AChE-R C-terminal sequence were prepared as detailed elsewhere (Sternfeld, et al., 2000). Secondary antibodies: goat anti-rabbit and donkey anti-mouse, horseradish peroxidase conjugated antibodies and ECL detection kit were all purchased from Santa Cruz Biotechnology (Santa Cruz, CA, USA).

Transgenic animals included FVB/N mice carrying the AChE-S transgene under control of the proximal 600 bp of the human *ACHE* promoter (Beeri, et al., 1995), transgenics which strongly express AChE-R under the cytomegalovirus (CMV) promoter (lines 45 and 70) (Sternfeld, et al., 2000) and an additional line of FVB/N transgenics expressing the AChE-C protein, also under the CMV promoter. Confined swim stress, anti-AChE exposure and isolation of the brain of these animals were as detailed elsewhere (Kaufer, Friedman et al. 1998; Kaufer, Friedman et al. 1999; Shapira, Tur-Kaspa et al. 2000); homogenates prepared from these brains were kept at –70°C until use.

Milk collection: Milk was collected from nursing mice 7 days after parturition. Two hr following the separation of the mothers from their pups, they were injected with 0.3 IU oxytocin. Milk was collected 10 min later by gentle massage of the mammary gland and was taken up by a capillary tube. The milk was diluted 1:4 with double distilled water and kept at –20°C.

***In situ* hybridization:** *In situ* hybridization was performed on 7 μm paraffin-embedded mouse mammary gland and gastrocnemius muscle slices with 50-mer 5' biotinylated, 2'-O-methylated AChE cRNA probes complementary to two alternative mouse reading frames: exon 6 for AChE-S and pseudo-intron 4 for AChE-R, all as detailed elsewhere (Grisaru, et al., 1999). Detection of the biotinylated probes involved streptavidin-conjugated alkaline phosphatase, using fast red substrate (Boehringer/Mannheim, Germany).

AChE-R antibodies: A full description of the preparation of the antibodies has been reported (Sternfeld, et al., 2000) . Briefly, by molecular biology techniques, ARP (AChE-R Peptide), with the sequence of the 26 C-terminal residues of AChE-R (GMQGPAGSGWEEGSGSPPGVTPLFSP) was fused to glutathione S-transferase (GST), and the fusion protein was expressed in *E. coli*. Rabbits were immunized with purified ARP-GST and specific serum antibodies adsorbed with GST.

AChE activity and inhibitor assays: Protein extraction from various brain regions was performed in low salt detergent solution (1% Triton X-100 in 0.01 M Na phosphate buffer, pH 7.4) and from muscle with high salt detergent solution (0.01 M

Tris HCl; 1 M Na chloride; 1% Triton and 1 mM EDTA), as described previously (Seidman, et al., 1994). AChE activity was measured spectrophotometrically (Ellman, et al., 1961) using a multiwell assay and a Molecular Dynamics (Palo Alto, CA, USA) reader. Iso-OMPA (10^{-5} M) was included in these assays to block BuChE activity. The activities of AChE-C and AChE-R were found to be stable for 5 hr at temperatures up to 42 °C and to resist freezing and thawing. For inhibition studies with reversible inhibitors, AChE from milk or gastrocnemius muscle and brain homogenates of stressed or AChE-R, AChE-C or AChE-S transgenic mice, purified human AChE-E and human recombinant AChE-S were pre-incubated for 10 min with the anti-cholinesterases in Ellman's reagent (Ellman, et al., 1961). ATCh (1 mM) was added and its hydrolysis rate was determined spectrophotometrically as described above. Inhibition was observed over inhibitor concentration ranges of 6 orders of magnitude. Inhibition of AChE activity values were determined from triplicate assays. IC_{50} values were calculated by Grafit (version 3, Erithacus Software, Staines, UK) and K_i values were then calculated by the method of Hobbiger and Peck (1969), based the K_m value of human AChE for ATCh of 0.14 mM (Ordentlich, et al., 1995). In the case of irreversible inhibitors, both k_{cat} and K_i were determined by adsorbing the chosen enzyme to antibody-coated wells of microtiter plates, exposing them to an inhibitor at several concentrations and for varying lengths of time, washing to remove the inhibitor, and assaying for remaining activity. (Schwarz, et al., 1995) The concentration dependence of the resultant pseudo-first order rate constants yielded an affinity constant, K_i, and their extrapolation yielded the catalytic rate constant, k_{cat}.

Polyacrylamide gel electrophoresis: Denaturing SDS-polyacrylamide gel electrophoresis and blotting were performed as described (Seidman, et al., 1995) using the noted antibodies. Blots were exposed to the proper secondary peroxidase-conjugated antibodies and chemiluminescently detected. Non-denaturing gel electrophoresis (120 V for 4-6 hr at 4°C) was performed in vertical 6% polyacrylamide gels using a 3% stacking gel and buffers identical to those employed for standard Laemmli SDS-PAGE except that 1% Triton X-100 replaced SDS in all solutions. Gels were rinsed 3 times with double distilled water and stained for catalytically active AChE for 1 hr under rotation at room temperature, using a histochemical staining procedure (Karnovsky and Roots, 1964).

Immunoblot analysis was performed essentially as detailed (Sternfeld, et al., 1998). Immunodetection was with pooled goat anti-mouse and anti-human AChE antibodies, directed at an N-terminal peptide common to the different variants (N-19 and E-19; Santa Cruz Biotechnology, Santa Cruz, CA). Signals were quantified using Image-Pro software (Media Cybernetics, Silver Spring, MD).

Sucrose gradient ultracentrifugation was performed with 20-80 µl samples containing catalytically active AChE sufficient to achieve a ΔA_{405} of approx. 2.4/min in the Ellman's assay. Muscle extracts were loaded with high salt buffer and somatosensory cortex extracts, with low salt buffer. Samples were applied to 12 ml 5-20% linear sucrose density gradients. Ultracentrifugation was for 20 hr, at 37,000 rpm at 4°C in the presence of bovine catalase (Sigma) as a sedimentation marker (11.4 S). Fractions were collected into 96-well microtiter plates and assayed for AChE activity essentially as described above.

RESULTS

Several lines of transgenic mice were screened for the level of muscle AChE and for their secretion of the appropriate recombinant AChE variants in milk (Table 1). For AChE-R, the highest expressor, line 70, was chosen for subsequent studies.

***In vivo* production of AChE-R in milk and muscle of transgenic mice**

Expression of the AChE-R transgene in the mammary gland and muscle of transgenic mice was first verified by *in situ* hybridization using a 5'-biotinylated 2'-O-methylated AChE cRNA probe targeted at the I4 pseudo-intron, which encodes the C-terminal sequence that characterizes AChE-R. AChE-R mRNA levels appeared to be considerably higher in mammary gland alveoli and around nuclei in the gastrocnemius muscle of AChE-R transgenics as compared with AChE-S transgenics or FVB/N control mice. In contrast, mouse AChE-S mRNA levels were essentially similar in these tissues (data not shown). This high expression level, consistent with previous finding of cmv-controlled expression of AChE (Seidman, et al., 1995), yielded over 350-fold excess of hydrolytic activities in muscle homogenates of AChE-R and AChE-C transgenics as compared with AChE-S and non-transgenic control mice (Table 1). No increase in milk AChE activity was observed in AChE-S transgenics, where the proximal human *ACHE* promoter limited expression to the nervous system (Beeri, et al., 1995). In contrast, milk enzyme activities were up to 230-fold higher than controls in both AChE-C and AChE-R pedeigrees (the BuChE-specific inhibitor iso-OMPA was used to block all but AChE activity) (Table 1). Muscle enzyme activities were similarly elevated. ***Although muscle AChE-R comprises both the host and the transgenic protein (Lev-Lehman, et al., 2000).*** AChE-R of either muscle or milk thus presented signal to noise ratios sufficiently high for testing inhibitor sensitivities of the AChE-R protein. Preincubation (10 min) of AChE-S with normal milk at the same dilution as that used in the assay of transgenic milk yielded the same activity as did preincubation with saline, indicating that milk contains no ChE inhibitor. The enzyme activities in these tissues appeared stable with time and under freezing and thawing, which enabled accumulation of enzyme preparations for comparative tests.

Transgenic AChE-R is subject to tissue-specific post-transcriptional modifications

Non-denaturing gel electrophoresis followed by cytochemical staining for catalytic activity revealed a diffuse fast-migrating band for AChE-R in trangenic milk, which was absent in the milk of control mice (Fig 1A). Muscle homogenates showed marked heterogeneity of staining, with two major diffuse bands, both different from the milk enzyme. This suggested tissue-specific post-transcriptional and/or post-translational modification. The transgene that expresses the AChE-R protein also includes exon 5, which produces the C-terminus peptide characteristic of AChE-E (Sternfeld, et al., 2000). This raised the possibility that the slower migrating enzyme band in muscle homogenates represented AChE-E-dimers produced from this transgene by alternative splicing. That purified erythrocyte AChE-E migrated yet more slowly again indicated tissue specificity for the post-translational processing of muscle as compared with erythrocyte enzyme, consistent with the variable AChE glycosylation reported by others (Meflah, et al., 1984). Recombinant AChE-S from HEK293 cells (Shafferman, et al., 1994) migrated yet more slowly (not shown), as did mouse brain AChE; and plasma BuChE presented a relatively sharp band co-migrating with AChE-E. A faint parallel band in the mouse milk probably represents the endogenous enzyme; AChE is known to be secreted also in human milk (Spitsyn and Bychkovskaia, 1994).

Tissue homogenates from normal and transgenic mouse lines did not differ in the presence of complex or high mannose chains, α(2-3) or α(2-6) terminal sialyl residues, or the presence of O-linked galactosyl-ß(1-3)galactosamine (as tested with the DIG Glycan Differentiation Kit, Boehringer/Mannheim, Germany) (data not shown). To further analyze the glycosylation of specific AChE variants, we subjected tissue homogenates to enzymatic hydrolysis by N-glycosidase F and endoglycosidase F (Boehringer), followed by denaturing gel electrophoresis and immunoblot analysis with antibodies targeted at the core domain common to all AChE variants. In this test, migration properties were similarly altered for AChEs from normal and all transgenic lines. We conclude that by these criteria the transgenic enzymes were indistinguishable in glycosylation from natural AChE.

Transgenic milk and muscle AChE variants display distinct electrophoretic mobilities and multimeric structures

When subjected to gel electrophoresis under denaturing conditions followed by immunoreaction with an antibody targeted to AChE-C, muscle homogenates from AChE-R transgenic mice revealed two bands of 62 and 67 KDa (Fig. 1B). The antibody did not detect mouse muscle AChE, but did recognize two proteins from mouse milk, and a third 62 KDa band which appeared only in the milk of AChE-R transgenics. Finally, recombinant AChE-S yielded a single band of 65 KDa.

Sucrose gradient sedimentation profiles (Fig. 2) indicated that milk AChE-R and AChE-C are monomeric, yet revealed both G1 monomers and G2 dimers in muscle extracts from AChE-R transgenics. Monomeric structure is consistent with AChE-R and AChE-C not having a C-terminus that contains a sulfhydryl group that can be oxidized to form a disulfide bridged dimer, like AChE-S. The G1 (monomer) peak was immunopositive for both an antibody generated against the unique C-terminal sequence of AChE-R, and an antibody that was directed to the core protein shared by all AChE variants. In contrast, the G2 material reacted only with the anti-core antibody (data not shown), suggesting that the dimeric enzyme most likely originated from E5-containing transcripts in the muscle tissue.

AChE-R displays distinct inhibitor sensitivities

Inhibition studies of AChE-R from transgenic mouse milk revealed clear differences between this variant and AChE-E or AChE-S purified from human red blood cells and transfected HEK 293 cells, respectively. Fig. 3 presents the inihibitors tested and inhibition curves for the different agents and Tables 2 and 3 present the apparent K_i values for the variant enzymes for reversible and pseudo-irreverrsible inhibitors. AChE-E appeared 10-fold more sensitive to the peripheral site inhibitor propidium than AChE-S. Conversely, AChE-R was 6-fold more sensitive than AChE-S to the parathion metabolite paraoxon, with AChE-E presenting an intermediate K_i value of 90 pM for this insecticide metabolite.

Because of the relatively low affinity of AChE for DFP, it was difficult by this method to evaluate the K_i; the second order rate constant, of 3×10^4 $M^{-1}min^{-1}$ for all the three variants is not dissimilar from the value of 7×10^4 $M^{-1}min^{-1}$ reported by Schwarz et al., (1995). The carbamate pyridostigmine showed essentially similar capacities to inhibit AChE-S and AChE-R, with slightly higher K_i of 100 pM for AChE-E. Rivastigmine, another carbamate inhibitor, was significantly more efficient

in inhibiting AChE-R than the two other variants. This was consistent with the selective affinity of rivastigmine for soluble brain AChE monomers (Anand, et al., 1996), as AChE-R lacks the potential for multimerization. Finally, both tacrine and donepezil inhibited the three AChE isoforms to the same extent (Table 2).

Substrate affinities were not dissimilar among the variants. All showed an apparent K_m values close to 0.2 mM for acetylthiocholine; the K_i that characterizes substrate inhibition was also fairly similar for the AChE-S, -R and -C variants, 2.7, 2.3 and 1.3 mM, respectively.

Inhibition of AChE-R is unaffected by the presence of its unique C-terminal sequence

A priori, the increased drug sensitivity of AChE-R may be due to an effect of the C-terminal peptide that is unique to this isoform. Alternatively, or additionally, it may reflect the inhibitor sensitivities of the core AChE protein, with this C-terminal peptide being inert with regard to inhibitor interactions but the peptides of AChE-S and AChE-E causing the differences. A third possibility was that the distinct sensitivities of the three variants reflect contributions of both their common core and their respective C-terminal peptides. To resolve these possibilities we compared the inhibition curves of AChE-R with those of AChE-C, also produced in transgenic mice, for rivastigmine, DFP and paraoxon. In all three cases, indistinguishable inhibitor senstivities were observed (Tables 2, 3), suggesting that the hydrophilic C-terminal peptide of AChE-R, unlike the AChE-S and AChE-E C-terminal sequences, does not significantly contribute to the inhibition profile of this enzyme isoform.

The inhibitor sensitivities of AChE-R are reflected *in vivo*

The normally rare AChE-R isoform accumulates in the mammalian brain following stress (Kaufer, et al., 1998). Its unique inhibitor sensitivities therefore predicted altered anti-cholinesterase sensitivities under post-stress conditions. Impaired assembly of brain AChE into multimeric molecules should reflect the accumulation of AChE-R in the stressed brain. This was tested by sucrose gradient centrifugation. Similar volumes of 1:10 (w/v) brain homogenates from AChE-R or AChE-S transgenics, untreated and stressed FVB/N mice revealed higher hydrolytic activities in transgenics and stressed mice, and different ratios between monomers and tetramers in transgenic or stressed as compared to control mice (Fig. 4). The striking increase in the monomeric fraction following stress (with the G1:G4 ratio increasing from 0.14 to 1.05) indicated a massive accumulation of the AChE-R protein in stressed brain. In comparison, G1:G4 ratios in AChE-R and AChE-S transgenics were 0.65 and 0.12, respectively. Accordingly, sensitivity to rivastigmine in the brain of stressed or AChE-R transgenic mice was two times higher than in control FVB/N mice, with IC_{50} values of 36.1 ± 2.2, 39.2 ± 10.8 and 78.5 ± 8.1 μM, respectively. In contrast, sensitivity of all cortex preparations to donepezil was similar (Fig. 4B). Thus, the *in vitro* inhibitor sensitivities of AChE-R are reflected *in vivo*.

DISCUSSION

Considering that anti-cholinesterase therapy has not one but three AChE targets, we found that each of these targets has a characteristic affinity for inhibitors. The proportion of total AChE activity that each of these targets represents varies with the physiological state of the individual, particularly under stress. Using muscle and milk of transgenic mice that over-produce the different human AChE variants, we observed

significant differences in their biochemical and immunochemical properties and their inhibitor sensitivities. These findings are important at several levels of human health and well being. First, they propose a molecular mechanism for at least some of the observed individual responses to anti-AChEs. Our data imply that the stress level of treated or exposed individuals or previous episodes of anti-AChE treatment or exposure may change their drug sensitivity. This helps to explain, for instance, the fluctuations over a wide range of neostigmine doses administered to individual patients with myasthenia gravis, and may contribute to an explanation of the neuromuscular consequences of their treatment by anti-AChEs (Evoli, et al., 1996). Similarly, the feedback response leading to AChE-R accumulation under anti-AChE exposure may explain the gradual increase in drug dose that is recommended at the onset of treatment for Alzheimer's disease (Winkler, et al., 1998).

Susceptibility to stress responses may be regarded as a quantitative trait dependent on the combined contributions of several genes. Such a genetic component implies that the distinction between "responders" and "non-responders" to anti-AChEs treatments may be due, at least in part, to their genetic predisposition to stress responses. In addition, environmental factors may contribute to such differences. These were suggested to include oxidative stress, in addition to previous anti-AChE exposure. The classification into anti-AChE responders and non-responders based on their apolipoprotein E-variants may be related to such stressors (Thal, et al., 1996). In addition, blood-brain barrier disruption under stress (Friedman, et al., 1996) would further contribute to the ease by which anti-AChEs reach brain neurons and complicate the effects of stress. Facilitation of the feedback response of AChE-R accumulation and change of individual's sensitivity to anti-AChEs may therefore be subject to drastic treatment- and/or stress-induced modulations.

Our sucrose gradient analyses extend previous reports that AChE-R increases under stress (Kaufer, et al., 1998, Kaufer and Soreq, 1999). Thus, a 30% increase in AChE activity in the brain of AChE-R transgenics (Sternfeld, et al., 2000) leads to a G1:G4 ratio of 0.65, but 90 min post-stress, this ratio is even higher at 1.05. AChE-R may, therefore, represent over a third of the brain enzyme in the post-stress state. Accordingly, the inhibition studies demonstrated more effective inhibition of AChE by rivastigmine, but not donepezil, in the post-stress brain. This would be consistent with the increased fraction of monomeric AChE-R under stress. Intriguingly, the fraction of AChE monomers increases in Alzheimer's disease (Arendt, Bruckner et al. 1992; Ogane) [Giacobini, 2000 #1585. Moreover, the therapeutic efficacy of rivastigmine for treating Alzheimer's disease patients has been attributed to its selective interaction with globular monomers of brain AChE, especially in the hippocampus (Anand, et al., 1996). Our current evidence demonstrates particular specificity for this drug for the AChE-R protein, which is, as we have shown, monomeric. This points to AChE-R as the protein target of choice for Alzheimer's disease therapy yet predicts potentially harmful accumulation of rivastigmine-blocked AChE-R in the brain of patients treated with an anti-cholinesterase. Because some of the morphogenic properties of AChE were shown to be unrelated to its catalytic activity (reviewed by Grisaru et al., 1999), blocked AChE may still lead to progressive damage, as is seen in AChE-transgenic mice (Beeri, et al., 1995, Beeri, et al., 1997). The alternative option of antisense-based suppression of AChE production (Shohami, et al., 2000, Seidman, et al., 1999) appears advantageous as it eliminates AChE production altogether, reducing both catalytic and non-catalytic activities.

Alternatively, or in addition, the design of the next generation of anti-cholinesterase drugs should take into consideration the individual properties of variants of the protein.

Finally, our findings demonstrate that measurements of AChE catalytic activity do not provide a complete picture of the outcome of treatment with or exposure to anti-AChEs. Rather, immunodetection of specific AChE variants is preferable. Such analyses can yield insights regarding the composition of AChE variants in exposed individuals and indicate the appropriate drug selection and dose determination for treatment.

ACKNOWLEDGEMENTS

We thank Dr. B. Norgaard-Pedersen (Copenhagen) for the gift of anti-AChE antibodies and Dr. M. Weinstock (Jerusalem) for rivastigmine.

REFERENCES

1. Anand, R., G. Gharabawi, and A. Enz (1996). Efficacy and safety results of the early phase studies with exelon (ENA-713) in Alzheimer's disease: an overview. *J Drug Dev Clin Pract* **8:**106-16.
2. Giacobini, E. (1998). Invited review: Cholinesterase inhibitors for Alzheimer's disease therapy: from tacrine to future applications. *Neurochem Int* **32:**413-9.
3. Davis, K. L., L. J. Thal, E. R. Gamzu, C. S. Davis, R. F. Woolson, S. I. Gracon, D. A. Drachman, L. S. Schneider, P. J. Whitehouse, T. M. Hoover, and et al. (1992). A double-blind, placebo-controlled multicenter study of tacrine for Alzheimer's disease. The Tacrine Collaborative Study Group. *N Engl J Med* **327:**1253-9.
4. Engel, A. G., K. Ohno, and S. M. Sine (1998). Congenital myasthenic syndromes: experiments of nature. *J Physiol Paris* **92:**113-7.
5. Friedman, A., D. Kaufer, J. Shemer, I. Hendler, H. Soreq, and I. Tur-Kaspa (1996). Pyridostigmine brain penetration under stress enhances neuronal excitability and induces early immediate transcriptional response. *Nat Med* **2:**1382-1385.
6. Loewenstein Lichtenstein, Y., M. Schwarz, D. Glick, B. Norgaard Pedersen, H. Zakut, and H. Soreq (1995). Genetic predisposition to adverse consequences of anti-cholinesterases in 'atypical' BCHE carriers. *Nat Med* **1:**1082-5.
7. Feldman, R. G. (1999). Organophosphorus compounds, in *Occupational and Environmental Neurotoxicology* 421-442, Lippincott-Raven, Philadelphia.
8. Feldman, R. G. (1999). Carbamates, in *Occupational and Environmental Neurotoxicology* 442-465, Lippincott-Raven, Philadelphia.
9. Dutta-Choudhury, T. A., and T. L. Rosenberry (1984). Human erythrocyte acetylcholinesterase is an amphipathic protein whose short membrane-binding domain is removed by papain digestion. *J Biol Chem* **259:**5653-60.
10. Jbilo, O., C. F. Bartels, A. Chatonnet, J. P. Toutant, and O. Lockridge (1994). Tissue distribution of human acetylcholinesterase and butyrylcholinesterase messenger RNA. *Toxicon* **32:**1445-57.
11. Soreq, H., and D. Glick (2000). Novel roles for cholinesterases in stress and inhibitor responses, in *Cholinesterases and Cholinesterase Inhibitors: Basic, Preclinical and Clinical Aspects* (E. Giacobini, ed.) 47-61, Martin Dunitz, London.

12. Prody, C. A., P. Dreyfus, R. Zamir, H. Zakut, and H. Soreq (1989). De novo amplification within a "silent" human cholinesterase gene in a family subjected to prolonged exposure to organophosphorous insecticides. *Proc Natl Acad Sci U S A* **86:**690-4.
13. Shapira, M., I. Tur-Kaspa, L. Bosgraaf, N. Livni, A. D. Grant, D. Grisaru, M. Korner, R. P. Ebstein, and H. Soreq (2000). A transcription-activating polymorphism in the ACHE promoter associated with acute sensitivity to anti-acetylcholinesterases. *Hum Mol Genet* **9:**1273-1281.
14. Li, Y., S. Camp, T. L. Rachinsky, D. Getman, and P. Taylor (1991). Gene structure of mammalian acetylcholinesterase. Alternative exons dictate tissue-specific expression. *J Biol Chem* **266:**23083-90.
15. Ben Aziz Aloya, R., S. Seidman, R. Timberg, M. Sternfeld, H. Zakut, and H. Soreq (1993). Expression of a human acetylcholinesterase promoter-reporter construct in developing neuromuscular junctions of Xenopus embryos. *Proc Natl Acad Sci U S A* **90:**2471-5.
16. Schwarz, M., Y. Loewenstein Lichtenstein, D. Glick, J. Liao, B. Norgaard Pedersen, and H. Soreq (1995). Successive organophosphate inhibition and oxime reactivation reveals distinct responses of recombinant human cholinesterase variants. *Brain Res Mol Brain Res* **31:**101-10.
17. Glick, D., M. Shapira, and H. Soreq (2000). Molecular neurotoxicology implications of acetylcholinesterase inhibition, in *Site-Specific Neurotoxicology* (P. GLazarovici and D. Lester, eds.)(in press), Plenum Press, New York.
18. Futerman, A. H., M. G. Low, K. E. Ackermann, W. R. Sherman, and I. Silman (1985). Identification of covalently bound inositol in the hydrophobic membrane-anchoring domain of Torpedo acetylcholinesterase. *Biochem Biophys Res Commun* **129:**312-7.
19. Seidman, S., M. Sternfeld, R. Ben Aziz Aloya, R. Timberg, D. Kaufer Nachum, and H. Soreq (1995). Synaptic and epidermal accumulations of human acetylcholinesterase are encoded by alternative 3'-terminal exons. *Mol Cell Biol* **15:**2993-3002.
20. Shafferman, A., A. Ordentlich, D. Barak, C. Kronman, R. Ber, T. Bino, N. Ariel, R. Osman, and B. Velan (1994). Electrostatic attraction by surface charge does not contribute to the catalytic efficiency of acetylcholinesterase. *EMBO J* **13:**3448-55.
21. Kaufer, D., A. Friedman, S. Seidman, and H. Soreq (1998). Acute stress facilitates long-lasting changes in cholinergic gene expression. *Nature* **393:**373-377.
22. Kaufer, D., A. Friedman, and H. Soreq (1999). The vicious circle: long-lasting transcriptional modulation of cholinergic neurotransmission following stress and anticholinesterase exposure. *The Neuroscientist* **5:**173-183.
23. Shohami, E., D. Kaufer, Y. Chen, S. Seidman, O. Cohen, D. Ginzberg, N. Melamed-Book, R. Yirmiya, and H. Soreq (2000). Antisense prevention of neuronal damages following head injury in mice. *J. Mol. Med.* **78:**228-236.
24. Lev-Lehman, E., T. Evron, E. S. Broide, E. Meshorer, I. Ariel, S. Seidman, and H. Soreq (2000). Synaptogenesis and myopathy under acetylcholinestrase overexpression. *J. Mol. Neurosci.* **14:**93-105.
25. Sternfeld, M., S. Shoham, O. Klein, C. Flores-Flores, T. Evron, G. H. Idelson, D. Kitsberg, J. W. Patrick, and H. Soreq (2000). Excess "readthrough" acetylcholinesterase attenuates but the "synaptic" variant intensifies neurodeterioration correlates. *Proc. Natl. Acad. Sci. USA* **97:**8647-8652.

26. Cousin, X., S. Bon, N. Duval, J. Massoulie, and C. Bon (1996). Cloning and expression of acetylcholinesterase from Bungarus fasciatus venom. A new type of cooh-terminal domain; involvement of a positively charged residue in the peripheral site. *J Biol Chem* **271:**15099-108.
27. Gough, N. R., and W. R. Randall (1995). Oligomerization of chicken acetylcholinesterase does not require intersubunit disulfide bonds. *J Neurochem* **65:**2734-41.
28. Gibney, G., and P. Taylor (1990). Biosynthesis of Torpedo acetylcholinesterase in mammalian cells. Functional expression and mutagenesis of the glycophospholipid-anchored form. *J Biol Chem* **265:**12576-83.
29. Beeri, R., C. Andres, E. Lev-Lehman, R. Timberg, T. Huberman, M. Shani, and H. Soreq (1995). Transgenic expression of human acetylcholinesterase induces progressive cognitive deterioration in mice. *Curr Biol* **5:**1063-71.
30. Kaufer, D., A. Friedman, S. Seidman, and H. Soreq (1999). Anticholinesterases induce multigenic transcriptional feedback response suppressing cholinergic neurotransmission. *Chem Biol Interact* **119-120:**349-60.
31. Grisaru, D., E. Lev-Lehman, M. Shapira, E. Chaikin, J. B. Lessing, A. Eldor, F. Eckstein, and H. Soreq (1999). Human osteogenesis involves differentiation-dependent increases in the morphogenically active 3' alternative splicing variant of acetylcholinesterase. *Mol Cell Biol* **19:**788-95.
32. Seidman, S., R. B. Aziz Aloya, R. Timberg, Y. Loewenstein, B. Velan, A. Shafferman, J. Liao, B. Norgaard Pedersen, U. Brodbeck, and H. Soreq (1994). Overexpressed monomeric human acetylcholinesterase induces subtle ultrastructural modifications in developing neuromuscular junctions of Xenopus laevis embryos. *J Neurochem* **62:**1670-81.
33. Ellman, G. L., D. Courtney, V. J. Andres, and R. M. Featherstone (1961). A new and rapid colorimetric determination of acetylcholinesterase activity. *Biochem. Pharmacol.* **7:**88-95.
34. Hobbiger, F., and A. W. Peck (1969). Hydrolysis of suxamethonium by different types of plasma. *Br J Pharmacol* **37:**258-71.
35. Ordentlich, A., D. Barak, C. Kronman, N. Ariel, Y. Segall, B. Velan, and A. Shafferman (1995). Contribution of aromatic moieties of tyrosine 133 and of the anionic subsite tryptophan 86 to catalytic efficiency and allosteric modulation of acetylcholinesterase. *J Biol Chem* **270:**2082-91.
36. Karnovsky, M. J., and L. Roots (1964). 'Direct coloring' thiocholine method for cholinesterase. *J. Histochem. Cytochem.* **12:**219-221.
37. Sternfeld, M., G. Ming, H. Song, K. Sela, R. Timberg, M. Poo, and H. Soreq (1998). Acetylcholinesterase enhances neurite growth and synapse development through alternative contributions of its hydrolytic capacity, core protein, and variable C termini. *J Neurosci* **18:**1240-9.
38. Meflah, K., S. Bernard, and J. Massoulie (1984). Interactions with lectins indicate differences in the carbohydrate composition of the membrane-bound enzymes acetylcholinesterase and 5'- nucleotidase in different cell types. *Biochimie* **66:**59-69.
39. Spitsyn, V. A., and L. S. Bychkovskaia (1994). [New locus of cholinesterase (E3) expressed in human milk]. *Genetika* **30:**172-5.
40. Evoli, A., A. P. Batocchi, M. Lo Monaco, S. Servidei, L. Padua, L. Majolini, and P. Tonali (1996). Clinical heterogeneity of seronegative myasthenia gravis. *Neuromuscul Disord* **6:**155-61.

41. Winkler, J., L. J. Thal, F. H. Gage, and L. J. Fisher (1998). Cholinergic strategies for Alzheimer's disease. *J Mol Med* **76:**555-67.
42. Thal, L. J., G. Schwartz, M. Sano, M. Weiner, D. Knopman, L. Harrell, S. Bodenheimer, M. Rossor, M. Philpot, J. Schor, and A. Goldberg (1996). A multicenter double-blind study of controlled-release physostigmine for the treatment of symptoms secondary to Alzheimer's disease. Physostigmine Study Group. *Neurology* **47:**1389-95.
43. Kaufer, D., and H. Soreq (1999). Tracking cholinergic pathways from psychological and chemical stressors to variable neurodeterioration paradigms. *Curr Opin Neurol* **12:**739-43.
44. Arendt, T., M. K. Bruckner, M. Lange, and V. Bigl (1992). Changes in acetylcholinesterase and butyrylcholinesterase in Alzheimer's disease resemble embryonic development--a study of molecular forms. *Neurochem Int* **21:**381-96.
45. Ogane, N., E. Giacobini, and E. Messamore (1992). Preferential inhibition of acetylcholinesterase molecular forms in rat brain. *Neurochem Res* **17:**489-95.
46. Beeri, R., N. Le Novere, R. Mervis, T. Huberman, E. Grauer, J. P. Changeux, and H. Soreq (1997). Enhanced hemicholinium binding and attenuated dendrite branching in cognitively impaired acetylcholinesterase-transgenic mice. *J Neurochem* **69:**2441-51.
47. Seidman, S., F. Eckstein, M. Grifman, and H. Soreq (1999). Antisense technologies have a future fighting neurodegenerative diseases. *Antisense Nucleic Acid Drug Dev* **9:**333-40.
48. Andres, C., R. Beeri, A. Friedman, E. Lev-Lehman, S. Henis, R. Timberg, M. Shani, and H. Soreq (1997). Acetylcholinesterase-transgenic mice display embryonic modulations in spinal cord choline acetyltransferase and neurexin Ibeta gene expression followed by late-onset neuromotor deterioration. *Proc Natl Acad Sci U S A* **94:**8173-8.

FOOTNOTES

*Supported by The Israel Science Foundation (590/97), the US Army Medical Research and Development Command (DAMD17-99-1-9547), The US-Israel Binational Science Foundation (99/115), the Eric Roland Center for Neurodegenerative Diseases and Ester Neuroscience, Ltd (to HS).

†To whom correspondence should be addressed, Department of Biological Chemistry, Institute of Life Sciences, Hebrew University of Jerusalem, 91904 Israel; tel. 972-2-6585109; fax. 972-2-6520258; e-mail soreq@shum.huji.ac.il.

Table 1. Production of human AChE variants in milk of transgenic mice

Three DNA constructs encoding alternative isoforms of recombinant human AChE (Sternfeld, et al., 1998) were used for introduction into transgenic mouse pedigrees. Milk of females from each of these lines was collected from nursing mice 7 days *post partum*. Milk and muscle hydrolysis rates of ATCh were determined spectrophotometrically using a modification of Ellman's assay (Andres, et al., 1997), in the presence or absence of 10^{-5} M of the selective BuChE inhibitor iso-OMPA. Activity is expressed as nmol ATCh hydrolyzed/min/µl (milk) or /mg protein (muscle).

promoter	protein	milk ChE activity	milk AChE activity[a]	muscle AChE activity[a]
hp	AChE-S	3.9 ± 0.2	0.5 ± 0.2	35.9 ± 1.3[b]
cmv	AChE-C	13 ± 2	7.1 ± 0.6	352 ± 59[c]
cmv	AChE-R (line 45)	11 ± 1	7.4 ± 0.3	190 ± 23[d]
cmv	AChE-R (line 70)	121 ± 4	115 ± 4.0	2700 ± 250[d]
FVB/N control		4.1 ± 0.4	0.5 ± 0.3	7.6 ± 0.6[d]

[a]Activity determined in the presence of 10^{-5} M iso-OMPA.
[b]Data taken from Andres et al. (1997).
[c]Values from 2 male mice (personal communication from T. Evron, Jerusalem).
[d]Data taken from Sternfeld et al. (1998).

Table 2. K_i values (µM) of human AChE variants for reversible inhibitors[a]

	donepezil	tacrine	propidium
AChE-R	0.098 ± 0.011	0.034 ± 0.002	1.3 ± 0.2
AChE-S	0.18 ± 0.02	0.040 ± 0.003	0.32 ± 0.04
AChE-E	0.19 ± 0.001	0.046 ± 0.007	2.9 ± 0.6
AChE-R/AChE-S	0.54	0.85	4.1

[a]The source of AChE-R was transgenic mouse milk and of AChE-S and AChE-E, the commercial human recombinant and human erythrocyte enzymes. The experiments were performed in triplicate.

Table 3. Kinetic constants for inhibition of AChE by pseudo-irreversible inhibitors[a]

	rivastigmine		paraoxon		pyridostigmine	
	k_i (min^{-1})	K_i (µM)	k_i (min^{-1})	K_i (µM)	k_i (min^{-1})	K_i (µM)
AChE-R	0.023	0.7	0.40	4.5	0.055	0.11
AChE-S	0.068	4.8	0.28	6.6	0.036	0.14
AChE-C	0.047	2.9	0.58	3.0	0.030	0.19

[a]The source of AChE-R and AChE-C was milk from the corresponding transgenic mice, and AChE-S was the commercial human recombinant enzyme. The experiments were performed in triplicate at 27 °C.

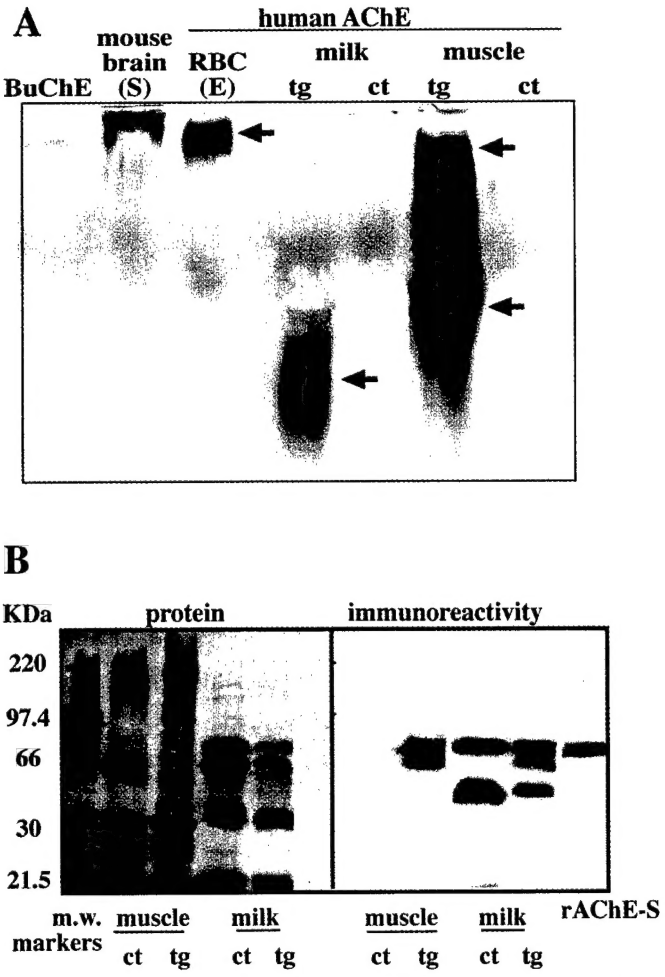

Fig. 1. AChE-R transgenic mice produce distinct AChE variants in muscle and milk

A. Activity gel. Samples of cholinesterases (with activity of ΔA_{405} of approx. 0.4/min in the Ellman's assay) were electrophoresed on non-denaturing polyacrylamide gels. Cholinesterase activity was detected using the Karnovsky method **(Karnovsky and Roots, 1964)**. Shown are (from left to right): human serum BuChE; AChE-S from transgenic mouse brain; AChE-E from human erythrocytes; milk and gastrocnemius muscle extracts from AChE-R transgenic and control mice. Upper bands (upper arrows) denote slowly migrating AChE-E. Lower bands (lower arrows) denote AChE-R. The different mobilities are probably due to different post-translational processing.

B. Immunodetection of recombinant human AChE in milk and muscle of transgenic mice. Right: Immunoblot; samples of milk and muscle extracts (40 µg of total protein) from AChE-R transgenic and control FVB/N mice, and purified recombinant AChE-S (6 I.U.) were subjected to 8% SDS-PAGE and blotted onto nitrocellulose filters. After blocking, the blot was reacted with monoclonal antibodies raised against denatured AChE-C (core) and then with horseradish peroxidase-conjugated goat anti-mouse IgG and subjected to chemiluminescent detection.

Two immunoreactive bands (72 and 54 KDa) appear both in transgenic and non-transgenic milk. The upper band, markedly stained by the Ponceau, co-migrates with mouse serum albumin which is abundant in mouse milk. However, a 62 KDa band, the predicted size of the AChE-R protein, appears in the milk and muscle of AChE-R transgenic, but not control mice. In the transgenic muscle, an additional immunopositive band of 70 KDa was detected, not found in non-transgenic muscle. This band most likely reflects muscle-specific production of AChE.

Left: Ponceau staining of the proteins on the nitrocellulose filter.

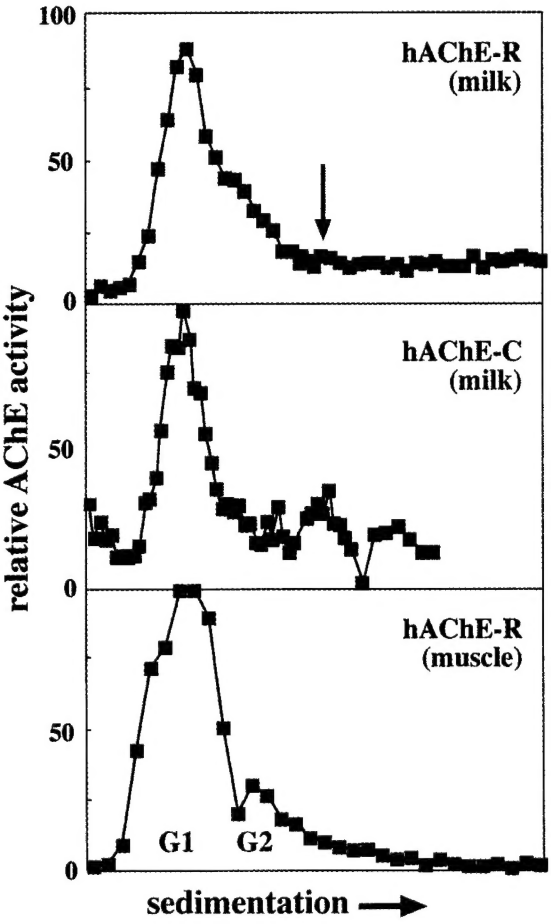

Fig. 2. Sedimentation profiles of variant AChEs from milk and muscle of female transgenic mice
Presented are one of 4 replicate sedimentation profiles in 5-20% sucrose gradients of AChE activities from milk and whole gastrocnemius muscle extract from mice expressing the AChE-R trangene and of milk from mice expressing AChE-C. All sedimentation profiles were aligned with bovine catalase as a sedimentation marker (11.4 S), whose position is indicated in the upper panel. Note the prominent peak of the monomer (G1), in milk of transgenics expressing either AChE-R or AChE-C; the similar sedimentation properties of AChE-R and AChE-C are compatible with the two monomers differing only by a short, hydrophilic sequence. An additional shoulder of AChE-E dimers (G2), is detectable in muscle from AChE-R transgenics.

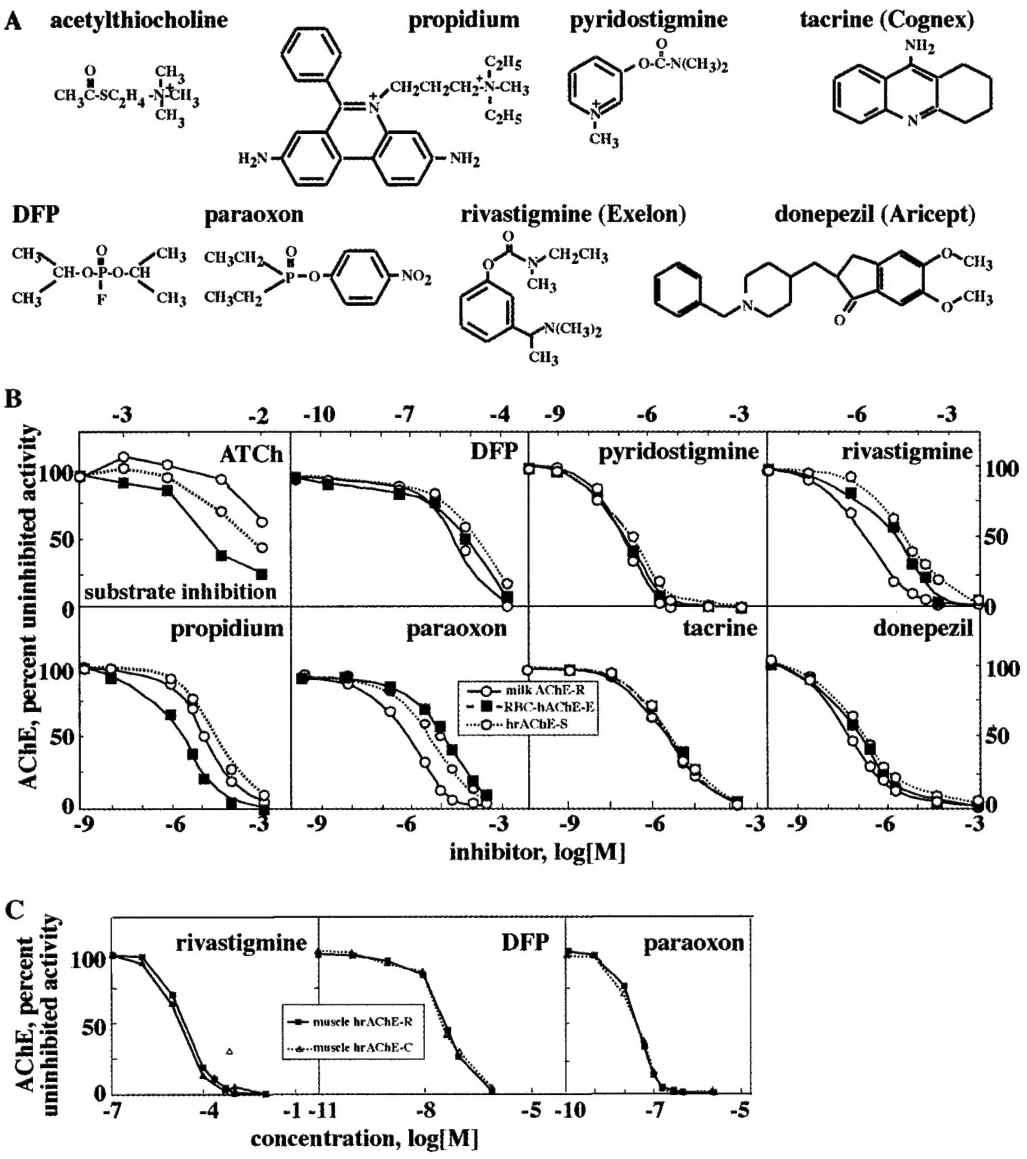

Fig. 3. AChE from transgenic AChE-R mouse milk displays high sensitivity to inhibitors

A. Structures of the AChE inhibitors used in this study.

B. AChE from the milk of AChE-R transgenic mice, human erythrocytes (RBC-hAChE-E) and human recombinant AChE-S (hrAChE-S) were pre-incubated for 10 min with the indicated concentrations of inhibitors in Ellman's reagent and AChE activity was measured. Data are presented for each AChE isoform as percent of uninhibited activity. Note that milk AChE-R, as expressed in AChE-R transgenic mice (open circles), is more sensitive to the organophosphates DFP and paraoxon and to the carbamate inhibitor rivastigmine than are the other AChE variants; AChE-R displays the same sensitivity as AChE-S and AChE-E to the carbamate pyridostigmine and tacrine, and is less sensitive than AChE-E to propidium. Note also that the range of the abscissae for the upper 4 panels is shown above them, and for the lower 4, below them.

C. AChE-R and AChE-C compared according to their inhibition by rivastigmine, DFP and paraoxon.

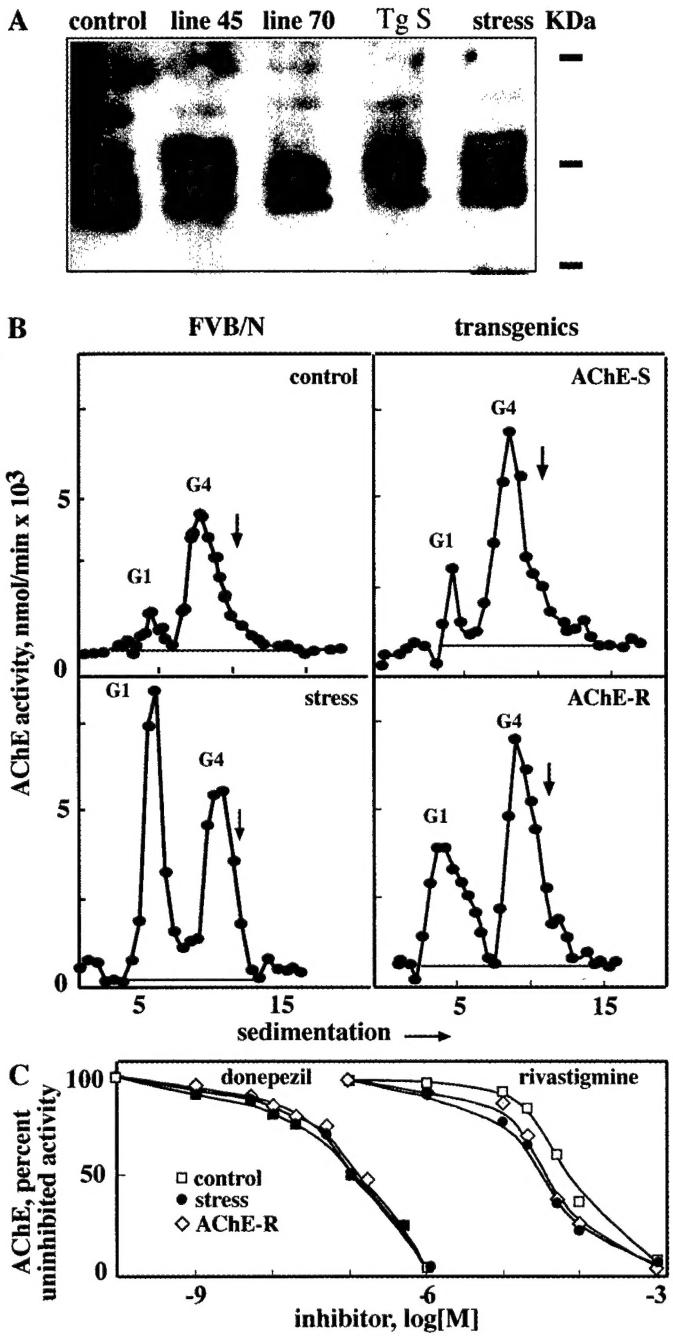

Fig. 4. Transgenic- and stress-induced alterations in brain AChE sedimentation profiles and inhibitor sensitivities

A. Immunoblot film, for transgenics and control and stressed control. The antibody was one targeted to the common core domain of human AChE; the positive signal obtained with this antibody in control mouse samples demonstrates massive cross reactivity with the mouse enzyme.

B. Shown are one of four sedimentation patterns of catalytically active AChE from the somatosensory cortices of untreated and 90 min post-stress FVB/N mice and from untreated AChE-S and -R transgenic mice. The total AChE activity of the control preparation was 0.97 ± 0.19; for the stressed group, 1.12 ± 0.16; for the AChE-S transgenics, 1.48 ± 0.34; and for the AChE-R transgenics, 1.36 ± 0.18 mmol/min/mg wet tissue weight. The G1:G4 ratios for these prepartations, caclulated from the areas under the peaks and above the lines constructed below them, are: control, 0.14; stress, 1.05; AChE-S, 0.12; and AChE-R, 0.65.

C. Shown are inhibition curves of pooled somatosensory cortex homogenates (n = 4 in each case), closely similar in dilution, of the above model systems (control and stressed FVB/N mice and AChE-R transgenics). Inhibition was with increasing doses of donepezil and rivastigmine. Note the increased sensitivity to the latter in experimental, as compared to control, samples.